Basin analysis and the geochemical signature of Paleoproterozoic sedimentary successions in northern Australia: Constraints on basin development in respect to mineralisation and paleoreconstruction models

Alexis Lambeck, (B.Sc, M.Sc)

Geology and Geophysics
School of Earth and Environmental Sciences
The University of Adelaide

This thesis is submitted in fulfilment of the requirements for the degree of Doctor of Philosophy in the Faculty of Science, University of Adelaide

December 2011

Table of Contents

List of Figures

List of Tables

Abstract

Secular changes in the characteristics of sedimentary basins and their associated mineral deposits in Proterozoic Australia are directly related to the evolving global tectonic regimes and global changes in atmospheric and oceanic redox states. Identifying these secular changes provides critical information to assist in applying first pass techniques for regional exploration in Australia. The break-up and formation of the Nuna supercontinent is recorded within sedimentary basins within Proterozoic Australia. Sedimentary basins deposited between 1910 Ma and 1810 Ma formed during the Nuna supercontinent amalgamation and host orogenic gold mineralisation, whereas those deposited between 1710 Ma ─ 1575 Ma are directly associated with the break-up of Nuna and host lead-zinc mineralisation.

Sediments in northern Australia deposited during the Nuna amalgamation, and before the Great Oxidation Event, consist of fine-grained iron-rich/mafic mudstones and siltstones which are geochemically characterised by high FeO contents, high Cr/Th and low Th/Sc values. This sedimentary assemblage includes the gold-bearing succession of the Dead Bullock Formation, Tanami region and Koolpin Formation, Pine Creek Orogen. This contrasts with the regionally overlying stratigraphy, which is characterised by low Cr/Th and FeO values and high Th/Sc values. These rocks are also characterised by lower abundances of gold deposits. These geochemical characteristics have successfully been applied by Newmont Tanami Operations to help design future drill programs in the Tanami region.

Sedimentological analysis has been applied in the poorly exposed Tanami basin. The results of these studies, in combination with isopach maps derived from seismic data, lithogeochemistry and U-Pb SHRIMP geochronology, have been used to establish a depositional model for gold-bearing Palaeoproterozoic rocks of the Tanami region. The identification of stratal surfaces between the Dead Bullock Formation (Callie Member) and the Killi Killi Formation permits a better understanding of stratigraphic architecture. The Killi Killi Formation consists of coarser grains in the northwest compared to the southeast which suggests that sediment was transported from the northwest. The maximum thickness of the Tanami Group is recorded in the northwest which then fines/thins to the southeast to a position south of the Callie Mine. The Callie Member was deposited as part of a condensed section below storm wave base. The conformably overlying Killi Killi Formation was also deposited below storm wave base and forms part of a low stand system tract.

Claystone and mudstone within the Killi Killi Formation are prospective for epigenetic gold deposits hosted by reduced mudstones (i.e., Callie style deposits). Within the Killi Killi Formation and the Callie Member, gold potential is enhanced by deep crustal faults that intersect black claystone forming overbank deposits of the Killi Killi Formation or condensed sections of the Callie Member. The claystone forms potential redox boundaries for oxidised gold bearing-fluid. Targeting the position of these thrust faults within claystone environments could help refine gold exploration methods in the Killi Killi Formation.

Possible analogies to iron-rich claystone in the Tanami province are suggested with similar iron-rich successions in the Pine Creek Orogen. Deposition of these iron-rich rocks in northern Australia may have involved similar processes that deposited iron-rich rocks between 2100 to 1800 Ma at Homestake, U.S.A., Ghana, West Africa, and Guyana, South America. Between ~2400 Ma to ~1850 Ma Superior-style BIF deposit were

deposited in many areas around the world, but after about 1800 Ma a global rise in oxygen content of the oceans led to the end of deposition of banded iron formations and iron-rich sediments. This transition from iron-rich sediments to iron-poor sediments corresponds to a general change in mineralisation style and correlates with the Nuna supercontinent break-up. Orogenic gold in northern Australia halted by ~1810 Ma, replaced by a major period of lead-zinc mineralisation between 1710 – 1575 Ma which is associated with the Nuna supercontinent break-up.

Basins that formed in the present day eastern part of Proterozoic Australia during Nuna break-up are characterised by an abrupt change in Sm-Nd isotopic characteristics of sediments at ~1650 Ma. Prior to ~1650 Ma, these rocks have bulk ε_{Nd}(1650 Ma) values of -8 to -6, interpreted to imply a relatively evolved sedimentary source. Sedimentary rocks that accumulated between 1650 Ma – 1600 Ma are characterised by bulk ε_{Nd} (1650 Ma) values of -2 to -1, indicating a more juvenile sedimentary source. Although Proterozoic felsic magmatism is known in eastern and central Australia, these rocks are either too young or too evolved to have acted as a source for juvenile detritus that characterises the sedimentary successions after ~1650 Ma, which indicates either a source exogenous to present day Australia or a source that was present within Proterozoic Australia that has been lost from the geological record. Juvenile felsic magmatic rocks with ages of around 1650 Ma are known in Laurentia and Baltica, both of which have been interpreted to have been adjacent to Australia at ~1650 Ma. Either of these sources could have been a source of juvenile detritus into Australian Proterozoic basins, but existing data are insufficient to be able to distinguish between these possibilities. Alternatively, the source could have been an endogenous source within Proterozoic Australia. Evidence of such a source may be preserved as "pinkites", thin felsic layers with a probable magmatic origin that are present in parts of the stratigraphy of interest. Present data do not allow discrimination of these three possible sources of juvenile detritus that were introduced into Proterozoic Australian basins at ~1650 Ma.

Sediment hosted Mt Isa-style Zn-Pb-Ag sediments can potentially be fingerprinted by Sm-Nd isotopic data. Future exploration could use this important isotopic boundary at 1650 Ma as an exploration tool for Mt Isa-style deposits in the Mt Isa Inlier, the Etheridge Province, and elsewhere in Proterozoic Australia.

Acknowledgements

By undergoing this PhD through Geoscience Australia and based at Adelaide University I have had the benefit of many people to 'bounce ideas' around and talk geology with, so I'm grateful to a lot of people who all collectively played a part in my PhD program. First and foremost I'd like to thank Geoscience Australia for supporting my PhD program, I'm grateful to the support given by James Johnson, Russell Korsch and GA Senior Management throughout my PhD program.

Secondly I'd like to thank my PhD supervisor at Geoscience Australia, David Huston, who was a fantastic help. Dave's unfaltering willingness to help out was greatly appreciated, especially during those 'Huston, I have a problem' moments! I'm also very grateful to Dave Champion for providing me with endless chats about geochemistry…and fishing. Time in the field was always fun with George Gibson and George's endless debates about geology. Andrew Retter provided much tireless enthusiasm in the field and Andrew's attention to detail made field work a really fun and enjoyable experience. Lesley Wyborn is also thanked for many thought provoking chats and Lesley's willingness 'to bounce ideas around' was much appreciated. Terry Mernagh was always happy to have chats about geochemistry and the dark art of 'geochemical modelling'. Tony Meixner's skills at GOCAD were greatly appreciated…as where endless chats about 24 hour mountain biking…

At Adelaide University, Karin Barovich and Martin Hand had the tough job of dealing with all my questions and work from afar and my endless stream of emails and 'stuff' to read through. I'm very thankful to Karin and Martin for those thought provoking questions and conversations through out my PhD program and with the brief time Martin and I spend 'kicking rocks' together in the Mount Isa region. David Bruce's tireless work in the labs at Adelaide University was also greatly appreciated, as was his attention to detail.

At Geoscience Australia; Richard Blewett, Peter Maher and John Wilford were always up for a run and a chat and a great way to break-up the day. Chats over coffee with Paul Henson about geology and 'life outside' of geology were also fun times. I'm very grateful to the Liz Webber, and Bill Pappas's geochemistry team, their help and willingness was greatly appreciated over the years! The GA geochronology group provided a fantastic resource and I'm entirely grateful to them all, especially Keith Sircombe, Andrews Cross, Chris Carson, and Chuck Magee for endless discussion down in the SHRIMP lab. Patrick Burke's enthusiasm to keep the SHRIMP running was also greatly appreciated. Chris Foudulis and his team in the zircon separation group also provided much enthusiastic support. At the University of Western Australia, Annette George provided many thoughtful suggestions and comments through out my PhD.

I am especially grateful to Ian Withnall and Allan Parsons from the Geological Survey of Queensland who put up with my endless stream of questions while 'kicking-rocks' in the field. The logistical support from GSQ while working in the Mount Isa Inlier was greatly appreciated during my PhD program. The GSQ team were always happy to talk geology and have a beer & BBQ with at the 'GSQ house' in Mount Isa.

My loving wife Andrea is also thanked for her all her support during my PhD program. I'm very grateful to Andrea's understanding of me disappearing off to remote places for weeks at a time with only brief and random sat phone conversations. Our two young children, Adah and Ashby, were always up for giggles and were a great way to really remember what's important in life!

Finally thanks to the University of Florida, Mike Perfit and David Foster for providing me with a 'quiet space' in the department to finish writing up my PhD.

Publications and selected conference Abstracts

Peer reviewed Journal Articles

Lambeck, A., Huston, D., and Barovich, K., 2010, Typecasting prospective Au-bearing sedimentary lithologies using sedimentary geochemistry and Nd isotopes in poorly exposed Proterozoic basins of the Tanami region, Northern Australia: Mineralium Deposita, v. 4, p. 497–515.

Lambeck, A., Mernagh, T. and Wyborn, L., A, I., 2011. Are iron-rich sedimentary rocks the key to the spike in orogenic gold mineralization in the Paleoproterozoic? Economic Geology 106 (3): 321-330.

Lambeck, A., Barovich, K., George, A.D., Cross, A. Huston, D., and Meixner T. Defining basin architecture in the poorly exposed Tanami Proterozoic turbiditic basin, northern Australia with implications for gold mineralisation (in press, Australian Journal of Earth Science)

Lambeck, A., Barovich, K., Gibson, G.M. and Huston, D., in review. An abrupt change in Nd isotopic composition in Australian basins at 1650 Ma: implications for the tectonic evolution of Australia and its place in Nuna. (in review. Precambrian Research).

Lambeck, A., C**ross, A.,** SHRIMP U-Pb detrital & volcanic zircon results, Georgetown Inlier, Mt Isa, Eastern Succession. (will form a future GA Record).

Selected Conference Abstracts

Lambeck, A., Gibson, G., Neumann, N., Huston, D. 2008, An integrated sedimentological, geochemical and geochronological analysis of Georgetown: Constraints on basin development and paleo reconstructions. Abstracts. Australian Earth Sciences Convention 2008.

Lambeck, A., Parsons, P., Barovich, K., Hand, M., Withnall, I., Huston, D., Neumann, N. and Carson, C. 2009, Sm-Nd isotopic fingerprinting defining a ~1650 Ma reference boundary in Mt Isa and Georgetown: Implications for Zn-Pb exploration. Digging Deeper, Abstracts, 2 December 2009, pg 12-15.

Lambeck, A., Huston, D., Neumann, N., Barovich, K. and Hand M., 2010, Reconstruction of the Australia-Laurentia link at 1650 Ma: constraints from Sm-Nd data from the Georgetown, Mount Isa, Curnamona, Yavapai and Mazatzal Provinces . Specialist Group in Tectonics and Structural Geology, Geological Society of Australia, Abstracts 25–29 January 2010, pg. 39.

Lambeck, A., Neumann, N., Barovich, K., Hand, M., Huston, D., Carson, C., Gibson, G., Withnall, I., and Parson, A., 2010, An Australian tectonic reconstruction at ~1650 Ma: A Baltica link. Abstracts. Australian Earth Sciences Convention 2010, pg. 132.

Lambeck, A., Mernagh, T. and Wyborn, L., A,I., 2010. The Spike in Orogenic Gold Mineralization in the Paleoproterozoic: Linked to Anomalously Iron-Rich Sedimentary rocks? Society of Economic Geology annual conference Keystone, Colorado pg 13.

Declaration

This thesis contains no material that has been accepted for the award of any other degree or diploma in any university or other tertiary institution and, to the best of my knowledge and belief, contains no material previously published or written by any other person, except where due reference has been made in the text.

I give consent to this copy of my thesis, when deposited in the University and Geoscience Australia libraries, being available for loan and photocopying.

_____

Alexis Lambeck

Chapter 1

Introduction

Geochemistry and mineralisation in the North Australia Craton

The break-up and formation of supercontinents through time has been linked to the temporal pattern of many types of ore deposits and their preservation potential (e.g. Barley and Groves, 1992; Titley, 1993; Kerrich et al., 2005; Goldfarb et al., 2009; Goldfarb et al., 2010). Although the timing of supercontinent break-up and amalgamation varies across the world, Goldfarb et al. (2010) discuss the approximate time periods for such supercontinent formation and break-up, which include 2800–2500 and 2450–2100 Ma, for Kenorland, 2100–1800 and 1600–1300 Ma for Nuna/Columbia, 1300–1100 and 850–600 Ma for Rodinia, and 600–300 and 200–60 Ma for Gondwana-Pangea.

Precambrian components of Australia consist of three cratons, the West Australian Craton, the North Australian Craton and the South Australian Craton (Myers et al., 1996). Each craton is separated by Paleoproterozoic to Neoproterozoic orogens with the Tasman Line marking the boundary of Precambrian rocks in eastern Australia (Myers et al., 1996; Direen and Crawford 2003). Intense debate continues over the geodynamic setting of the Australian orogenic systems with both intracratonic and plate margin settings proposed for the orogenic belts (e.g. Etheridge et al., 1987; Myers et al., 1996; Fraser et al., 2007; Cawood and Korsch 2008; Payne et al., 2009).

Cawood and Korsch (2008) refer to the pre-1840 Ma entity of Australia as the Diamantina Craton, which consists of the Western, Northern and South Australia cratons. The North Australia Craton (NAC) includes the continental mass that existed after ~1700 Ma with the amalgamation of provinces from the West Kimberley in the west to Georgetown in the east.

The late Paleoproterozoic to early Mesoproterozoic in Australia (Fig. 1.1 & 1.2) is the timing of formation of most of Australia's Proterozoic mineral deposits. Huston et al. (2010) suggested this period of mineralisation was linked to the formation and break-up of Nuna (Hoffman, 1991 aka Columbia; Rogers and Santosh, 2002). Large areas of the Diamantina Craton were covered by thick sedimentary basins which host world-class gold and lead-zinc deposits (Fig. 1.1 & 1.2). Within these thick sedimentary basins, anoxic stratigraphy, consisting of black mudstones, hosts metal-enriched deposits of varying types. Goldfarb et al. (2010) noted that, in general, particular ore deposit types form predominantly within particular time periods while at other times in the geological history these deposit types are scarce or absent.

The motivation behind quantifying the sedimentary successions of northern Australia was to build and improve on earlier regional correlations and ultimately provide suggestions which could be applied to help lower exploration risk in northern Australia. The study helps typecast sediments that were deposited during the Nuna supercontinent amalgamation and then uses isotopic typecasting to study rocks that were deposited during the break-up of Nuna, with a discussion of the tectonic evolution of Australia and potential continental reconstruction models.

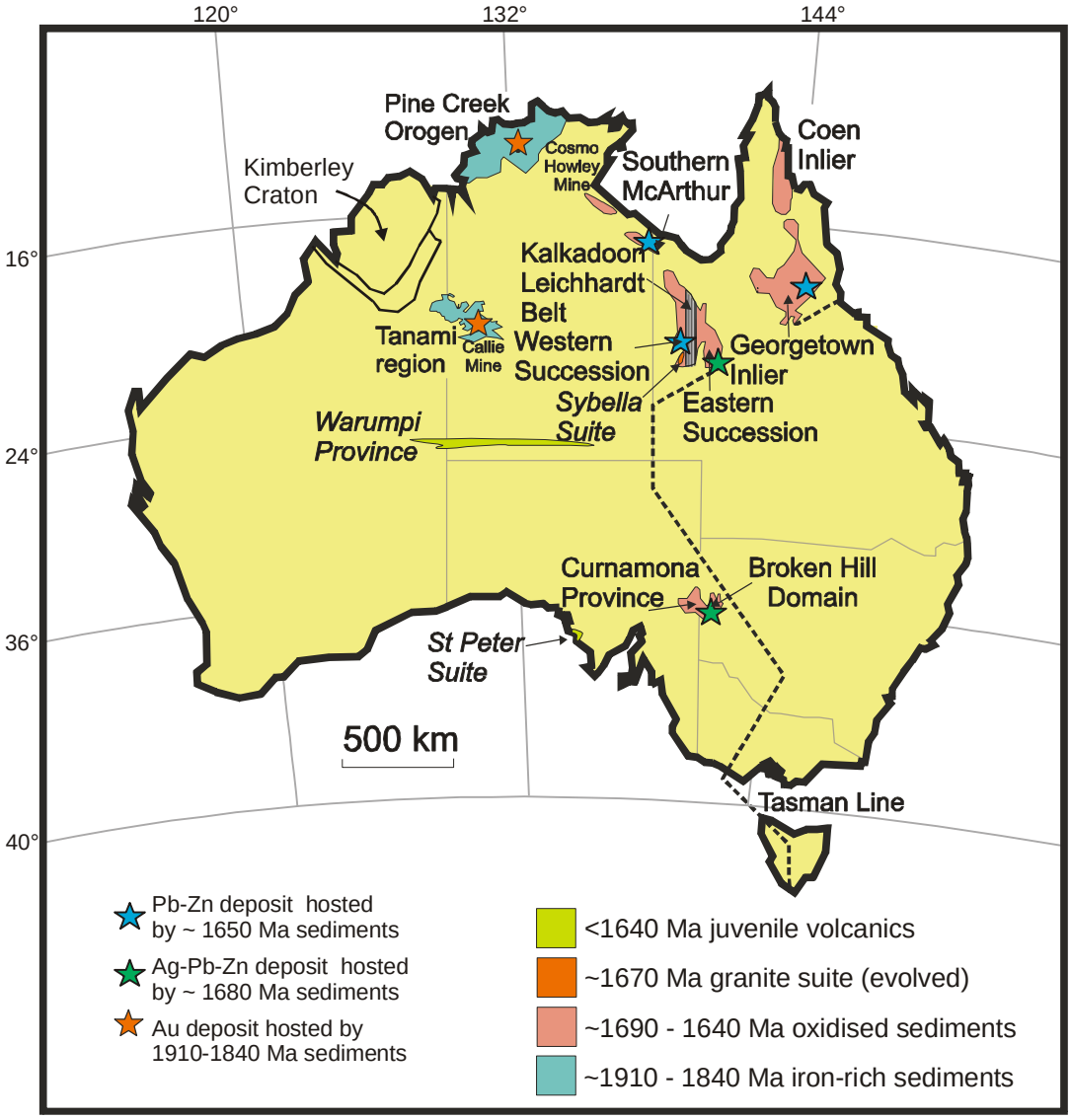

Fig. 1.1 - Proterozoic map of Australia showing location of Proterozoic gold and lead-zinc mines within regional stratigraphy.

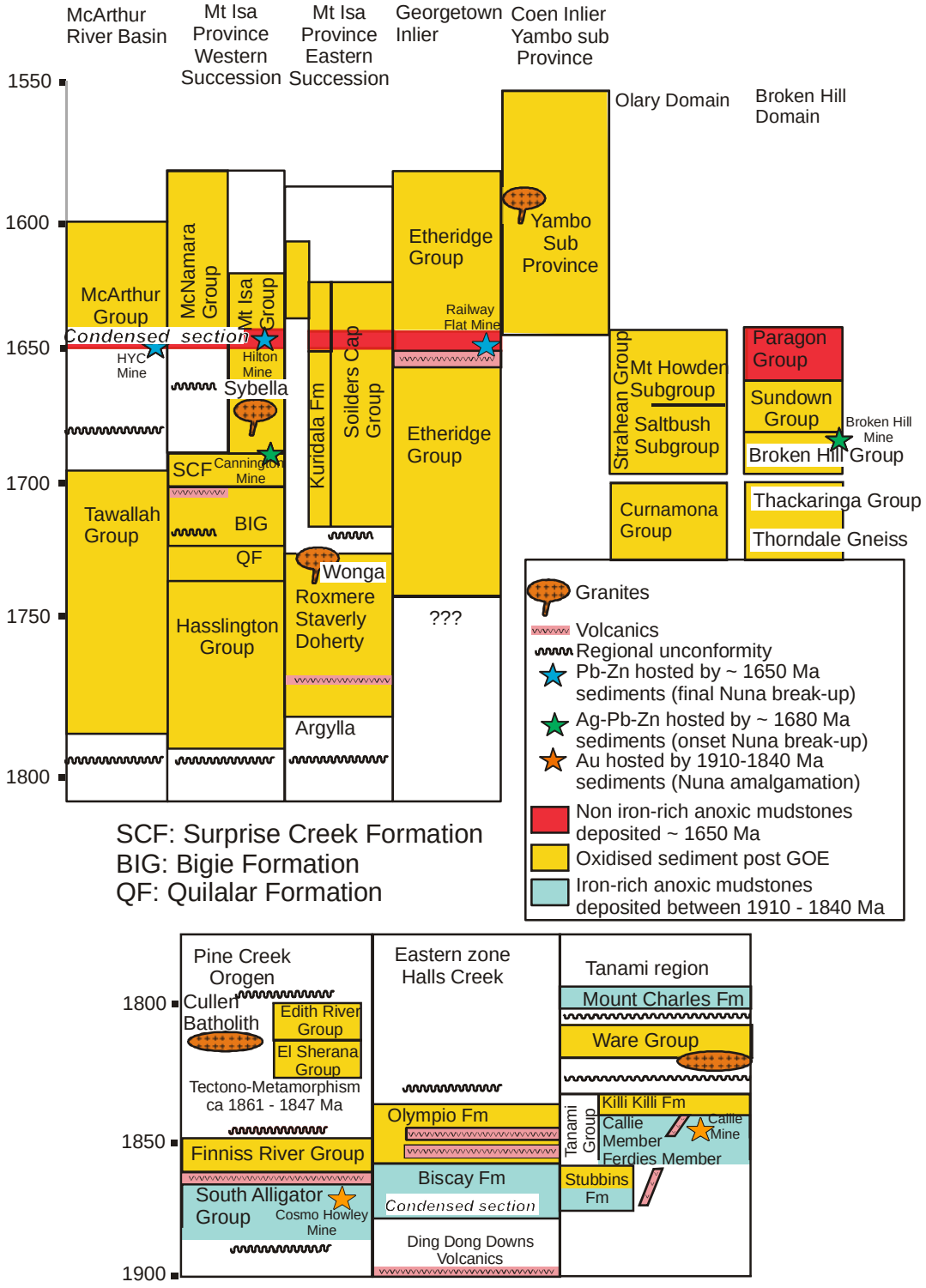

Figure 1.2 - Schematic and simplified time-space diagram for Proterozoic Australia modified from Blewett et al. (1998), R. Page in Blake et al., (1999), Page et al. (2005), Betts and Giles (2006), Cross and Crispe (2007), Worden et al. (2008).

The time period from 2100 to 1800 Ma is recognised as the third largest period of orogenic gold mineralization globally (Goldfarb et al., 2001). The ca. 1910 Ma - 1800 Ma mudstones in northern Australia host significant gold deposits which formed during the amalgamation of the Nuna supercontinent (Fig. 1.2). The Paleoproterozoic Tanami region and Pine Creek Orogen of northern Australia host one world-class gold mine and many other gold deposits in anomalously iron–rich marine mudstones. Oceans before ~1850 Ma are thought to have been largely iron-rich (Holland 1984). However, as a delayed consequence of the first Great Oxidation Event (GOE) the rise in the oxygen content in the oceans increased sulfate content and caused the oxidation of soluble ferrous iron (Fe^{2+}) to ferric iron (Fe3+). As ferric iron is highly insoluble, the period between 1900 and 1850 Ma is marked by a major period of deposition of iron-rich sedimentary rocks, including banded iron formation (Huston and Logan, 2004; Bekker et al., 2010).

Between 1800 – 1580 Ma after the GOE, the mineralisation style changed significantly, probably in response to changes both in geodynamics and the oxidation of the atmosphere and hydrosphere. In northern Australia (and in parts of Canada) there was a major period of lode gold mineralisation between 1820 and 1790 Ma, possibly in response to the assembly of Nuna. However, the major period of lead-zinc mineralisation between 1685 and 1575 Ma may have been the consequence of Nuna break-up (Leach et al., 2010). Leach et al. (2010) has subdivided lead-zinc deposits into two types, clastic dominated (CD lead-zinc deposits, former SEDEX deposits e.g. Mt Isa and Hilton deposits) and Mississippi Valley-type (MVT). As MVT deposits reached their maximum abundance during the final assembly of Pangea, they are not discussed here (see Leach et al. (2010) for more details). The final mineralisation stage in the Australian Proterozoic is the transition to iron-oxide copper-gold deposits at 1590 ─ 1500 Ma.

The oxygenation state of sediments through time varies considerably as do the types of deposits and minerals. Some of the most significant orogenic gold deposits in the Australian Paleoproterozoic are found in anoxic iron-rich sediments deposited before the GOE. In contrast, younger, more oxidised successions are important hosts for lead-zinc deposits (Cooke et al., 2000; Huston et al., 2006) These oxidised fluids interacted with reduced mudstones deposited between 1655 and 1575 Ma to form the world-class Mt Isa and HYC lead-zinc deposits. The initial driver of these fluids has been attributed to prominent inflections and bends in the Australian Proterozoic apparent polar wander path which drove episodes of fluid circulation (Loutit et al., 1994; Idnurm 2000).

Ireland and Mayer (1984) initially proposed that gold mineralisation in the Tanami region was syngenetic, however an epigenetic origin is now generally accepted (Huston et al., 2007). However, debate about the role of magmas in the ore genesis continues. Mayer (1990); Nicholson (1990) and Smith et al., (1998) infer a metamorphic origin perhaps driven by a granitic intrusion. An alternative to this hypothesis is proposed by Wall and Taylor (1990), Tunks and Marsh (1998) and Wall (2005) who suggest a mixed magmatic-metamorphic origin with gold fluids derived from nearby granites.

Xenotime SHRIMP U-Pb data of Cross et al. (2005) and $^{40}Ar/^{39}Ar$ of Fraser (2002) suggest gold mineralisation is not a single event in the Tanami region and Pine Creek Orogen and instead gold mineralisation occurred between ca. 1810 Ma and ca. 1780 Ma. The timing of mineralisation is potentially broadly consistent with the collision

between the Kimberley Craton and North Australia Craton at ~ 1850 Ma (Sheppard et al., 1999).

Lead-zinc deposits, a diverse group of ores, are hosted by a wide variety of siliclastic and carbonate rocks. The minerals consist mainly of sphalerite, galena, and generally lesser amounts of iron sulfides (Leach et al., 2010). Sedimentary brines are attributed as the main ore-fluids in CD deposits with mineralisation occurring contemporaneously by exhalative processes or replacement processes below the sea floor (Leach et al., 2010). Parts of the Mount Isa basin were extensively altered by K-feldspar-hematite alteration at ~1640 Ma. Cooke et al. (1998) suggested this alteration and loss of both Zn and Pb was an important metal source for the overlying Mt Isa style mineralisation. The main attributes of lead-zinc deposits in the Mount Isa Inlier and globally are attributed by Leach et al. (2005) to be determined by the tectonic setting in which ore deposition occurred.

The aim of this project is to improve understanding of regional geology and provide novel approaches to establishing temporal correlations of stratigraphy across regional Australia. The project uses field observations and facies interpretation to suggest a potential 'first-pass' regional stratigraphy with potential links to the global occurrence of similar sedimentary facies forming distinct time periods within the earths evolution. Given the problems of scale and detail of mine stratigraphy and the difficulty of relating this to a regional stratigraphy with usually less stratigraphic detail and greater scale, a large portion of this research is undertaken to provide a detailed quantifiable mine-stratigraphy that could be reproduced by interested parties.

1.1 Thesis Outline and summary of results

This study was approached by successive chapters: The first three chapters are based around sediments that were associated with the Nuna amalgamation. **Chapter 2** provides background geology and field observations for chapter 3, using sedimentological interpretation of outcrop, drillcore integrated with seismic interpretation and regional chemostratigraphy to establish a depositional model for gold-bearing Paleoproterozoic rocks of the Tanami region. **Chapter 3** establishes a regional geochemical stratigraphy in the Tanami region that that has implications to gold exploration in northern Australia. **Chapter 4** then expands the facies and geochemical knowledge gathered in the Tanami province assessing relationships between the composition of the sediments to the global ocean chemistry and the timing of Proterozoic orogenic gold deposits. **Chapter 5** describes a Sm-Nd isotopic change through much of Australia at 1650 Ma which is interpreted to relate to the final break-up of Nuna. The isotopic characteristics of these 1650 Ma rocks in northern Australia are used to investigate the tectonic break-up of Australia with a discussion of potential global tectonic reconstruction models at 1650 Ma.

This thesis has been written in the form of individual manuscripts addressing the main mineralising events in the Paleoproterozoic to early Mesoproterozoic evolution of the North Australian Craton. The manuscripts have been left in their original state to allow the reader to follow the progression through the Paleo- and early Mesoproterozoic. This leads to some repetition but highlights the contribution of this research project to the current understanding of the North Australian Craton as well as helping to highlight some of the new significant changes in understanding the timing and deposition of orogenic gold and clastic dominated lead-zinc deposits.

1.2 Geological background

1.2.1 Tanami region and Pine Creek Orogen

The Paleoproterozoic Tanami region is a poorly exposed province within northern Australia that hosts a number of significant gold deposits (Figure 1.1; Chapters 2-4). The Callie deposit is the largest and is hosted by black mudstones of the Dead Bullock Formation: Global gold resources (production plus resources) from the Dead Bullock Formation are ~275 t (Huston et al 2007). The stratigraphically overlying Killi Killi Formation consists of poorly sorted turbidite and black mudstone facies. The Killi Killi Formation hosts about 30 t Au (Huston et al 2007). The Paleoproterozoic Pine Creek Orogen hosts the Cosmo Howley deposit and associated deposits within black mudstones of the Koolpin Formation which have produced ~99 t gold (Ahmad et al., 2009). The Koolpin Formation, like the Dead Bullock Formation of the Tanami region, is overlain by poorly-sorted turbidities, the Finiss River Group.

Effective exploration in the Tanami region and Pine Creek Orogen is severely hampered due to poor knowledge of the regional stratigraphy and potential correlation between regions (e.g. Pine Creek Orogen, and Tanami region, Fig. 1.1). As large areas are covered by regolith, regional correlations within and between geological regions are difficult (Blake et al., 1979; Hendrickx et al., 2000; Crispe et al., 2007; Huston et al., 2007).

1.2.2 Eastern Proterozoic Australia at ~1650 Ma

The 1710 Ma ─ 1575 Ma lead-zinc events in the Mount Isa Province and Georgetown Inliers provide continued mining and exploration interest in northern Australia (Fig. 1.1). Within the Mount Isa and Georgetown provinces however, regional field correlations are difficult as the successions have been extensively deformed, tectonically displaced, and metamorphosed. This is particularly the problem in comparison of the Eastern and Western Successions of the Mt Isa Province and correlations with other Proterozoic sedimentary basins, e.g. Curnamona Province and Georgetown Inlier. While detailed studies within the terrains are clearly possible (eg. Western Succession, Mt Isa: Southgate et al., 2000; Jackson et al., 2005), comparisons with the Eastern Succession and other regional terrains are still debatable (Foster and Austin 2008; Neumann et al., 2009). The collection of Sm-Nd and U-Pb isotopic characteristics of basin fill combined with U-Pb isotopes of dolerities/gabbros units intruding the basin presents a record of tectonic processes and paleogeography of potential source regions (e.g. Barovich and Hand, 2008; Betts et al., 2008; Lambeck Chapter 5).

1.3 Results

Chapter 2 provides background geology and uses detailed facies analysis, isopach maps, seismic data and U-Pb SHRIMP geochronology to establish a depositional model of the Tanami Group sediments in the Tanami region. The chapter suggests gold exploration success could be increased in the Killi Killi Formation sediments if fine-grained sediments proximal to deep crustal penetrating thrust faults are targeted for further drilling. The gold-bearing Dead Bullock Formation, while having limited areal extent, can potentially be extrapolated west from the Callie Mine. This chapter is in press in the Australian Journal of Earth Science as ‘Proterozoic turbiditic depositional system (Tanami Group) in the Tanami region, northern Australia, and implications for gold

mineralisation' by Lambeck, A., Barovich K., George A.D., Cross A., Meixner T., and Huston D.

Chapter 3 typecasts the gold-bearing stratigraphy in the Tanami region geochemically and provides a suggested tectonic evolution. The chapter follows on from a previously published detailed study on the Callie mine stratigraphy (Lambeck et al., 2008) and builds a regional geochemical stratigraphy with respect to potential gold mineralisation. The chapter was published as 'Typecasting prospective Au-bearing sedimentary lithologies using sedimentary geochemistry and Nd isotopes in poorly exposed Proterozoic basins of the Tanami region, Northern Australia' by Lambeck, A., Huston, D., and Barovich K. 2010. Mineralium Deposita, 45(5): 497-515.

Chapter 4 suggests a global context for the Proterozoic rocks of northern Australia. In the Paleoproterozoic, sedimentary rocks deposited between 2400 Ma and 1800 Ma are known to preferentially host orogenic gold deposits, as opposed to the Archean, where the hosts are predominantly mafic igneous rocks (Goldfarb et al., 2001). The Paleoproterozoic Tanami region and Pine Creek Orogen of northern Australia host one world-class gold mine and many other gold deposits in anomalously iron–rich marine mudstones. World-class gold deposits associated with iron-rich sedimentary rocks are also known at the Homestake deposit, USA, and in Ghana, West Africa (Roddaz et al., 2007; Morelli et al., 2010). This chapter was published 'Are iron-rich sedimentary rocks the key to the spike in orogenic gold mineralization in the Paleoproterozoic?' by Lambeck, A., Mernagh, T.P., and Wyborn L. Economic Geology, 106(3): 321-330.

Chapter 5 investigates late Paleoproterozoic sedimentary basins across the Mt Isa and Georgetown Provinces in northern Queensland. The basins record a significant change in their neodymium isotopic composition to more positive epsilon Nd values at ca. 1650 Ma. This isotopic change is interpreted to reflect the break-up of the Nuna supercontinent, and also has been defined in the Curnamona Province in South Australia and NSW (Barovich and Hand, 2008). Volcanism and extension between 1690 – 1640 Ma in Proterozoic Australia with a previously undefined juvenile volcanic suite is the most probable source to explain the presence of tuffs/peperites and thin rhyolite in the sedimentary basins. Juvenile sedimentary detritus is perhaps evidence of a once larger magamatic source active between 1690 to at least 1640 Ma that has been removed either by erosion or tectonically during the break-up of Nuna. Chapter 5 concludes that the extension and rifting could have been part of back-arc extension associated with a convergent margin along eastern Proterozoic Australia, or it could be associated with divergence between Proterozoic Australia and the cratonic block to the east during Nuna time (possibly Laurentia or Baltica). This chapter is in review in Precambrian Research as 'An abrupt change in Nd isotopic composition in Australian basins at 1650 Ma: implications for the tectonic evolution of Australia and its place in Nuna' by Lambeck A., Barovich K., Gibson G, and Huston D.

In addition to the manuscripts listed, project results have been presented as conference abstracts which are listed in the introductory section of this thesis.

1.4 Supplementary Appendices

Geochronology; collected and processed during PhD candidature, has formed the basis of a Geoscience Australia Record, (Lambeck and Cross in review) in the thesis appendix. The GA record, at the back of this thesis, details U-Pb data from:

- A sample of Lane Creek Formation. Detrital zircons from this sample yielded a maximum depositional age of **1789 ± 8** Ma.
- A sample of felsic unit intruding Candlow Formation in Georgetown area. This sample yielded an age of **1675 ± 8** Ma, and is interpreted as a maximum depositional age, an interpretation consistent with the morphology of the zircons.
- Two samples of sandstone hosting the Croyden Zn-Cu-Pb-Sn prospect. Both samples yielded **Phanerozoic** detrital zircons **(~500** Ma) in a rock unit previously inferred to have a Proterezoic age.
- A sample of black mudstone from the Kuridala Formation. This sample, which has an 'evolved' $\varepsilon_{Nd}1650$ value, yielded an age of **1686 ± 7** Ma

An additional paper is in draft which further utilizes whole-rock and Sm-Nd data collected during PhD study but not referenced in this thesis. All geochemical data are found in the CD attached and briefly outlined below.

Whole-rock and trace element geochemistry; Files of whole-rock and trace element geochemistry used in this PhD study from the Mount Isa Inlier and Tanami region. The Tanami data has been referenced in Chapters 2, 3 & 4; Lambeck et al. (2008); Lambeck et al. (2010) and (Lambeck et al., 2011). All Mount Isa whole-rock data collected during PhD study is included in the attached CD.

Sm-Nd data from Eastern Succession, Mount Isa and Etheridge Province, Georgetown Inlier; Files of detailed Sm-Nd data from black mudstone sequences collected through out the Eastern succession and Etheridge Province. Sm-Nd data and whole-rock geochemistry data will be referenced in an Australian Journal of Earth Sciences paper (in prep; data on CD at back of thesis).

Whole rock Sm-Nd and Pb-Pb data collected from ironstones and host rocks in the Tennant Creek goldfield; Data were collected from five mineralised and five unmineralised samples. The purpose of the study was to determine if gold is associated with juvenile magmatic fluids (data on CD at back of thesis). A brief abstract outlining the project is included on attached CD.

1.5 References

Ahmad, M., Wygralak, A.S. and Ferenczi, P.A., 2009. Gold deposits of the Northern Territory (Second Edition). Northern Territory Geological Survey, (Second Edition update by Wygralak AS and Scrimgeour IR), Report 11.

Barley, M.E. and Groves, D.I., 1992. Supercontinent cycles and the distribution of metal deposits through time. Geology, 20(4): 291-294.

Barovich, K. and Hand, M., 2008. Tectonic setting and provenance of the Paleoproterozoic Willyama Supergroup, Curnamona Province, Australia: Geochemical and Nd isotopic constraints on contrasting source terrain components. Precambrian Research, 166(1-4): 318-337.

Bekker,A, Slack ,J.F. Planavsky,N., Krapez,B., Hofmann,A., Konhauser,K.O., Rouxel, O.J. 2010. Iron Formation: The Sedimentary Product of a Complex Interplay among Mantle, Tectonic, Oceanic, and Biospheric Processes

Betts, P. and Giles, D., 2006. The 1800-1100 Ma tectonic evolution of Australia. Precambrian Research, 144: 92-125.

Betts, P.G., Giles, D. and Schaefer, B.F., 2008. Comparing 1800-1600 Ma accretionary and basin processes in Australia and Laurentia: Possible geographic connections in Columbia. Precambrian Research, 166(1-4): 81-92.

Blake, D., Hodgson, I. and Muhling, P., 1979. Geology of The Granites-Tanami Region. Bureau of Mineral Resources, Australia, Canberra, Bulletin 197.

Blake, D., Tyler, I., Griffin, T., Sheppard, S., Thorne, A. and Warren, R., 1999. Geology of the Halls Creek 1:100 000 Sheet area (4461), Western Australia. Australian Geological Survey Organisation Record, Department of Industry, Science & Resources.

Blewett, R.S., Black, L.P., Sun, S.s., Knutson, J., Hutton, L.J. and Bain, J.H.C., 1998. U-Pb zircon and Sm-Nd geochronology of the Mesoproterozoic of North Queensland: implications for a Rodinian connection with the Belt supergroup of North America. Precambrian Research, 89(3-4): 101-127.

Cawood, P.A. and Korsch, R.J., 2008. Assembling Australia: Proterozoic building of a continent. Precambrian Research, 166(1-4): 1-35.

Cooke, D., Bull, S., Large, R. and McGoldrick, P., 2000. The importance of oxidized brines for the formation of Australian Proterozoic stratiform sediment-hosted Pb-Zn (sedex) deposits. Economic Geology, 95: 1-17.

Cooke, D.R., Bull, S.W., Donovan, S. and Rogers, J.R., 1998. K metasomatism and base metal depletion in volcanic rocks from the McArthur basin, Northern Territory-implications for base metal mineralisation. Economic Geology, 93: 1237-1263.

Crispe, A.J., Vandenberg, L.C. and Scrimgeour, I.R., 2007. Geological framework of the Archaean and Palaeoproterozoic Tanami Region, Northern Territory. Mineralium Deposita, 42: 3-26.

Cross, A. and Crispe, A.J., 2007. SHRIMP U-Pb analyses of detrital zircon: A window to understanding the Palaeoproterozoic development of the Tanami Region, northern Australia. Mineralium Deposita, 42: 27-50.

Cross, A.J., Fletcher, I.F., Crispe, A.J., Huston, D.L. and Williams, N., 2005. New constraints on the timing of deposition and mineralisation in the Tanami Group. Annual Geoscience Exploration Seminar (AGES) 2005: record of abstracts. Northern Territory Geological Survey Record 2005/0001.

Direen, N.G. and Crawford, A.J. 2003. The Tasman Line: Where is it; what is it, and is it Australia's Rodinian break-up boundary? Australian Journal of Earth Science, 50:4 , 491-502.

Etheridge, M., A., Rutland, R., W,R. and Wyborn, L., A,I., 1987. Orogenesis and tectonic processes in the Early to Middle Proterozoic of northern Australia. Proterozoic Lithospheric Evolution 17. American Geophysical Union Geodynamics Series 17, 131-147 pp.

Foster, D.R.W. and Austin, J.R., 2008. The 1800-1610 Ma stratigraphic and magmatic history of the Eastern Succession, Mount Isa Inlier, and correlations with adjacent Paleoproterozoic terranes. Precambrian Research, 163(1-2): 7-30.

Fraser, G.L., 2002. Geochronology of Tanami ores and host rocks. Annual Geoscience Exploration Seminar (AGES) 2002: record of abstracts. Northern Territory Geological Survey Record 2002/0003.

Fraser, G.L., Huston, D., Gibson, G.M., Neumann, N., Maidment, D., Kositcin, N., Skirrow, R.G., Jaireth, S., Lyons, P., Carson, C., Cutten, H. and Lambeck, A., 2007. Geodynamic and metallogenic evolution of Proterozoic Australia from 1870 - 1550 Ma: a discussion. Geoscience Australia Record 2007/16: 76.

Goldfarb, R.J., Bradley, D. and Leach, D.L., 2010. Secular Variation in Economic Geology. Economic Geology, 105(3): 459-465.

Goldfarb, R.J., Groves, D.I. and Gardoll, S., 2001. Orogenic gold and geologic time: a global synthesis. Ore Geology Reviews, 18(1-2): 1-75.

Goldfarb, R.J., Groves, D.I., Kerrich, R. and Leach, D.L., 2009. Metallogenic evolution on an evolving Earth. Proceedings of the Tenth Bienniel SGA Meeting, Townsville, Australia: 11–13.

Hendrickx, M.A., Slater, K., Crispe, A.J., Dean, A.A., Vanderberg, L.C. and Smith, J., 2000. Paleoproterozoic stratigraphy of the Tanami Region: regional correlations and relation to mineralization-preliminary results. Northern Territory Geological Survey Record 2000-13, 2000-13, 66 pp.

Hoffman, P.F., 1991. Did the Breakout of Laurentia Turn Gondwanaland Inside-Out? Science, 252(5011): 1409-1412.

Holland, H.D., 1984. The Chemical Evolution of the Atmosphere and Ocean. . Princeton Series in Geochemistry,, Princeton University Press, New Jersey.

Huston, D., 2006. Mineral systems and tectonic evolution of the North Australian Craton. In: P. Lyons and D.L. Huston (Editors), Evolution and metallogenesis of the North Australian Craton. Geoscience Australia, Alice Springs.

Huston, D., Wygralak, A., Mernagh, T., Vandenberg, I.C., Crispe, A.J., Lambeck, A., Bagas, L., Cross, A., Fraser, G., Williams, N., Worden, K. and Meixner, T., 2007. Lode gold mineral systems of the Tanami Region, northern Australia. Mineralium Deposita, 42: 175-204.

Huston, D.L., Pehrsson, S., Eglington, B.M. and Zaw, K., 2010. The Geology and Metallogeny of Volcanic-Hosted Massive Sulfide Deposits: Variations through Geologic Time and with Tectonic Setting. Economic Geology, 105(3): 571-591.

Idnurm, M., 2000. Towards a high resolution Late Paleoproterozoic-earliest Mesoproterozoic apparent polar wander path for northern Australia. Australian Journal of Earth Sciences, 47: 405-429.

Ireland, T.J. and Mayer, T.E., 1984. The geology and mineralisation of the The Granites gold deposits, Northern Territory. Proceedings of the Australasian Institute of Mining and Metallurgy Conference, Darwin, Northern Territory, pp 397-405.

Jackson, M.J., Southgate, P., Black, L. and Domagala, J., 2005. Overcoming Proterozoic quartzite sandbody miscorrelations: integrated sequence stratigraphy and SHRIMP U-Pb dating of the Surprise Creek Formation, Torpedo Creek and Warrina Park Quartzites, Mt Isa Inlier. Australian Journal of Earth Sciences, 52: 1-25.

Kerrich, R., Goldfarb, R.J. and Richards, J., 2005. Metallogenic provinces in an evolving geodynamic framework. Economic Geology 100th anniversary volume 1097–1136.

Lambeck, A., Huston, D., Maidment, D. and Southgate, P., 2008. Sedimentary geochemistry, geochronology and sequence stratigraphy as tools to typecast stratigraphic units and constrain basin evolution in the gold mineralised Palaeoproterozoic Tanami Region, Northern Australia. Precambrian Research, 166(1-4): 185-203.

Lambeck, A., Mernagh, T. and Wyborn, L., A, I., 2011. Are iron-rich sedimentary rocks the key to the spike in orogenic gold mineralization in the Paleoproterozoic? Economic Geology, 106(3).

Leach, D.L., Bradley, D.C., Huston, D., Pisarevsky, S.A., Taylor, R.D. and Gardoll, S.J., 2010. Sediment-Hosted Lead-Zinc Deposits in Earth History. Economic Geology, 105(3): 593-625.

Leach, D.L., Sangster, D.F., Kelley, K.D., Large, R.R., Garven, G., Allen, C.R., Gutzmer, J. and Walters, S., 2005. Sediment-Hosted Lead-Zinc Deposits: A Global Perspective. Economic Geology, 100th Anniversary Volume: 561-607.

Loutit, T., Wyborn, L.A.I., Hinman, M.C. and Idnurm, M., 1994. Palaeomagnetic, tectonic, magmatic and mineralisation events in the Proterozoic of Northern Australia. Australasian Institute of Mining and Metallurgy, Publication Series, 5/94: 123-128.

Mayer, T.E., 1990. The Granites gold field. Aus IMM Monogr, 14: 715-719.

Morelli, R., Bell, C., Creaser, R. and Simonetti, A., 2010. Constraints on the genesis of gold mineralization at the Homestake Gold Deposit, Black Hills, South Dakota from rhenium–osmium sulfide geochronology. Mineralium Deposita, 45(5): 461-480.

Myers, J., Shaw, R. and Tyler, I., 1996. Tectonic evolution of Proterozoic Australia. Tectonics, 1: 1431–1446.

Neumann, N.L., Southgate, P.N. and Gibson, G.M., 2009. Defining unconformities in Proterozoic sedimentary basins using detrital geochronology and basin analysis--An example from the Mount Isa Inlier, Australia. Precambrian Research, 168(3-4): 149-166.

Nicholson, P.M., 1990. Tanami gold deposit. Aus IMM Monogr, 14: 719-724.

Page, R.W., Conor, C.H.H., Stevens, B.P.J., Gibson, G.M., Preiss, W.V. and Southgate, P.N., 2005. Correlation of Olary and Broken Hill Domains, Curnamona Province: Possible Relationship to Mount Isa and Other North Australian Pb-Zn-Ag-Bearing Successions. Economic Geology, 100(4): 663-676.

Payne, J.L., Hand, M., Barovich, K.M., Reid, A. and Evans, D.A.D., 2009. Correlations and reconstruction models for the 2500-1500 Ma evolution of the Mawson Continent. Geological Society, London, Special Publications, 323(1): 319-355.

Roddaz, M., Debat, P. and Nikiéma, S., 2007. Geochemistry of Upper Birimian sediments (major and trace elements and Nd-Sr isotopes) and implications for weathering and tectonic setting of the Late Paleoproterozoic crust. Precambrian Research, 159(3-4): 197-211.

Rogers, J.J.W. and Santosh, M., 2002. Configuration of Columbia, a Mesoproterozoic supercontinent. Gondwana Research, 5: 5-22.

Sheppard, S., Tyler, I. and Page, R.W., 1999. Palaeoproterozoic subduction-related and passive margin basalt in the Halls Creek Orogen, northwest Australia. Australian Journal of Earth Sciences, 46: 679-690.

Smith, M.E., Lovett, D.R., Pring, P.I. and Sando, B.G., 1998. Dead Bullock Soak gold deposits. Aust IMM Monogr 22:449–460, 22: 449-460.

Southgate, P., Bradshaw, B., Dimagala, J., Jackson, M.J., Idnurm, M., Krassay, A.A., Page, R.W., Sami, T., Scott, D., Lindsay, J., McConachie, B. and Tarlowski, C., 2000. Chronostratigraphic basin framework for Palaeoproterozoic rocks (1730-1575 Ma) in northern Australia and implications for base-metal mineralisation. Australian Journal of earth Sciences, 47(3): 461-483.

Titley, S.R., 1993. Relationship of stratabound ores with tectonic cycles of the phanerozoic and proterozoic. Precambrian Research, 61(3-4): 295-322.

Tunks, A.J. and Marsh, S., 1998. Gold deposits of the Tanami Corridor. Aust. IMM Monogr., 22: 443-448.

Wall, V.J., 2005. TAG: Thermal aureole (pluton-related) gold systems. AIG News, 79: 1-7.

Wall, V.J. and Taylor, J.R., 1990. Granite emplacement and temporally related gold mineralisation. Geological Society of Australia Abstracts, 25: 264-265.

Worden, K., Carson, C., Scrimgeour, I., Lally, J. and Doyle, N., 2008. A revised Palaeoproterozoic chronostratigraphy for the Pine Creek Orogen, northern Australia: Evidence from SHRIMP U-Pb zircon geochronology. Precambrian Research, 166(1-4): 122-144.

Alexis Lambeck

PhD THESIS TITLE

"Basin analysis and the geochemical signature of Paleoproterozoic sedimentary successions in northern Australia: Constraints on basin development in respect to mineralisation and paleoreconstruction models"

CHAPTER 2

Proterozoic turbiditic depositional system (Tanami Group) in the Tanami region, northern Australia, and implications for gold mineralisation

Lambeck, A.[1,2]
Barovich, K.[1]
George, A.[3]
Cross, A.[2]
Huston, D.[2]
Meixner, T.[2]

[1] Centre for Tectonics Resources and Exploration, University of Adelaide, Adelaide, SA 5005.
[2] Geoscience Australia, GPO Box 378, Canberra, ACT 2601, Australia
[3]School of Earth & Environment, University of Western Australia, Perth, WA 6009, Australia

Australian Journal of Earth Sciences (in press)

NOTE:
Statements of authorship appear on pages 16-17 in the print copy of the thesis held in the University of Adelaide Library.

Chapter 2

Proterozoic turbiditic depositional system (Tanami Group) in the Tanami region, northern Australia, and implications for gold mineralisation

In press: Lambeck, A., Barovich, K., George, A.D., Cross, A. Huston, D., and Meixner T. Proterozoic turbiditic depositional system (Tanami Group) in the Tanami region, northern Australia, and implications for gold mineralisation. Australian Journal of Earth Science (2012).

Abstract

Sedimentological interpretation of outcrop and drillcore, integrated with previously published seismic interpretation and regional chemostratigraphy, is used to establish a depositional model for gold-bearing Paleoproterozoic rocks of the Tanami region. Analyses of the Dead Bullock Formation and Killi Killi Formation of the Tanami Group form a basis for future correlations across northern Australia. Poorly-exposed Paleoproterozoic sandstone, siltstone and claystone of the Killi Killi Formation record development of a deep-water, basin-floor turbidite system composed of channelised sandy lobes with muddy lobe fringes. The sediment source was located to the northwest. Underlying the Killi Killi Formation are the poorly exposed dark claystones of the upper Dead Bullock Formation, forming a condensed section.

We interpret that this depositional system was an important control on gold mineralisation in both the Killi Killi Formation and the underlying Dead Bullock Formation of the Tanami Group. Gold deposition is enhanced within the Dead Bullock Formation where crustal faults intersect claystone facies. Similar facies in the Killi Killi Formation may also host gold mineralisation. Deep exploration holes at the Titania and Old Pirate prospects could potentially intersect the stratigraphically underlying gold-bearing claystones of the Dead Bullock Formation.

2.1 Introduction

The Tanami region, of the North Australian Craton (Myers *et al.* 1996) hosts a number of significant gold deposits that makes it the richest gold-bearing Proterozoic region in northern Australia (Crispe *et al.* 2007; Huston *et al.* 2007; Figures 2.1, 2.2). Production over the last 20 years has exceeded 4.8 Moz, with unmined resources of over 7.7 Moz (Huston *et al.* 2007). There is a very strong lithological control on the location of these deposits. Sedimentary rocks host nearly 80% of the gold resource with 61% in carbonaceous units and 16% in iron formations, mostly in the Callie Member of the Dead Bullock Formation (Huston *et al.* 2007; Figure 2.3). The Paleoproterozoic rock record is poorly exposed. Regolith covers much of the region, making detailed lithostratigraphic correlation difficult (see Figure 2.4) and mapping the distribution of favourable host rocks for gold problematic. In this contribution, we combine the chemostratigraphic correlation proposed earlier (Lambeck *et al.* 2008, 2010) with detailed core logs to establish depositional facies associations. We then combine these associations with seismic data (Goleby *et al.* 2009) to construct a stratigraphic model for the evolution of the Tanami region. Understanding controls on the areal extent of

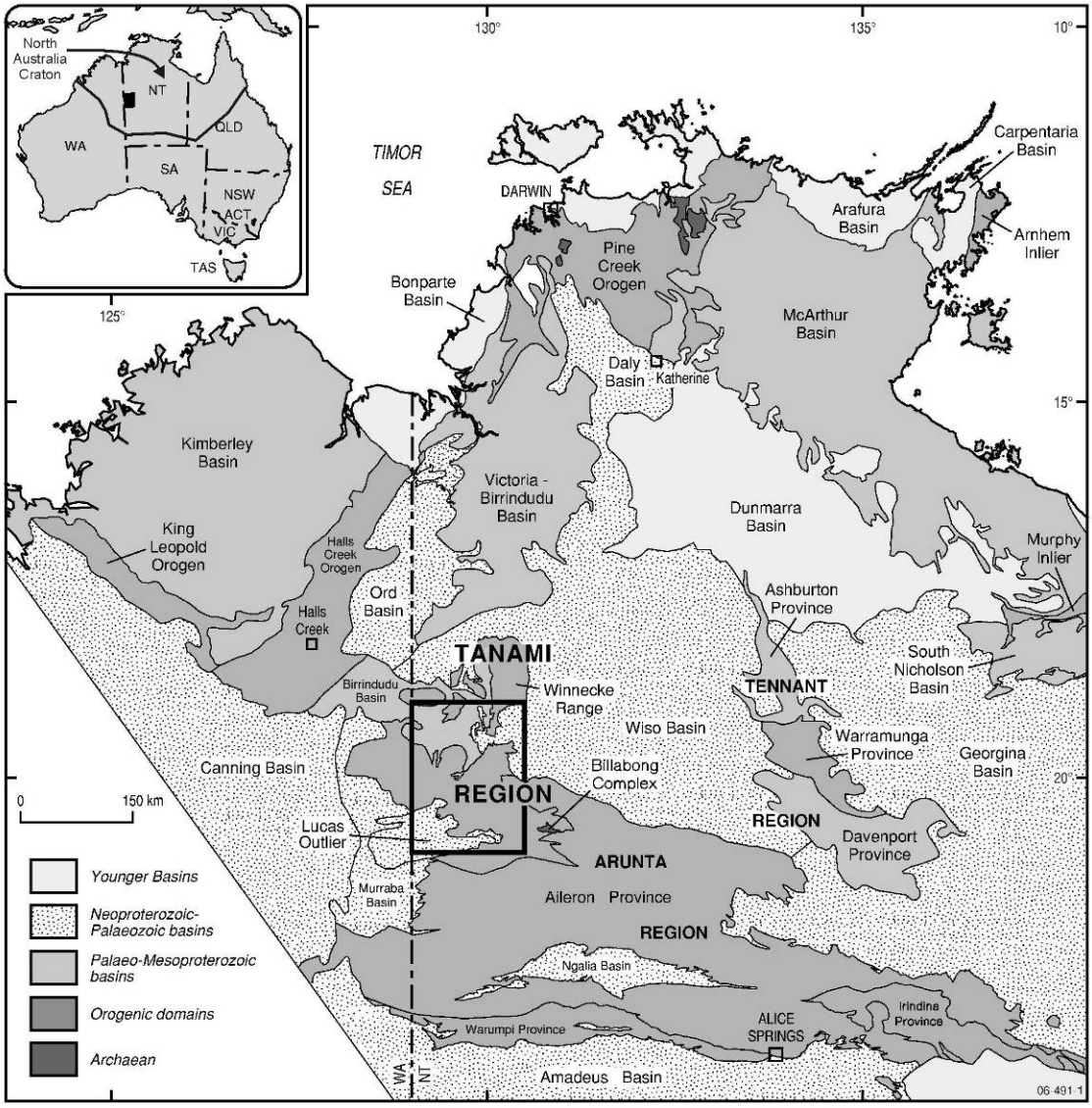

Fig. 2.1. Location of Tanami region in northern Australia showing distribution of major basins and orogenic domains (from Cross and Crispe, 2007).

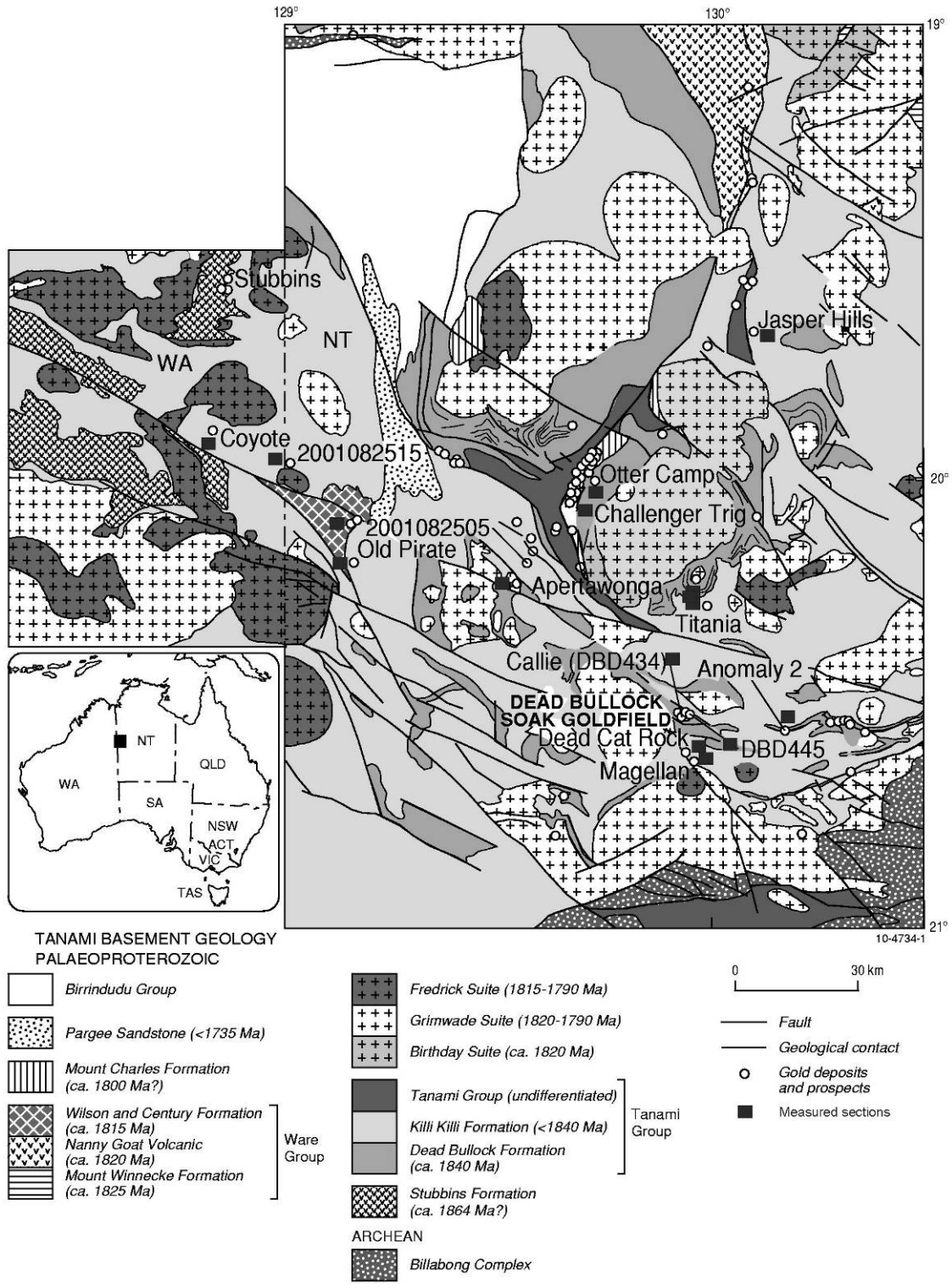

Fig. 2.2. Geological map showing distribution of Proterozoic lithostratigraphic and igneous units in the Tanami region (from Huston et al., 2007). Note location of the Northern Territory – Western Australian border.

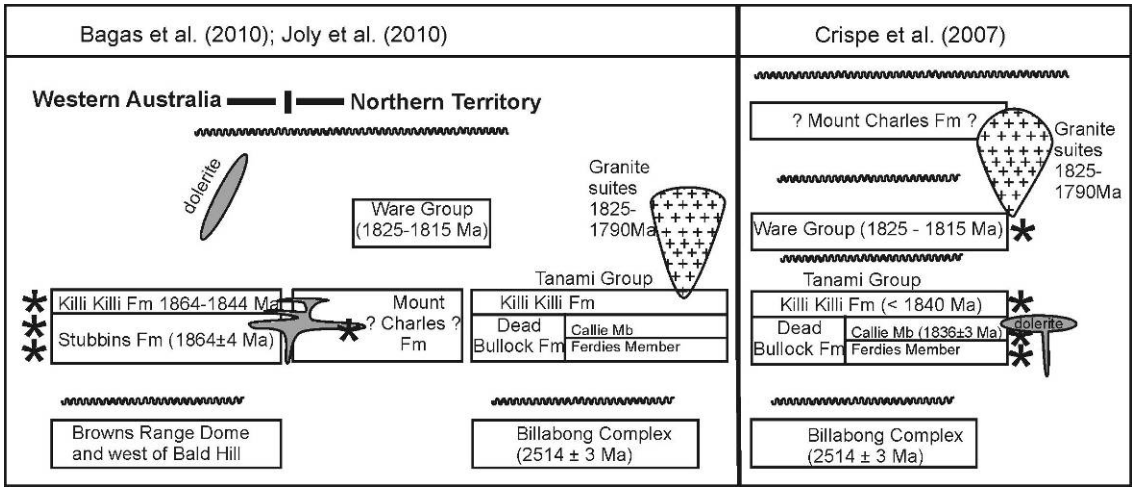

Fig. 2.3. Regional stratigraphy of the Tanami region after Crispe et al (2007) with an alternative Tanami stratigraphy proposed by Bagas et al. (2010) and Joly et al. (2010). Gold deposits within regional stratigraphy are shown by *.

Fig. 2.4 Outcrop view (Dead Cat Rock, Figure 2.2) of the Proterozoic Tanami region consisting mainly of regolith cover and poorly exposed stratigraphic succession dominated by more resistant horizons. Tape is 5 m long. View to the north.

siltstone that could develop redox fronts with oxidised mineralised gold fluid in the Tanami region may aid the potential to find gold deposits and refine gold exploration methods for the Dead Bullock and Killi Killi Formations.

Gold mineralisation in the Tanami region forms part of a worldwide episode of orogenic gold deposition between 2100 Ma and 1800 Ma (Goldfarb et al. 2001; 2010). Iron-rich and carbonaceous sedimentary rocks have been linked as potential chemical traps for gold enrichment during the Proterozoic (Lambeck et al. 2011). Similar stratigraphy to the Dead Bullock Formation, which consists of iron-rich sediments (Lambeck et al. 2011) overlain by non iron-rich stratigraphy, has also been identified in the Pine Creek Orogen (Figure 2.1).

In the Pine Creek Orogen (Figure 2.1), the basal Koolpin Formation of the South Alligator Group consists of iron-rich siltstones and mudstones (Needham et al. 1988). Similar to the Tanami region, the iron-rich rocks of the South Alligator Group are overlain by those of the Finniss River Group, which comprises iron-poor turbidites consisting of poorly sorted sandstones. The depositional age of rocks of the Koolpin Formation is inferred to be between ca 2020 Ma and ca 1860 Ma based on detrital zircons and an overlying tuffaceous unit (Worden et al. 2008).

While the Pine Creek stratigraphy is potentially older than the Tanami Group, the mineralisation process of oxidised gold fluid forming a redox boundary with the anoxic claystones, is the same. Similar regional stratigraphy is found globally in Proterozoic basins of West Africa, Birimian craton, and South America in Brazil, Suriname and French Guinea. In both West Africa and South America, gold-bearing stratigraphy consists of gold trapped within claystones/mudstones rocks (Milési et al. 1992; Gosselin & Dubé 2005; Roddaz et al. 2007; Béziat et al. 2008; Lambeck et al. 2011).

2.1.1 Geological background and regional stratigraphy

The Tanami region is centred 600 km northwest of Alice Springs in northern Australia (Figure 2.1) and forms part of the Paleoproterozoic basement of the North Australian Craton. Although all units in the Dead Bullock and Killi Killi Formations have undergone greenschist facies metamorphism the prefix ‘meta-’ is omitted from the following descriptions.

The Tanami region lies between two neighbouring regions of Paleoproterozoic basement: the Aileron Province of the Arunta region to the southeast and the Halls Creek Orogen to the northwest (Figure 2.1; Crispe et al. 2007). Compressional and extensional structures have been interpreted in the Tanami region, overlying the Archean basement (Goleby et al. 2009). While the interpretation of these structures remains unclear, it suggests that these structures have played a part in the development of the Tanami region and the Tanami Group sediments (Goleby et al. 2009).

The oldest exposed rocks are high-grade metasedimentary rocks and leucogranites of the Billabong Complex, with a likely Neoarchean age (ca 2514 ± 3 Ma; Page 1995, figure 2.2). The remainder of the region comprises siliciclastic sedimentary rocks deposited after ca 1865 Ma and intruded by post-1830 Ma granites, with both sedimentation and granite emplacement largely concluded by ca 1790 Ma (Crispe et al. 2007; Huston et al. 2007; Lambeck et al. 2008; Figure 2.3). Figure 2.3 details the stratigraphy of Crispe et al. (2007) and a suggested alternative by Bagas et al. (2010) and Joly et al. (2010).

The oldest known Paleoproterozoic rocks form the Stubbins Formation in Western Australia (Bagas et al. 2008). The Stubbins Formation consists of a succession of banded-iron formation, shale, chert, basalt, dolerite sills, and rhyodacite that is conformably overlain by the Killi Killi Formation (Bagas et al. 2008). The relationship between the Stubbins Formation and the remainder of the Tanami region is not clear because the Stubbins Formation is either fault bounded or not exposed (Bagas et al. 2008; Joly et al. 2010). SHRIMP U–Pb zircon data from turbiditic sandstone within the Stubbins Formation provide maximum depositional ages of 1870 ± 6 Ma and 1864 ± 3 Ma (D. Maidement in Bagas et al. 2008). A cross-cutting quartz-porphyry rhyodacite near the top of the Stubbins Formation is interpreted to have an igneous crystallisation age of 1864 ± 4 Ma (D. Maidement in Bagas et al. 2008). The combined maximum depositional age of 1864 ± 3 Ma and the igneous crystallisation age of 1864 ± 4 Ma provide the depositional age of the Stubbins Formation (Bagas et al. 2008). Bagas et al. (2010) and Joly et al. (2010; Figure 2.3) interpret the Stubbins Formation in the western Tanami region as a lateral equivalent to the Dead Bullock Formation in the eastern Tanami region (see Figure 2.3).

In the Northern Territory, the Tanami Group overlies the Billabong Complex and is divided into the basal Dead Bullock Formation and overlying Killi Killi Formation. Goleby et al. (2009) interpreted southeasterly thinning of the Tanami Group from deep crustal seismic data. The formations are geochemically distinguished by Th/Sc, Zr/Sc and Cr/Th ratios and total Fe values (Lambeck et al. 2008, 2010, 2011). The poorly outcropping Dead Bullock Formation contains mafic sediment that is iron-rich compared to felsic sediment of the overlying Killi Killi Formation (Lambeck et al. 2008, 2011). The Dead Bullock Formation is characterised by a U–Pb detrital zircon pattern with a dominant peak at 2500 Ma, and subsidiary peaks at 2700 and 3200 Ma; no peak younger than 2200 Ma is present (Cross & Crispe 2007). This detrital zircon pattern is attributed to a general northern Australia source (Cross & Crispe 2007; Lambeck et al. 2010); however, other southern Proterozoic and/or Archean sources cannot be ruled out (e.g. Fraser et al. 2010). The Dead Bullock Formation is divided into the basal Ferdies Member and the upper Callie Member (Crispe et al. 2007). The Ferdies Member consists of fining-upward sandy siltstone overlain by ~600 m of siltstone–claystone (Tde beds, Bouma 1962) of the Callie Member, interpreted to have been deposited during decreased rates of clastic deposition (Lambeck et al. 2008). An interpreted tuffaceous unit within the Callie Member has a magmatic crystallisation age of 1838 ± 6 Ma. However, its stratigraphic position within the Callie Member is not clear (Cross & Crispe 2007).

The overlying Killi Killi Formation is the most areally extensive lithostratigraphic unit in the Tanami region. It consists of fine-grained, micaceous-lithic muddy sandstone interbedded with siltstone and claystone. Coarser grained and geochemically distinctive turbidites of the Killi Killi Formation are interpreted as lowstand deposits associated with a basinward shift in facies distinguishing a provenance change in sedimentary source (Lambeck et al. 2008). This geochemical transition suggests a progressive conformable change in provenance as detailed in Lambeck et al. (2008). Visually this transition is marked by the relatively rapid influx of coarse quartz-rich sediments overlying generally quartz-poor sediments. Little evidence of reworking from the underlying iron-rich Dead Bullock Formation into the Killi Killi Formation is observed (Lambeck et al. 2008, 2011). The age of the Killi Killi Formation is constrained by its range in detrital zircons and the underlying depositional age of the Dead Bullock Formation. A maximum detrital zircon depositional age of between 1870 Ma and 1860

Ma was reported by Cross & Crispe (2007), but this unit must be younger than the ca 1838 Ma tuffaceous unit in the Dead Bullock Formation. Hence, as discussed by Cross & Crispe (2007), the Killi Killi Formation is interpreted to be deposited at least 20 Ma after the age of its youngest detrital zircon component. An alternative view is proposed by Bagas et al. (2009), who suggest the interpreted tuffaceous unit is potentially an intrusion, implying the Tanami Group could be older than ca 1838 Ma (Figure 2.3). Bagas et al. (2009) calculated a maximum depositional age of 1864 ± 6 Ma for the Killi Killi Formation where it directly overlies the 1864 ± 4 Ma Stubbins Formation in the Western Tanami region.

The Ware Group is interpreted to unconformably overlie the Tanami Group and is dominated by felsic volcanic rocks and coarse-grained lithic sandstone, with minor siltstone (Crispe et al. 2007). Claoúe-Long et al. (2008) note that clastic sediments within the Ware Group have detrital zircon provenance patterns similar to (and probably recycled from) the underlying Killi Killi Formation. The Ware Group also contains a younger detrital component between 1830 and 1820 Ma (Cross & Crispe 2007), which is interpreted to derive from proximal felsic volcanism within the group (Claoue-Long et al. 2008). SHRIMP U–Pb zircon dating of a rhyolite (Mount Winnecke Formation) within the Ware Group yielded an age of 1824 ± 5 Ma (sample #87495029, Ozchron database, Geoscience Australia). As detailed in Lambeck et al. (2010) both the Killi Killi Formation and Ware Group were deposited during regional extension, with a dominant felsic source and minor Archean input. While sedimentary detritus has probably been recycled into the Ware Group from the underlying Killi Killi Formation, the broader depositional setting remains unchanged between the sedimentation of Killi Killi Formation and the Ware Group sediments.

The Mount Charles Formation consists of fine- to coarse-grained clastic sedimentary rocks intercalated with basalt (Crispe et al. 2007; Cross & Crispe 2007). The Mount Charles Formation is dominated by zircons with Archean ages but in addition, contains a youngest detrital component at ca 1910 Ma (Cross and Crispe 2007). Crispe et al. (2007) interpret that the Mount Charles Formation was deposited about 100 Ma after its depositional age. Although contacts are not exposed, Crispe et al. (2007) interpret the Mount Charles Formation to unconformably overlie the Ware Group. Alternatively, Bagas et al. (2010) and Joly et al. (2010) place the Mount Charles Formation as a lateral equivalent to the Dead Bullock Formation (Figure 2.3). The regional stratigraphic position of the Mount Charles Formation requires further work. The older detritus, represented by the detrital zircon patterns (Cross and Crispe 2007), less intense structural deformation (Crispe et al. 2007) and contrasts in whole-rock geochemistry between the Mount Charles (Lambeck et al. 2010), and the Dead Bullock Formations, provide evidence against a correlation between these units as suggested by Bagas et al. (2010) and Joly et al. (2010). An alternative explanation to Bagas et al. (2010) and Joly et al. (2010) is provided by Crispe et al. (2007), Cross & Crispe (2007) and Lambeck et al. (2010), who suggested the Dead Bullock and the Mount Charles Formations were deposited at different times and in different geological settings.

2.1.2 Gold deposits and gold prospects of the Tanami region

Huston et al. (2007) and Goleby et al. (2009) both proposed that known lode-gold deposits are typically associated with antiformal structures nested on thrust systems that transect the whole Tanami Group. The thrust systems are interpreted to have acted as fluid conduits for gold mineralisation, transporting gold to higher structural levels, including the Dead Bullock and Killi Killi Formations. As dark claystone in the Dead

Bullock Formation has acted as an important redox boundary for gold mineralisation (Huston et al. 2007; Williams 2007), by inference dark claystone in the Killi Killi Formation could also act as a redox boundary to the oxidised gold fluid. Hence, gold prospectivity in the Killi Killi Formation is increased where crustal-penetrating structures interact with thick claystone facies.

The richest gold-bearing host rocks, the Dead Bullock and Mount Charles Formations, have very limited areal extent (<10%) (Figure 2.2; Lambeck et al. 2010). Approximately 40% of the exposed area of the region is represented by the Killi Killi Formation, which is currently known to contain ~30 tonnes of gold (Huston et al. 2007), with the remaining exposed outcrop mainly consisting of granites. Other smaller deposits that occur in the Tanami region are granite-, dolerite-, sandstone- and mudstone-hosted gold mineralisation, but their deposition is controlled by lithology, structural, pressure, and temperature constraints (Huston et al. 2007).

2.2 Methods

Eleven diamond-drillholes, selected to minimise potential structural repetition, and seven outcrop sections were logged (Figures 2.5, 2.6). These cores and outcrops are assigned to the Killi Killi Formation based on their whole-rock and trace-element geochemical and geochronological data (Cross & Crispe 2007; Lambeck et al. 2008, 2010). An additional drillcore, DBD 445 (Figure 2.5), interpreted by Lambeck et al. (2008) to intersect Killi Killi Formation, is also included in this study. Sedimentary facies were defined for each core and outcrop section based on lithological characteristics. Except at Dead Bullock Soak where the transition between the Dead Bullock and Killi Killi Formations is recorded, the exact stratigraphic position of the Killi Killi cores within the Killi Killi Formation remains unknown (Figures 2.5, 2.6; Lambeck et al. 2008). In this study, all cores within the Killi Killi Formation are placed above the datum line.

Grain-size information was recorded on a graphic log. Composite cores were constructed at Dead Bullock Soak (DBD 434) and Coyote (CYD050 & CYD072; Figure 2.2) using the established mine lithostratigraphy (Williams 2007; Lambeck et al. 2010; Figures 2.5, 2.6), because no single core intersects the entire succession. Gaps are shown on the composite logs to illustrate uncertainty in the stratigraphic relationships between drillholes. The upper part of the Dead Bullock Soak composite drill core from Lambeck et al. (2008) is used in this study to represent the Callie Member and the Killi Killi Formation.

Two surfaces were constructed from the seismic interpretation of Goleby et al. (2009), one at the base of the Dead Bullock Formation and one stratigraphically higher, at the base of the Killi Killi Formation. These surfaces were generated in Paradigm 2009 GOCAD 2.6.0™ software to visualise the stratigraphic packages. An isopach map of the Dead Bullock Formation was generated to show stratal thickness variation between these two surfaces. The stratal package overlying the upper surface is composed of the Killi Killi Formation and Ware Group because they are indistinguishable on seismic data. The isopach map of this stratal package was constructed using Earth's surface or the seismically interpreted base of granite bodies to define thickness variation across the region. Drillholes were located on the isopach surface as minimum thicknesses as drill holes did not intersect underlying stratigraphy. Positions of deep crustal thrust faults

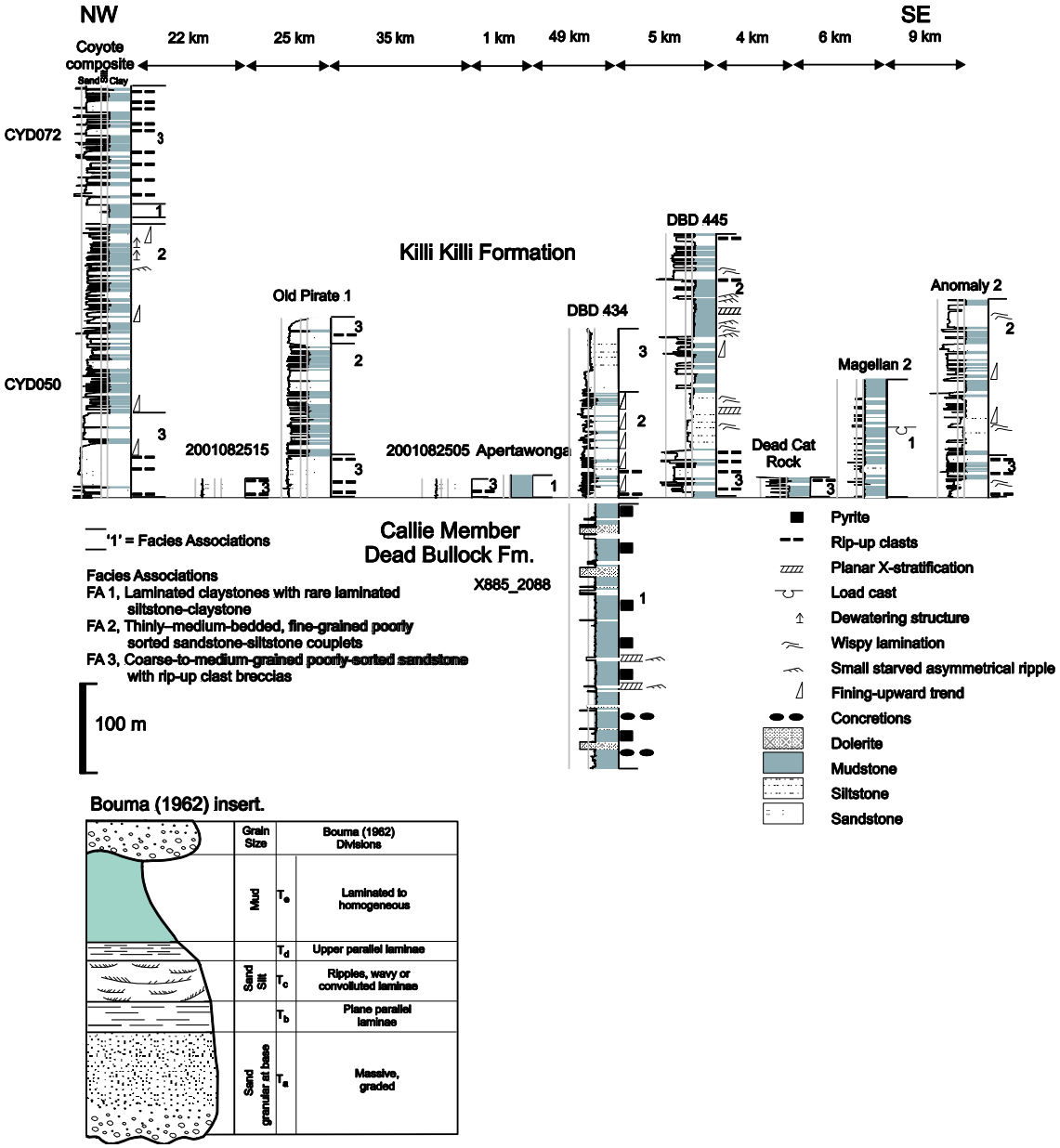

Fig. 2.5 - Northwest–southeast of the Tanami region shows the lateral facies variation of the Killi Killi Formation and the limited extent of the Dead Bullock Formation. The strata coarsen to the western Tanami Coyote drill hole. The datum was chosen on the inferred contact between the Killi Killi Formation and the Dead Bullock Formation. The insert displays the Bouma Sequence showing Te, Td, Tc, Tb and Ta divisions from Bouma (1962). Formation abbreviated to Fm in figure.

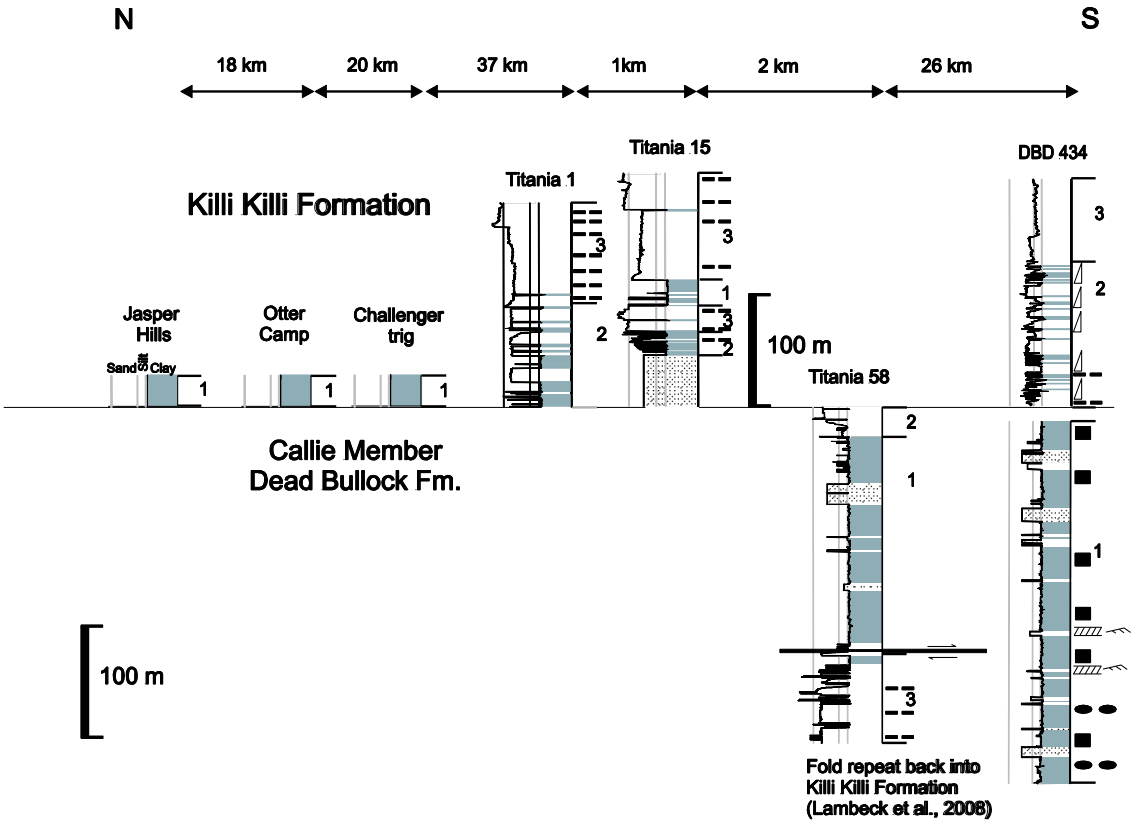

Fig. 2.6 North–south transect of the Tanami region showing the lateral facies variation of the Killi Killi Formation. The cross-section implies that sediment fines to the north. The datum was chosen on the inferred contact between the Killi Killi Formation and the Dead Bullock Formation. Formation abbreviated to Fm in figure.

based on seismic interpretation (Goleby *et al.* 2009) are located on the isopach surfaces (Figures 2.7, 2.8).

2.3 Facies Associations

Six facies are recognised in the Callie Member and the Killi Killi Formation based on bedding characteristics, fabric, texture and sedimentary structures (Figure 2.9; Table 2.1). The presence of normally-graded sandstone-claystone couplets with incomplete Bouma sequences is consistent with their interpretation as sediment-gravity flow deposits, mainly by turbidity currents (e.g. Walker 1978; Posamentier & Walker 2006). Abundant siltstone and claystone facies also indicate significant deposition by suspension settling (Table 2.1). Lack of any sedimentary structures indicative of wave activity suggests the facies were deposited below storm wave base.

Three facies associations are defined in this study (FA1–FA3) based on common intercalation of genetically related facies (Figure 2.10). Typically the boundaries between facies associations are sharp. Recognition of these facies associations is the basis for attributing these deposits to a turbiditic depositional system. In the following descriptions, turbidites that form the bulk of the Killi Killi Formation and Callie Member of the Dead Bullock Formation are described using the standard Bouma (1962) subdivisions (Ta–e; Figure 2.5).

2.3.1 Facies Association 1 (FA1)

Description: FA1 is characterised by thick successions (up to 600 m) of dark grey–black, massive to laminated claystone (Facies F1; Figure 2.10a; Table 2.1) with rare laminated siltstone–claystone Tde beds (Facies F2; Figure 2.10b). Starved ripples and micro-scale cross laminations are locally developed in F2. Concretionary horizons in F1 represent local quartz cementation. FA1 is recognised in both the Callie Member and Killi Killi Formation.

Interpretation: The dominance of claystone and observations of starved ripples indicates deposition mostly by suspension settling with limited bottom current activity. The concretionary horizons in the claystone are interpreted to represent condensation associated with minimum rates of clastic deposition in the basin, allowing early diagenetic growth at, or close to, the sediment water interface (Raiswell 1987). This association indicates a low energy, basin-floor setting (Johnson et al. 2001; Martinsen et al. 2003).

2.3.2 Facies Association 2 (FA2)

Description: FA2 is composed of thinly–medium-bedded, poorly sorted, fine sandstone–siltstone couplets (Tbde , Tbcde beds, Facies F3; Figure 2.10c; Table 2.1) and minor massive fine sandstone with dewatering structures and associated rip-up clast breccias (Ta, Tab beds, Facies F4). Scoured bed bases and amalgamation of sandstone beds are locally present. FA2 is recognised only in the Killi Killi Formation.

Interpretation: Facies F3 and F4 record deposition by sandy turbidity currents. Local scoured bases and amalgamated sandstones in F3 suggest scouring and filling of channels. The thinly-bedded, fine sandy turbidites lacking Ta bases represent deposition by dilute turbidity currents at channel margins and/or in interchannel areas. Stacked fining-upward patterns (e.g. Titania 1 and DBD 434 in Figures 2.6, 2.10c) between F4

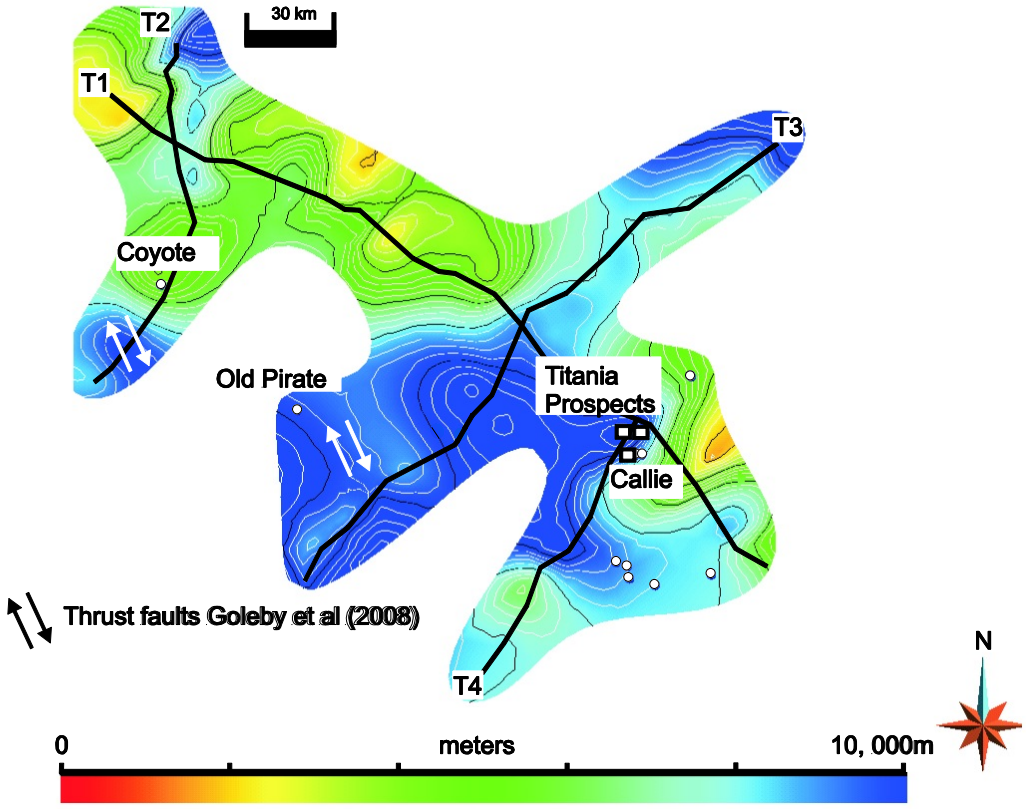

Fig. 2.7 - Isopach of the Dead Bullock Formation. The depicted surface represents the interpreted thickness derived from seismic interpretation of Goleby et al. (2009) with colder colours representing maximum basin depocentres. The positions of the regional seismic lines are shown labelled T1–T4 and key Au-prospect and drill holes shown. See Figure 2.1 for location of all names. Open squares are where drill holes have intersected Dead Bullock Formation and open circles are where drill holes intersect Killi Killi Formation (Lambeck et al. 2008).

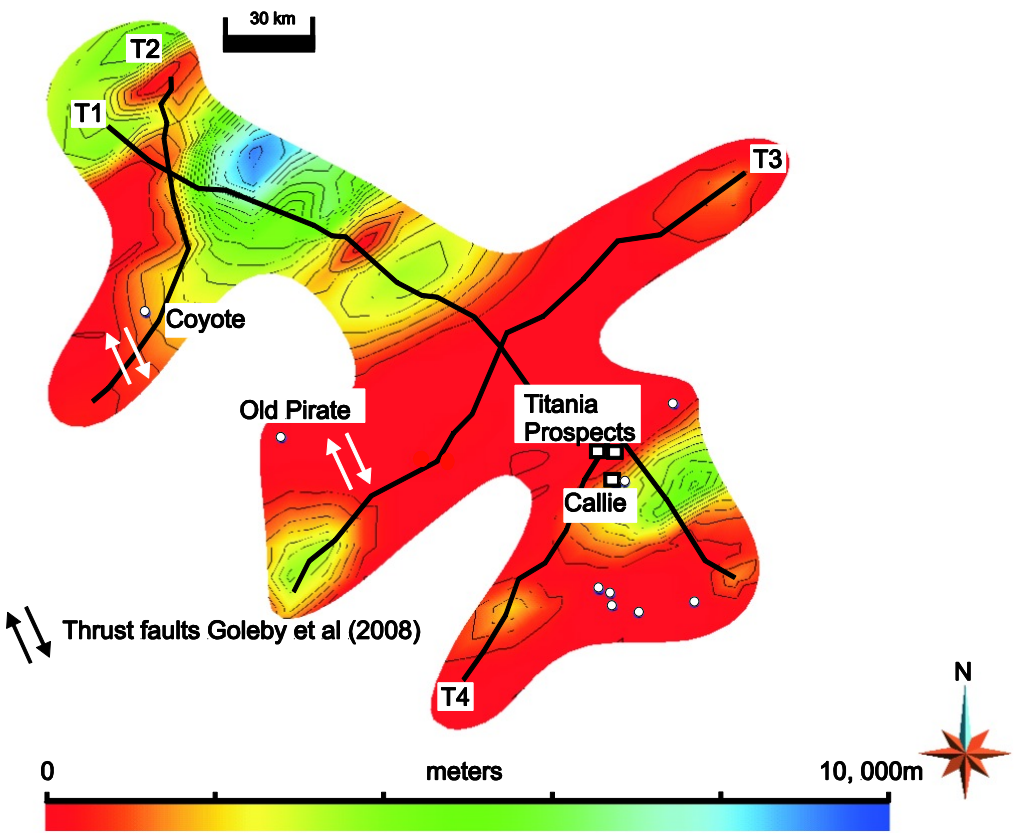

Fig. 2.8 Isopach of the combined Killi Killi Formation–Ware Group assemblage. The depicted surface represents the interpreted thickness derived from seismic interpretation of Goleby et al. (2009) with colder/darker colours representing maximum basin depocentres. The positions of the regional seismic lines are shown labelled T1–T4 and key Au-prospect and drill holes shown. See Figure 2.1 for location of all names. Open squares are where drill holes have intersected Dead Bullock Formation and open circles are where drill holes intersect Killi Killi Formation (Lambeck et al. 2008).

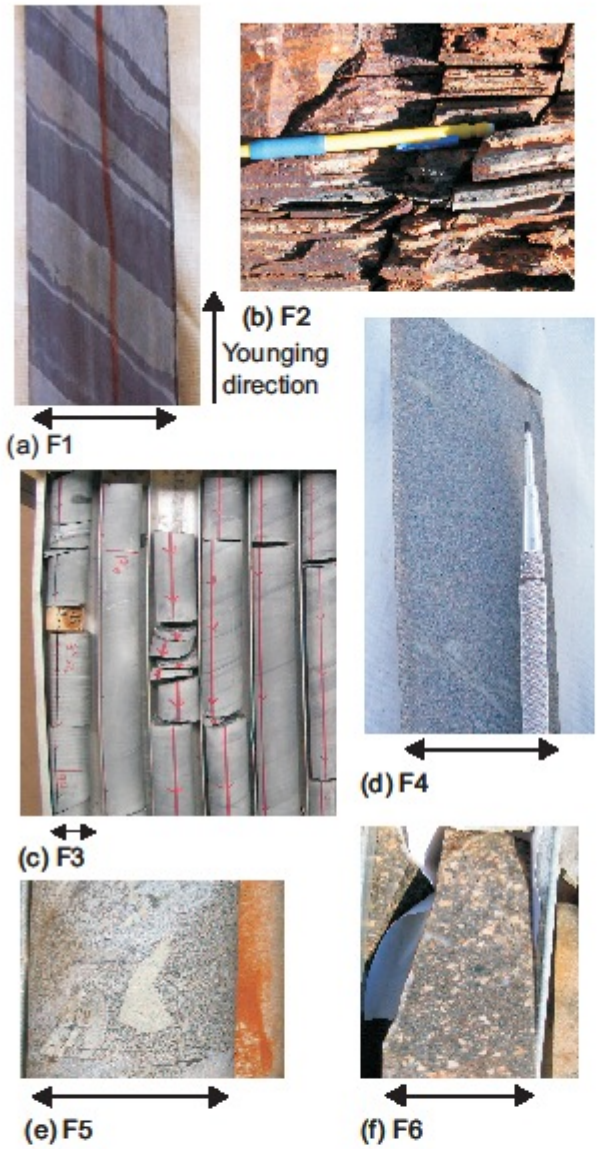

Fig. 2.9 Example photographs of each of Facies 1–6 as described in Table 1; see Figure 2 for locations. (a) F1: Drill core X885_2088, laminated claystone, displaying 'Zebra rock' alternating black claystone and pale decarbonised claystone. (b) F2: Apertawonga outcrop, laminated claystone and siltstone. (c) F3: DBD 434, thinly medium-bedded fine sandstone-siltstone couplets (note: arrows in the photograph point down hole). (d) F4: DBD 445, Massive fine muddy sandstone, claystone rip-up clasts breccias. (e) F5: DBD445, Medium-bedded sandstone, claystone rip-up clasts breccias. (f) F6: CYD050, Thickly bedded medium-to-coarse sandstone. Horizontal arrows in all pictures represent core width 4.7 cm; younging direction is at the top of page.

Facies associations	Facies No.	Facies name	Description	Bouma Division	Bed/ Contacts	Facies Thickness	Other features	Depositional Process
FA1	F1	Laminated claystone.	Thin (mm to cm scale) planar laminated to lenticular claystone or massive claystone.	T_{de}	Planar base and top; rare loading on bed bases.	commonly up to ~200 m thick.	Commonly pyrite cubes, local development of 'zebra rock' with alternating black claystone and pale decarbonised claystone (Williams 2007).	Suspension settling and dilute turbidity currents.
	F2	Laminated claystone with rare laminated siltstone-claystone.	Normally graded pale-coloured siltstone– very dark claystone. Siltstone has planar lamination, mm-scale starved ripples, cross-lamination; dewatering pipes are rare.	Incomplete Bouma sequences T_{de}	Sharp planar contacts with local scouring.	10 cm to > 1 m	Pyrite cubes; $CaCO_2$ cement in cross-stratified sandstone, chloritized zones.	Dilute muddy turbidity currents.
FA 2	F3	Thinly-medium bedded fine sandstone-siltstone couplets.	Normally graded fine sandstone–siltstone couplets.	Incomplete Bouma sequences T_{bde}, T_{bcde}	Sharp planar contacts with local scouring.	Amalgamated units with thickness up to 30 m.	Claystone rip-up clast breccias; $CaCO_2$ cement, chloritic zones.	Deposition by sandy turbidity currents.
	F4	Massive medium muddy sandstone.	Commonly massive, very poorly sorted medium sandstone may have normal grading; dewatering pipes are rare.	T_{a-b}	bases.	Amalgamated units with thickness up to 5m.	Claystone rip-up clasts breccias; chloritic zones, $CaCO_2$ cement.	High-concentration deposition by high-density turbidity currents.
FA 3	F5	Medium bedded sandstone.	Massive medium sandstone with claystone rip-up clast breccias up to 5 cm long.	T_a	Irregular base and top.	Up to 2 m thick; thickness variation between drill cores.	Claystone rip-up clast breccias; chloritiic zones, $CaCO_2$ cement.	High-concentration deposition by high-density turbidity currents.
	F6	Thickly bedded medium-to-coarse sandstone and rip-up clast breccias.	Massive medium to coarse sandstone with claystone rip-up clast breccias up to 5 cm long.	T_a, T_{ae}	Scoured bed bases are common.	Amalgamated thickly bedded turbidities up to 30 m thick in drill core.	Elongate and irregular claystone rip-up clast breccias.	High-concentration deposition by high high-density turbidity currents and sandy debris flows.

Table 2.1. Facies characteristics of the Callie Member of the Dead Bullock Formation and Killi Killi Formation, Tanami Group, Tanami region.

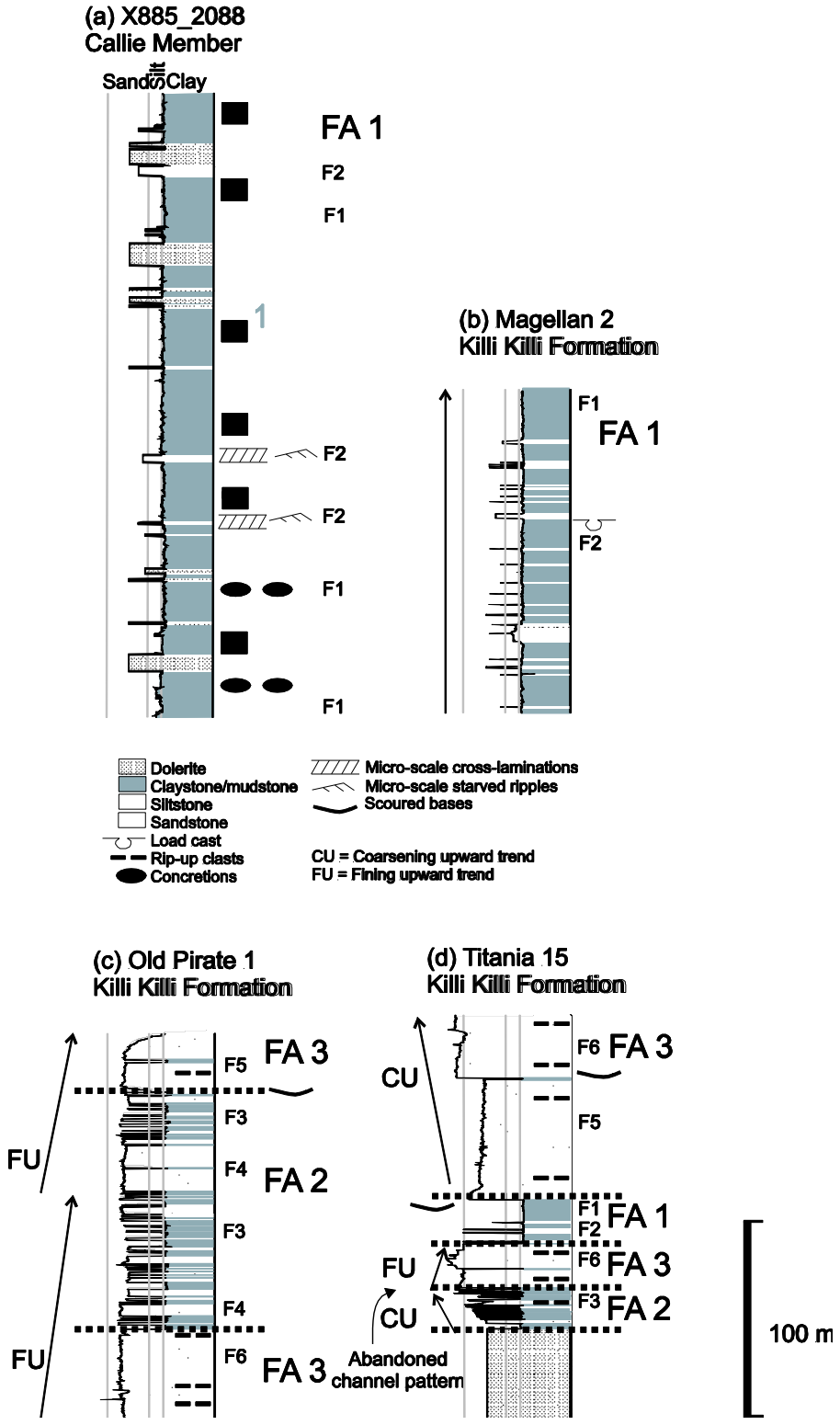

Fig. 2.10 Six facies, (F1–F6, Table 2.1), are recognised in the Callie Member and the Killi Killi Formation on the basis of bedding characteristics, fabric, texture and sedimentary structures with three facies associations defined (FA1–FA3, Table 2.1). Measured stratigraphic sections of; (a) Callie Member at Callie Mine, (b) Magellan 2, (c) Old Pirate, and (d) Titania. See Figure 2.2 for locations, Figure 2.9 for example photographs of recognised Facies.

and F3 also support channel and channel margin/interchannel area deposition respectively.

2.3.3 Facies Association 3 (FA3) and interpretation

Description: FA3 is composed of poorly sorted, medium sandstones with thickly to very thickly bedded rip-up clast breccias (debrites, Facies F5) and medium- to thick-bedded muddy coarse sandstone with rare muddy tops (Ta, Tae beds: F6; Figure 2.10c, d; Table 2.1). Scoured bed bases are common and the thickly bedded turbidites form amalgamated stratal packages up to 30 m thick in drillcore. Structural repetition may have contributed to the thickness of these packages (e.g. Vandenberg et al. 2001) although no obvious tectonic structures were identified in core. FA3 is recognised only in the Killi Killi Formation.

Interpretation: High-density turbidites and associated rip-up clast breccias arranged in fining-upward patterns suggest a channel-fill origin (e.g. Mayall et al. 2006). The rip-up clasts indicate scouring and entrainment of fragments of the muddy substrate by erosive flows. The geochemical composition of the claystone confirms that the rip-up clasts were derived from the Killi Killi Formation (Lambeck et al. 2008).

In summary, the facies associations identified in this study are interpreted as representing deposition in different parts of a deep-water turbidite system and share sedimentological similarities with sub-environments described in studies elsewhere (Richards et al. 1998; Johnson et al. 2001; Gervais et al. 2006; Mayall et al. 2006). The lack of wave-formed structures and systematic recognition of sandstone–mudstone couplets and Bouma sequences supports a deepwater depositional setting below storm wave base. The distribution of coarser sand-rich facies towards the northwest (e.g. Figure 2.5) suggests that the sediment source was most likely located in this direction. This is also consistent with the interpretation by Goleby et al. (2009) that the Tanami Group thins to the southeast.

A schematic summary of the interpreted facies relationships between drillcore locations suggests formation of channelised sandy lobes with muddy lobe fringes on the basin floor (Figure 2.11). Similar lobe complexes have been recognised in well exposed outcrop examples (e.g. Eschard et al. 2003; Beaubouef 2004; Prélat et al. 2009) and modern marine settings (e.g. Samuel et al. 2003; Gervais et al. 2006; Deptuck et al. 2008).

2.4 Regional Stratigraphic Transects and Isopach maps

North–south and east–west trending transects were constructed across the Tanami region to summarise variations in stratigraphic thickness of the Killi Killi Formation (Figures 2.5, 2.6). The basal Callie Member was only observed at the Callie Mine and 26 km northwest at Titania (Figure 2.2). The east–west-trending cross-section (Figure 2.5) displays a general coarsening of facies from the east (Anomaly 2) to the west (Coyote). Two separate zones of claystone deposits are observed in drill core at Magellan 2 and in outcrop at Apertawonga (Figure 2.5), potentially indicating lower sediment input between sediment lobes.

The north-trending transect extends from Callie mine (Dead Bullock Soak composite core) to a surface exposure at Jasper Hills (Figure 2.6). Within the Killi Killi Formation the most obvious feature of this transect is the increase in claystone facies (Te) to the

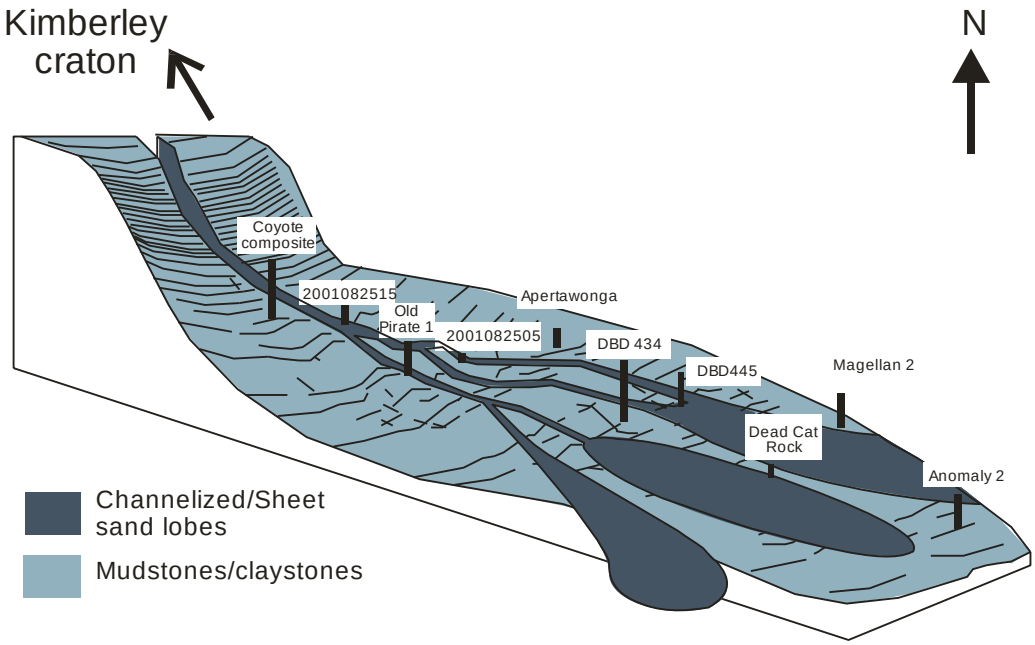

Fig. 2.11 - Schematic diagram illustrating the lateral facies relationships and depositional model for the Killi Killi Formation. See Figure 2.2 for location of logged drillcore and outcrop sections.

north with surface exposures in the northern Tanami region consisting almost entirely of claystone. Structural complexity makes determining thickness of the claystone problematic. In logs on the transects claystones are only shown to be thin beds but are regionally extensive around Jasper Hills (Figure 2.2). The undrilled claystone facies most likely represent thick, hundred metre-scale successions as depicted in the Killi Killi Formation isopach surface (Figure 2.8).

Figures 2.7 and 2.8 present the isopach maps established from the seismic data of Goleby et al. (2009) for the Dead Bullock Formation and the combined Killi Killi Formation–Ware Group, respectively. The surface extension of crustal penetrating structures, proximal to the Old Pirate Prospect, are shown on the isopach maps (Figures 2.7, 2.8). These thrust faults could be important conduits for gold-bearing fluid and potentially form the plumbing system to gold mineralisation in the Tanami region (Huston et al. 2007; Goleby et al. 2009).

Some caution must be taken in interpreting these diagrams. It should be noted that isopach maps relate to stratigraphic thickness and do not necessarily relate to outcrop patterns in Figure 2.2. The surfaces used to construct the maps should be considered form surfaces that mark boundaries between major units. Strata between these form surfaces are deformed, which means that the isopach maps are a combination of true stratigraphic thickness and structural thickening. As documented by Goleby et al. (2009) and shown in Figures 2.7 and 2.8, there are systematic regional patterns in the thickness of the Tanami succession. Determining true stratigraphic thickness of the sedimentary packages remains difficult.

Broadly, Figures 2.7 and 2.8 show opposing thickness. That is, where the Dead Bullock Formation appears thick, the Killi Killi–Ware Group appears relatively thin, and vice versa. Although the extent and thickness of the Dead Bullock Formation generally remains untested by drilling, the main depocentre during Dead Bullock Formation time was located in the southwestern part of the Tanami province. This depocentre trends broadly northeast, although thickness distributions indicate a possible northeast-trending boundary along the far east of the Tanami region. The Callie and Titania deposits are located along this margin (Figures 2.2, 2.6; Lambeck et al. 2008). The apparent thickening of the Dead Bullock Formation along seismic line T-3, directly north of Titania, remains untested by drilling. More regional geochemistry, combined with carefully placed drill holes are required to test the regional extent of the Dead Bullock Formation.

During Killi Killi–Ware time, the depocentre shifted to the northwest with minimal deposition in the southeast. This is consistent with a decrease in the thickness of the Tanami Group to the southeast as suggested by Goleby et al. (2009), and a broad increase in grain size and occurrence of proximal Bouma sequences in the Killi Killi Formation to the northwest (Figure 2.5; see above). The claystone-dominated successions at Jasper Hills, Otter Camp and Challenger Trig correspond to the thinnest parts the Killi Killi–Ware Group stratal package (Figure 2.8).

2.5 Depositional history of the Killi Killi Formation

The facies data and facies association data are suggestive of a deepwater below wave base turbiditic setting with currently no interpreted evidence for a wave-dominated environment. As more data becomes available, e.g. structural studies to determine true

stratigraphic thickness of regional units, these new data can be incorporated into the current deep-water facies model to help refine understanding of the localisation of gold deposits within the Tanami region.

The deepest water conditions during deposition of the Tanami Group are interpreted to be represented by the ~600 m thick succession of Facies 1 (Callie Member) at the Callie mine (Figure 2.7). Limited exposure makes regional correlations problematic. However, the isopach map suggests that thick sequences of the Dead Bullock Formation may extend to the Old Pirate prospect (Figure 2.7). The isopach map of the Killi Killi-Ware stratal package (Figure 2.8), combined with its mapped regional distribution (Figures 2.5, 2.6, 2.10), suggests that it was part of a much larger depositional system. Progradation led to deposition of sandy lobes on an otherwise muddy substrate (Callie Member). The claystone-dominated succession in the northern part of the Tanami basin and at sites such as Apertawonga and Magellan are interpreted as interchannel or lobe fringe settings similar to those described by Prélat et al. (2009) from the Permian Karoo Basin, South Africa.

Whole-rock geochemistry indicates a change in provenance between the Dead Bullock and Killi Killi Formations. The influx of coarser sediment of different provenance and development of a turbidite complex is attributed to a major relative sea-level fall (e.g. Lambeck et al. 2008).

The depositional model (Figure 2.11) combined with the isopach maps in Figures 2.7 and 2.8 provide some basis for predicting the distribution of iron-rich and claystone facies, which are important hosts for gold in the Tanami region. The depocentre of the highly prospective Dead Bullock Formation is located in the southeastern part of the Tanami basin, and extends to the south and west of the Callie and Titania deposits. This area, much of which is poorly exposed, should be considered highly prospective for gold. Claystone facies of the Killi Killi Formation, which should also have significant potential to host gold are more likely distributed in the northern part of the Tanami basin. The intersection of this favourable stratigraphy with structures that acted as fluid pathways (e.g. faults identified in seismic data (Goleby et al. 2009) and from geological mapping) is suggested to be the most favourable site for gold mineralisation. However, other rock types (e.g. dolerite or basalt) or structural settings could potentially also localise gold deposition.

Facies assemblage data suggest sedimentary units of the Killi Killi Formation were sourced from the northwest (Figures 2.5, 2.6, 2.10). Two different tectonic models have been proposed that could help explain the source of the Killi Killi Formation sediments. The initial model of Etheridge et al. (1987) suggests basin convergence on continental crust with little horizontal movement suggesting an eroding continent directly to the northwest of the Tanami region. In contrast, Griffin et al. (2000), based on work by Sheppard et al. (1999) and Tyler et al. (1999), interpreted convergence between the Kimberley and proto-North Australian cratons with collision between plates at ca 1850 Ma. In this model, the Tanami region was a foreland basin as subsequently proposed by Tyler et al. (2005) and Huston (2006). Neither model is entirely definitive, mainly due to lack of geochronology in the Tanami region.

2.6 Conclusions

Sedimentological analysis and seismic interpretation has been undertaken on the poorly exposed Paleoproterozoic Tanami Group in northern Australia. The results of these studies, in combination with isopach maps derived from seismic data, lithogeochemistry and U–Pb SHRIMP geochronology, have been used to develop a depositional model for the Tanami Group. The identification of stratal surfaces between the Dead Bullock Formation (Callie Member) and the Killi Killi Formation, permits a better understanding of stratigraphic architecture. The maximum thickness of the Tanami Group is recorded in the northwest, which then fines/thins to the southeast to a position south of the Callie Mine. The Killi Killi Formation consists of sandstone-dominated facies, which thin and become more muddy to the southeast. This suggests a sediment source located to the northwest. The Callie Member was deposited as part of a condensed section below storm wave base. The conformably overlying Killi Killi Formation, also deposited below storm wave, base forms part of a basin-floor fan previously interpreted as a lowstand system tract. The claystone facies form potential redox boundaries for oxidised gold-bearing fluid. Targeting these thrust faults within claystone-dominated stratigraphic successions could help refine gold exploration methods in the Killi Killi Formation. It is suggested that the original architecture of the Tanami basin influenced the later lode-gold mineral system. Gold exploration success could be enhanced if deep holes are drilled within the Titania and Old Pirate Prospects to intersect the underlying Dead Bullock Formation.

2.7 Acknowledgements

This study could not have taken place without the support and enthusiasm of Newmont Australia and Tanami Gold. Many thanks are given to Pascal Hill, Martin Smith and Rosalyn Da Costa from Newmont and Tim Smith from Tanami Gold who provided initial collaboration opportunities. The Northern Territory Geological Survey also provided logistical support and Andrew Crispe provided many useful discussions. At Geoscience Australia George Gibson, Lesley Wyborn, and David Champion provided helpful and fun discussions. We are grateful to Jamie Vinnels who provided many discussions and critically read an earlier version of the manuscript. Ian Tyler and Simon Bodorkos and two anomalous reviewers are thanked for there detailed reviews and their suggestions greatly improved the focus of the paper. This contribution is published with permission of the Chief Executive Officer of Geoscience Australia.

2.8 References

Bagas, L., Bierlein, F.P., Anderson, J.A.C. and Maas, R., 2010. Collision-related granitic magmatism in the Granites-Tanami Orogen, Western Australia. Precambrian Research, 177(1-2): 212-226.

Bagas L., Anderson J. A. C. & Bierlein F. 2009. Palaeoproterozoic evolution of the Killi Killi Formation and orogenic gold mineralization in the Granites–Tanami Orogen, Western Australia. Ore Geology Reviews 35, 47–67.

Bagas, L., Bierlein, F.P., English, L., Anderson, J.A.C., Maidment, D. and Huston, D.L., 2008. An example of a Palaeoproterozoic back-arc basin: Petrology and geochemistry of the ca. 1864 Ma Stubbins Formation as an aid towards an improved understanding of the Granites-Tanami Orogen, Western Australia. Precambrian Research, 166(1-4): 168-184.

Beaubouef, R.T., 2004. Deep-water leveed-channel complexes of the Cerro Toro Formation, Upper Cretaceous, southern Chile. AAPG Bulletin, 88(11): 1471-1500.

Béziat, D., Dubois, M., Debat, P., Nikiéma, S., Salvi, S. and Tollon, F., 2008. Gold metallogeny in the Birimian craton of Burkina Faso (West Africa). Journal of African Earth Sciences, 50(2-4): 215-233.

Bouma, A.H., 1962. Sedimentology of Some Flysch Deposits: a Graphic Approach to Facies Interpretation. Elsevier, Amsterdam, 168 pp.

Bouma, A.H., 2001. Fine-grained submarine fans as possible recorders of long- and short-term climatic changes. Global and Planetary Change, 28(1-4): 85-91.

Claoué-Long, J., Edgoose, C. and Worden, K., 2008. A correlation of Aileron Province stratigraphy in central Australia. Precambrian Research, 166(1-4): 230-245.

Crispe, A.J., Vandenberg, L.C. and Scrimgeour, I.R., 2007. Geological framework of the Archaean and Palaeoproterozoic Tanami Region, Northern Territory. Mineralium Deposita, 42: 3-26.

Cross, A. and Crispe, A.J., 2007. SHRIMP U-Pb analyses of detrital zircon: A window to understanding the Palaeoproterozoic development of the Tanami Region, northern Australia. Mineralium Deposita, 42: 27-50.

Deptuck, M.E., Piper, D.J.W., Savoye, B. and Gervais, A., 2008. Dimensions and architecture of late Pleistocene submarine lobes off the northern margin of East Corsica. Sedimentology, 55(4): 869-898.

Eschard, R., Albouy, E., Deschamps, R., Euzen, T. and Ayub, A., 2003. Downstream evolution of turbiditic channel complexes in the Pab Range outcrops (Maastrichtian, Pakistan). Marine and Petroleum Geology, 20(6-8): 691-710.

Etheridge, M., A., Rutland, R., W,R. and Wyborn, L., A,I., 1987. Orogenesis and tectonic processes in the Early to Middle Proterozoic of northern Australia. Proterozoic Lithospheric Evolution 17. American Geophysical Union Geodynamics Series 17, 131-147 pp.

Fraser, G., McAvaney, S., Neumann, N., Szpunar, M. and Reid, A., 2010. Discovery of early Mesoarchean crust in the eastern Gawler Craton, South Australia. Precambrian Research, 179(1-4): 1-21.

Gervais, A., Savoye, B., Mulder, T. and Gonthier, E., 2006. Sandy modern turbidite lobes: A new insight from high resolution seismic data. Marine and Petroleum Geology, 23(4): 485-502.

Goldfarb, R.J., Bradley, D. and Leach, D.L., 2010. Secular Variation in Economic Geology. Economic Geology, 105(3): 459-465.

Goldfarb, R.J., Groves, D.I. and Gardoll, S., 2001. Orogenic gold and geologic time: a global synthesis. Ore Geology Reviews, 18(1-2): 1-75.

Goleby, B.R., Huston, D.L., Lyons, P., Vandenberg, L., Bagas, L., Davies, B.M., Jones, L.E.A., Gebre-Mariam, M., Johnson, W., Smith, T. and English, L., 2009. The Tanami deep seismic reflection experiment: An insight into gold mineralization and Paleoproterozoic collision in the North Australian Craton. Tectonophysics, 472(1-4): 169-182.

Gosselin, P. and Dubé, B., 2005. Gold deposits of the world: distribution, geological parameters and gold content. Geological Survey of Canada, Open File 4895: 271.

Griffin, T.J., Page, R.W., Sheppard, S. and Tyler, I.M., 2000. Tectonic implications of Palaeoproterozoic post-collisional, high-K felsic igneous rocks from the Kimberley region of northwestern Australia. Precambrian Research, 101(1): 1-23.

Huston, D., 2006. Mineral systems and tectonic evolution of the North Australian Craton. In: P. Lyons and D.L. Huston (Editors), Evolution and metallogenesis of the North Australian Craton. Geoscience Australia, Alice Springs.

Huston, D., Wygralak, A., Mernagh, T., Vandenberg, I.C., Crispe, A.J., Lambeck, A., Bagas, L., Cross, A., Fraser, G., Williams, N., Worden, K. and Meixner, T., 2007. Lode gold mineral systems of the Tanami Region, northern Australia. Mineralium Deposita, 42: 175-204.

Johnson, S.D., Flint, S., Hinds, H. and De Ville Wickens, H., 2001. Anatomy, geometry and sequnce stratigraphy of basin floor to slope turbidite systems, Tanqua Karoo, south Africa. Sedimentology, 48: 987-1023.

Joly, A., McCuaig, T.C. and Bagas, L., 2010. The importance of early crustal architecture for subsequent basin-forming, magmatic and fluid flow events. The Granites-Tanami Orogen example. Precambrian Research, 182(1-2): 15-29.

Lambeck, A., Mernagh, T. and Wyborn, L., A, I., 2011. Are iron-rich sedimentary rocks the key to the spike in orogenic gold mineralization in the Paleoproterozoic? Economic Geology 106 (3): 321-330.

Lambeck, A., Huston, D. and Barovich, K., 2010. Typecasting prospective Au-bearing sedimentary lithologies using sedimentary geochemistry and Nd isotopes in poorly exposed Proterozoic basins of the Tanami region, Northern Australia. Mineralium Deposita, 45(5): 497-515.

Lambeck, A., Huston, D., Maidment, D. and Southgate, P., 2008. Sedimentary geochemistry, geochronology and sequence stratigraphy as tools to typecast stratigraphic units and constrain basin evolution in the gold mineralised Palaeoproterozoic Tanami Region, Northern Australia. Precambrian Research, 166(1-4): 185-203.

Martinsen, O.J., Lien, T., Walker, R.G. and Collinson, J.D., 2003. Facies and sequential organisation of a mudstone-dominated slope and basin floor succession: the Gull Island Formation, Shannon Basin, Western Ireland. Marine and Petroleum Geology, 20(6-8): 789-807.

Mayall, M., Jones, E. and Casey, M., 2006. Turbidite channel reservoirs--Key elements in facies prediction and effective development. Marine and Petroleum Geology, 23(8): 821-841.

Milési, J.-P., Ledru, P., Feybesse, J.-L., Dommanget, A. and Marcoux, E., 1992. Early proterozoic ore deposits and tectonics of the Birimian orogenic belt, West Africa. Precambrian Research, 58(1-4): 305-344.

Myers, J., Shaw, R. and Tyler, I., 1996. Tectonic evolution of Proterozoic Australia. Tectonics, 1: 1431–1446.

Page, R.W., Sun, S.-S. and Blake, D., 1995. Geochronology of an exposed late Archæan basement terrane in The Granites-Tanami region. AGSO Research Newsletter, 22: 19-20.

Prélat, A., Hodgson, D.M. and Flint, S.S., 2009. Evolution, architecture and hierarchy of distributary deep-water deposits: a high-resolution outcrop investigation from the Permian Karoo Basin, South Africa. Sedimentology, 56(7): 2132-2154.

Posamentier, H.W., Walker, R.G., 2006. Deep-water turbidites and submarine fans. Special Publication 84. In: Posamentier, H.W., Walker, R.G. (Eds.), Facies Models Revisited. SEPM, pp. 399-520.

Raiswell, R., 1987. Non-steady state microbiological diagenesis and the origin of concretions and nodular limestones. Geological Society, London, Special Publications, 36(1): 41-54.

Richards, M., Bowman, M. and Reading, H., 1998. Submarine-fan systems i: characterization and stratigraphic prediction. Marine and Petroleum Geology, 15(7): 689-717.

Roddaz, M., Debat, P. and Nikiéma, S., 2007. Geochemistry of Upper Birimian sediments (major and trace elements and Nd-Sr isotopes) and implications for weathering and tectonic setting of the Late Paleoproterozoic crust. Precambrian Research, 159(3-4): 197-211.

Rutland, R., W,R., 1973. Tectonic evolution of the continental crust in Australia. In: D. Tarlings, H. and S.K. Runcorn (Editors), Continental Drift Sea Floor Spreading and Plate Tectonics: Implications for the Earth Sciences. Academic Press, London, pp. 1003-1025.

Samuel, A., Kneller, B., Raslan, S., Sharp, A. and Parsons, C., 2003. Prolific deep-marine slope channels of the Nile Delta, Egypt. AAPG Bulletin, 87(4): 541-560.

Sheppard, S., Tyler, I. and Page, R.W., 1999. Palaeoproterozoic subduction-related and passive margin basalt in the Halls Creek Orogen, northwest Australia. Australian Journal of Earth Sciences, 46: 679-690.

Tyler, I.M., Page, R.W. and Griffin, T.J., 1999. Depositional age and provenance of the Marboo Formation from SHRIMP U-Pb zircon geochronology: Implications for the early Palaeoproterozoic tectonic evolution of the Kimberley region, Western Australia. Precambrian Research, 95(3-4): 225-243.

Tyler, I.M., Sheppard, S., Bodorkos, S. and Page, R.W., 2005. Tectonic significance of detrital zircon profiles across paleoproterozoic orogens in the Kimberely region of northern Australia. In: M. Wingate and S. Pisarevsky (Editors), Fremantle TSRC Supercontinents and Earth Evolution Symposium. Geological Society of Australia Abstracts 81 p. 33, Perth.

Vandenberg, I.C., Hendrick, M.A. and Crispe, A.J., 2001. Structural geology of the Tanami Region. Northern Territory Geological Survey Record 2001-004, 28 pp.

Walker, R.G., 1978. Deep-water sandstone facies and ancient submarine fans; models for exploration for stratigraphic traps. AAPG Bulletin, 62(6): 932-966.

Williams, N., 2007. Controls on mineralisation at the world-class Callie gold deposit, Tanami desert, Northern Territory, Australia. Mineralium Deposita, 42: 65-87.

Alexis Lambeck

PhD THESIS TITLE

“Basin analysis and the geochemical signature of Paleoproterozoic sedimentary successions in northern Australia: Constraints on basin development in respect to mineralisation and paleoreconstruction models”

CHAPTER 3

Typecasting prospective Au-bearing sedimentary lithologies using sedimentary geochemistry and Nd isotopes in poorly exposed Proterozoic basins of the Tanami region, Northern Australia

Lambeck, A.[1,2]
Huston, D.,[2]
Barovich, K.[1]

[1] Centre for Tectonics Resources and Exploration, University of Adelaide, Adelaide, SA 5005.
[2] Geoscience Australia, GPO Box 378, Canberra, ACT 2601, Australia

MIneralium Deposita – 2010, 45, 497-515

STATEMENT OF AUTHORSHIP

Typecasting prospective Au-bearing sedimentary lithologies using sedimentary geochemistry and Nd isotopes in poorly exposed Proterozoic basins of the Tanami region, Northern Australia

Mineralium Deposita – 2010, 45, 497-515

Alexis Lambeck (PhD. Candidate)

Collected all samples, interpreted data, wrote manuscript and acted as corresponding author

I hereby certify that the statement of contribution is accurate

Signed …… ……Date…21 June 2011.

David Huston (co-author name)

Supervised development of work, provided assistance with data interpretation and manuscript evaluation

I hereby certify that the statement of contribution is accurate and I give permission for the inclusion of the paper in the thesis

Signed …… ……Date…21 June 2011.

Karin Barovich (co-author name)

Provided assistance with data interpretation and manuscript evaluation

I hereby certify that the statement of contribution is accurate and I give permission for the inclusion of the paper in the thesis

Signed …… ……Date…21 June 2011.

Chapter 3

Typecasting prospective Au-bearing sedimentary lithologies using sedimentary geochemistry and Nd isotopes in poorly exposed Proterozoic basins of the Tanami region, Northern Australia

Published as: Lambeck, A., Huston, D., and Barovich, K. 2010. Typecasting prospective Au-bearing sedimentary lithologies using sedimentary geochemistry and Nd isotopes in poorly exposed Proterozoic basins of the Tanami region, Northern Australia Mineralium Deposita (2010) 45:497–515.

Abstract

The development of a regional stratigraphy in Paleoproterozoic basins within the Tanami region, Northern Australia has been hindered by the difficulty of discriminating sedimentary units and facies across this isolated and poorly exposed basin. A regional stratigraphy is important as it provides constraints on sedimentary basin evolution and assists in gold exploration. Gold is known to be more concentrated in certain rock formations. Based on Nd isotopes and whole rock geochemistry, five main sedimentary events have been identified in the Tanami region. Some sedimentary units were derived from homogeneous local sources, whereas others contain evidence of a well-mixed fine-grained remote provenance. Within the basins, major gold-bearing lithologies are characterised by mafic source indicators: (1) high Cr/Th ratios; (2) low Th/Sc ratios; (3) low $(La/Yb)_{PAAS}$ ratios relative to Post-Archean Average Shale (Taylor and McLennan 1985); (4) Eu anomalies equal to ~1; and (5) distinctive ranges in initial ε_{Nd} values. Potential future exploration target areas have been identified in the Tanami region at the Cashel and Sunline prospects using these geochemical parameters.

3.1 Introduction

The Tanami region is a poorly exposed, mostly Paleoproterozoic province within Northern Australia that hosts a number of significant gold deposits (Fig. 3.1 Plumb et al. 1990; Smith et al. 1998; Huston et al. 2007; Bagas et al. 2009). The Callie deposit is the largest (6.0 Moz Au) and is hosted by black mudstones of the Dead Bullock Formation (Smith et al. 1998). Effective exploration of the Tanami region, however, has been severely hampered by poor knowledge of the regional stratigraphy. It is difficult to identify and correlate exposed packages of poorly sorted sandstones, siltstones and black mudstones separated by large regions of regolith cover (Blake et al. 1979; Hendrickx et al. 2000; Crispe et al. 2007; Huston et al. 2007).

Lode-gold provinces such as the Yilgarn and Superior cratons host gold in a variety of lithologic types and structural settings (Hodgson 1993). In contrast to these regions, two of the three major goldfields in the Tanami region the Granites and Dead Bullock Soak goldfields are hosted exclusively by carbonaceous or iron-rich sedimentary units (Huston et al. 2007). Smaller sediment-hosted gold deposits in the Tanami region include Oberon, Coyote and Minotaur. Huston et al. (2007) calculated that sediment-hosted gold deposits contain 77% of the Tanami gold resource (carbonaceous sedimentary rocks 61%, banded iron formation 16%). Given the lack of outcrop and the complex geophysical character of the lithology types, this paper focuses on sedimentary geochemistry as a means of creating criteria that will aid in the classification of gold-

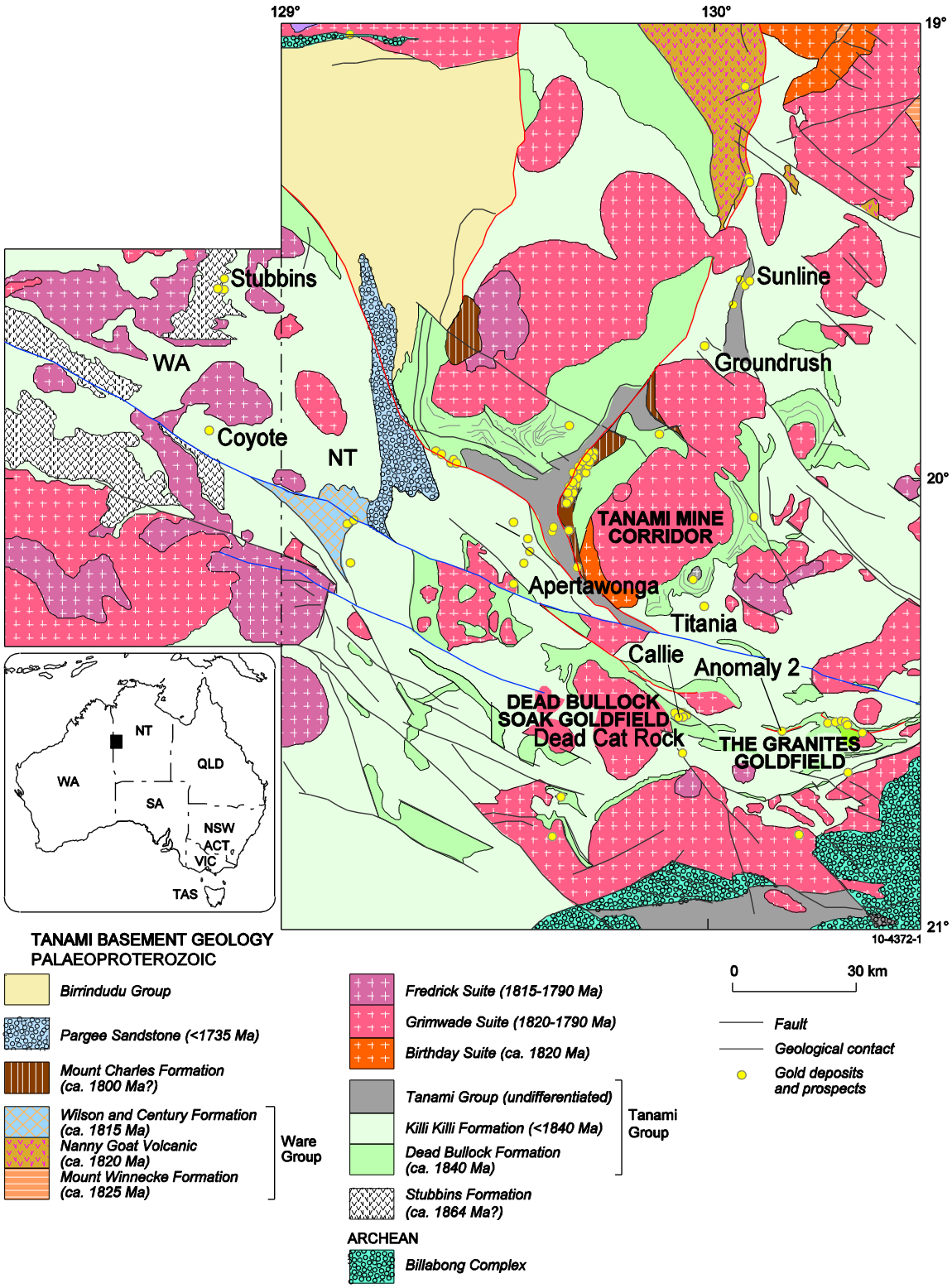

Fig 3.1 - Solid geology of the Proterozoic units in the Tanami region (Huston et al. 2007). The Cashel Prospect is 39 km east of Anomaly 2 within mapped undifferentiated Tanami Group

bearing successions. Ultimately, exploration costs can be lowered by geochemically distinguishing gold-bearing stratigraphic units within an overall regional fine-grained succession.

Lambeck et al. (2008) typecast the Stubbins, Dead Bullock and Killi Killi Formations using Zr/Sc and Th/Sc ratios, Cr values and REE patterns combined with detrital zircon populations and differentiated between the more gold-prospective Dead Bullock Formation from the less gold-prospective Stubbins and Killi Killi Formations. In this paper, we build upon the techniques developed by Lambeck et al. (2008) and use Cr/Th ratios, Th/Sc ratios, $(La/Yb)_{PAAS}$ and Eu/Eu* values, combined with Sm–Nd isotopic variations, to identify changes in sedimentary source for the Proterozoic Tanami region. These characteristics allow us to typecast the major gold-bearing lithologies within the poorly exposed fine-grained siltstones and black mudstones of the Tanami gold province

3.1.1 Geological setting and stratigraphy

The Tanami region is situated in northwest central Australia (Fig 3.1) within the North Australia Craton (Myers et al. 1996). The characteristics, relationships and ages of supracrustal rock units and granites in the Tanami region are described by Crispe et al. (2007) and Cross and Crispe (2007), and only a summary is provided here. Table 3.1 and Fig. 3.2 provide an overview of the Tanami regional stratigraphy. The oldest rocks in the Tanami region are high-grade Neoarchean metasedimentary rocks and leucogranites (~2,514±3 Ma) that occur within the Billabong Complex (Page et al. 1995 Fig. 3.1). Although the outcrop of Archean rocks is <5% of the total area in the Tanami region, Page et al. (1995) used Sm–Nd isotope data from granites to suggest that Archean rocks are more extensive at depth.

The sedimentary successions within the Tanami region have been subdivided into five events based on geochemistry and geochronology (Table 3.1). The oldest know Paleoproterozoic rocks form the Stubbins Formation in Western Australia. This package, described in detail by Bagas et al. (2008), consists of a 2- to 3-km-thick lower succession of interlaid turbiditic sandstone, siltstone, mudstone and dolerite sills conformably overlain by an upper ~200-m-thick succession of iron-rich siltstone and mudstone, carbonaceous mudstone, chert, pillow basalt and dolerite sills with rare rhyolite and lamprophyre dykes. The relationship between the Stubbins Formation and the remainder of the Tanami region is not clear as the Stubbins Formation is everywhere fault-bounded (Bagas et al. 2008). Two SHRIMP U–Pb zircon dates provide maximum depositional ages of 1,870±6 and 1,864±3 Ma (Bagas et al. 2008). A quartz–porphyry rhyodacite interpreted to intrude the upper part of the Stubbins Formation yields an igneous crystallisation age of 1,864±3 Ma and is interpreted as the approximate age of the host succession (Bagas et al. 2008).

The Tanami Group consists of the basal Dead Bullock Formation overlain by the Killi Killi Formation (Fig. 3.2). The basal Ferdies Member of the Dead Bullock Formation consists of a sandy siltstone fining upwards into graphitic units and banded iron formation of the Callie Member (Lambeck et al. 2008). The Callie Member at Dead Bullock Soak is the largest gold-producing region in the Northern Territory.

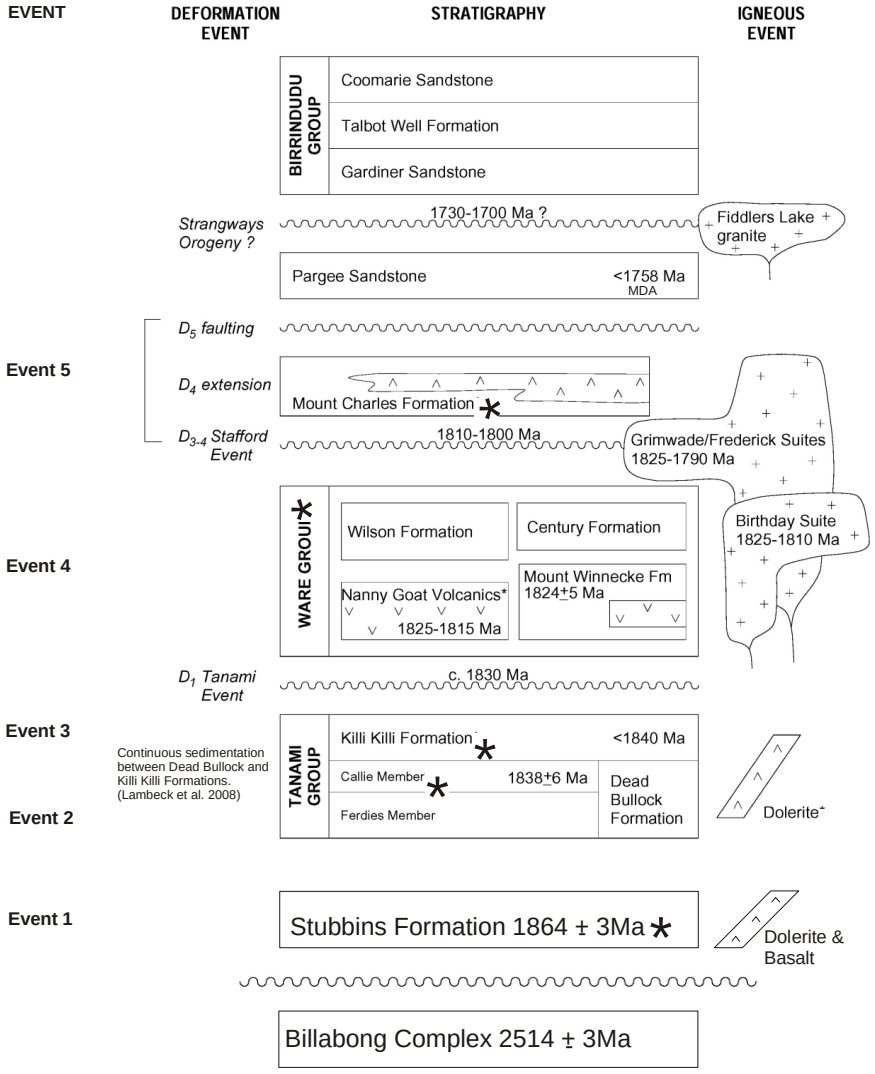

Fig. 3.2 - Regional straigraphy of the Tanami region from Crispe et al (2007). Asterisks indicate significant gold mineralisation. Geochronology of the Tanami region is detailed in Table 3.1

Table 3.1 Summary of regional stratigraphy for the Tanami region in respect to total gold tonnage

Regional Stratigraphy	Total Au (tonnes)	Average Cr/Th	Average Th/Sc	Average REE (PAAS)	Eu/Eu*	ε_{Nd}	Geochronology
Mount Charles Formation	*56.6*	*22.2 ± 9.8*	< 1	*[La/Yb]$_{PAAS}$ = 0.5 (range = 0.1 - 3.4)*	*1.4 ± 0.1*	*Range, -7.2 to +1.6*	*1800 Ma (dep age) (Cross and Crispe 2006)*
Ware Group	**2.3**	**1.9 ± 1.2**	**2.9 ± 1.2**	**[La/Yb]$_{PAAS}$ = 1.1 (range = 0.3 - 2.7)**	***0.9* ± 0.1**	**-2.4, - 2.7**	**1815±13 Ma, (max dep) (Claoue Long et al. 2001)**
Killi Killi Formation	**33**	**2.7 ± 1.3**	***2.1* ± 0.8**	**[La/Yb]$_{PAAS}$ = 1.3 (range = 0.5 - 2.4)**	***0.9* ± 0.1**	**Range, - 6.5 to +3.1**	**~1860 Ma (max dep) (Cross and Crispe 2007)**
Dead Bullock Formation	*270*	*63.5 ± 45.6*	*< 1*	*[La/Yb]$_{PAAS}$ = 0.5, with 98 % of the data in the range of 0.1 - 1.0)*	*1.3 ± 0.2*	*Range, -6.0 to -6.4*	*1838±6 Ma (max dep) (Cross and Crispe 2007)*

Average and standard deviation for whole rock and trace element geochemistry of sedimentary rock, Nd isotopes and geochronology. The Dead Bullock and Mount Charles Formations, shown in *italics*, are the main gold-bearing lithologies and are used as gold 'proxies' for further exploration in the Tanami region

max dep maximum deposition

Correlations among units within the Tanami are largely dependent on detrital zircon age data. The detrital spectra of Dead Bullock and Killi Killi Formations are significantly different. The Dead Bullock Formation contains a main peak at 2,500 Ma with subsidiary peaks at 2,700 and 3,200 Ma (Cross and Crispe 2007). No peaks are present younger than 2,200 Ma, which contrasts with the overlying Killi Killi Formation which contains a dominant detrital zircon peak at 1,860 Ma with minor peaks at 2,500 Ma and older (Cross and Crispe 2007).

The youngest zircon component of the Killi Killi Formation provides a maximum depositional age of between 1,870 and 1,860 Ma. As reported by Cross and Crispe (2007), however, this unit and the underlying Dead Bullock Formation is geochronologically well constrained by an inferred "tuffaceous unit" in the Dead Bullock Formation with an age of 1,838±6 Ma. Hence, the Killi Killi Formation is interpreted to be deposited at least 20 Ma after the age of its youngest detrital zircon component. The Killi Killi Formation, composed of turbiditic siliciclastic rocks consisting of micaceous sandstone, lithic sandstone interbedded with siltstones and carbonaceous mudstones, also hosts gold, but it is less extensively mineralised (Crispe et al. 2007). The Killi Killi Formation (and its time correlative, the Lander Rock beds) occurs extensively across the Tanami and northern Arunta regions (Crispe et al. 2007).

Multiple generations of dolerite sills intrude the Tanami Group and are described in detail by Dean (2001). At Dead Bullock Soak, the Dead Bullock Formation is cross-cut by the locally named Coora Dolerite and End it All Dolerite. The dolerites are up to 200 m thick and are affected by the same major deformation and metamorphic events as the Tanami Group (Crispe et al. 2007). Crispe et al. (2007) observed peperitic textures on the lower contact of the Coora Dolerite with Dead Bullock Formation and suggested intrusion of the Coora dolerite into soft sediment.

The Ware Group forms part of a regionally widespread episode of volcanism and clastic sedimentation in the Tennant Creek region (Crispe et al. 2007) and the Pine Creek Orogen (Lally and Worden 2004). The Ware Group is dominated by felsic volcanics and coarse-grained lithic sandstones, with minor siltstone and basalt. It includes the Mount Winnecke Formation (Traves 1955; Blake et al. 1975), Nanny Goat Volcanics (Hendrickx et al. 2000), Wilson Formation and Century Formation (Crispe et al. 2007 Fig 3.2). The relationship with the underlying Tanami Group is not exposed, but Crispe et al. (2007) infer an unconformity based on structural observations. SHRIMP U–Pb dating of the Ware Group provides a maximum deposition age of 1,815±13 Ma (Claoué-Long et al. 2001).

Regional deformation and granite plutonism at ~1,800 Ma, the Stafford Event, caused extension and localised sedimentation, forming the Mount Charles Formation (Cawood and Korsch 2008). The Mount Charles Formation (Fig. 3.2) is a succession of fine- to coarse-grained clastic sedimentary rocks intercalated with basalt interpreted to be restricted to the Tanami mine corridor (Crispe et al. 2007). Within the Tanami mine corridor, gold mineralisation was restricted to within the sedimentary and basaltic volcanic rocks (Tunks and Cooke 2007). The Mount Charles Formation consists of mafic volcanic rocks that are consistent with the existence of an intra-continental rift setting at the time of deposition (Tunks and Cooke 2007). The pillow basalts within the Mount Charles Formation are described by Tunks (1996) as intracontinental tholeiites.

An unconformity between the underlying Dead Bullock Formation and the basal, thinly

bedded lithic sandstone is exposed; however, the top of the Mount Charles Formation is not exposed (Crispe et al. 2007). Cross and Crispe (2007) note that obtaining reliable geochronological data from the Mount Charles Formation is problematic. The lack of regional deformation and metamorphism within the Mount Charles Formation suggests it postdates the ~1,830–1,810 Ma metamorphic and deformational events in the Tanami Group (Crispe et al. 2007). The Mount Charles Formation is interpreted to have a depositional age of ~1,810 Ma, 100 Ma younger than the ~1,910 Ma age based on the youngest detrital zircons (Cross and Crispe 2007).

The Pargee Sandstone is a thick succession of interbedded conglomerate, pebbly sandstone, quartz-rich sandstone and minor siltstone. Based on $^{40}Ar/^{39}Ar$ thermogeochronology and detrital zircon geochronology, sediments forming the Pargee Sandstone may have been sourced from the Arunta Block (Crispe et al. 2007). The Pargee Sandstone has a maximum deposition age of 1,768± 14 Ma (Claoué-Long et al. 2001; Cross and Crispe 2007). This unit unconformably overlies cleaved siltstone of the Killi Killi Formation and is unconformably overlain by the Gardiner Sandstone, the basal unit of the Birrindudu Group (Blake et al. 1975; 1979). As no significant gold prospects are found within the Pargee Sandstone or the overlying Birrindudu Group, they are not included as part of this study.

3.2 Sampling and analytical methods

Drill cores were selected in consultation with Newmont and Tanami Gold mine geologists to cover the full stratigraphic succession and minimise structural complications. The Stubbins, Dead Bullock, Mount Charles and Killi Killi Formations and Ware Group were sampled from either drill holes or limited outcrop from regions where the regional stratigraphy is known (Crispe et al. 2007). Lambeck et al. (2008) have previously reported composite stratigraphy and lithologic geochemical sections through the Stubbins Formation, Callie deposit, the Cashel and Sunline prospects and the Dead Cat Rock and Apertawonga outcrop sections. The composite section of the Mount Charles Formation stratigraphy was constructed in a similar fashion to the composite section completed at the Dead Bullock Soak goldfield (Lambeck et al. 2008). Lack of available core limited sampling of the full Mount Charles stratigraphic section, and only ~300 m of representative core was sampled. The Mount Charles Formation, including significant occurrences of pillow basalts, is estimated to be ~3,000 m thick (Tunks 1996). Diamond drill holes RGD 116, DDH076, CAD053 and HRD003 were used for the Mount Charles Formation composite downhole profile.

Whole rock and trace element analyses were carried out on 434 samples in three batches. The first batch (62 samples) consisted of split pulp samples crushed in tool steel by Newmont Australia. The second batch (225 hand samples, 50–300 g) was prepared in either a tungsten–carbide mill or tool steel mill at Geoscience Australia. The third batch (147 samples) consisted of samples from drill core ground on-site to a fine powder (approximately 20 g) using a diamond core grinder. Between samples, the core grinder was cleaned with compressed air to avoid contamination. The ground powder from the cores was visually inspected and found to contain small chips from the diamond-grinding wheel. To exclude potential contamination, the chemistry of the cutting wheel was determined, and elements that were major components of the wheel (W, Ag, Cu, Zn, Mn, Ni and Fe) were removed from the geochemical database for data analysis and interpretation. In addition, seven outcrop samples, including a sample of felsic volcanics, were taken from the Ware Group and were analysed for whole rock and

trace element geochemistry. Three representative samples of whole rock geochemistry from each of the regional stratigraphic units are given in Table 3.2 The total dataset for whole rock major and trace element analysis can be accessed from the Electronic supplementary material, Supplementary data for the Mount Charles Formation and Ware Group and in Lambeck et al. (2008) for the Stubbins Formation, Tanami Group and Sunline and Cashel Prospects. Data is also available in the appendix of this thesis.

Abundances of major and trace elements were determined at Geoscience Australia, Canberra using X-ray fluorescence (XRF) and inductively coupled plasma mass spectroscopy (ICP-MS) techniques. Major and minor elements (Si, Ti, Al, Fe, Mn, Mg, Ca, Na, K, P and S) were determined by wavelength-dispersive XRF on fused discs using methods similar to those of Norrish and Hutton (1969). Precision for these elements is better than ±1% of the reported values. Arsenic, Ba, Cr, Cu, Ni, Sc, V, Zn and Zr were determined by pressed pellet on a wavelength-dispersive XRF using methods similar to those described by Norrish and Chappell (1977). Selected trace elements (Cs, Ga, Nb, Pb, Rb, Sb, Sn, Sr, Ta, Th, U and Y) and the rare earth elements were analysed at Geoscience Australia by ICP-MS (Agilent 7500ce with reaction cell) using methods similar to those of Eggins et al. (1997), but on solutions obtained by dissolution in distilled HF and HNO_3 acid of the fused glass discs (Pyke 2000). Precisions are 5% and 10% at low levels. Agreement between XRF and ICP-MS (Ba, Nb, Pb, Rb, Sr, Y and Zr) are within 10%.

Based on the existing and new geochemical data, a suite of 28 sedimentary samples, eight basalts and dolerites and a felsic volcanic rock were analysed for Sm–Nd isotopic composition as part of this study. Isotope analyses were determined by isotope dilution in two batches. Fifteen samples were completed at Adelaide University using techniques detailed in Wade et al. (2005). Samples were evaporated in HF–HNO_3 overnight, digested in hot HF–HNO_3 in sealed Teflon vials for 5 days, then evaporated to dryness in HF–HNO_3. Samples were subsequently evaporated in 6 M HCl and then bombed with 6 M HCl overnight. Nd and Sm concentrations were calculated by isotope dilution, with Nd isotope ratios measured by thermal ionisation mass spectrometry on a Finnigan MAT 262 mass spectrometer and Sm isotope ratios measured on a Finnigan MAT 261 mass spectrometer. The running average for the La Jolla standard is 0.511289±8 (n=134). Twenty-one samples were analysed at La Trobe University using techniques detailed in Wade et al. (2005) and in Waight et al. (Waight et al. 1998; 2000).

3.3 Geochemical results

To enable a direct comparison, all analyses were recalculated to 100% volatile-free, and all samples containing >5% CaO or >5% loss of ignition were excluded from further consideration (Roser and Korsch 1986). This minimised any possible effect of disturbance by alteration and allows drill cores to be compared regionally.

3.3.1 Major elements

Ternary diagrams of major element plots using Nesbitt and Young (1984; 1989) display a separation in the data (Fig. 3.3a, b). The Dead Bullock and Mount Charles Formations appear to be more enriched in Al_2O_3 compared to the Stubbins and Killi Killi Formation and Ware Group. The ternary diagram of Al_2O_3–($CaO + Na_2O + K_2O$)– ($FeO^T + MgO$) (Nesbitt and Young 1989; Bierlein et al. 1998) is modified here to show two separate sedimentary provenances, a felsic provenance and a mafic provenance (Fig. 3.3b). The

Table 3.2 Representative samples from the Tanami regional stratigraphy (all data found in appendix)

	Regional stratigraphy														
	Stubbins Formation	Stubbins Formation	Stubbins Formation	Dead Bullock Formation	Dead Bullock Formation	Dead Bullock Formation	Killi Killi Formation	Killi Killi Formation	Killi Killi Formation	Ware Group	Ware Group	Ware Group	Mount Charles Formation	Mount Charles Formation	Mount Charles Formation
Sample no.	2004-085495[a]	2004-085523[a]	2004-085535[a]	2003-085201[a]	2003-085092[a]	2003-085280[a]	2003-085073[a]	2003-085072[a]	2003-085071[a]	2005-085302[a]	2005-085303[a]	2005-085307[a]	2005-085134[a]	2005-085115[a]	2005-085146[a]
Lithology	Mudstone	Mudstone	Mudstone	Claystone	Claystone	Claystone	Fine sandstone	V.Fine sandstone	V.Fine sandstone	Fine sandstone	Fine sandstone	Fine sandstone	Fine sandstone	Mudstone	Fine sandstone
Latitude	-19.5849	-19.5849	-19.5849	-20.5224	-20.5224	-20.5224	-20.5088	-20.5088	-20.5088	-18.7723	-18.6769	-18.2547	-20.0396	-20.1033	-20.1033
Longitude	128.8657	128.8657	128.8657	130.944	130.944	130.944	129.9531	129.9531	129.9531	130.3007	130.339	130.1495	129.6694	129.5404	129.5405
SiO_2	61.9	64.2	61.1	56.1	57.7	65.7	72.1	77.9	56.2	62.9	89.8	81.0	61.6	44.2	55.3
TiO_2	0.5	0.6	0.5	1.5	0.9	0.9	0.6	0.5	0.6	0.4	0.3	0.3	0.8	1.9	2.3
Al_2O_3	18.4	18.1	18.2	16.0	14.8	14.3	14.3	10.8	21.5	18.6	5.1	8.1	11.4	19.2	17.2
Fe_2O_3	*5.8*	*5.4*	*6.5*	14.4	11.7	9.4	2.9	3.4	8.8	7.3	1.2	4.3	*11.6*	*21.3*	*15.7*
MnO	*< 0.1*	*< 0.1*	*< 0.1*	0.1	0.1	<0.1	<0.1	<0.1	<0.1	<0.1	<0.1	<0.1	*0.2*	*0.1*	*<0.1*
MgO	2.7	1.7	2.7	4.2	5.3	2.1	0.7	1.0	2.1	1.0	0.2	0.9	3.6	2.9	0.4
CaO	0.4	0.2	0.2	1.2	1.2	0.4	0.2	0.2	0.2	0.1	0.0	0.1	2.4	1.0	0.2
Na_2O	0.4	0.5	0.2	1.3	2.8	0.5	1.4	0.3	0.2	0.1	<0.1	0.3	0.2	0.6	0.2
K_2O	5.6	5.2	5.3	1.9	1.0	3.4	4.1	4.5	5.7	5.4	1.1	0.7	1.8	4.7	4.4
P_2O_5	0.1	0.1	0.1	0.1	0.2	0.1	0.2	0.1	0.1	0.1	0.1	0.1	0.1	0.1	0.1
SO_3	1.2	0.0	0.7	1.5	0.1	0.1	0.0	0.0	0.2	<0.1	0.0	0.0	0.0	0.0	0.0
LOI	2.7	3.7	4.4	2.1	4.1	2.9	3.2	1.1	4.2	3.9	2.1	3.9	6.2	3.8	4.0
Total	99.8	99.8	99.8	100.5	100.0	100.1	99.9	99.9	100.0	99.8	99.9	99.9	99.9	99.8	99.9
Cs	18.5	26.5	22.3	2.4	3.6	2.6	8.5	7.2	7.8	28.1	2.5	1.7	3.1	5.0	3.8
Ba	1017.0	450.0	517.0	1445.0	126.0	997.0	312.0	404.0	726.0	738.0	155.0	165.0	192.0	363.0	105.0
Rb	258.7	266.8	265.9	81.8	49.0	83.6	307.1	322.5	298.7	302.8	76.6	54.4	50.4	138.3	122.0
Sr	23.3	20.2	25.1	357.7	75.2	32.8	33.5	30.8	46.9	45.5	334.6	67.0	26.7	27.8	23.1
Pb	12.0	22.0	24.0	13.0	15.0	5.0	10.0	4.0	21.0	16.0	4.0	8.0	5.0	6.0	3.0
La	49.9	54.9	57.7	18.5	28.2	3.4	48.0	33.2	55.3	42.6	31.3	70.3	11.2	14.1	16.9
Ce	96.4	107.4	105.0	36.8	51.9	6.3	96.6	66.0	105.3	83.4	59.9	81.6	22.4	38.5	41.4
Pr	11.4	12.6	12.6	4.6	6.7	0.8	12.6	8.6	14.0	10.7	7.6	13.6	2.9	4.1	5.1
Nd	39.9	43.1	42.2	18.1	26.1	3.7	43.1	30.6	48.1	37.2	27.9	45.5	11.4	15.2	21.1
Sm	8.8	8.6	8.6	3.9	5.2	1.1	8.4	6.1	9.2	7.4	5.9	8.4	2.9	3.4	4.9
Eu	1.2	1.3	1.3	0.9	2.4	0.3	1.4	0.9	1.6	1.2	0.8	1.4	0.9	1.1	1.3
Gd	6.4	6.6	5.5	3.4	4.8	1.2	6.3	4.8	6.8	6.1	2.9	6.1	2.9	3.4	4.1
Tb	1.0	1.1	0.8	0.6	0.8	0.2	1.0	0.7	1.0	1.0	0.4	0.9	0.5	0.7	0.7
Dy	5.6	5.9	4.4	3.6	5.3	1.4	5.2	4.0	5.3	6.1	2.3	4.1	3.0	4.1	4.7
Ho	1.1	1.2	0.9	0.8	1.1	0.3	1.0	0.8	1.1	1.3	0.5	0.8	0.6	1.0	1.0
Er	3.3	3.2	2.5	2.3	3.4	1.1	3.0	2.3	3.1	3.7	1.6	2.1	1.7	2.6	2.9
Yb	3.0	3.0	2.4	2.2	2.7	1.4	2.9	2.2	2.9	3.3	1.6	1.9	1.5	2.6	2.9
Lu	0.4	0.4	0.4	0.4	0.3	0.2	0.4	0.3	0.5	0.5	0.2	0.3	0.2	0.4	0.5
Y	35.1	37.8	24.2	19.3	34.7	8.7	31.0	25.2	32.7	42.5	16.2	26.9	19.4	19.1	27.2

Table 3.2 (continued)

	Regional stratigraphy														
	Stubbins Formation	Stubbins Formation	Stubbins Formation	Dead Bullock Formation	Dead Bullock Formation	Dead Bullock Formation	Killi Killi Formation	Killi Killi Formation	Killi Killi Formation	Ware Group	Ware Group	Ware Group	Mount Charles Formation	Mount Charles Formation	Mount Charles Formation
Th	19.6	22.8	17.7	8.2	20.5	2.3	24.6	20.2	24.0	27.6	15.8	15.5	7.9	4.6	4.6
U	7.3	6.6	5.3	2.4	6.1	0.4	4.1	4.8	3.2	5.1	1.8	1.7	0.7	0.6	0.8
Zr	110.0	180.0	102.0	169.0	148.0	67.0	243.0	216.0	121.0	141.1	144.4	295.5	99.6	152.7	175.8
Hf	3.1	4.8	3.0	4.2	3.8	1.7	7.2	6.3	3.6	4.0	3.8	7.0	2.7	5.1	5.0
Nb	13.3	16.4	12.9	9.7	8.9	4.5	16.2	12.3	14.4	11.8	6.0	8.4	4.9	8.9	11.3
Sn	6.9	8.5	6.9	1.7	1.2	2.0	8.5	5.3	7.0	6.5	2.1	8.5	0.8	1.9	1.6
Ta	0.9	1.3	1.1	0.7	0.6	0.3	1.7	1.6	1.3	1.0	0.6	0.8	0.2	0.5	0.5
Mo	0.9	0.5	1.0	1.3	1.6	1.4	1.1	1.5	0.7	<0.1	2.1	5.4	0.5	< 0.1	< 0.1
Cr	87.0	75.0	90.0	307.0	398.0	179.0	61.0	39.0	113.0	53.0	11.0	45.0	147.0	113.0	177.0
V	81.0	67.0	94. 0	230.0	197.0	285.0	58.0	34.0	103.0	74.0	11.0	40.0	164.0	327.0	321.0
Sc	15.0	12.0	13.0	39.0	28.0	38.0	11.0	6.0	17.0	15.0	4.0	9.0	19.0	47.0	33.0
Cu	*42.0*	*23.0*	*273.0*	95.0	62.0	69.0	53.0	26.0	25.0	1.0	1.0	4.0	*137.0*	*94.0*	*35.0*
Zn	*145.0*	*90.0*	*131.0*	148.0	92.0	64.0	15.0	22.0	45.0	94.0	4.0	40.0	*119.0*	*160.0*	*55.0*
Ag	*4.5*	*1.0*	*0.8*	0.2	0.1	<0.01	<0.01	<0.01	<0.01	<0.01	<0.01	6.4	*26.5*	*2.4*	*15.6*
As	<0.1	4.6	55.5	<0.4	9.5	<0.4	4.6	1.9	1.4	6.7	4.5	8.4	3.8	6.4	4.9
Be	4.0	4.7	4.6	1.6	1.7	1.0	4.1	2.6	4.8	4.2	1.0	2.2	0.9	1.0	0.9
Bi	0.4	0.7	0.6	0.1	0.1	<0.01	0.1	0.3	0.2	0.8	<0.1	0.9	<0.1	0.1	<0.1
Ga	26.5	24.6	23.7	22.1	17.4	16.8	21.4	13.8	29.8	25.5	6.6	10.7	16.3	27.2	27.3
F	723.0	888.0	837.0	737.0	1140.0	723.0	1822.0	1283.0	1690.0	1888.0	512.0	2009.0	266.0	<37	161.0
Ge	1.5	1.7	1.8	2.0	2.9	2.8	1.9	1.8	2.3	1.9	1.0	2.1	1.6	1.6	2.2
Sb	3.1	1.9	8.2	4.6	0.5	0.2	1.5	5.1	1.0	8.3	4.4	4.4	0.8	1.8	7.6
La/Sc	3.3	4.6	4.4	0.5	1.0	0.1	4.4	5.5	3.3	2.8	7.8	7.8	0.6	0.3	0.5
Zr/Sc	7.3	15.0	7.8	4.2	5.2	1.8	22.8	38.9	7.1	9.4	36.1	32.8	5.2	3.2	5.3
Th/Sc	1.3	1.9	1.4	0.2	0.7	0.1	2.2	3.4	1.4	1.8	4.0	1.7	0.4	0.1	0.1
(La/Yb) $_{PAAS}$	1.2	1.3	1.8	0.6	0.8	0.2	1.2	1.1	1.4	1.0	1.4	2.7	0.6	0.4	0.4
Eu/Eu*	0.7	0.8	0.9	0.7	1.5	0.9	0.5	0.5	0.6	0.9	0.9	0.9	1.5	1.5	1.4

Major elements reported in oxide weight per cent, trace elements reported in parts per million, Eu/Eu* = (Eu/1.1)/((Sm/5.6 + Gd/4.7)/2). Subscript PAAS refers t0 PAAS normalised ratios;normalising factors from Taylor and McLennan (1985). Elements in italics and listed here contain contamination from grinding wheel and analysis of the contaminated elements has not been used in this study Fe_2O_3, MnO, Cu, Zn and Ag

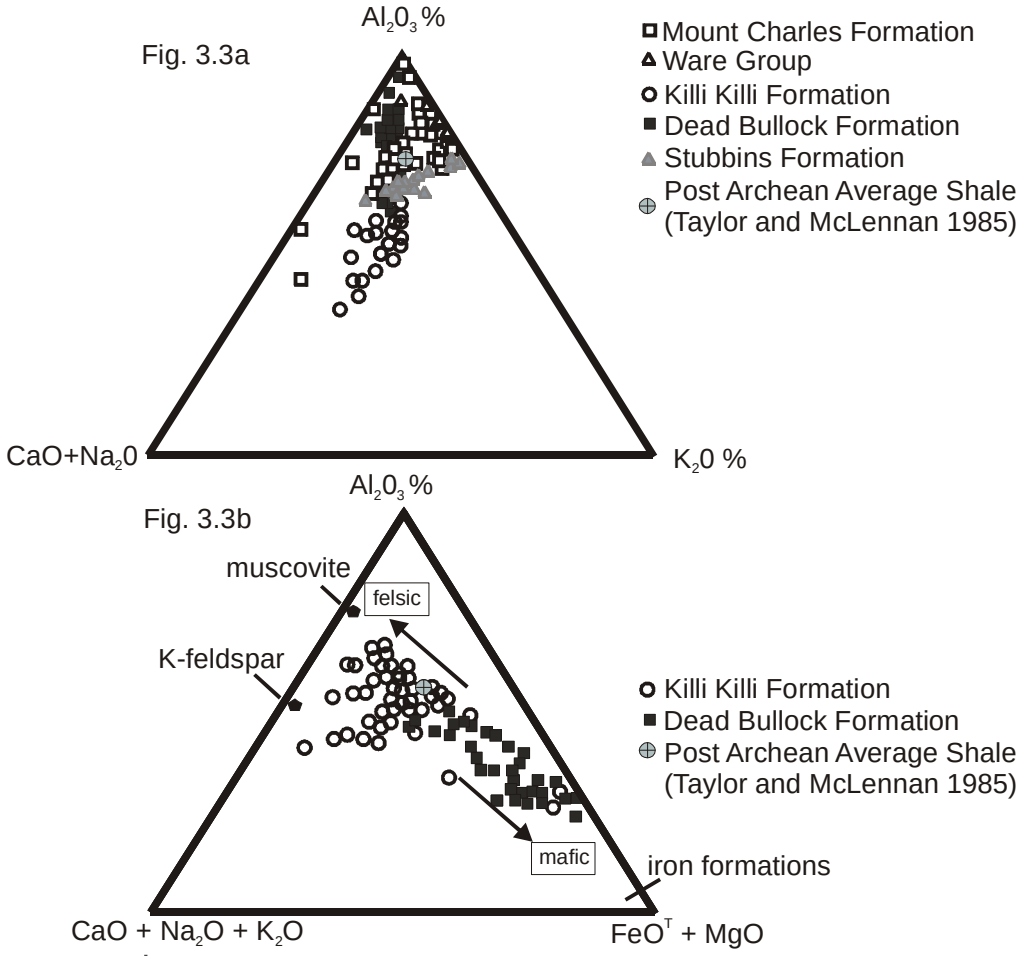

Fig. 3.3 a - Triangular diagram of molecular Al_2O_3–CaO + Na_2O–K_2O (cf. Nesbitt and Young 1984). The gold-bearing Dead Bullock and Mount Charles Formations have high Al_2O_3 and can be distinguished from the less aluminous Stubbins and Killi Formations and Ware Group sedimentary rocks. **b** Triangular diagram of molecular Al_2O_3– (CaO + Na_2O + K_2O)–(FeO^T + MgO) (Nesbitt and Young 1989) showing compositional variations between the Dead Bullock and Killi Killi Formations. The Stubbins and Mount Charles Formations are not shown in this plot due to contamination as described in "Sampling and analytical methods".

Dead Bullock Formation samples contain higher FeO^T + MgO than the Killi Killi Formation samples which are more dominated by muscovite and K-feldspar. Samples from the Stubbins Formation, Ware Group and Mount Charles Formation that were prepared under different laboratory conditions and contain potential Fe contamination as detailed in the methods and the data were excluded in this plot.

Effects of alteration associated with hydrothermal and regional metamorphic processes must be taken into account when defining changes in regional sedimentary provenance in the Tanami region (Williams 2007). Bagas et al. (2008) discussed hypogene alternation in the Tanami region due to either greenschist facies metamorphism or associated mineralising events and showed that the more mobile elements have been affected (e.g. CaO, Na_2O and K_2O). Therefore, to define changes in regional sedimentary provenance using sedimentary geochemistry, selected immobile elements need to be used.

3.3.2 Regional chemostratigraphy

Variations in sedimentary provenance can be used to understand geological evolution of regions (e.g. Prame and Pohl 1994; Slack and Stevens 1994; Dabard et al. 1996; Garzione et al. 1997; Roser et al. 2002). Condie and Wronkiewicz (1990) concluded that the Cr/Th ratio in pelites can provide an important geochemical index of early Precambrian crustal evolution and can be used to monitor changes in source composition with strong correlations to Th/Sc, Sc/Th and La/Sc ratios. The use of rare earth elements (REE) as provenance indicators requires assumptions to be met: (1) They are not significantly modified by metamorphism and diagenesis (Michard 1989; Bau 1991) and (2) that the REE were quantitatively transported in the detrital component (McLennan and Taylor 1982; Crichton and Condie 1993; Ugidos et al. 1997; Robinson et al. 2001).

Sedimentary geochemistry, detrital U–Pb ages and Nd isotopic signatures provide independent tools to help discriminate tectonic setting and sedimentary provenance (e.g. McLennan et al. 1993; González-Álvarez et al. 2006; Payne et al. 2006; Barovich and Hand 2008; McLennan et al. 1995; Yamashita et al. 2000; Goodge et al. 2002; Lahtinen et al. 2002; Tran et al. 2003; 2008). U–Pb geochronology of zircon-bearing sources provides an age spectrum and maximum depositional age of the sediment. Limitations of detrital zircon geochronology discussed by Barovich and Hand (2008) include: (1) loss of small zircons in separation; (2) lack of contribution from fine-grained sources; and (3) lack of contribution from less felsic sources. Once weathering and sorting processes are accounted for (e.g. Cullers and Podkovyrov 2000; López et al. 2005), Sm–Nd studies combined with REE and detrital U–Pb studies record information on the average crustal residence time of sediment from all contributing protoliths and distinguish between mantle-derived igneous and evolved crustal evolved sources. Sm–Nd data, however, are unable to separate individual protolith ages (McLennan et al. 1993). Through a combination of sedimentary geochemistry, detrital zircon U–Pb and Sm–Nd isotope studies, a relatively clear picture of the crustal segments from which the sedimentary package was sourced can be created. Detrital zircon SHRIMP U–Pb ages (Cross and Crispe 2007; Bagas et al. 2008) provide lower and upper age constraints on the regional stratigraphic succession of the Tanami Basin.

The geochemical and REE data for each of the regional stratigraphic units are presented in Table 3.1 and Figs. 3.4, 3.5, 3.6 and 3.7. The Callie composite section from Lambeck et al. (2008) and a new composite section for the Mount Charles Formations are

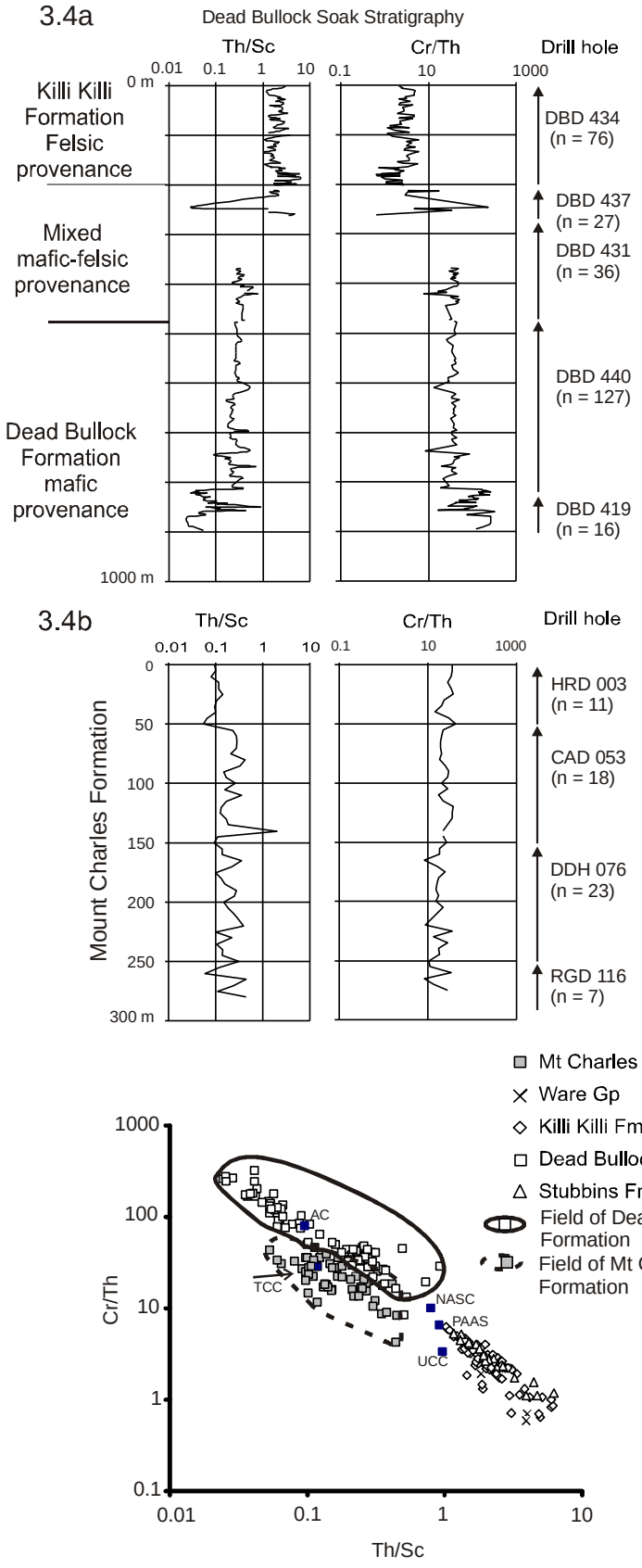

Fig. 3.4 Downhole unsmoothed curves for Th/Sc and Cr/Th values for Dead Bullock Soak *(DBS)* composite core (a) (Lambeck et al. 2008) and Mount Chales composite core (b). The Th/Sc and the Cr/Th values for DBS show inverse trends. The Killi Killi Formation has high Th/Sc and is assigned a felsic provenance. The Dead Bullock Formation has low Th/Sc and high Cr/Th interpreted to reflect a mafic provenance. The Mount Charles Formation has low Th/Sc values and high Cr/Th abundances also interpreted to have a mafic provenance.

Fig. 3.5 Cr/Th-Th/Sc compositions of the Tanami regional stratigraphy. The Dead Bullock and Killi Killi Formations described in Lambeck et al. (2008) are used as a template for the regional stratigraphy. Black squares are as follows: *AC* Archean crust, *TCC* total continental crust, *NASC* North american shale composition, PAAS Post-Archean average australian shale, *UCC* upper continental crust (Taylor and McLennan 1985)

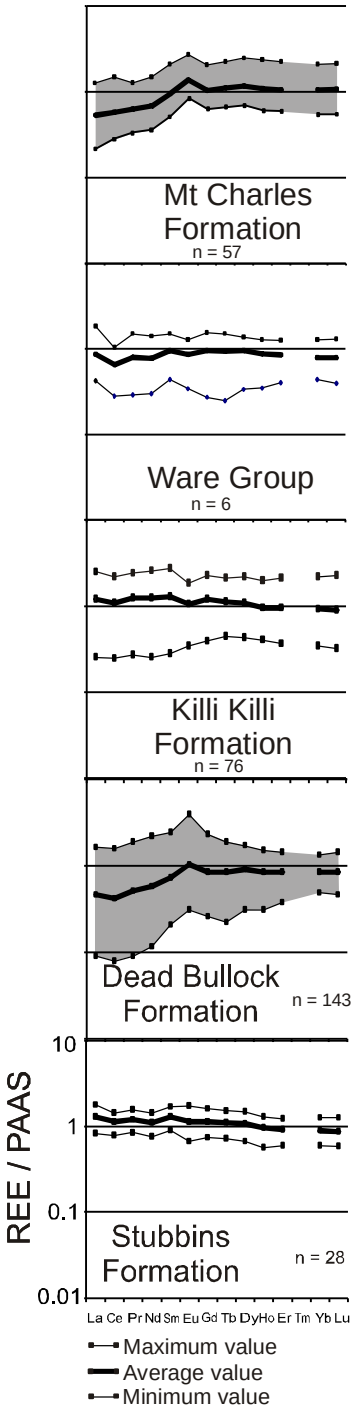

◄ **Fig. 3.6** - REE pattern for each sedimentary regional stratigraphic unit in stratigraphic order normalised to PAAS (Taylor and McLennan 1985). The Dead Bullock and Mount Charles Formations, which are the major gold-bearing units, are charterised by moderate depletion in LREE and highlighted in grey. In contrast, the Stubbins Formation, Killi Killi Formation and Ware Group REE patterns are flat.

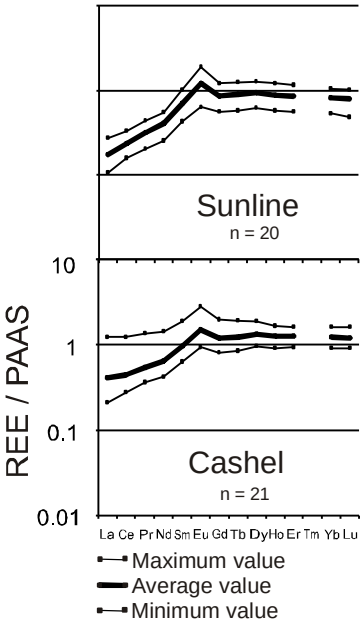

Fig. 3.7 - The Cashel and Sunline prospect REE patterns are characterised by LREE depletion relative to HREE.

presented in Fig. 3.4. Downhole composite plots of Th/Sc and Cr/Th ratios at Dead Bullock Soak and in the Mount Charles Formation show that the Dead Bullock Formation has low Th/Sc and high Cr/Th ratios compared to the Killi Killi Formation. The composite downhole log of the Mount Charles Formation is highlighted by high Cr/Th ratios and low Th/Sc ratios. Data from the Cr/Th-Th/Sc plot distinguish the Dead Bullock Formation and Mount Charles Formations from the remainder of the regional stratigraphy by having Cr/Th values >10 and Th/Sc values <1 (Fig. 3.5). The Dead Bullock and Mount Charles Formations are light REE-depleted, relative to PAAS, and the remainder of the regional stratigraphic units have flat REE patterns (Fig. 3.6), apart from the Cashel and Sunline Prospects which are light REE-depleted (Fig. 3.7).

3.3.3 Stubbins Formation

Twenty-nine geochemical analyses of drill core samples were analysed from the Stubbins Formation which have high Th/Sc ratios (3–6) and low (<100 ppm) Cr abundances and flat REE patterns relative to PAAS (Lambeck et al. 2008). The mixed coarse- to fine-grained sedimentary rocks of the Stubbins Formation have average Cr/Th and Th/Sc ratios of 3.1 and 2.3, respectively (Figs. 3.4 and 3.5). The REE patterns relative to PAAS are flat and almost identical to PAAS, with an average $(La/Yb)_{PAAS}$ value of 1.5; the average Eu anomaly (Fig. 3.6) is 0.8 (Eu/Eu* = (Eu/1.1)/((Sm/5.6 + Gd/4.7)/2). Three initial ε_{Nd} values (calculated at 1,860 Ma) of sedimentary rocks from the Stubbins Formation range between −6.3 and −5.7. Two ε_{Nd} values were calculated for the Stubbins Basalt at 1.4 and 0.6, respectively (Table 3.3 and Fig. 3.8).

3.3.4 Dead Bullock Formation

One hundred and two geochemical analyses were obtained from the Dead Bullock Formation, as defined by Lambeck et al. (2008), and have low Th/Sc ratios (<2), high (>100 ppm) Cr abundances and light REE (LREE)-depleted PAAS normalised REE patterns. The mixed coarse- to fine-grained sedimentary rocks of the Dead Bullock Formation have average Cr/Th and Th/Sc ratios of 63.5 and 0.2, respectively (Figs. 3.4 and 2.5). The REE patterns are light REE-depleted with an average $(La/Yb)_{PAAS}$ value of 0.5; the average Eu anomaly is 1.3 (Fig. 3.6). One initial ε_{Nd} (calculated at 1,860 Ma) of sedimentary rock from the Ferdies Member at the Callie Mine is −6.0 (Table 3.3). Samples assigned to the basal Ferdies Member of the Dead Bullock Formation from the Groundrush area by Crispe et al. (2007) have initial ε_{Nd} values of −10.9 and −9.7 at 1,860 Ma (Fig. 3.8 and Table 3.3). Initial ε_{Nd} values at 1,838 Ma for the Callie Member, Dead Bullock Formation, vary from −6.9 to −6.4. Initial values for the Coora Dolerite, one from about 5 m from the basal contact and one from the middle of the ~200-m-thick dolerite are +1.6 and +1.1, respectively, at 1,838 Ma.

3.3.5 Killi Killi Formation

Twenty-nine geochemical analyses of drill core samples were completed for the Killi Killi Formation. These have high Th/Sc ratios (3–6), low (<100 ppm) Cr abundances and flat REE patterns relative to PAAS (Lambeck et al. 2008). The coarse- to fine-grained sedimentary rocks of the Killi Killi Formation have average Cr/Th and Th/Sc ratios of 2.7 and 2.1, respectively (Figs. 3.4 and 3.5). The REE patterns are flat and almost identical to PAAS with an average $(La/Yb)_{PAAS}$ value of 1.3; the average Eu anomaly is 0.9 (Fig. 3.6). Initial ε_{Nd} (1,840 Ma) values from the Killi Killi Formation range from −6.3 to +3.1 (Fig. 3.8 and Table 3.3).

Table 3.3 Sm-Nd isotope data for selected regional Tanami samples, locations in GDA 94

Sample # (laboratory)	Regional Stratigraphy	Longitude	Latitude	Depth m	Prospect/local name/drill core	Lithology	Age (Ma)	Sm ppm	Nd ppm	$^{147}Sm/^{144}Nd$	$^{143}Nd/^{144}Nd$	2SE	ε_{Nd} (øMa)	ε_{Nd} (t)
2005085051 (A)	Mount Charles Formation	130.94396	-20.522376	140.5	Cashel/002	Sandy Slst.	1810	4.9	18.0	0.1637	0.512276	20	-7.1	+ 0.6
2005085064 (A)	Mount Charles Formation	130.94396	-20.522376	83.0	Cashel /002	Sandy Slst.	1810	7.6	41.0	0.1118	0.511618	20	-19.9	-0.2
2005085083 (A)	Mount Charles Formation	130.084303	-19.566657	178.0	Sunline/HYD003	Sandy Slst.	1810	4.5	17.6	0.1542	0.512138	20	-9.8	+ 0.1
2005085203 (B)	Mount Charles Formation	129.6670772	-20.058092	Outcrop sample from pit	Dinky bouncer	Basalt	1810	4.9	21.5	0.1386	0.512301	8.7	-7.5	+ 6.0
2005085145 (B)	Mount Charles Formation	129.716439	-19.961145	60.7	Hurricane/003	Poorly-sorted c.-Sst.	1810	4.8	20.2	0.1448	0.511703	11.2	-19.2	-7.2
2005085154 (A)	Mount Charles Formation	129.6861808	-20.022533	26.0	Money/RDG116	Poorly-sorted c.-Sst.	1810	7.6	29.6	0.1542	0.512213	20	-8.3	+ 1.6
2005085158 (B)	Mount Charles Formation	129.6861808	-20.022533	111.0	Money/RDG117	Slst.	1810	6.9	27.3	0.1526	0.511945	11.1	-14.5	-4.2
2005085202 (A)	Mount Charles Formation	129.6670531	-20.022433	Outcrop sample from pit	Money/RDG118	Basalt	1810	6.2	23.4	0.1605	0.512098	20	-10.5	-2.1
2005085201 (B)	Mount Charles Formation	129.6670372	-20.022520	Outcrop sample from pit	Southern Pit	Basalt	1810	12.4	46.8	0.1598	0.512138	11.4	-10.9	-2.3
2005085100 (A)	Mount Charles Formation	129.6670772	-20.05809	96.5	Dogbolter/076	Slst.	1810	7.1	37.5	0.1139	0.511451	20.	-23.2	-3.9
2005085116 (B)	Mount Charles Formation	129.6670772	-20.05809	201.8	Dogbolter/076	Poorly-sorted c.-Sst.	1810	4.8	20.8	0.1388	0.511600	8.3	-20.8	-7.4
8749 5001 (B)	Nanny Goat Volcanics	130.080408	-19.107752	Outcrop sample	Ware Group	Felsic Volcanic	1820	1.8	7.5	0.1447	0.511562	16.4	-22.4	-10.3
2005085302 (A)	Ware Group	130.3007753	-18.772307	Outcrop sample	Ware Group	Fine Sst.	1820	7.1	36.5	0.1175	0.511565	20	-20.9	-2.4
2005085 307 (A)	Ware Group	130.1494073	-18.254666	Outcrop sample	Ware Group	Fine Sst	1820	8.1	45.6	0.1073	0.511429	20	-23.8	-2.7
2004085415 (B)	Killi Killi Formation	128.831278	-19.899652	248.2	Coyote CYD050	Poorly-sorted c.-Sst.	1840	5.9	32.7	0.1085	0.509975	8.2	-26.7	-5.6
2004085428 (A)	Killi Killi Formation	128.831676	-19.899966	315.0	Coyote CYD072	Poorly-sorted c.-Sst.	1840	11.1	63.0	0.1067	0.511370	20	*-25.0*	-3.7
2002082007 (A)	Killi Killi Formation	128.831676	-19.899966	200.0	Coyote CYD072	Poorly-sorted c.-Sst.	1840	5.6	31.4	0.1083	0.511365	20	-25.1	-4.2
2004085003 (B)	Killi Killi Formation	129.965654	-20.539965	Outcrop sample	Dead Cat Rock	Poorly-sorted c.-Sst.	1840	8.1	40.8	0.1199	0.509939	13.3	-24.3	-6.3
2004085001 (B)	Killi Killi Formation	129.965654	-20.539965	Outcrop sample	Dead Cat Rock	Poorly-sorted c.-Sst.	1840	6.0	34.5	0.1043	0.411506	20	-22.3	-0.5
2005085301 (B)	Killi Killi Formation	129.546003	-20.23718	Outcrop sample	Apertawonga	Mst.	1840	3.4	22.4	0.0915	0.510296	15.4	-24.1	+ 0.7
2005085300 (A)	Killi Killi Formation	129.545945	-20.23719	Outcrop sample	Apertawonga	Mst.	1840	6.9	50.3	0.0830	0.511430	20	*-23.8*	+ 3.1
2003085079 (A)	Killi Killi Formation	129.953133	-20.508792	181.3	Callie/DBD434	Slst.	1840	7.0	36.4	0.1167	0.511357	20	-25.2	-6.4
2003085089 (B)	Killi Killi Formation	129.953133	-20.508792	136.1	Callie/DBD434	Slst.	1840	4.3	22.5	0.1164	0.509929	7.8	-25.4	-6.5
2003085091 (B)	Killi Killi Formation	129.953133	-20.508792	127.7	Callie/DBD434	V.fine Sst	1840	0.6	3.3	0.1160	0.509925	7.8	-25.5	-6.5
2004085004 (B)	Dead Bullock Formation	129.932398	-20.525999	185.0	Coora Dolerite X885_2088	Dolerite	1840	1.5	5.1	0.1814	0.510342	8.8	-2.0	+ 1.6
2004085005 (B)	Dead Bullock Formation	129.932398	-20.525999	250.0	Coora Dolerite X885_2089	Dolerite	1840	1.6	5.3	0.1847	0.510313	11.6	-1.7	+ 1.1
2003085265 (A)	Dead Bullock Formation	129.914437	-20.533068	327.5	Orac/DBD440	Slst.	1838	4.7	23.2	0.1210	0.511371	20	*-24.7*	-6.9

Table 3.3 (continued)

Sample # (laboratory)	Regional Stratigraphy	Longitude	Latitude	Depth m	Prospect/local name/drill core	Lithology	Age (Ma)	Sm ppm	Nd ppm	$^{147}Sm/^{144}Nd$	$^{143}Nd/^{144}Nd$	2SE	ε_{Nd} (øMa)	ε_{Nd} (t)
2003085142 (A)	Dead Bullock Formation	129.914437	-20.533068	158.3	Upper Blake Beds/DBD440	Mst.	1838	4.3	20.9	0.1254	0.511450	20	-23.2	-6.4
2003085289 (A)	Dead Bullock Formation	129.922206	-20.530549	574.3	Calli Laminated Beds/DBD431	Slst.	1860	13.5	66.3	0.1229	0.511429	20	-23.6	-6.0
2004085327 (A)	Ferdies Member	129.991425	-19.712445	326.0	Groundrush/GHD045	Poorly-sorted c.-Sst.	1860	*6.2*	35.6	0.1045	0.510956	20	-32.8	-10.9
2004085340 (A)	Ferdies Member	129.991425	-19.712445	415.0	Groundrush/GHD045	Poorly-sorted c.-Sst.	1860	6.0	28.9	0.1255	0.511274	20	-26.6	-9.7
2004085464 (A)	Stubbins Formation	128.865741	-19.584874	388.9	Stubbins Formation/BLRCD02	Poorly-sorted m. - Sst.	1860	9.3	48.1	0.1162	0.511364	20	*-19.9*	-5.7
2004085467 (B)	Stubbins Formation	128.864297	-19.589202	205.2	Stubbins Formation/LKD100	Poorly-sorted m. -Sst.	1864	5.5	29.6	0.1125	0.511367	9.6	-25.6	-5.6
2004085504 (B)	Stubbins Formation	128.863563	-19.589147	164.0	Stubbins Formation/LKD54	Poorly-sorted m. -Sst.	1864	5.7	29.8	0.1156	0.511370	8.7	-25.7	-6.3
177280 (A)	Stubbins Formation	128.864297	-19.589202	151.8	Stubbins Formation/BLRCD01	Basalt	1860	2.9	10.9	0.1597	0.512216	20	-8.2	0.6
178804 (B)	Stubbins Formation	128.865741	-19.584874	123.7	Stubbins Formation/BLRCD01	Basalt	1860	4.1	14.5	0.1695	0.512375	20	-5.1	1.4

Mst. mudstone, Slst. siltstone, Sst. sandstone, m.Sst. medium sandstone, c.Sst coarse sandstone. (A) La Trobe University, (B) Adelaide University, 2 SE = 0.511289 ± 0.00002

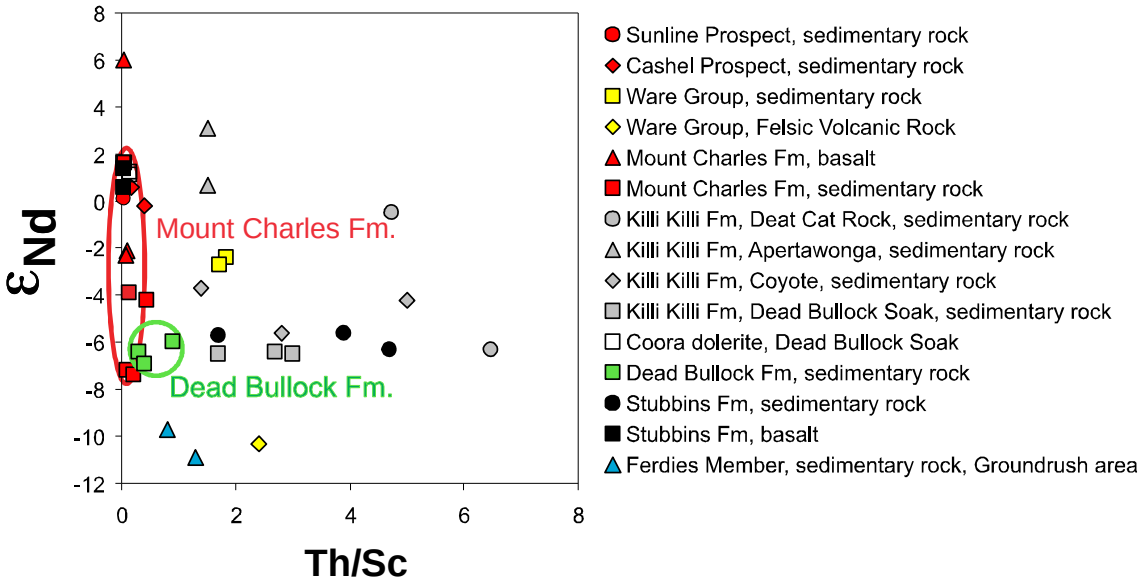

Fig. 3.8 - ε_{Nd} initial values plotted against Th/Sc help differentiate the Tanami regional stratigraphy

3.3.6 Ware Group

Seven outcrop samples were analysed from the Ware Group and have high Th/Sc ratios (3–4), low (<100 ppm) Cr abundances and flat REE patterns relative to PAAS. They include six coarse- to fine-grained sedimentary samples and one felsic volcanic (analysed for Nd isotopes). The fine-grained sandstone samples have an average Cr/Th and Th/ Sc ratios of 1.9 and 2.9, respectively (Figs. 3.4 and 3.5). The REE patterns are flat and almost identical to PAAS with an average $(La/Yb)_{PAAS}$ value of 1.1, and the average Eu anomaly is 0.9 (Fig. 3.6). Two initial ε_{Nd}(1,820 Ma) values from the Ware Group are −2.4 and −2.7. The felsic Nanny Goat Volcanics have an ε_{Nd}(1,820 Ma) value of −10.3 (Fig. 3.8 and Table 3.3).

3.3.7 Mount Charles Formation

Fifty-seven geochemical analyses of drill core samples were completed for the Mount Charles Formation. These have low Th/Sc ratios (<2) and high (>100 ppm) Cr abundances. The poorly sorted coarse- to fine-grained sedimentary rocks have average Cr/Th and Th/Sc ratios of 22.2 and 0.2, respectively (Figs. 3.4 and 3.5). The REE patterns are light REE-depleted relative to PAAS with an average $(La/Yb)_{PAAS}$ value of 0.5, and the average Eu anomaly is 1.4 (Fig. 3.6). ε_{Nd}(1,810 Ma) values range from −7.2 to 1.6, which suggests that there is a large range of crustal residence ages in the source materials for the sedimentary rocks. Three ε_{Nd}(1,810 Ma) values from basalts within the Mount Charles Formation are −2.3, −2.1 and +6.0. The fine-grained sedimentary rocks of the Cashel and Sunline Prospect sampled by Lambeck et al. (2008) have average Cr/Th ratios of 45.8 and 238, respectively, low Th/Sc and $(La/Yb)_{PAAS}$ values and Eu anomalies of ~0.9. Three samples from the Cashel and Sunline Prospect have ε_{Nd}(1,810 Ma) values ranging from −0.2 to +0.6.

3.4 Discussion

Groves (1993) suggested that gold deposits in the Tanami region may illustrate the continuum model of lode-gold deposition which was confirmed by Mernagh and Wygralak (2007) who illustrated ore deposition occurring at a range of depths from 1.5 to 11 km. Whilst the Tanami region contains a range in mechanisms of lode-gold deposition, Huston et al. (2007) documented that many of these Tanami lode-gold deposits are hosted by reactive rock units such as carbonaceous siltstone and iron formation. The lode-gold deposits hosted within the Dead Bullock and Mount Charles Formations formed during times of regional extension associated with voluminous mafic and felsic magmatism (Crispe et al. 2007; Huston et al. 2007).

Condie (1997) suggested that mixing of sediments derived from Archean and Paleoproterozoic sources, as documented in Lambeck et al. (2008), could occur in basins adjacent to active continental margins (i.e. back-arc to foreland basin). The tectonic setting and timing of regional extension has been documented by Bagas et al. (2008) who suggested that sedimentary and basalt geochemistry of the Tanami region forms a back-arc basin. Similarly, the Mount Charles Formation was deposited during a period of regional extension, (Stafford Event: Cawood and Korsch 2008) in which turbiditic sedimentary rock and basalt were deposited in the post-rift basin.

The fine-grained facies of the Dead Bullock Formation were interpreted by Lambeck et al. (2008) to have been deposited in a deepwater environment to form ~600 m of well-bedded carbonaceous rocks. These acted as reductants to oxidised metalliferous fluid

that travelled along D5 shears and deposited gold when thick carbonaceous horizons were encountered (Huston et al. 2007; Williams 2007). Gold in the Mount Charles Formation is hosted mainly within basalt, but also present in the base of carbonaceous mudstone units above basalt flows (Huston et al. 2007).

Being able to geochemically discriminate these gold-prospective carbonaceous units within the predominantly fine-grained regional stratigraphy will ultimately help reduce gold exploration risk. Traditionally, coarse-grained sedimentary rocks in the Tanami region have been mapped as Killi Killi Formation, and fine-grained sedimentary rocks and black mudstones have been mapped as Dead Bullock Formation or Mount Charles Formation (Smith et al. 1998). As shown by Lambeck et al. (2008), this criterion is not entirely reliable, and thick black mudstones can be found within the Killi Killi Formation. When gold tonnage (sum of gold resources, production and stockpiles) is calculated for the regional stratigraphy (Table 3.1), the main gold-bearing units of the Dead Bullock and Mount Charles Formations are highlighted containing in excess of 320 tonnes of gold, representing 90% of the known gold in the Tanami region.

3.4.1 Suggested evolution of the Tanami region geochemical variations

In this section, the model of the early Tanami evolution discussed by Cross and Crispe (2007) is assessed using the regional sedimentary geochemical data (Fig. 3.9). Five geochemical events are defined in this paper and discussed in geochronological order starting at the basal geochemical event.

3.4.2 Stubbins Formation: event 1

The stratigraphic relationship of the Stubbins Formation, which is only known in the western Tanami region, is enigmatic within the regional stratigraphy. Based on the ~1,864 Ma depositional age (Bagas et al. 2008), the Stubbins Formation is stratigraphically below the ~1,838 Ma interpreted “tuffaceous sandstone” of the Dead Bullock Formation in the northern Tanami region. It should be noted, however, that both the Stubbins and Killi Killi Formations contain detrital zircon populations with ages between 1,860 and 1,870 Ma; the Dead Bullock Formation only contains detrital zircons older than 2,500 Ma (Bagas et al. 2008; Cross and Crispe 2007).

Samples from the Stubbins Formation have REE patterns that are almost identical to that of PAAS (Fig. 3.6). Small standard deviations for La/Yb_{PAAS} indicate a very homogeneous source. Th/Sc and Cr/Th ratios of ~2.3 and ~3.1, respectively, suggest that the Stubbins Formation is derived from a felsic source (Taylor and McLennan 1985; Condie and Wronkiewicz 1990; McLennan et al. 1990; Lahtinen 2000; Lahtinen et al. 2002). The source must have been strongly evolved, as reflected by the average ε_{Nd}(1,860 Ma) value of approximately −5. Due to the local occurrence of the coarse- to fine-grained siliciclastic rocks, our data support the interpretation of Lambeck et al. (2008) and suggest that the Stubbins Formation was deposited in a restricted basin with a chemically differentiated source (Fig. 3.9). Based on whole rock geochemistry, Bagas et al. (2008) proposed that the basalts in the Stubbins Formation were formed in an extensional setting.

3.4.3 Dead Bullock Formation: event 2

Both the Ferdies and Callie Members of the Dead Bullock Formation are interpreted to have been derived from Archean mafic and felsic rocks on the basis of Th/Sc, Zr/Sc, Cr

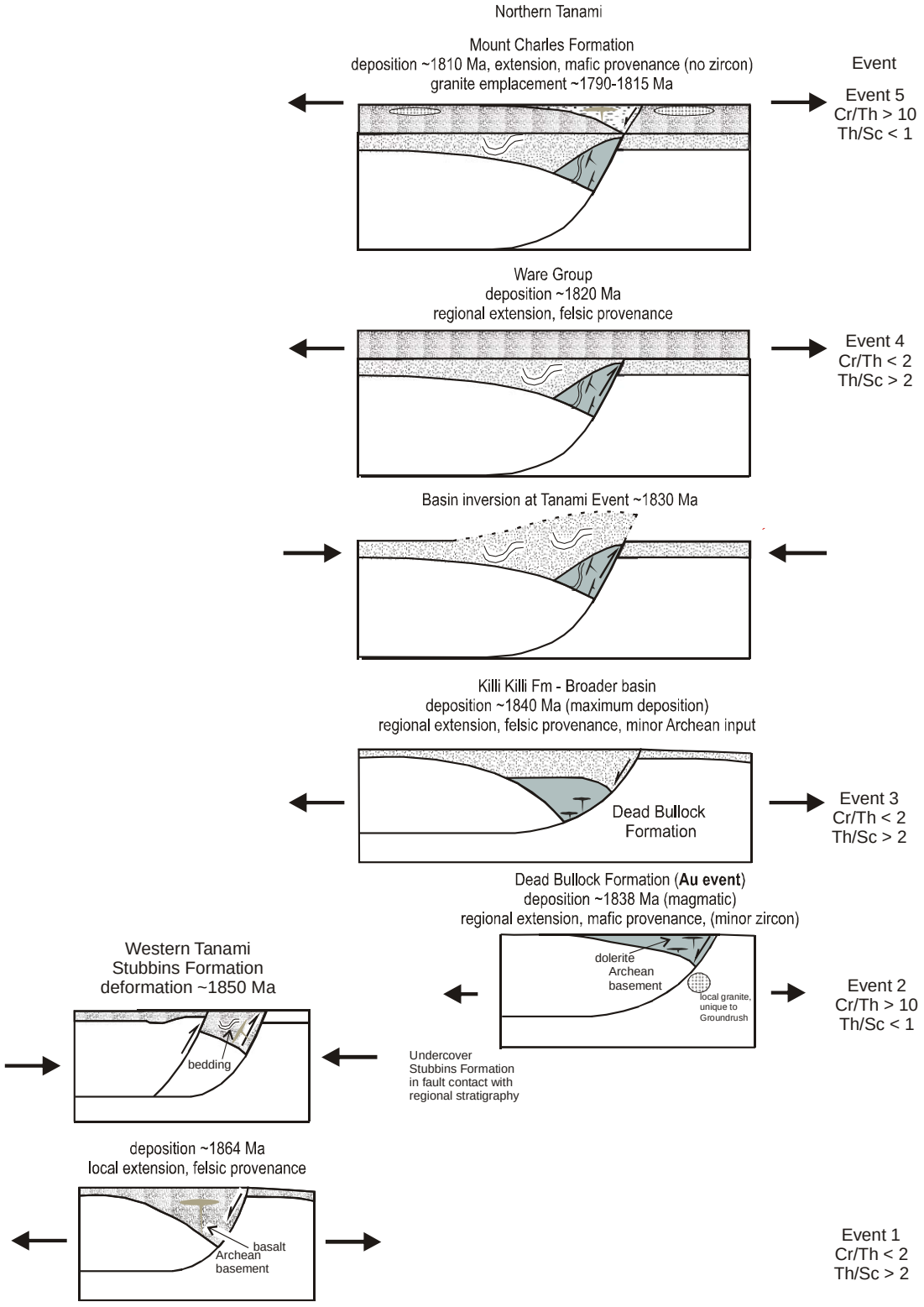

Fig. 3.9 - Schematic tectonic reconstruction models for the five main geochemical events in the Tanami region.

and REE values (Lambeck et al. 2008). The basal Ferdies Member, as represented by samples from the Groundrush area, was derived from an evolved source with ε_{Nd}(1860Ma) approximately −10, and is unique in the Tanami region (Fig. 3.8). The overlying Callie Member also records an evolved source ε_{Nd}(1,840 Ma) approximately −6. Page et al. (1995) used U–Pb ages combined with Nd isotope model ages and whole rock geochemistry to infer the existence of largely concealed late Archean crust in this region. The evolved ε_{Nd} values from the Ferdies and Callie Members (Fig. 3.8 and Table 3.3) support the interpretation of Page et al. (1995) that the source of the sedimentary rocks was dominantly Archean granitic crust. This is consistent with the presence of 2,500, 2,700 and 3,200 Ma zircons in the Dead Bullock Formation (Cross and Crispe 2007).

The source of the sedimentary rocks in the Dead Bullock Formation is not known, but possibilities include Archean provinces in the West Australia Craton or Archean rocks of the Tanami Province. Goleby et al. (2009) suggests that deposition of the Dead Bullock Formation may have occurred during regional extension (Fig. 3.9). The sandy siltstone and black mudstones were probably deposited in a deepwater setting and were derived from a remote Archean mafic and felsic source (Lambeck et al. 2008; Fig. 3.9). The depositional age of the Ferdies Member is poorly constrained between ~2,110 and 1,840 Ma (Cross and Crispe 2007).

3.4.4 Killi Killi Formation: event 3

Lambeck et al. (2008) concluded that the contact between the Dead Bullock and overlying Killi Killi Formations is conformable, but a change in sedimentary source is recorded. The Killi Killi Formation (Th/Sc > 2.1, Table 3.1) was derived from sources with variable crustal residence ages as shown by the wide range of ε_{Nd}(1,840 Ma) values: approximately −6 to +3 (Table 3.3). Detrital U–Pb zircon data (Cross and Crispe 2007) place maximum depositional ages for the Killi Killi Formation at ~1,860 Ma. Lambeck et al. (2008) suggested that black mudstones of Apertawonga are part of the Killi Killi Formation based on high Th/Sc ratios. The most juvenile ε_{Nd} values of the fine-grained turbidites are +1.0 and +3.3 at Apertawonga. These sedimentary rocks are attributed to a relatively local juvenile source not previously recorded in the Tanami region (Table 3.3 and Fig. 3.9). The varied ε_{Nd} values are interpreted to indicate deposition in localised basins. This may be due to the development of separate rift shoulders with poor mixing among canyon slope systems. Sedimentation of the Killi Killi facies was terminated by regional deformation at about 1,840–1,825 Ma.

3.4.5 Ware Group deposition: event 4

Unconformably overlying the Tanami Group sedimentary rocks is the regionally extensive Ware Group, deposited during a time of regional extension at 1,825–1,810 Ma (Cross and Crispe 2007; Fig. 3.9). The highly negative initial ε_{Nd} value from the felsic Nanny Goat Volcanics (−10.3) suggests an evolved source derived from the melting of Archean crust. Figures 3.5 and 3.6 suggest relative enrichment of LREE and Th, and lower Cr values relative to the underlying Dead Bullock and overlying Mount Charles Formations imply a more felsic source component. The shallow water/fluvial sedimentation was halted by uplift resulting from regional deformation and granite plutonism (Crispe et al. 2007).

3.4.6 Mount Charles Formation: event 5

The Mount Charles Formation was deposited at a time of localised extension during the regional Stafford Event (Claoué-Long and Hoatson 2005; Cawood and Korsch 2008; Fig. 3.9). The fine to coarse clastic sedimentary rocks have a low $(La/Yb)_{PAAS}$ ratio of 0.5 interpreted to reflect a relatively mafic source.

The mafic Mount Charles Formation is distinguished from the mafic Dead Bullock Formation by Cr/Th ratios (Fig. 3.4). Initial ε_{Nd} isotopic values for both units can also help differentiate between them (Fig. 3.8). The Dead Bullock Formation has ε_{Nd}(1,860 Ma) of approximately −6, whereas the Mount Charles Formation yields a range of ε_{Nd} values from approximately −7 to +1.6 at 1,810 Ma. The ε_{Nd} (1,838 Ma) values from the dolerite units within the Dead Bullock Formation are approximately +1 compared to ε_{Nd} values from the Mount Charles Basalts which range from −2.1 to +6.0. Nd isotope data from the Dead Bullock Formation support derivation from a long-lived mantle source. ε_{Nd} values from sedimentary rocks of the Mount Charles Formation range from −7.2 to +1.6 at 1,810 Ma and may indicate a mixed source of Archean and Proterozoic mafic–felsic volcanic rocks.

3.5 Implications for gold exploration

The gold-prospective Dead Bullock and Mount Charles Formations cannot be distinguished in hand specimen from other regional stratigraphic units, but can be identified using whole rock, trace element and Nd isotopic values. Figure 3.5 shows that the Dead Bullock and Mount Charles Formations have lower Th/Sc and higher Cr/Th ratios than the Stubbins and Killi Killi Formations and Ware Group, which we interpret to indicate a more mafic source. Although gold is known in most units in the Tanami region, the largest deposits are hosted by the Dead Bullock and Mount Charles Formations, probably because these units were more effective as chemical trap rocks (Huston et al. 2007; Bagas et al. 2008). To illustrate the relationship between chemostratigraphy and gold mineralisation, the Cr/ Th, Th/Sc, $(La/Yb)_{PAAS}$ and Eu/Eu* values for each regional stratigraphic unit are plotted relative to gold tonnage (Fig. 3.10a–d). The Sm–Nd data from the Tanami regional stratigraphy are shown in Table 3.3. The data presented above suggest that geochemical parameters can be used to identify the more fertile Dead Bullock and Mount Charles Formations. These diagrams show that in the Tanami region, geochemical signatures can be used to discriminate more prospective hosts which display Cr/Th > 10, Th/Sc < 1, $(La/Yb)_{PAAS}$ < 1 and positive or negative Eu anomalies. The “mafic” Dead Bullock and Mount Charles Formations can be distinguished by Cr/Th and initial ε_{Nd} values.

The Sunline and Cashel Prospects contain high Cr values (>110 ppm), low Th/Sc ratios (<1) (Lambeck et al. 2008 (Lambeck et al. 2008) and are LREE-depleted (Fig. 3.7). The whole rock and trace element data from the Cashel and Sunline prospects, combined with initial ε_{Nd} isotopic values, suggest that the prospects are hosted by the Mount Charles Formation (Figs. 3.7 and 3.9 and Table 3.3). These results suggest new prospects for further exploration within possible Mount Charles stratigraphy. Whereas potential ore-bearing stratigraphy has been identified, detailed work is still required to find prospective chemical traps (cf. Huston et al. 2007; Williams 2007). At this stage, Dead Bullock Formation has only been identified at Callie and possibly at Titania (Lambeck et al. 2008).

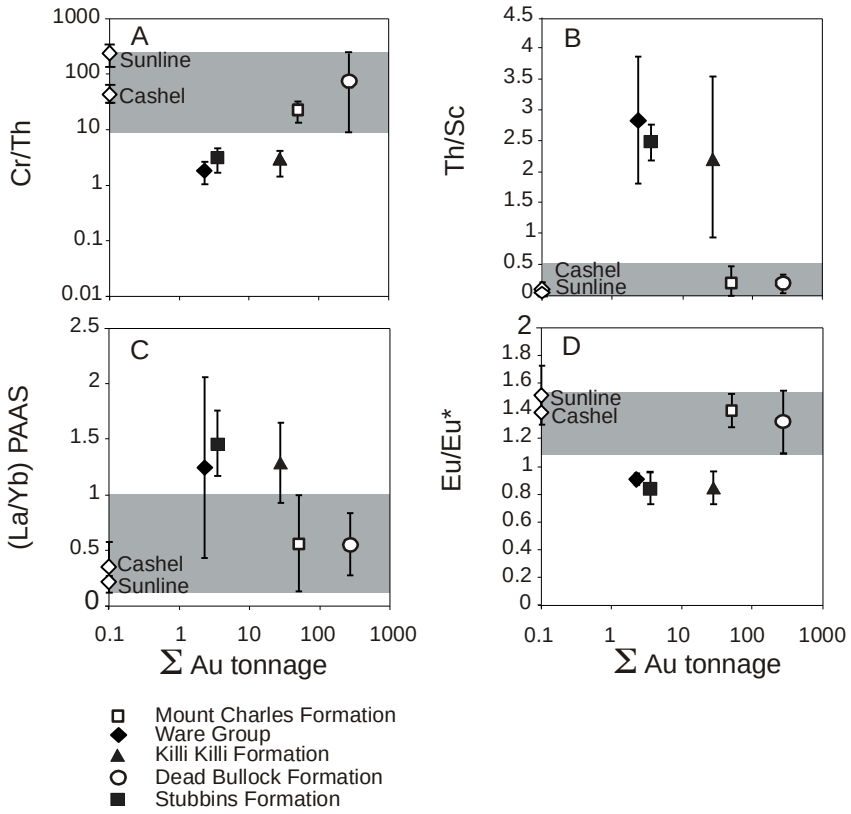

Fig. 3.10 a - Total gold tonnage plotted against Cr/Th. For this case, total gold tonnage was calculated as the sum of gold resources, production and stockpile; error bars show ±1 standard deviation. Major gold-bearing formations are shaded in grey. Dead Bullock and Mount Charles Formations are clearly distinguished by Cr/Th values > 10. **b** Gold Tonnage plotted against Th/Sc; the Dead Bullock and Mount Charles Formations are distinguished by Th/Sc Values < 1. **c** Gold Tonnage plotted against $(La/Yb)_{PAAS}$ further highlights the division of the regional stratigraphy in respect to gold mineralisation. **d** Gold Tonnage plotted against Eu/Eu*. samples from Sunline and Cashel Prospects fall within the same range as the Dead Bullock and Mount Charles Formation.

Linking the geochemical and geochronological methodology in this way permits development of an enhanced paleogeographic model and provides a new regional exploration strategy for the Tanami region. The geochemical approach discussed in this paper can be applied to other Proterozoic terrains, though the individual diagnostic geochemical features (i.e. specific REE patterns, $(La/Yb)_{PAAS}$ values, Th/Sc values, Cr/Th values and ε_{Nd}) discussed in this paper are clearly terrain-specific.

3.6 Conclusions

Gold-prospective stratigraphy in the Tanami region can be identified in deepwater turbidite facies, within which rocks derived from sediments deposited under anoxic conditions form a reductant for the oxidised gold-bearing fluid. The gold-prospective black carbonaceous stratigraphy can be geochemically identified from other non-gold-bearing stratigraphy by Cr/Th ratios combined with Th/Sc values, La/Yb_{PAAS} ratios and the Eu anomaly. The ε_{Nd} values may also provide important geochemical indicators of basin evolution and deepwater facies in the Tanami region.

Our results from the Tanami region indicate that a series of events occurred over more than 50 Ma. The data suggest that these were a series of separate events involving extension and contraction. Of the sedimentary units formed during these events, the Dead Bullock and the Mount Charles Formations contain the largest gold resource and are geochemically characterised by:

1. High Cr/Th values (>10);
2. Low Th/Sc values (<1);
3. Low $(La/Yb)_{PAAS}$ (<1);
4. Eu anomaly + or −; and
5. ε_{Nd} values that assist in defining stratigraphic position.

The geochemical techniques described may assist the exploration for lode-gold deposits in other basins. Identifying the deepest parts of sedimentary basins and discriminating the prospective stratigraphy using the sort of geochemical proxies discussed in this paper could reduce exploration risk. Geochemically discriminating deepwater facies such as thick carbonaceous horizons within the poorly exposed Tanami region can help in the discrimination of prospective packages. The Sunline and Cashel Prospects contain geochemical evidence of a mafic provenance similar to that of the highly prospective Mount Charles Formation.

3.7 Acknowledgements

This work could not have been carried out without support and assistance from Newmont Australia and Tanami Gold. Many thanks are given to Chris Campbell from Newmont for his continued support during this project and to Cathy Crowther from Newmont for her help and enthusiasm in sampling the Mount Charles Formation. We are grateful to Tim Smith, Jim Anderson and Luc English from Tanami Gold for their help in gathering samples. The Northern Territory Geological Survey also provided logistical, support and Andrew Crispe and Leon Vandenberg provided many useful discussions. At Geoscience Australia, much help was received; many thanks to David Champion, Nick Williams and Natalie Kositcin for their discussions, advice and reviews. Many thanks to John Pyke, Bill Pappas, Liz Webber and Mike Smith for sample preparation and geochemical analyses. We are grateful to Martin Hand from Adelaide University and Russell Korsch from Geoscience Australia who critically read

an earlier version of the manuscript and two anonymous reviewers who greatly helped in improving the manuscript. Many thanks to David Bruce at Adelaide University and Graeme Luther and John Webb from La Trobe University for Sm–Nd analysis.

3.8 References

Bagas L, Anderson JAC, Bierlein FP (2009) Palaeoproterozoic evolution of the Killi Killi Formation and orogenic gold mineralization in the Granites-Tanami Orogen, Western Australia. Ore Geology Reviews 35: 47-67.

Bagas L, Bierlein FP, English L, Anderson JAC, Maidment D, Huston DL (2008) An example of a Palaeoproterozoic back-arc basin: Petrology and geochemistry of the ca. 1864 Ma Stubbins Formation as an aid towards an improved understanding of the Granites-Tanami Orogen, Western Australia. Precambrian Research 166: 168-184.

Barovich K, Hand M (2008) Tectonic setting and provenance of the Paleoproterozoic Willyama Supergroup, Curnamona Province, Australia: Geochemical and Nd isotopic constraints on contrasting source terrain components. Precambrian Research 166: 318-337.

Bau M (1991) Rare-earth element mobility during hydrothermal and metamorphic fluid-rock interaction and the significance of the oxidation state of europium. Chemical Geology 93: 219-230.

Bierlein FP, Fuller T, Stüwe K, Arne DC, Keays RR (1998) Wallrock alteration associated with turbidite-hosted gold deposits. Examples from the Palaeozoic Lachlan Fold Belt in central Victoria, Australia. Ore Geology Reviews 13: 345-380.

Blake D, Hodgson I, Muhling P (1979) Geology of The Granites-Tanami Region. Bureau of Mineral Resources, Australia, Canberra Bulletin 197.

Blake D, Hodgson I, Smith P (1975) Geology of the Birrindudu and Tanami 1:250 0000 Sheet Areas, Northern Territory. Bureau of Mineral Resources, Australia, Canberra Report 174.

Cawood PA, Korsch RJ (2008) Assembling Australia: Proterozoic building of a continent. Precambrian Research 166: 1-35.

Claoué-Long J, Cross A, Smith J (2001) NTGS-AGSO Geochronology Project, Report 4. AGSO Record 2001/06.

Claoué-Long JC, Hoatson DM (2005) Proterozoic mafic-ultramafic intrusions in the Arunta Region, central Australia: Part 2: Event chronology and regional correlations. Precambrian Research 142: 134-158.

Condie KC (1997) Plate Tectonics and Crustal Evolution. Heinemann, Butterworth.

Condie KC, Wronkiewicz DJ (1990) The Cr/Th ratio in Precambrian pelites from the Kaapvaal Craton as an index of craton evolution. Earth and Planetary Science Letters 97: 256-267.

Crichton JG, Condie KC (1993) Trace elements as source indicators in cratonic sediments; a case study from the early Proterozoic Libby Creek Group, southeastern Wyoming. J. Geol 101: 319-332.

Crispe AJ, Vandenberg LC, Scrimgeour IR (2007) Geological framework of the Archaean and Palaeoproterozoic Tanami Region, Northern Territory. Mineralium Deposita 42: 3-26.

Cross A, Crispe AJ (2007) SHRIMP U-Pb analyses of detrital zircon: A window to understanding the Palaeoproterozoic development of the Tanami Region, northern Australia. Mineralium Deposita 42: 27-50.

Cullers RL, Podkovyrov VN (2000) Geochemistry of the Mesoproterozoic Lakhanda shales in southeastern Yakutia, Russia: implications for mineralogical and provenance control, and recycling. Precambrian Research 104: 77-93.

Dabard MP, Loi A, Peucat JJ (1996) Zircon typology combined with Sm---Nd whole-rock isotope analysis to study Brioverian sediments from the Armorican Massif. Sedimentary Geology 101: 243-260.

Dean A (2001) Igneous rocks of the Tanami Region. Northern Territory Geological Survey Record 2001-003.

Eggins SM, Woodhead JD, Kinsley LPJ, Mortimer GE, Sylvester P, McCulloch MT, Hergt JM, Handler MR (1997) A simple method for the precise determination of >40 trace elements in geological samples by ICPMS using enriched isotope internal standardisation. Chemical geology 134: 311-326.

Garzione CN, Patchett JP, Ross GM, Nelson J (1997) Provenance of Paleozoic sedimentary rocks in the Canadian Cordilleran miogeocline: a Nd isotopic study. Canadian Journal of Earth Sciences 34: 1603-1618.

Goleby BR, Huston DL, Lyons P, Vandenberg L, Bagas L, Davies BM, Jones LEA, Gebre-Mariam M, Johnson W, Smith T, English L (2009) The Tanami deep seismic reflection experiment: An insight into gold mineralization and Paleoproterozoic collision in the North Australian Craton. Tectonophysics 472: 169-182.

González-Álvarez I, Agnieszka Kusiak M, Kerrich R (2006) A trace element and chemical Th-U total Pb dating study in the lower Belt-Purcell Supergroup, Western North America: Provenance and diagenetic implications. Chemical Geology 230: 140-160.

Goodge J, Myrow P, Williams I, Bowring S (2002) Age and provenance of the Beardmore Group, Antarctica: Constraints on Rodinia Supercontinent break up. Journal of Geology 110 (4): 393-406.

Groves DI (1993) The crustal continuum model for late-Archæan lode gold deposits of the Yilgarn block, Western Australia. Mineralium Deposita 28: 366-374.

Hendrickx MA, Slater K, Crispe AJ, Dean AA, Vanderberg LC, Smith J (2000) Paleoproterozoic stratigraphy of the Tanami Region: regional correlations and relation to mineralization-preliminary results. Northern Territory Geological Survey Record 2000-13.

Hodgson C (1993) Mesothermal lode gold deposits. Geol Assoc Can (Special Paper) 40: 635-678.

Huston D, Wygralak A, Mernagh T, Vandenberg IC, Crispe AJ, Lambeck A, Bagas L, Cross A, Fraser G, Williams N, Worden K, Meixner T (2007) Lode gold mineral systems of the Tanami Region, northern Australia. Mineralium Deposita 42: 175-204.

Lahtinen R (2000) Archean-Proterozoic transition: geochemistry, provenance and tectonic setting of metasedimentary rocks in central Fennoscandian Shield, Finland. Precambrian Research 104: 147-174.

Lahtinen R, Huhma H, Kouse J (2002) Contrasting source components of the Palaeoproterozoic Svecofennian metasediments: Detrital zircon U-Pb, Sm-Nd and geochemical data. Precambrian Research 116: 81-109.

Lally J, Worden K (2004) Geochronology in the Pine Creek Orogen-new results from NTGS. Annual Geoscience Exploration Seminar (AGES 2004) Record of Abstracts, Northern Territory Geological Survey Record 2004-001.

Lambeck A, Huston D, Maidment D, Southgate P (2008) Sedimentary geochemistry, geochronology and sequence stratigraphy as tools to typecast stratigraphic units

and constrain basin evolution in the gold mineralised Palaeoproterozoic Tanami Region, Northern Australia. Precambrian Research 166: 185-203.

López JMG, Bauluz B, Fernández-Nieto C, Oliete AY (2005) Factors controlling the trace-element distribution in fine-grained rocks: the Albian kaolinite-rich deposits of the Oliete Basin (NE Spain). Chemical Geology 214: 1-19.

McLennan SM, Hemming S, McDaniel DK, Hanson GN (1993) Geochemical approaches to sedimentation, provenance and tectonics Geological Society of America Special Paper 284. pp 21-40.

McLennan SM, Hemming SR, Taylor SR, Eriksson KA (1995) Early Proterozoic crustal evolution: Geochemical and Nd---Pb isotopic evidence from metasedimentary rocks, southwestern North America. Geochimica et Cosmochimica Acta 59: 1153-1177.

McLennan SM, Taylor SR (1982) Geochemical constraints on the growth of the continental crust. Journal of Geology 90: 347-361.

McLennan SM, Taylor SR, McCulloch MT, Maynard JB (1990) Geochemical and Nd---Sr isotopic composition of deep-sea turbidites: Crustal evolution and plate tectonic associations. Geochimica et Cosmochimica Acta 54: 2015-2050.

Mernagh TP, Wygralak AS (2007) Gold ore-forming fluids of the Tanami region, Northern Australia. Mineralium Deposita 42: 145-173.

Michard A (1989) Rare earth element systematics in hydrothermal fluids. Geochimica et Cosmochimica Acta 53: 745-750.

Myers J, Shaw R, Tyler I (1996) Tectonic evolution of Proterozoic Australia. Tectonics 1: 1431–1446.

Nesbitt HW, Young GM (1984) Prediction of some weathering trends of plutonic and volcanic rocks based on thermodynamic and kinetic considerations. Geochimica et Cosmochimica Acta 48: 1523-1534.

Nesbitt HW, Young GM (1989) Formation and Diagenesis of Weathering Profiles. The Journal of Geology 97: 129-147.

Norrish K, Chappell BW (1977) X-ray fluorescence spectrometry. Academic Press, London.

Norrish K, Hutton JT (1969) An accurate X-ray spectrographic method for the analysis of a wide range of geological samples. Geochimica Cosmochimica Acta 33: 431-453.

Page RW, Sun S-S, Blake D (1995) Geochronology of an exposed late Archæan basement terrane in The Granites-Tanami region. AGSO Research Newsletter 22: 19-20.

Payne J, Barovich K, Hand M (2006) Provenance of metasedimentary rocks in the northern Gawler Craton, Australia: Implications for Palaeoproterozoic reconstructions. Precambrian Research 148: 275-291.

Plumb K, Ahmad M, Wygralak AS (1990) Mid-Proterozoic basins of the North Australia Craton-regional geology and mineralisation In: Hughes F (ed) Geology of the Mineral Deposits of Australia and Papua New Guinea. Australasian Institute of Mining and Metallurgy, Mongraph 14, pp 881-902.

Prame WKBN, Pohl J (1994) Geochemistry of pelitic and psammopelitic Precambrian metasediments from southwestern Sri Lanka: implications for two contrasting source-terrains and tectonic settings. Precambrian Research 66: 223-244.

Pyke J (2000) Minerals laboratory staff develops new ICP-MS preparation method. AGSO-Geoscience Australia Research Newsletter 33. Canberra, pp 12-14.

Robinson DM, DeCelles PG, Patchett PJ, Garzione CN (2001) The kinematic evolution of the Nepalese Himalaya interpreted from Nd isotopes. Earth and Planetary Science Letters 192: 507-521.

Roser BP, Coombs DS, Korsch RJ, Campbell JD (2002) Whole-rock geochemical variations and evolution of the arc-derived Murihiku terrane, New Zealand. Geological Magazine 139: 665-685.

Roser BP, Korsch RJ (1986) Determination of tectonic setting of sandstone-mudstone suites using SiO_2 content and Na_2O/K_20 ratio. Journal of Geology 94: 635-650.

Slack JF, Stevens BPJ (1994) Clastic metasediments of the Early Proterozoic Broken Hill Group, New South Wales, Australia: Geochemistry, provenance, and metallogenic significance. Geochimica et Cosmochimica Acta 58: 3633-3652.

Smith ME, Lovett DR, Pring PI, Sando BG (1998) Dead Bullock Soak gold deposits. Aust IMM Monogr 22:449–460 22: 449-460.

Taylor SR, McLennan SM (1985) The continental crust: its Composition and Evolution. Blackwell Scientific.

Tran HT, Ansdell K, Bethune K, Watters B, Ashton K (2003) Nd isotope and geochemical constraints on the depositional setting of Paleoproterozoic metasedimentary rocks along the margin of the Archean Hearne craton, Saskatchewan, Canada. Precambrian Research 123: 1-28.

Tran HT, Ansdell KM, Bethune KM, Ashton K, Hamilton MA (2008) Provenance and tectonic setting of Paleoproterozoic metasedimentary rocks along the eastern margin of Hearne craton: Constraints from SHRIMP geochronology, Wollaston Group, Saskatchewan, Canada. Precambrian Research 167: 171-185.

Traves D (1955) The geology of the Ord-Victoria region, northern Australia. Bureau of Mineral Resources, Australia. Bulletin 27.

Tunks A (1996) Structure and origin of gold mineralization, Tanami Mine, Northern Territory. PhD thesis, University of Tasmania, Hobart.

Tunks A, Cooke D (2007) Geological and structural controls on gold mineralization in the Tanami District, Northern Territory. Mineralium Deposita 42: 107-126.

Ugidos JM, Valladares MI, Recio C, Rogers G, Fallick AE, Stephens WE (1997) Provenance of Upper Precambrian-Lower Cambrian shales in the Central Iberian Zone, Spain: evidence from a chemical and isotopic study. Chemical Geology 136: 55-70.

Wade BP, Hand M, Barovich KM (2005) Nd isotopic and geochemical constraints on provenance of sedimentary rocks in the eastern Officer Basin, Australia: implications for the duration of the intracratonic Petermann Orogeny. Journal of the Geological Society 162: 513-530.

Waight T, Maas R, Nicholls I (2000) Fingerprinting feldspar phenocrysts using crystal isotopic composition stratigraphy: implications for crystal transfer and magma mingling in S-type granites. Contributions to Mineralogy and Petrology 139: 227-239.

Waight TE, Weaver SD, Muir RJ, Maas R, Eby GN (1998) The Hohonu Batholith of North Westland, New Zealand: granitoid compositions controlled by source H20 contents and generated during tectonic tranition. Contributions to Mineralogy and Petrology 130: 225-239.

Williams N (2007) Controls on mineralisation at the world-class Callie gold deposit, Tanami desert, Northern Territory, Australia. Mineralium Deposita 42: 65-87.

Yamashita K, Creaser RA, Villeneuve ME (2000) Integrated Nd isotopic and U-Pb detrital zircon systematics of clastic sedimentary rocks from the Slave Province, Canada: evidence for extensive crustal reworking in the early- to mid-Archean. Earth and Planetary Science Letters 174: 283-299.

Alexis Lambeck

PhD THESIS TITLE

"Basin analysis and the geochemical signature of Paleoproterozoic sedimentary successions in northern Australia: Constraints on basin development in respect to mineralisation and paleoreconstruction models"

CHAPTER 4

ARE IRON-RICH SEDIMENTARY ROCKS THE KEY TO THE SPIKE IN OROGENIC GOLD MINERALIZATION IN THE PALEOPROTEROZOIC?

Lambeck, A.[1,2]
Mernagh, T.P. [2]
Wyborn, L.[2]

[1] Centre for Tectonics Resources and Exploration, University of Adelaide, Adelaide, SA 5005.
[2] Geoscience Australia, GPO Box 378, Canberra, ACT 2601, Australia

Economic Geology – 2011,(3) May, 321-330

NOTE:
Statements of authorship appear on page 76 in the print copy of the thesis held in the University of Adelaide Library.

Chapter 4

Are iron-rich sedimentary rocks the key to the spike in orogenic gold mineralisation in the Paleoproterozoic?

Lambeck, A., Mernagh, T.P., & Wyborn, L. (2011). Are iron-rich sedimentary rocks the key to the spike in orogenic gold mineralisation in the Paleoproterozoic?
Economic Geology, v. 106 (3), pp. 321-330

Alexis Lambeck

PhD THESIS TITLE

"Basin analysis and the geochemical signature of Paleoproterozoic sedimentary successions in northern Australia: Constraints on basin development in respect to mineralisation and paleoreconstruction models"

CHAPTER 5

An abrupt change in Nd isotopic composition in Australian basins at 1650 Ma: implications for the tectonic evolution of Australia and its place in Nuna

Lambeck, A.[1,2]
Barovich, K.[1]
Gibson, G. [2]
Huston, D.,[2]

[1] Centre for Tectonics Resources and Exploration, University of Adelaide, Adelaide, SA 5005.
[2] Geoscience Australia, GPO Box 378, Canberra, ACT 2601, Australia

Precambrian Research – 2011, (submitted)

NOTE:
Statements of authorship appear on page 100 in the print copy of the thesis held in the University of Adelaide Library.

Chapter 5

An abrupt change in Nd isotopic composition in Australian basins at 1650 Ma: Implications for the tectonic evolution of Australia and its place in Nuna

In review as: An abrupt change in Nd isotopic composition in Australian basins at 1650 Ma: implications for the tectonic evolution of Australia and its place in Nuna. Precambrian Research (in review, Precambrian Research)

Abstract

Late Paleoproterozoic sedimentary basins across eastern Australia record a significant change in their neodymium isotopic composition at ca. 1650 Ma. Prior to ca. 1650 Ma, detritus was derived from comparatively evolved sources generating bulk $\varepsilon_{Nd(1650\ Ma)}$ values of generally -8 to -6. Subsequent sedimentary successions, which accumulated between ca. 1650 Ma – 1600 Ma, have bulk $\varepsilon_{Nd\ (1650\ Ma)}$ values of -2 to -1. This change is interpreted to reflect the input of sediments from a new, probable felsic volcanic source, indicating a fundamental change in the tectonic history of Australia. Although the data are not definitive, a possible driver to this change in sedimentary source is the initiation of renewed rifting from 1650 Ma along the eastern margin of Paleoproterozoic Australia. As the 1650-1600 Ma sedimentary successions that record the isotopic change are voluminous, a large, juvenile source of volcanic detritus must have been present, either within Paleoproterozoic Australia or in the cratonic block immediately to the present-day east of Australia in the Nuna supercontinent. Although voluminous juvenile felsic magmatic sources are known in eastern and central Australia (e.g. 1639 Ma – 1631 Ma volcanics in the Warumpi Province; 1620 Ma – 1610 Ma granites of the St Peter Suite in the Gawler Province), these sources are too young to have acted as a source for the juvenile detritus. Felsic intrusions of ~1650 Ma age are present in the Mount Isa Province, but the known exposed volume is very small. Either a major ~1650 Ma magmatic province has not yet been discovered (or has been lost from the geologic record), or the source of the juvenile detritus lies elsewhere, possibly in once adjacent parts of the Nuna supercontinent of which the Mount Isa region was part.

5.1 Introduction

It is well established that the fill of sedimentary basins preserves a record of tectonism and uplift within their hinterlands even though the source rocks themselves may have long been removed through erosion or tectonic divergence. This statement is no less true for modern sedimentary basins as it is for much older ones of Proterozoic age preserved within the Mt Isa Province and Coen and Georgetown Inliers of northern Australia, and within the Curnamona Province of south-central Australia (Fig. 5.1). Although now variably deformed and metamorphosed, these basins still retain important information about tectonic events affecting large tracts of Proterozoic Australia, including evidence for a 50 Ma felsic magmatic event that occurred intermittently from at least ca. 1690 to 1640 Ma. This magmatism is expressed at several different stratigraphic levels within these basins and takes the form of thin tuff horizons or shallow intrusions, previously described as "pinkites" in the Mount Isa region (Page et

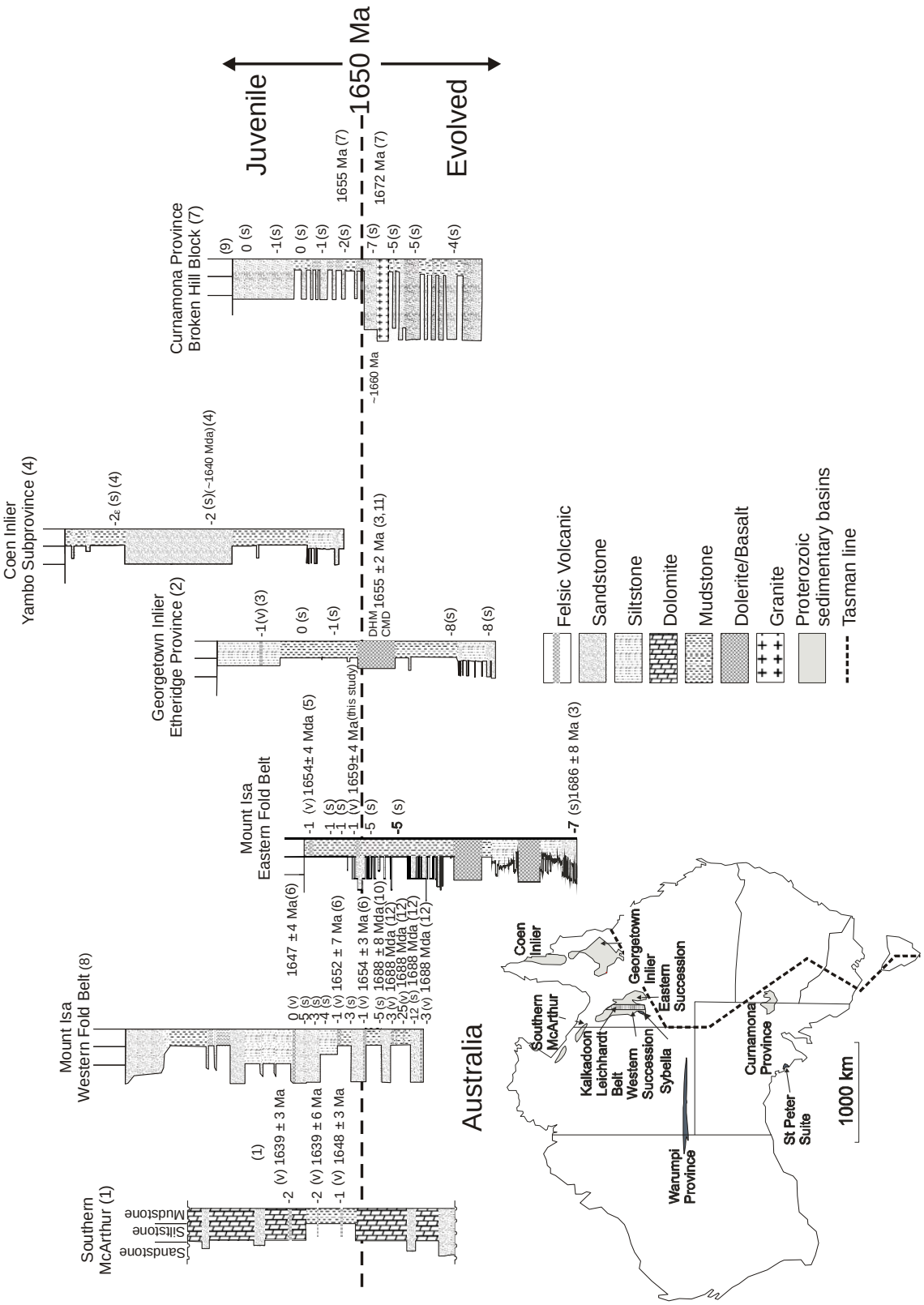
Juvenile
1650 Ma
Evolved
Curnamona Province
Broken Hill Block (7)
1655 Ma (7)
1672 Ma (7)
~1660 Ma
Coen Inlier
Yambo Subprovince (4)
Georgetown Inlier
Etheridge Province (2)
DHM 1655 ± 2 Ma (3,11)
CMD
Mount Isa
Eastern Fold Belt
1647 ±4 Ma(6)
1654± 4 Mda (5)
1659± 4 Ma(this study)
1654 ± 3 Ma (6)
1688 ± 8 Mda(10)
1652 ± 7 Ma (6)
1686 ± 8 Ma (3)
Mount Isa
Western Fold Belt (8)
Southern
McArthur (1)
Sandstone
Siltstone
Mudstone
(1)
(V) 1639 ± 3 Ma
(V) 1639 ± 6 Ma
(V) 1648 ± 3 Ma
Felsic Volcanic
Sandstone
Siltstone
Dolomite
Mudstone
Dolerite/Basalt
Granite
Proterozoic
sedimentary basins
Tasman line
Australia
Coen
Inlier
Georgetown
Inlier
Eastern
Succession
Southern
McArthur
Kalkadoon
Leichhardt
Belt
Western
Succession
Sybella
Curnamona
Province
St Peter
Suite
Warumpi
Province
1000 km

Fig. 5.1 - Regional chronostratigraphic columns in Precambrian eastern Australia showing juvenile felsic input at ca. 1650 Ma. Detrital zircon U-Pb, inferred maximum depositional ages (Mda) and stratigraphic ages (Ma) derived from magmatic rocks, rhyolite and dolerite. Epsilon Nd data on bulk volcanics (v) and bulk sediments (s). DHM = the Dead Horse meta-basalt and CMD = the Cobbold meta-dolerite as described in Black et al. (1998) and Baker et al. (2010). Regional stratigraphic data are from this study and following references marked on figure in brackets Page (1981) (1); Withnall et al., (1988) (2); Black et al., (1998) (3); Blewett et al., (1998) (4); Page and Sun (1998) (5); Page et al., (2000) (6); Page et al., (2005) (7); Southgate et al., (2006) (8); Barovich and Hand (2008) (9); Neumann et al., (2009) (10); Baker et al., (2010) (11); Jackson et al. (2005). Epsilon Nd data for the Curnamona Province is from Barovich and Hand (2008) and one data in the Etheridge Province is from Black and McCullock (1984). Data from the Sybella Granite and Carters Bore Rhyolite are in Table 1.

al., 2000) but now known to include some peperites (Neumann et al., 2006; Gibson et al., 2008). These rocks point to a higher level of ongoing magmatic activity during basin formation than hitherto proposed and thus provide additional clues to the tectonic processes that accompanied basin formation and evolution in Proterozoic Australia.

In particular, these rocks serve as a useful means of correlation between sedimentary sequences where the basins are widely dispersed and separated by large distances. Although detailed correlations of sedimentary successions within individual geological provinces have already been attempted (e.g. Southgate, 2000; Jackson et al. 2005; Neumann et al. 2009), comparisons and correlation between Proterozoic terrains across Australia are much more difficult because large areas of the terrains of interest are under cover, and the host terrains may themselves have undergone different degrees of deformation and metamorphism so that primary sedimentary features and structures are no longer preserved. Here we present Sm-Nd characteristics and U-Pb geochronology of basin fill for late Paleoproterozoic successions in the Mount Isa Province and Georgetown Inlier. These new data, and existing data for the Curnamona Province (Barovich and Hand, 2008) and Coen Inlier (Blewett et al., 1998), record a major influx of juvenile magmatic detritus at ca. 1650 Ma. Based on this evidence, we speculate on the volcanic and tectonic processes that could have provided this detritus.

5.1.1 Geological setting and stratigraphy

The evolution of the interior of the proto-Australian continent between 1800 and 1600 Ma is characterised by the development of numerous intracratonic volcano-sedimentary basins (e.g. Plumb et al., 1990; Eriksson et al., 1993; Southgate et al., 2000; Giles et al., 2002; Betts et al., 2008). A back-arc, dominantly extensional setting for basin development is generally inferred with syn-extensional magmatism, deformation and low-pressure/high-temperature metamorphism linked at higher crustal levels to normal growth faulting and sedimentation (Giles et al., 2002; Betts and Giles 2006; Gibson et al., 2008). Basin fill is dominated by sub-aerial to shallow and deep marine clastic sequences (e.g. Southgate et al., 2000; Neumann et al., 2009).

Three north-south trending tectonic units are recognised in the Mount Isa region. The Western Fold Belt and the Eastern Fold Belt are both predominantly made up of sedimentary rocks whereas the third unit (Kalkadoon-Leichhardt Belt) is older and comprises mainly felsic volcanic and plutonic rocks dated as being no younger than 1850 Ma in age (Blake and Stewart 1992; Bierlein et al., 2008 Fig. 5.1.). The Eastern Fold Belt comprises mainly deep-water sedimentary facies with intercalated mafic sills, interpreted to have developed in a rift environment as part of an extensional system active from ca. 1690 to 1660 Ma (Page and Sun, 1998; Gibson et al., 2008; Rubenach et al., 2008). In contrast, deposition in the Western Fold Belt occurred under fluviatile to near shore to shallow marine conditions, and mainly gave rise to sandstone-dominated sequences in which siltstone, dolostone and black shales are subsidiary components. SHRIMP dating of thin ‘tuffaceous’ beds and detrital zircons constrains the age of this western sedimentary succession to between 1690 and 1660 Ma (Southgate et al., 2000; Jackson et al., 2005).

After ca. 1650 Ma, late-stage rift sediments were deposited across the Mount Isa Province, with sedimentation terminated at ca. 1600 Ma (Betts et al., 2008). These 1650 Ma – 1600 Ma sequences and correlatives in the McArthur Basin further west (Fig. 5.1) contain persistent horizons, interpreted as ash fall tuff, that have been used to constrain deposition ages (Page 1981; Page and Sun 1998; Page et al., 2000).

Siliciclastic successions, interpreted as rift successions, have been identified in the Georgetown Inlier (Etheridge Province), and Curnamona Province (Willis et al., 1983; Withnall et al., 1988; Page et al., 2005). Within the Etheridge Province, syn-depositional mafic igneous rocks of the lower Etheridge Group (Fig. 5.1), were emplaced around ca. 1650 Ma (Black et al., 1998; Baker et al., 2010). Deposition of the upper Etheridge Group is constrained by emplacement of mafic igneous rocks in the lower Etheridge Group (these rock *do not* extend into the upper Etheridge Group), which provides a maximum age of 1655.9 ±2.2 Ma (Black et al (1998), and subsequent regional deformation, which began sometime after 1625 Ma (Cihan et al., 2006). North of the Etheridge Province, the Coen Inlier consists of fine-grained siliciclastic rocks with depositional ages constrained between 1643 Ma and 1585 Ma (Blewett et al., 1998). In southern Australia, basal units in the Curnamona Province were deposited between 1715 Ma – 1672 Ma (Page et al., 2005). These units are overlain by fine-grained siliciclastic rocks, with ages between ca. 1650 Ma and 1590 Ma (Page et al., 2005).

5.1.2 Syn-sedimentary "pinkites" in the Mount Isa Province

Critical to most recent interpretations of basin formation and evolution in the Mount Isa Province is the supposed age and timing of sedimentation as determined by the dating of intercalated igneous rocks and so-called "pinkites". A small body of meta-rhyolite in the Eastern Fold Belt has a crystallisation age of 1654 ± 4 Ma which is interpreted as the minimum stratigraphic age of the Eastern Fold Belt (Page and Sun 1998). New SHRIMP U-Pb dating of a fractionated dolerite sill within the upper Eastern Fold Belt stratigraphy provides a crystallisation age of 1659 ± 4 Ma (Fig. 5.2, Supplementary data at end of this chapter), confirming the minimum stratigraphic age reported by Page and Sun (1998).

No less important in the Western Fold Belt are the published ages of the "tuffites". Initially these rocks, informally called "pinkites", were interpreted as airfall tuffs and, hence, were thought to provide a direct measurement of stratigraphic age (Page et al., 2000). Recent observations suggest a more complicated picture in which at least some of the pinkites are better interpreted as shallow-level felsic sills intruded into wet, as yet unconsolidated sediment. In their original description of Western Succession 1688 Ma 'pinkites', Jackson et al. (2005) reported that these rocks occur as 3 – 10 cm-thick pink, felsic layers within very fine-grained sediment (Fig. 5.3a) and interpreted this layering to represent bedding. Omitted from this description is the important observation that while many tuffites have a sharp, planar lower boundary with the underlying sedimentary host rock (Fig. 5.3b), the upper surface is often irregular, and in some cases clearly brecciated with isolated shards and angular blocks of pinkite disseminated throughout the lower part of the immediately overlying sedimentary bed. Some of these shards and blocks extend for several centimetres into the overlying sediment and have no physical connection with the main body of pinkite. Such relations are more suggestive of formation through an explosive process as occurs during devolatilisation of wet sediment following the introduction of hot magma. Some pinkites are thus better described as peperites with their emplacement ages accordingly reinterpreted as providing a minimum depositional age for their sedimentary host rocks. It is nevertheless evident that in most cases this age will probably be identical to or within a few million years of the true sedimentation age. The more important point in the context of this paper is that these pinkites are sufficiently widely distributed and occur at all stratigraphic levels to provide a robust means of constraining both the age of local sedimentation and the duration of basin formation itself. It is further evident that the

magnitude and volume of peperite formation has an important bearing on the proximity of magmatism. If, as originally interpreted, the pinkites are airfall tuffs, the magmatic source could have been located very far from the Mt Isa Province. However, if these bodies are interpreted, at least in part, as high level intrusions, then magmatism need not be distal but could have occurred within the same region as sedimentation.

Elsewhere in the Mount Isa Province and in the McArthur River Basin, "tuff" layers between 120 cm and 5 m in thickness thick occur in successions with ages between ca. 1650 – 1613 Ma (Page 1981; Page et al., 2000). Although we have not observed these units, they are describe in the literature (Page 1981; Page et al., 2000) as having sharp contacts at the base but gradational contacts with the overlying sediments. These descriptions are indicative of a tuffaceous origin, but, based upon our observations in parts of the Mount Isa Province, it is possible, or even likely, that some of these felsic units could be peperites. Despite this uncertainty in processes, these rocks must have been emplaced penecontemporaneously with sedimentation, probably from a proximal magmatic source.

Less juvenile pinkites occurring at ca. 1680 Ma in the Western Succession (Jackson et al., 2005) intruded into relatively evolved sediment (Table 5.1). In contrast sediments in the Eastern Succession, Georgetown and Coen Inliers by 1650 Ma contain juvenile volcanic detritus (Table 5.1; Blewett et al. 1998). The juvenile detritus records that the influx of volcanism was probably at its peak by ca. 1650 Ma. The decreasing influence westward of juvenile sedimentary detritus (Fig. 5.1) and the thickness of these tuffs is suggestive of a potential volcanic source that is either intracratonic or very proximal to the east or north of Australia at ca. 1650 Ma.

5.2 Sampling and analytical methods

Representative transects to collect sedimentary and volcanic rock covering the age interval 1700 Ma – 1600 Ma were undertaken in the Etheridge Province of the Georgetown Inlier, and in the Eastern and Western Fold Belts of the Mt Isa Province. Representative sandstones and mudstones were sampled in each transect for Sm-Nd analysis (Table 5.1) and added to previously collected samples of felsic volcanic rocks in the Southern McArthur Basin and Western Fold Belt (taken from the Geoscience Australia rock store: (Page 1981; Page et al., 2000 Fig. 5.1). Neodymium isotopes were analysed on selected samples at the University of Adelaide following techniques described in Wade et al. (2006). SHRIMP U-Pb analyses of a metadolerite in the Eastern Succession was completed as part of this study.

Whole-rock geochemistry for tuffaceous samples (pinkites) of Page et al. (1981; 2000), rhyolite of Page and Sun (1998), tuffs/peperites of Jackson et al. (2005) and the dolerite sample (this study) was determined at Geoscience Australia following methods of Jenner et al. (1990) and Pyke (2000) (Table 5.2). Abundances of major and trace elements were determined using X-ray fluorescence (XRF) and inductively coupled plasma mass spectroscopy (ICP-MS) techniques. Major and minor elements (Si, Ti, Al, Fe, Mn, Mg, Ca, Na, K, P and S) were determined by wavelength-dispersive XRF on fused discs using methods similar to those of Norrish and Hutton, (1969). Precision for these elements is better than ±1% of the reported values. Arsenic, Ba, Cr, Cu, Ni, Sc, V, Zn and Zr were determined by pressed pellet on a wavelength-dispersive XRF using methods similar to those described by Norrish and Chappell (1977). Selected trace elements (Cs, Ga, Nb, Pb, Rb, Sb, Sn, Sr, Ta, Th, U and Y) and the rare earth elements

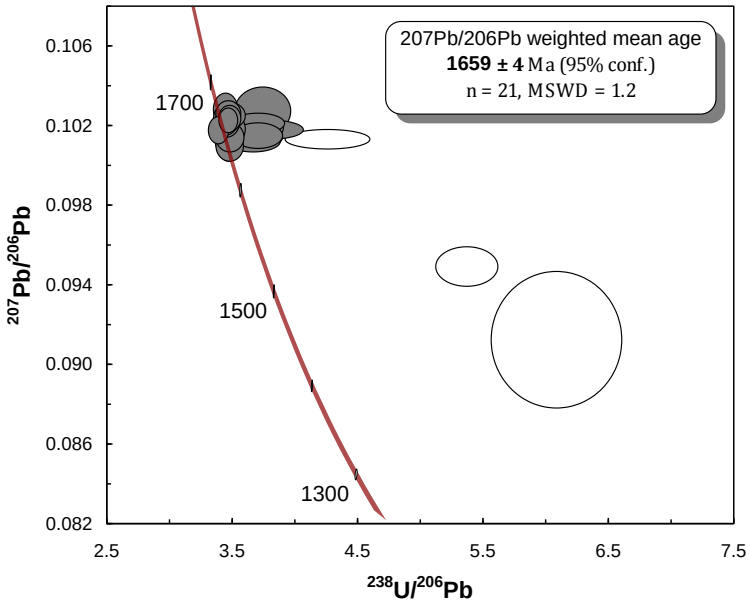

Fig. 5.2 - Tera-Wasserburg Concordia diagram of all zircon analyses from the Eastern Succession Dolerite (2009165033). Three grains more discordant than an arbitrary threshold level of 10 %, represented by open ellipses, are not included in age determination and have been excluded from further consideration.

Fig. 5.3a - Peperite (pinkite) dated by Jackson et al. (2005). Note angular fragments of pinkite in overlying clastic sedimentary layer to left of knife. Esperanza Waterhole.

Fig. 5.3b - Peperite (pinkite) with the upper surface showing irregular, and brecciated contact with overlying sediment. Crocodile Waterhole.

Table 5.1. Sm-Nd isotope data for eastern Australia collected for this work. Stratigraphic ages from 1: Page (1981), 2: Black et al., (1998), 3: Page et al. (2000 and references therein), Neumann et al. (2009, and references therein), 5: Jackson et al., (2005).

Region	Sample #	Formation	Lithology	Easting WGS84 Zone 54	Northing WGS84	Strat age (Ma, ref)	Sm (ppm)	Nd (ppm)	$^{147}Sm/^{144}Nd$	$^{143}Nd/^{144}Nd$ [a]	2S.E.	$\varepsilon_{Nd(0)}$ [b]	$\varepsilon_{Nd}(T)$
Eastern Fold Belt	2006169027	Mt Norna Qzt	Black mudstone	472021	7684709	1680 (4)	5.4	31.8	0.1025	0.511354	9	-25.1	-4.8
Eastern Fold Belt	2006165025	Mt Norna Qzt	Black mudstone	469044	7683286	1680 (4)	4.3	24.4	0.1058	0.511360	9	-24.9	-5.3
Eastern Fold Belt	2009165012	Mt Norna Qzt	Black mudstone	471706	7683721	1655 (3)	10.1	58.4	0.1040	0.511273	11	-26.6	-7.0
Eastern Fold Belt	1945980	Toole Creek Volcanics	Sandy siltstone	570827	7692891	1655 (3)	10.7	65.8	0.0979	0.511532	9	-21.6	-0.6
Eastern Fold Belt	2006165013	Toole Creek Volcanics	Black mudstone	473166	7687257	1655 (3)	5.2	30.7	0.1016	0.511575	9	-20.7	-0.5
Eastern Fold Belt	92208013	Mt Norna Rhyolite	Flow-banded Rhyolite	471900	7663200	1654 (3)	1.3	6.7	0.1181	0.511726	11	-17.8	-1.1
Eastern Fold Belt	2009165033	Toole Creek Volcanics	Dolerite with Gabbro domains	448041	7647452	1658	2.0	5.8	0.2071	0.512714	20	1.5	-0.8
Western Fold Belt	2009165014	Urquhart Shale	Sandy siltstone	340860	7724516	1652 (3)	3.1	17.3	0.1080	0.511505	10	-22.1	-3.3
Western Fold Belt	2009165015	Urquhart Shale	Sandy siltstone	340860	7724416	1652 (3)	3.8	21.4	0.1077	0.511442	10	-23.3	-4.4
Western Fold Belt	2009165020	Kennedy Siltstone	Sandy siltstone	340710	7709480	1652 (3)	7.0	41.8	0.1017	0.511470	8	-22.8	-2.7
Western Fold Belt	2009165049	Lady Loretta Fm	Sandy siltstone	295620	7811762	1647 (3)	3.9	21.8	0.1074	0.511 440	9	-23.4	-4.5
Western Fold Belt	91779005	Urquhart Shale	tuff	340856	7724416	1652 (3)	3.8	25.0	0.0927	0.511440	9	-23.4	-1.4
Western Fold Belt	95779090	Lady Loretta - felsic	tuff	295692	7811922	1647 (3)	10.9	74.1	0.0891	0.511493	12	-22.3	0.4
Western Fold Belt	95779104	Paradise Creek - felsic tuff	tuff	325920	7819872	1654 (3)	4.6	32.5	0.0854	0.511362	20	-24.9	-1.3

Table 5.1 (continued)

Region	Sample #	Formation	Lithology	Easting WGS84 Zone 54	Northing WGS84	Strat age (Ma, ref)	Sm (ppm)	Nd (ppm)	$^{147}Sm/^{144}Nd$	$^{143}Nd/^{144}Nd$[a]	2S.E.	$\varepsilon_{Nd(0)}$ [b]	$\varepsilon_{Nd}(T)$
Western Fold Belt	2008165104	Moondara Slt	Siltstone	352178	7816876	1668 (4)	9.1	49.8	0.1111	0.511431	11	-23.5	-5.3
Western Fold Belt	95779098	Lower Gunpowder Creek Formation	Pinkite	325620	7819772	1688 (5)	8.9	61.4	0.0888	0.511313	50	-25.8	-3.0
Western Fold Belt	2008165068	Prize Supersequence	Pinkite	325479	7819811	1688 (5)	9.6	59.9	0.09877	0.511383	41	-24.5	-3.8
Western Fold Belt	2008165076	Gun supersequence	Pinkite	325933	7819949	1688 (5)	3.4	9.2	0.22524	.511670	39	-18.9	-25.1
Western Fold Belt	2008165077	Gun supersequence	Siltstone	325915	7819948	1688 (5)	1.9	7.0	0.16302	.511644	44	-19.4	-12.3
Georgetown Inlier	2007169006	Heliman Fm	Fine-grained Sst	724837	7944946	1655 (2)	3.8	22.5	0.1021	0.511632	14	-19.6	0.4
Georgetown Inlier	2007169005	Townley Fm	Fine-grained Sst	727953	7945315	1655 (2)	6.6	40.0	0.1001	0.511545	10	-21.3	-0.8
Georgetown Inlier	2007169004	Corbett Fm	Poorly sorted coarse Sst	761665	7880614	1700 (2)	3.5	19.8	0.1074	0.511221	9	-27.6	-8.2
Georgetown Inlier	2007169002	Bernecker Fm	Fine-grained Sst	763956	7877996	1700 (2)	4.4	25.2	0.1049	0.511208	10	-27.9	-7.9
Southern McArthur	91779034	Teena Dolomite	Pink tuff	613853	8177608	1639 (1)	5.5	33.1	0.1006	0.511488	8	-22.4	-2.3
Southern McArthur	91779032	Barney Creek Formation	Tuffaceous felsic shale	617525	8182767	1639 (1)	7.2	35.8	0.1214	0.511783	7	-16.7	-0.9
Southern McArthur	91779042	Tatoola Sandstone	Tuffaceous clastic siltstone	572674	8168788	1648 (1)	12.6	61.0	0.1246	0.511772	6	-16.9	-1.7
Western Fold Belt	2004169015	Guns Knob Granite, central Sybella region	Granite	332902	771552	1674 (4)	10.5	64.6	0.0985	0.511281	10	-26.5	-5.4
Western Fold Belt	2004169018	Widgewarra Granite, southern Sybella region	Granite	330928	7682946	1670 (4)	19.6	108.6	0.1089	0.511414	9	-23.9	-5.1
Western Fold Belt	74205211	Carters Bore Rhyolite	Rhyolite	317700	7745700	1678 (4)	14.1	77.7	0.1099	0.511456	10	-23.1	-4.4

Table 5.1.

a $^{143}Nd/^{144}Nd$ ratios are normalised to $^{146}Nd/^{144}Nd = 0.7219$

b present day $^{143}Nd/^{144}Nd$ (CHUR) = 0.512638 and $^{147}Sm/^{144}Nd$ (CHUR) = 0.1967 (DePaolo and Wasserburg, 1976). The running average for the La Jolla standard is 0.511860 with an uncertainty of 0.5 ε_{Nd}. For all discussion, ε_{Nd} was calculated at 1650 Ma.

Table 5.2. Whole-rock geochemistry of syn-sedimentary "pinkites". Samples from Page (1981; 2000) and geochemical data from this study.

Lithology/ location/ sample number	Tuff, Hilton-Isa 9177-9005	Tuff, Paradise Creek, 9577-9104	Tuff, Paradise Creek, 9577-9101	Tuff, Lady Loretta, 9577-9090	Tuff, River-sleigh Fm, 9610-0501	Tuff, River-sleigh Fm, 9677-9133	tuff, HYC Pyritic Shale Member, 9177-9032	Tuff, Teena Dolomite, 9177-9034	tuffaceous sandstone, Tatoola Sst, 9177-9042	Rhyolite, Eastern Isa, 9220-8013	Dolerite, Eastern Isa 2009-165032	Basalt, Eastern Isa, 2008-165055	Basalt, Eastern Isa, 2008-165056	Basalt, Eastern Isa, 2008-165057	Pinkite, Western Isa 2008-165068	Pinkite, Western Isa 2008-165076
SiO_2	56.25	58.67	60.66	68.89	53.71	65.65	73.99	57.13	69.81	73.28	71.74	46.90	48.23	46.56	59.61	61.64
TiO_2	0.16	0.15	0.27	0.24	0.43	0.21	0.27	0.40	0.36	0.36	0.46	1.38	1.25	1.41	0.17	0.17
Al_2O_3	16.97	10.03	12.42	15.45	23.10	16.10	10.09	13.56	14.28	13.70	12.95	13.77	13.93	13.17	15.78	15.99
Fe_2O_3	1.17	0.13	0.74	1.14	2.28	2.87	1.51	1.01	1.83	2.12	0.62	18.11	14.32	16.91	1.68	1.62
MnO	0.07	0.03	0.05	< 0.005	0.07	0.09	0.21	0.17	0.01	0.03	< 0.005	0.32	0.21	0.31	0.07	0.01
MgO	0.99	4.06	2.79	0.41	2.94	0.16	1.39	2.88	0.87	1.07	0.79	5.80	6.73	6.47	1.06	0.92
CaO	4.43	6.51	4.63	0.03	1.04	0.12	2.17	5.02	0.11	0.55	0.17	9.35	9.80	9.84	3.09	1.74
Na_2O	0.18	0.11	0.14	0.06	0.03	0.20	4.55	0.13	0.15	2.05	0.06	2.55	2.36	2.64	0.17	0.13
K_2O	12.69	8.88	10.44	11.08	8.21	13.58	1.30	11.87	10.40	5.34	3.54	0.32	0.67	0.64	13.79	14.17
P_2O_5	0.03	0.05	0.11	0.04	0.08	0.08	0.09	0.21	0.08	0.05	0.04	0.10	0.09	0.12	0.09	0.05
$C0_2$	4.01	4.10	3.76	0.20	0.20	0.10	3.50	6.62	0.54	–	–	–	–	–	–	–
SO_3	2.90	2.10	1.77	0.11	1.57	0.16	1.13	0.53	1.53	0.26	0.01	0.02	0.04	0.01	0.07	0.02
MLOI	< 0.1	5.10	2.11	2.27	6.38	0.61	< 0.1	0.37	< 0.21	0.98	9.51	1.31	2.29	1.86	4.09	3.40
Total	99.85	99.92	99.89	99.91	100.03	99.93	100.20	99.90	99.97	99.78	99.87	99.94	99.92	99.92	99.66	99.85
Cs	< 3	0.9	1.7	3.96	30.1	2.19	< 3	< 3	< 3	1.14	2.93	0.15	0.15	0.14	1.58	1.73
Ba	1031	927	924	2068	327.9	777.3	236	538	398	1397	608	168	144	95	2314	771
Rb	215	144	189	239	525.6	256.8	39	183	178	147.5	144.6	3.8	30.9	22.7	296.9	202.7
Sr	23	17	21	36.3	14.7	27.4	13	12	19	79.7	39.1	107.9	108.1	74.8	28.1	7.2
Pb	195	5.5	10	6.6	107.5	471.4	34	21	5	14.03	7.25	4.52	2.61	0.87	7	11
La	28	42.2	27.4	68.3	76.8	18.9	35	40	46	38.9	35.5	4.61	6.03	3.85	43.72	7.88
Ce	63	85.2	55.9	153	154.2	42.79	82	94	122	78.22	65.5	10.63	15.37	10.3	129.1	17.94
Pr	7	9.4	6.3	19.44	17.88	6.26	8	10	13	9.46	7.31	1.57	2.07	1.66	15.28	2.02
Nd	24	32.3	22	73.7	63.7	24.4	36	34	62	35.3	27.8	8.45	10.23	9.26	60.08	8.94
Sm	–	5	3.5	11.98	12.5	4.84	–	–	–	6.33	5.22	3.02	3.05	3.5	10.07	3.46
Eu	–	0.6	0.5	1.595	1.333	0.82	–	–	–	0.851	0.698	1.221	1.057	2.024	0.974	0.63
Gd	–	3.7	2.8	6.79	11.71	3.47	–	–	–	4.6	4.81	4.16	3.92	5.25	4.99	3.67
Tb	–	0.6	0.4	0.79	2.15	0.52	–	–	–	0.62	0.77	0.74	0.69	1.02	0.6	0.62
Dy	–	4.1	2.7	4.16	14.04	3.41	–	–	–	3.76	4.85	4.74	4.33	6.37	2.73	4.03
Ho	–	0.9	0.6	0.86	2.96	0.64	–	–	–	0.76	1.03	0.99	0.93	1.33	0.43	0.92
Er	–	3.1	2	2.56	8.73	1.88	–	–	–	2.18	3.11	2.74	2.56	3.72	1.01	2.81
Yb	–	3.2	2.2	2.92	7.83	1.73	–	–	–	2.14	2.88	2.62	2.37	3.7	0.9	2.89
Lu	–	0.5	0.3	0.49	1.27	0.27	–	–	–	0.37	0.49	0.36	0.35	0.55	0.13	0.41
Y	26	29.2	19.6	24.2	80	20.1	52	33	50	21.6	34.8	23.6	18.2	32.4	10.8	30.1

Table 5.2. (continued)

Lithology/ location/ sample number	Tuff, Hilton-Isa 9177-9005	Tuff, Paradise Creek, 9577-9104	Tuff, Paradise Creek, 9577-9101	Tuff, Lady Loretta, 9577-9090	Tuff, River-sleigh Fm, 9610-0501	Tuff, River-sleigh Fm, 9677-9133	tuff, HYC Pyritic Shale Member, 9177-9032	Tuff, Teena Dolomite, 9177-9034	tuffaceous sandstone, Tatoola Sst, 9177-9042	Rhyolite, Eastern Isa, 9220-8013	Dolerite, Eastern Isa 2009-165032	Basalt, Eastern Isa, 2008-165055	Basalt, Eastern Isa, 2008-165056	Basalt, Eastern Isa, 2008-165057	Pinkite, Western Isa 2008-165068	Pinkite, Western Isa 2008-165076
Th	29	16.8	14.2	22.9	73.79	20.9	24	26	27	15.5	11.8	0.3	0.81	0.41	29.17	24.78
U	6	6.2	8.2	5.56	16.18	8.52	6	7	6	2.46	10.2	0.13	0.4	0.16	1.05	6.09
Zr	199	187	180	130	465	106	228	181	227	233	185	67	72	70	41	268
Hf	10	–	–	4.05	14.42	3.65	7	7	8	6.63	4.8	1.98	2.09	2.05	1.46	7.76
Nb	21	10.7	12.9	15.8	33.3	15.5	15	14	17	15.3	15.5	4.3	5.3	4.7	11.6	20.3
Sn	3	< 0.5	1	5.4	11.5	1	< 2	5	4	0.9	0.5	0.8	0.9	1.6	0.7	0.1
Ta	4	0.9	1	1.63	3.27	2.09	< 2	< 2	< 2	0.8	0.89	0.26	0.35	0.29	1.37	1.45
Mo	5	0.3	0.5	< 0.3	< 0.3	2.1	< 2	< 2	4	< 0.3	< 0.3	1.4	0.8	< 0.3	1.1	1.1
Cr	58	5	15	14	< 1	15	10	22	35	11	36	40	182	181	3	4
V	8	6.5	31.5	24	10	29	17	27	29	21	134	417	369	460	2	2
Sc	7	9.5	8	6	10	8	10	12	6	7	9	44	45	50	3	2
Ni	20	4	6	10	3	32	4	3	18	1	21	49	85	86	23	30
Cd	–	–		0.11	0.15	0.6	–	–	–	0.07	0.02	0.08	0.06	< 0.02	0.12	0.05
Cu	2	12	24	94	10	25	15	8	9	16	96	3	15	4	50	2
Zn	2441	5	6	11	86	213	6	44	14	15	57	52	71	69	164	1
Ag	2	< 0.1	0.5	< 0.6	< 0.6	< 0.6	1	2	1	< 0.6	< 0.6	< 0.6	< 0.6	< 0.6	< 0.6	< 0.6
As	24	2.7	7.4	10	88.9	55.6	17	2	31	0.5	5.6	82.7	21	2.5	68.9	66.6
Be	2	0.3	0.8	1.9	9	0.5	< 1	< 1	2	3.9	1.9	1.2	0.5	0.8	< 1	0.4
Bi	< 2	0.2	0.3	0.69	1.73	2.24	< 2	< 2	< 2	0.26	< 0.02	0.29	0.07	0.47	0.23	0.43
Ga	19	6.9	6.7	9.4	29.1	6.4	9	9	13	13	18.2	23.1	19.7	23.3	2.9	12.8
F	–	< 200	677	852	2802	90	–	–	–	448	604	670	422	707	< 200	< 200
Ge	32	1.5	1.1	1.4	3.6	1.4	4	3	6	1.9	< 0.2	1.8	1.3	2.3	0.7	1.2
Sb	–	0.3	1.1	1.6	5.8	2.3	–	–	–	< 0.8	< 0.8	1.6	0.9	< 0.8	3.6	2.9

Major elements reported in oxide weight per cent, trace elements reported in parts per million.

were analysed using ICP-MS (Agilent 7500ce with reaction cell) and following methods similar to those of Eggins et al. (1997). Analyses were obtained by dissolution in distilled HF and HNO3 acid of the fused glass discs (Pyke 2000). Precisions are 5% and 10% at low levels. Agreement between XRF and ICP-MS (Ba, Nb, Pb, Rb, Sr, Y and Zr) are within 10%.

5.3 Trends in Sm-Nd and U-Pb isotope data

Figure 5.1 shows stratigraphic columns from eastern Proterozoic Australia between ca. 1690 Ma and 1600 Ma, with corresponding Nd isotope composition (expressed as ε_{Nd} at 1650 Ma. As ε_{Nd} changes of only ~1 epsilon per 100 million years, the results of the calculations are not affected substantially by using any age within the depositional age range). Prior to ca. 1650 Ma, the Eastern Fold Belt (Mount Isa) is characterised by evolved ε_{Nd} values of ca. -6 and detrital U-Pb spectra dominated by 2600-1680 Ma zircons (Neumann et al., 2009). After ca. 1650 Ma, metasedimentary rocks in the Eastern Fold Belt record more juvenile ε_{Nd} values of ca. -1, a dominant detrital zircon peak at ca. 1650 Ma, and little or no Archean detrital zircons (Page et al., 2000; Carson et al., 2009). The 1659 ± 4 Ma fractionated dolerite (Fig. 5.2; Supplementary data at end of this chapter) and 1654 ± 2 Ma rhyolite (Page and Sun 1998) are characterised by more juvenile ε_{Nd} values of ca. -1. Griffin et al. (2006) record a similar trend in ε_{Hf} values of zircon from stream sediment samples collected specifically from catchments within the Eastern Fold Belt. The zircon data show a greater juvenile input with higher mean ε_{Hf} values after ca 1700 Ma.

The Etheridge Province largely mimics the ε_{Nd} patterns observed in the Eastern Fold Belt. Units older than ca. 1650 Ma (Black et al., 1998 and references therein) have evolved ε_{Nd} values of ca. -8, whereas sedimentary units younger than ca. 1650 Ma are characterized by more juvenile Nd isotope ratios, with ε_{Nd} values of ca. 0 to -1. To the north of the Etheridge Province, ca. 1640 Ma sedimentary units in the Coen Inlier also have relatively juvenile Nd isotopes, with ε_{Nd} values of ca. -2 (Blewett et al., 1998). In southern Australia, the Willyama Supergroup of the Curnamona Province records a similar change in Nd isotopic composition with sedimentary units older than 1650 Ma recording ε_{Nd} values between -7 and -4, whereas rocks younger than 1650 Ma (Paragon Group) are characterised by more juvenile values of -2 to 0 (Barovich and Hand 2008).

Changes in Nd isotopic composition in the Western Fold Belt (Mount Isa) are less systematic (Fig. 5.1). Sedimentary rocks are characterized by relatively uniform, evolved Nd isotopic compositions through the time period for which data are available. Magmatic rocks record more juvenile Nd isotopic compositions of ca. -1. Similar isotopic compositions characterise ca. 1640 Ma felsic tuffs in the southern McArthur Basin (Page 1981 Fig. 5.1, Table 5.1). Two outliers are recorded in the ca. 1680 Ma pinkites in the Western Fold Belt which provide anomalous results of epsilon values of ~ -25 and -12 (Table 5.1).

Although the geochemistry of the ca. 1690 - 1650 Ma felsic magmatic rocks in Proterozoic Australia suggests these rocks have been altered, REEs, which are immobile during most types of alterations, can be used to see though alteration (e.g. Michard 1989; Bau 1991; Robinson et al. 2001). The REEs suggest ca. 1690 - 1650 Ma magmatic rocks from Australia consist of a bimodal magmatic suite of tholeiitic basalts and felsic volcanic rocks (Fig. 5.4, Table 5.2). Tholeiites show flat to very slightly light

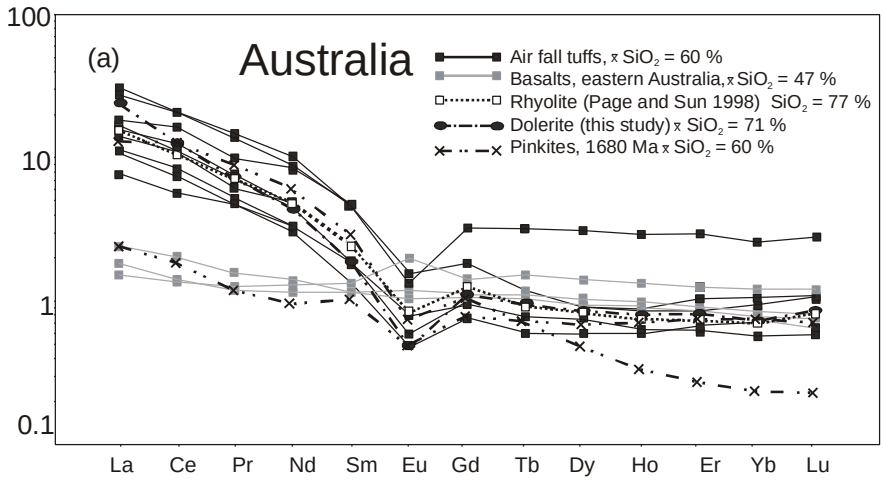

Fig. 5.4 - Rare earth element plots of basalts, tuffaceous airfall deposits and rhyolite, from ca. 1650 Ma – 1620 Ma recorded in Proterozoic Australia (Page 1981; Page and Sun 1998; Page et al., 2000; Jackson et al., 2005). Normalised to NMORB Sun and McDonough (1989).

REE enrichment patterns with no Eu anomaly. In contrast, felsic volcanic rocks are generally all light REE enriched with negative Eu anomalies (Fig. 5.4). The ca. 1680 Ma pinkites first described by Jackson et al. (2005) and further elaborated on here show a range in REE chemistry from light REE enrichment to flat REE patterns. The REE patterns of a 1680 Ma pinkite and proximal siltstone suggest evidence of geochemical disturbance with some loss of the light REE fraction ultimately affecting the epsilon value of the 1680 Ma pinkite and siltstone. The cause of this highly evolved data at ca. 1680 Ma is not fully understood but it is postulated here that it is related to light REE element loss through late alternation caused by mineralizing fluids.

The Sm-Nd data indicate that the isotopic change is most pronounced in the very eastern most parts of Proterozoic Australia, appearing both in the sedimentary and magmatic record. In contrast, further to the west, the change is not apparent in the sedimentary record, although still present in low-volume magmatic and/or volcanic rocks. This suggests that the source of the juvenile sediments was likely located either along the eastern margin of Proterozoic Australia or in cratonic blocks that were contiguous with eastern Australia at around 1650 Ma.

5.4 Tectonic setting of the ~1650 Ma magmatic source

Magmatic activity was well advanced by 1690–1680 Ma and included the intrusion of granites as well as mafic dykes and sills throughout Proterozoic Australia (e.g. Wyborn et al., 1987; Rubenach et al., 2008). An extensional tectonic regime was operating from at least prior to 1690 and to ca. 1640 Ma (Betts and Giles, 2006; Betts et al., 2008; Gibson et al., 2008). Basin formation and resulting sedimentary fill is associated with volcanism and siliciclastic sedimentation within north- to northwest-trending extensional basins throughout Proterozoic Australia (Betts and Giles, 2006). Gibson et al. (2008) further suggested that the 1670 Ma Sybella granite had been partially unroofed and transported upwards from midcrustal levels along major extensional shear zones before 1640 Ma. Bimodal magmatic activity and extension continued to ca. 1640 Ma with intercalations of tuffs/peperites and basalts though out Proterozoic Australia (Fig. 5.1). The voluminous influx of juvenile magmatism in Australia appears to be directly linked with active extension and bimodal volcanism as part of regional Proterozoic rifting in Australia.

The Australian Proterozoic basins appear to broadly follow the simple asymmetric stretching model for basin evolution of (Lister et al., 1986) as evidenced by their formation above a regionally developed mid-crustal detachment in which kinematic indicators in the more strongly deformed (mylonitised) lower plate are themselves asymmetric and consistently oriented top-to-the-south (Passchier and Williams 1989; Holcombe et al., 1991; Gibson et al., 2008). Sediments are deposited in individual fault-bounded grabens with a period of continuous, or near continuous, bimodal magmatic activity from about ~1690 - ~1640 Ma. Felsic volcanism potentially continued as late as 1613 Ma in the McArthur Province (Page et al., 2000). This extension and rifting could have been part of a back-arc setting linked to the retreat of a magmatic arc system off Australia and which now lies in the Mojave terrane of western Laurentia (Karlstrom et al., 2001).

5.5 1690 – 1640 Ma magmatism in Australia; a possible source of juvenile detritus?

Data from Australian Proterozoic sedimentary basins indicate a major influx of juvenile, felsic detritus from within or very proximal to basins at ca. 1650 Ma, as indicated both by Nd isotopic data and zircon inheritance patterns (Table 5.1; Carson et al., 2009; Neumann et al., 2009). To determine the source of this proximal detritus, isotopic and geochronological data from Proterozoic Australia were assessed for similar-age, juvenile felsic magmatism.

5.5.1 Possible sources from Proterozoic Australia

Four possible magmatic suites are source candidates based on age and felsic geochemistry (Fig. 5.1): (1) the Sybella suite in the Western Fold Belt of the Mount Isa Inlier, (2) the Argilke magmatic suite in the Warumpi Province, (3) the St Peter magmatic suite in the southern Gawler Province and (4) an unrecognised major magmatic province in Proterozoic Australia for which there is only little remaining evidence (mostly pinkites described above).

Volumetrically significant felsic magmatism is found in the Western Fold Belt as the ca. 1670 Ma Sybella Suite (Page and Bell 1986), which consists of the Sybella Granite and the Carters Bore Rhyolite (Wyborn et al., 1988; Page et al., 2000). Intercalated with these granites are lesser amounts of gabbro and dolerite, indicating that this phase of magmatism was bimodal rather than unimodal in character. ε_{Nd} values at 1650 Ma for the Sybella Suite are all ca. -5 (Table 5.1).

The Warumpi Province is an east-trending 1690 Ma – 1600 Ma terrane along the southern margin of the Arunta region. Scrimgeour et al. (2005) interpret it to be an exotic terrane that accreted onto the southern margin of the North Australian Craton during a single tectonic cycle that peaked at 1640–1635 Ma. ε_{Nd} values of -2.6 and -1.3 are reported for 1631 ± 4 Ma granite and a 1638 ± 2 Ma charnockite (Cross et al., 2004; Close et al., 2006). The 1639 ± 5 Ma Mount Webb Granite in the western extension of the Warumpi Province in Western Australia records an ε_{Nd} value of -2 (Wyborn et al., 1998).

In South Australia, the south west Gawler craton includes the 1620 – 1610 Ma St. Peter Suite consisting of both felsic and mafic rocks with a comagmatic origin (Flint 1987; Flint et al., 1990). ε_{Nd} values at 1620 Ma are between -2 and +2 (Ferris 2001; Swain et al., 2005). The St Peter Suite has been attributed to a volcanic arc by Ferris et al. (2002).

Bimodal volcanism in the Mt Isa Province as discussed above, is recorded by pinkites/tuffs and dolerite sills. Dolerites are recorded through out the Eastern Fold belt from 1688 Ma (Rubenach et al., 2008) to 1659 Ma (Fig. 5.2) with deposition of peperites/tuffs between 1688 – 1613 Ma farther west in Western Fold Belt (Page et al., 2000; Jackson et al., 2005).

Although there are four identified 1690 – 1600 Ma volcanic events listed above in Proterozoic Australia, the combination of available geochronology and isotopic data suggest three of these are not suitable sources. Isotopic data from the Sybella Suite are evolved and inconsistent with the Nd data from the <1650 Ma successions (Table 5.1). Magmatic events at 1630 – 1640 Ma in the Warumpi Province and at 1610 – 1620 Ma for St Peter Suite have appropriate Nd isotope compositions, but are too young based on

SHRIMP U-Pb volcanic data to account for the ≤1650 Ma source (Flint 1987; Flint et al., 1990; Wyborn et al., 1998; Cross et al., 2004; Barovich and Hand 2008). Potentially a large previously unidentified juvenile volcanic suite as part of bimodal magmatism during regional extension between ca. 1690 – 1640 Ma could have been active with volcanism present in the McArthur basin until ca. 1613 Ma (Page et al., 2000). The only remaining evidence for a juvenile source is from one thin rhyolite and the thin but regionally widely distributed juvenile tuffs/peperites recorded in the regional stratigraphy (Table 5.1). A potentially larger intracratonic system could have eroded to form the juvenile sedimentary detritus in the Eastern Succession and the Georgetown Inlier.

5.5.2 Possible sources from outside of Australia

No voluminous felsic magmatic province has yet been identified in Australia that could have sourced the juvenile detritus recorded in Proterozoic Australia basins at ~1650 Ma. An alternative possibility is that the detritus was sourced from crustal blocks contiguous with eastern Australia at the time that the latter formed part of the Nuna supercontinent (Hoffman 1997 aka Columbia; Rogers and Santosh 2002). Although most workers (e.g. Karlstrom et al., 2001; Betts et al., 2008) have suggested that eastern Australia was adjacent to Laurentia when Nuna was assembled, other workers have suggested that Australia was adjacent to South China (Li et al., 1995), Siberia (Sears and Price 2003) and Baltica (Pesonen et al., 2003). The data presented in this paper have a bearing on this issue. Below we assess each of these crustal blocks as a possible source of ~1650 Ma juvenile detritus.

Major juvenile magmatism is also recorded in Laurentia in the Matzatzal province at 1650 Ma (Karlstrom et al., 2001; Amato et al., 2008). Tectonic reconstruction models for 1650 Ma (e.g., SWEAT: (Dalziel 1991; Moores 1991) and SWEAT-like: (Betts et al., 2008) suggest the volcanic source in Laurentia is potentially too distal to have produced the volumetrically significant volcanic detritus in Australia. Between 1690 and 1640 Ma rocks of eastern Australia and southwest Laurentia, while sharing some similarities in metamorphic style were not subject to a common contractional orogenic event (Gibson et al. 2008). As interpreted by Gibson et al (2008) the terranes of southwest Laurentia may have developed outboard of the Broken Hill and Mount Isa terranes, possibly as part of a continental magmatic arc that rifted off eastern Australia from ca. 1800 Ma onward.

An alternative source of juvenile magmatism is present in Baltica at ca. 1650 Ma (Brewer et al., 1998; Åhäll and Connelly 2008), although existing paleomagnetic data and current tectonic reconstructions do not allow assessment of this possibility. No ca. 1650 Ma volcanic or magmatic sources of juvenile detritus are known in either South China or Siberia, making them unlikely sources.

The source of the ~1650 Ma juvenile detritus in Proterozoic Australian basins is unclear. None of the potential sources in Australia and overseas are clear matches, either because of volume or age constraints or because tectonic reconstructions and other data are either not definitive enough or are not compatible with a proximal source for the detritus. Resolution of this source problem could be key to understanding the tectonic setting and reconstruction of Australia in the late Paleoproterozoic as Nuna was breaking up.

5.6 Conclusions

Sm-Nd isotopic data from late Paleoproterozoic basins located throughout eastern Precambrian Australia indicate an abrupt change in sediment provenance from evolved to more juvenile compositions at ca. 1650 Ma. Known voluminous Australian sources for the juvenile detritus (e.g. the 1640-1630 Ma Warumpi Province, the 1620 Ma – 1610 Ma St Peters Suite or the 1670 Ma Sybella Suite) are unlikely as the events are either too young or the magmas too evolved.

A previously unrecognised intracratonic juvenile volcanic suite active over a 50 Ma period of documented continental rifting and bimodal volcanism between 1690 – 1640 Ma within Australia is the most probable source to explain the thin rhyolite and tuffs/peperites up to 5 m thick in northern Australia. The juvenile sedimentary detritus is potentially evidence of a once larger, presently eroded magmatic province that was active in Proterozoice Australia from ca. 1690 to at least 1640 Ma.

The influx of felsic volcanism into Proterozoic Australia during regional extension could be associated with rifting and break-up of Nuna which began at ca. 1800 and may have concluded at ca. 1650 Ma. The extension and rifting could have been part of back-arc extension associated with a convergent margin along eastern Proterozoic Australia, or it could be associated with divergence between Proterozoic Australia and the cratonic block to the east during Nuna time (possibly Laurentia or Baltica). Existing data are insufficient to distinguish these possibilities. Felsic juvenile magmatism documented at 1650 Ma in either Laurentia or Baltica could be the source of juvenile detritus into Australian Proterozoic basins. Lack of a similar geological evolution between Laurentia and Australia between 1690 to 1600 Ma and current paleomagnetic data suggests Laurentia was potentially too distal to Australia to be the source of voluminous volcanism. Juvenile volcanism in Baltica at 1650 Ma could have been a source of volcanic detritus, but lack of paleomagnetica data and potentially large areas between source in Baltica and detritus recorded in Australia, while possible, are unlikely.

5.7 Acknowledgements

This study could not have taken place without the support of The Geological Survey of Queensland; Thanks are given to Ian Withnall, Allan Parsons and Laurie Hutton. Xstrata are thanked for providing drill core in the Western Fold Belt. Sergei Pisarevsky, University of Western Australia, and Martin Hand. University of Adelaide, provided enlightening debate about paleomagmatism and tectonic reconstruction models. David Bruce at Adelaide University is thanked for his dedicated help with Sm-Nd analysis. At Geoscience Australia Richard Blewett, David Champion and Russell Korsch provided many fun discussions and critically read earlier versions of the manuscript. Andrew Cross provided assistance with the geochronology data and Andrew Retter provided much dedicated help with field work. The paper benefited from earlier reviews by Pete Betts, Karl Karlstrom and Åke Johansson.

5.8 References

References

Åhäll, K.-I. and Connelly, J.N., 2008. Long-term convergence along SW fennoscandia: 330 m.y. of proterozoic crustal growth. Precambrian Research, 161(3-4): 452-474.

Amato, J.M., Boullion, A.O., Serna, A.M., Sanders, A.E., Farmer, G.L., Gehrels, G.E. and Wooden, J.L., 2008. Evolution of the Mazatzal province and the timing of the Mazatzal orogeny: Insights from U-Pb geochronology and geochemistry of igneous and metasedimentary rocks in southern New Mexico. Geological Society of America Bulletin, 120(3-4): 328-346.

Baker, M.J., Crawford, A.J. and Withnall, I.W., 2010. Geochemical, Sm-Nd isotopic characteristics and petrogenesis of Paleoproterozoic mafic rocks from the Georgetown Inlier, north Queensland: Implications for relationship with the Broken Hill and Mount Isa Eastern Succession. Precambrian Research, 177(1-2): 39-54.

Barovich, K. and Hand, M., 2008. Tectonic setting and provenance of the Paleoproterozoic Willyama Supergroup, Curnamona Province, Australia: Geochemical and Nd isotopic constraints on contrasting source terrain components. Precambrian Research, 166(1-4): 318-337.

Bau M (1991) Rare-earth element mobility during hydrothermal and metamorphic fluid-rock interaction and the significance of the oxidation state of europium. Chemical Geology 93: 219-230.

Betts, P. and Giles, D., 2006. The 1800-1100 Ma tectonic evolution of Australia. Precambrian Research, 144: 92-125.

Betts, P.G., Giles, D. and Schaefer, B.F., 2008. Comparing 1800-1600 Ma accretionary and basin processes in Australia and Laurentia: Possible geographic connections in Columbia. Precambrian Research, 166(1-4): 81-92.

Bierlein, F.P., Black, L.P., Hergt, J. and Mark, G., 2008. Evolution of Pre-1.8 Ga basement rocks in the western Mt Isa Inlier, northeastern Australia-Insights from SHRIMP U-Pb dating and *in-situ* Lu-Hf analysis of zircons. Precambrian Research, 163(1-2): 159-173.

Black, L. and McCulloch, M.T., 1984. Sm-Nd ages of the Arunta, Tennant Creek and Georgetown Inliers of northern Australia. Australian Journal of Earth Sciences, 31: 49-60.

Black, L.P., Gregory, P., Withnall, I.W. and Bain, J.H.C., 1998. U-Pb zircon age for the Etheridge Group, Georgetown region, north Queensland: Implications for relationship with the Broken Hill and Mt Isa sequences. Australian Journal of Earth Sciences: An International Geoscience Journal of the Geological Society of Australia, 45(6): 925 - 935.

Blake, D. and Stewart, A. (Editors), 1992. Stratigraphy and tectonic framework, Mount Isa Inlier. Detailed Studies of the Mount Isa Inlier, 243. Australian Geological Survey Organisation 243, 1-11 pp.

Blewett, R.S., Black, L.P., Sun, S.s., Knutson, J., Hutton, L.J. and Bain, J.H.C., 1998. U-Pb zircon and Sm-Nd geochronology of the Mesoproterozoic of North Queensland: implications for a Rodinian connection with the Belt supergroup of North America. Precambrian Research, 89(3-4): 101-127.

Brewer, T.S., Daly, J.S. and Åhäll, K.-I., 1998. Contrasting magmatic arcs in the Palaeoproterozoic of the south-western Baltic Shield. Precambrian Research, 92(3): 297-315.

Carson, C., Hutton, L.J., Withnall, I.W. and Perkins, W., 2009. Summary of results: Joint GSQ-GA NGA geochronology project Mount Isa Region URANDANGI, CLONCURRY, DUCHESS and DOBBYN 1:250 000 Sheet areas August 2007 - June 2008. Geoscience Australia Record: 69.

Cihan, M., Evins, P., Lisowiec, N. and Blake, K., 2006. Time constraints on deformation and metamorphism from EPMA dating of monazite in the

Proterozoic Robertson River Metamorphics, NE Australia. Precambrian Research, 145(1-2): 1-23.

Close, D., Scrimgeour, I. and Edgooose, C., 2006. Evolution and mineral potential of the Palaeoproterozoic Warumpi Province. In: P. Lyons and D. Huston (Editors), Evolution and metallogenesis of the North Australian Craton. Conference Abstracts. Geoscience Australia Record 2006/16, Alice Springs 2006.

Cross, A., Claoué-long, J., Scrimgeour, I.R., Close, D.F. and Edgoose, C.J., 2004. Summary of results. Joint NTGS-GA geochronological project: southern Arunta Region 2000-2003. Northern Territory Geological Survey Record 2004-003.

Dalziel, I.W.D., 1991. Pacific margins of Laurentia and East Antarctica-Australia as a conjugate rift pair: Evidence and implications for an Eocambrian supercontinent. Geology, 19(6): 598-601.

DePaolo, D.J. and Wasserburg, G.J., 1976. Nd isotopic variations and petrogenetic models. Geophys. Res. Lett, 3: 249–252.

Eggins, S.M., Woodhead, J.D., Kinsley, L.P.J., Mortimer, G.E., Sylvester, P., McCulloch, M.T., Hergt, J.M. and Handler, M.R., 1997. A simple method for the precise determination of >40 trace elements in geological samples by ICPMS using enriched isotope internal standardisation. Chemical geology, 134: 311-326.

Eriksson, K.A., Simpson, E. and Jackson, M.J. (Editors), 1993. Stratigraphical evolution of a Proterozoic syn-rift to post-rift basin: constraints on the nature of lithospheric extension in the Mount Isa Inlier, Australia. Tectonic Controls and Signatures in Sedimentary Successions, 20. International Association of Sedimentologists Special Publication, 203-221 pp.

Ferris, G.M., 2001. The geology and geochemistry of granitoids in the Childara region, western Gawler craton, South Australia: Implications for the Proterozoic tectonic history of the western Gawler craton and the development of lode-style gold mineralisation at Tunkillia, University of Tasmania, Australia MSc. Thesis, 175 pp.

Ferris, G.M., Schwarz, M.P. and Heithersay, P., 2002. The geological framework, distribution and controls of Fe-oxide and related alteration, and Cu- Au mineralisation in the Gawler craton, South Australia. Part I: geological and tectonic framework. Hydrothermal iron oxide copper-gold and related deposits: A global perspective. GeoConsultancy Publishing, Adelaide, 9-31 pp.

Flint, R.B., 1987. NUYTS, South Australia: Adelaide, Primary Industries and Resources South Australia. 30.

Flint, R.B., Rankin, L.R. and Fanning, C.M., 1990. Definition; the Palaeoproterozoic St. Peter Suite of the western Gawler craton. Geological Survey of South Australia, Quarterly Geological Notes, 114: 2-8.

Gibson, G.M., Rubenach, M.J., Neumann, N.L., Southgate, P.N. and Hutton, L.J., 2008. Syn- and post-extensional tectonic activity in the Palaeoproterozoic sequences of Broken Hill and Mount Isa and its bearing on reconstructions of Rodinia. Precambrian Research, 166(1-4): 350-369.

Giles, D., Betts, P. and Lister, G., 2002. Far-field continental backarc setting for the 1.80-1.67 Ga basins of northeastern Australia. Geology, 30(9): 823-826.

Griffin, W., Belousova, E., Walters, S. and O'Reilly, S., 2006. Archaean and Proterozoic crustal evolution in the Eastern Succession of the Mt Isa district, Australia: U-Pb and Hf-isotope studies of detrital zircons. Australian Journal of Earth Sciences, 53: 125-149.

Hoffman, P.F., 1997. Tectonic genealogy of North America. In: B.A. Van der Pluijm and S. Marhak (Editors), Earth Structure, an Introduction to Structural Geology and Tectonics. New York, McGraw Hill, pp. 459-464.

Holcombe, R.J., Pearson, P.L. and Oliver, N.H.S., 1991. Geometry of a Middle Proterozoic extensional decollement in north-eastern Australia. Tectono[hysics. Tectonophysics, 191: 255-274.

Jackson, M.J., Southgate, P., Black, L. and Domagala, J., 2005. Overcoming Proterozoic quartzite sandbody miscorrelations: integrated sequence stratigraphy and SHRIMP U-Pb dating of the Surprise Creek Formation, Torpedo Creek and Warrina Park Quartzites, Mt Isa Inlier. Australian Journal of Earth Sciences, 52: 1-25.

Jenner, G.A., Longerich, H.P., Jackson, S.E. and Fryer, B.J., 1990. ICP-MS A powerful tool for high-precision trace-element analysis in earth sciences: Evidence from analysis of selected USGS reference samples. Chemical Geology, 83: 133-148.

Karlstrom, K.E., Åhäll, K.-I., Harlan, S.S., Williams, M.L., McLelland, J. and Geissman, J.W., 2001. Long-lived (1.8-1.0 Ga) convergent orogen in southern Laurentia, its extensions to Australia and Baltica, and implications for refining Rodinia. Precambrian Research, 111(1-4): 5-30.

Li, Z.-X., Zhang, L. and Powell, C.M., 1995. South China in Rodinia: Part of the missing link between Australia-East Antarctica and Laurentia? Geology, 23(5): 407-410.

Lister, G.S., Etheridge, M.A. and Symonds, P.A., 1986. Detachment faulting and the evolution of passive continental margins. Geology, 14(3): 246-250.

Michard A (1989) Rare earth element systematics in hydrothermal fluids. Geochimica et Cosmochimica Acta 53: 745-750.

Moores, E., 1991. Southwest United-States-East Antarcric (Sweat) connection-a hypothesis. Geology, 19: 425-428.

Neumann, N., Southgate, P., Gibson, G. and McIntyre, A., 2006. New SHRIMP geochronology for the western fold belt of the Mt Isa inlier: Developing a 1800-1650 Ma event framework. Australian Journal of Earth Sciences, 53: 1023-1039.

Neumann, N.L., Southgate, P.N. and Gibson, G.M., 2009. Defining unconformities in Proterozoic sedimentary basins using detrital geochronology and basin analysis--An example from the Mount Isa Inlier, Australia. Precambrian Research, 168(3-4): 149-166.

Norrish, K. and Chappell, B.W., 1977. X-ray fluorescence spectrometry. Physical methods in determination mineralogy. Academic Press, London, 201-272 pp.

Norrish, K. and Hutton, J.T., 1969. An accurate X-ray spectrographic method for the analysis of a wide range of geological samples. Geochimica Cosmochimica Acta, 33: 431-453.

Page, R.W., 1981. Depositional ages of the stratiform base metal deposits at Mount Isa and McArthur River, Australia, based on U-Pb zircon dating of concordant tuff horizons. Economic Geology, 76: 648-658.

Page, R.W. and Bell, T.H., 1986. Isotopic and structural responses of granite to successive deformation and metamorphism. Journal of Geology, 94: 365–379.

Page, R.W., Conor, C.H.H., Stevens, B.P.J., Gibson, G.M., Preiss, W.V. and Southgate, P.N., 2005. Correlation of Olary and Broken Hill Domains, Curnamona Province: Possible Relationship to Mount Isa and Other North Australian Pb-Zn-Ag-Bearing Successions. Economic Geology, 100(4): 663-676.

Page, R.W., Jackson, M.J. and Krassay, A.A., 2000. Constraining sequence stratigraphy in northern Australia basins: SHRIMP U-Pb zircon geochronology between Mt Isa and McArthur River. Australian Journal of Earth Sciences, 47: 431-459.

Page, R.W. and Sun, S.S., 1998. Aspects of geochronology and crustal evolution in the Eastern Fold Belt, Mt Isa Inlier. Australian Journal of Earth Sciences, 45(3): 343 - 361.

Passchier, C.W. and Williams, P.R., 1989. Proterozoic extensional deformation in the Mount Isa Inlier, Queensland, Australia. Geol. Mag., 126: 43-53.

Pesonen, L.J., Elming, S.Å., Mertanen, S., Pisarevsky, S., D'Agrella-Filho, M.S., Meert, J.G., Schmidt, P.W., Abrahamsen, N. and Bylund, G., 2003. Palaeomagnetic configuration of continents during the Proterozoic. Tectonophysics, 375(1-4): 289-324.

Plumb, K., Ahmad, M. and Wygralak, A.S., 1990. Mid-Proterozoic basins of the North Australia Craton-regional geology and mineralisation. In: F. Hughes (Editor), Geology of the Mineral Deposits of Australia and Papua New Guinea. Australasian Institute of Mining and Metallurgy, Mongraph 14, pp. 881-902.

Pyke, J., 2000. Minerals laboratory staff develops new ICP-MS preparation method., AGSO-Geoscience Australia Research Newsletter 33, Canberra, pp. 12-14.

Robinson DM, DeCelles PG, Patchett PJ, Garzione CN (2001) The kinematic evolution of the Nepalese Himalaya interpreted from Nd isotopes. Earth and Planetary Science Letters 192: 507-521.

Rogers, J.J.W. and Santosh, M., 2002. Configuration of Columbia, a Mesoproterozoic supercontinent. Gondwana Research, 5: 5-22.

Rubenach, M.J., Foster, D.R.W., Evins, P.M., Blake, K.L. and Fanning, C.M., 2008. Age constraints on the tectonothermal evolution of the Selwyn Zone, Eastern Fold Belt, Mount Isa Inlier. Precambrian Research, 163(1-2): 81-107.

Scrimgeour, I.R., Kinny, P.D., Close, D.F. and Edgoose, C.J., 2005. High-T granulites and polymetamorphism in the southern Arunta Region, central Australia: Evidence for a 1.64 Ga accretional event. Precambrian Research, 142(1-2): 1-27.

Sears, J.W. and Price, R.A., 2003. Tightening the Siberian connection to western Laurentia. Geological Society of America Bulletin, 115(8): 943-953.

Southgate, P., Bradshaw, B., Dimagala, J., Jackson, M.J., Idnurm, M., Krassay, A.A., Page, R.W., Sami, T., Scott, D., Lindsay, J., McConachie, B. and Tarlowski, C., 2000. Chronostratigraphic basin framework for Palaeoproterozoic rocks (1730-1575 Ma) in northern Australia and implications for base-metal mineralisation. Australian Journal of earth Sciences, 47(3): 461-483.

Southgate, P.N., Kyser, T.K., Scott, D.L., Large, R.R., Golding, S.D. and Polito, P.A., 2006. A Basin System and Fluid-Flow Analysis of the Zn-Pb-Ag Mount Isa-Type Deposits of Northern Australia: Identifying Metal Source, Basinal Brine Reservoirs, Times of Fluid Expulsion, and Organic Matter Reactions. Economic Geology, 101(6): 1103-1115.

Sun, S.S. and McDonough, W.F., 1989. Chemical and isotopic systematics of oceanic basalts: implications for mantle composition and processes. Geological Society, London, Special Publications, 42(1): 313-345.

Swain, G., Barovich, K., Hand, M. and Ferris, G., 2005. Proterozoic magmatic arcs and oroclines: St Peter Suite, Gawler craton, South Australia. In: M.T.D. Wingate and S.A. Pisarevsky (Editors), Supercontinents and Earth Evolution Symposium Geological Society of Australia, Abstracts p. 42.

Wade, B., Barovich, K., Hand, M., Scrimgeour, I. and Close, D., 2006. Evidence for Early Mesoproterozoic Arc Magmatism in the Musgrave Block, Central Australia: Implications for Proterozoic Crustal Growth and Tectonic Reconstructions of Australia. The Journal of Geology, 114(1): 43-63.

Willis, I.L., Brown, R.E., Stroud, W.J. and Stevens, B.P.J., 1983. The Early Proterozoic Willyama Supergroup: Stratigraphic subdivision and interpretation pf high- to

low-grade metamorphic rocks in the Broken Hill block, New South Wales. Geological Society of Australia Journal, 30: 195-224.

Withnall, I.W., Bain, J.H.C., Draper, J.J., MacKenzie, D.E. and Oversby, B.S., 1988. Proterozoic stratigraphy and tectonic history of the Georgetown Inlier, northeastern Queensland. Precambrian Research, 40-41: 429-446.

Wyborn, L.A.I., Hazell, M., Page, R., Idnurm, M. and Sun, S.-S., 1998. A newly discovered major Proterozoic granite-alteration system in the Mount Webb region, central Australia, and implications for Cu-Au mineralisation. Aust. Geol. Surv. Organ. (AGSO) Res, Newslett. 28: 1–6.

Wyborn, L.A.I., Page, R.W. and McCulloch, M.T., 1988. Petrology, geochronology and isotope geochemistry of the post-1820 Ma granites of the Mount Isa Inlier: mechanisms for the generation of Proterozoic anorogenic granites. Precambrian Research, 40-41: 509-541.

Wyborn, L.A.I., Page, R.W. and Parker, A.J. (Editors), 1987. Geochemical and geochronological signatures in Australian Proterozoic igneous rocks. Geochemistry and mineralization of Proterozoic volcanic suites, 33. Geological Society Special Publications, 377-394 pp.

5.9 Supplementary data

U-Pb dating of the Hampden Mine dolerite, Eastern Fold Belt, Mt. Isa.

2009165033: Eastern Succession Mt Isa (Hampden Mine)

GA sample ID: 2009165033
GA mount No.: GA6108
1:100 000 sheet: Kuridala Region
1:250 000 sheet: Duchess SF54-6
Geographic area: Mount Angelay and Malbon
Region: Mount Isa Eastern Fold Belt
Grid Reference (WGS84) 448041 **E** 7647452 **N**
Formal name: Metadolerite
Lithology: Dolerite

Sample details
SHRIMP U–Pb dating was undertaken to establish the age of dolerites between black mudstones within the Kuridala/Hampton Mine sequence. The Kuridala sequence is described by Parsons et al., (2008) as a lithological equivalent to the Soldiers Cap Group. The sample collected for analysis was a silica rich small-scale pegmatitic phase from an area < 1 m across consisting of coarse hornblende which graded into surrounding dolerite.

Zircon description
The heavy mineral concentrate separated from this sample was dominated by titanite and only 40 zircons of a generally poor quality were recovered. The grains are typically small (~20 to ~40 μm); however, a few are up to ~80 μm in diameter. They are colourless, clear to turbid, variably cracked and fragmented, the majority with angular margins and only a few having crystal faces. The grains are strongly to moderately luminescent and faint, often normal growth banding is present in many of the grains however, some appear structureless and are moderately luminescent. Almost all grains have thin (~1 to 5 μm) strongly luminescent streaks which can occur within the interior of some grains, discordant to the primary growth zones, or concordantly along grain margins or between what may be separate growth phases.

Analytical procedures
SHRIMP U-Pb isotopic analyses were conducted on Geoscience Australia's SHRIMP IIe using the procedures outlined in Carson et al., (2009). The unknown zircons were mounted together with the $^{206}Pb/^{238}U$ standard zircon Temora 2 (416.8 Ma Black et al., 2004) and $^{207}Pb/^{206}Pb$ standard zircon OG1 (3465Ma, Stern et al., 2009). Cathodoluminescence (CL) images were taken of the zircons to reveal their internal zoning. These images were obtained with a JEOL JSM-6490LV scanning electron microscope located at Geoscience Australia and operating at 15kV with a working distance of 16mm. Data reduction was carried out using SQUID 1.13b and ISOPLOT 3 Microsoft Excel-based macros (Ludwig, 2001; 2003). The pooled age is calculated from the ^{204}Pb corrected $^{207}Pb/^{206}Pb$ ages using ISOPLOT 3 (Ludwig, 2003) and the final age is given at the 95% confidence interval. Error ellipses on the concordia diagram are plotted at the 1σ level.

U–Pb isotopic results

Twenty four analyses were undertaken on twenty one zircons from this sample (Figure 5.A.1, Table 5.A.1). U contents range from 202 to 640ppm and Th/U from 0.04 to 2.62.Common Pb contents are all below 0.1% (f_{206}). Three analyses are more discordant than an arbitrary threshold of 10 % and have been removed from further consideration. The remaining 21 analyses all have the same radiogenic $^{207}Pb/^{206}Pb$ ratio within analytical error (MSWD = 1.2) and combine to give an age of 1659 ± 4 Ma. This is interpreted as the magmatic age of these zircons and their host rock. It is also within error of a previous SHRIMP U–Pb zircon age for the Foxes Creek rhyolite sample of 1654 ± 4 Ma (Page and Sun, 1998) and within error of detrital zircons in the Toole Creek Formation (1658 ± 5 Ma; Carson et al., 2009).

Table 5.A.1: SHRIMP U–Pb zircon isotopic data from the Hampden Mine dolerite (2009165033)

SHRIMP U–Pb zircon isotopic data from the Hampden Mine dolerite (20091650

Grain area	$^{206}Pb_c$ (%)	U (ppm)	Th (ppm)	$^{232}Th/^{238}U$	$^{238}U/^{206}Pb^*$	± (%)	$^{207}Pb^*/^{206}Pb^*$	± (%)	$^{207}Pb/^{206}Pb$ Age (Ma)	± (1σ)	Discordance %
magmatic zircons											
359.Z.1.1.1	0.01	514	412	0.83	3.69	3.77507	0.1021	0.33296	1663	6	8
359.Z.3.1.1	0.02	556	190	0.35	3.79	4.54732	0.1018	0.30829	1657	6	10
359.Z.4.1.1	0.01	202	199	1.02	3.73	3.99105	0.1027	0.78909	1674	15	10
359.Z.6.1.1	0.02	432	18	0.04	3.65	3.96669	0.1012	0.35649	1646	7	6
359.Z.7.1.1	0.06	354	168	0.49	3.66	4.07865	0.1014	0.40896	1650	8	6
359.Z.8.1.1	-0.03	312	215	0.71	3.69	3.62913	0.1019	0.44044	1658	8	8
359.Z.9.1.1	0.00	298	197	0.68	3.69	3.49257	0.1015	0.41999	1651	8	7
359.Z.10.1.1	-0.02	345	56	0.17	3.44	1.96114	0.1022	0.50807	1664	9	1
359.Z.12.1.1	-0.01	385	384	1.03	3.47	2.14507	0.1014	0.48512	1650	9	1
359.Z.13.1.1	0.04	388	397	1.06	3.46	2.07939	0.1010	0.50694	1642	9	0
359.Z.14.1.1	0.00	453	220	0.50	3.47	2.2171	0.1025	0.41709	1670	8	3
359.Z.15.1.1	0.04	337	162	0.50	3.47	2.13491	0.1018	0.51761	1657	10	2
359.Z.16.1.1	-0.03	562	64	0.12	3.45	1.86453	0.1026	0.41673	1672	8	2
359.Z.17.1.1	-0.01	294	250	0.88	3.45	1.88806	0.1012	0.56511	1647	10	1
359.Z.18.1.1	0.00	539	334	0.64	3.45	1.44646	0.1023	0.40546	1666	8	2
359.Z.19.1.1	0.00	505	132	0.27	3.46	1.7155	0.1024	0.42383	1667	8	2
359.Z.18.2.1	0.01	346	413	1.23	3.44	1.98906	0.1024	0.51182	1667	9	2
359.Z.13.2.1	0.03	362	346	0.99	3.43	1.9376	0.1023	0.51014	1666	9	1
359.Z.20.1.1	0.04	371	416	1.16	3.43	1.87258	0.1028	0.51833	1676	10	2
359.Z.22.1.1	0.04	339	181	0.55	3.46	2.23561	0.1018	1.02681	1657	19	1
359.Z.1.2.1	0.01	473	381	0.83	3.37	1.51661	0.1018	0.44374	1656	8	-1
greater than 10% discordant											
359.Z.2.1.1	0.01	631	385	0.63	4.25	5.28863	0.1013	0.31744	1648	6	19
359.Z.5.1.1	0.06	640	666	1.07	5.36	3.0656	0.0948	0.69078	1525	13	30
359.Z.11.1.1	0.05	547	1389	2.62	6.08	5.67051	0.0911	2.49914	1450	48	35

1. $\%^{206}Pbc$ indicates the proportion of common ^{206}Pb in the total measured ^{206}Pb.
2. Pb isotopic ratios corrected for common Pb by reference to the measured ^{204}Pb.
3. All errors quoted as 1**σ**.

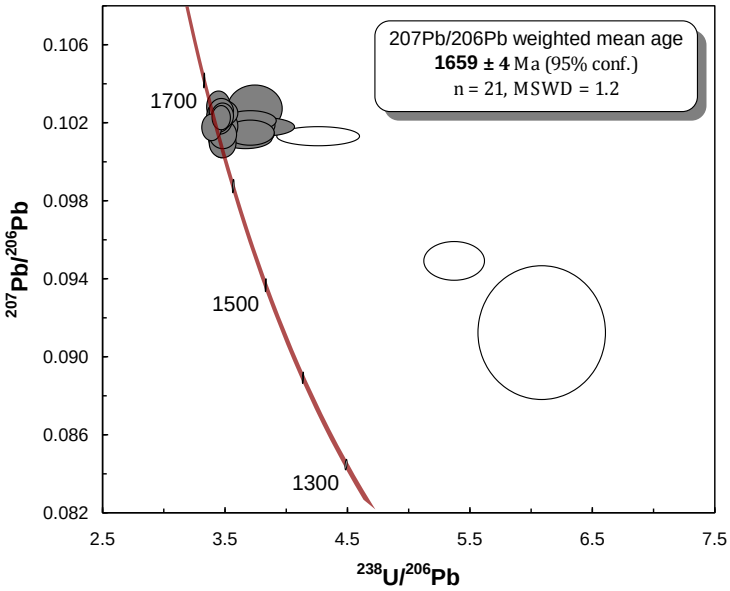

Figure 5.A.1. Terra-Wasserburg Concordia diagram showing results of all zircon analyses from the Hampden Mine dolerite (2009165033). Three grains more discordant than an arbitrary threshold level of 10 %, represented by open ellipses, are not included in age determination and have been excluded from further consideration.

Supplementary data references

Black, L.P., Kamo, S.L., Allen, C.M., Davis, D.W., Aleinkoff, J.N., valley, J.W., Mundil, R., Campbell, I.H., Korsch, R.J., Williams, I.S. and Foudoulis, C., 2004. Improved 206Pb/238U microprobe geochronology by the monitoring of a trace-element-related matrix effect; SHRIMP, ID–TIMS, ELA–ICP–MS and oxygen isotope documentation for a series of zircon standards. Chemical Geology, 205: 115–140.

Carson, C., Hutton, L.J., Withnall, I.W. and Perkins, W., 2009. Summary of results: Joint GSQ-GA NGA geochronology project Mount Isa Region URANDANGI, CLONCURRY, DUCHESS and DOBBYN 1:250 000 Sheet areas August 2007 - June 2008. Geoscience Australia Record: 69.

Ludwig, K.R., 2001. Squid 1.03: a user's manual. Berkeley Geochronology Center, Special Publication 2.

Ludwig, K.R., 2003. Isoplot 3.00: a user's manual. Berkeley Geochronology Center, Special Publication 4.

Page, R.W. and Sun, S.S., 1998. Aspects of geochronology and crustal evolution in the Eastern Fold Belt, Mt Isa Inlier. Australian Journal of Earth Sciences, 45(3): 343 - 361.

Parsons, A., Withnall, I.W., Neumann, N.L., Carson, C.J. and Lambeck, A., 2008. The Tectono-Stratigraphic framework of the Cloncurry-Selwyn Zone: working towards a resolution. Digging Deeper 6 Proceedings, Geological Survey of Queensland.

Stern, R.A., Bodorkos, S., Kamo, S.L., Hickman, A.H. and Corfu, F., 2009. Measurements of SIMS instrumental mass fraction of Pb-isotopes during zircon dating. Geostandards and Geoanalytical Research, 33(2): 145-168.

Chapter 6

Conclusions

The work presented here outlines multidisciplinary techniques including; facies analysis, whole-rock and trace element geochemistry, U-Pb and Sm-Nd isotope geochemistry to identify evidence for secular changes in Proterozic Australia and relate this to gold and zinc-lead-silver mineralising events. Understanding this secular variation of deposit types is therefore a potentially powerful tool for mineral exploration in Proterozoic Australia. This study shows the age and geochemistry of the potential host rock within Proterozoic Australia can help provide a rapid filter for determining favourable regions and deposit styles for future gold and lead-zinc exploration programs. These secular variations in Proterozoic Australia appear to be related to changes in tectonic cycles and processes, and changes in the composition of the hydrosphere, and may be applicable to other parts of the world.

The Australian Proterozoic is broadly characterized by a general transition through time from lode gold deposits at 1910 ─ 1800 Ma, to sediment-hosted zinc-lead-silver deposits at 1710 ─ 1575 Ma, and then to iron-oxide copper-gold deposits at 1590 ─ 1500 Ma ((Goldfarb et al., 2001; Goldfarb et al., 2010a; Huston et al., 2010). The latter two epochs are the most significant in Australia's geologic history for zinc-lead-silver and copper-gold-uranium systems. The general timing of these mineralisation events corresponds broadly to the formation and break-up of the Nuna supercontinent during the late Paleoproterozoic to early Mesoproterozoic. The geological expression of this mineralisation occurs within thick sedimentary basins which cover large areas of northern Australia. These siliciclastic basins host world-class gold and lead-zinc deposits within anoxic mudstones sequences.

Goldfarb et al. (2010a) discusses the complex interplay between metallogeny and the evolving global tectonic regime, global changes in atmospheric and oceanic redox states through time. Particular ore deposit types are either abundant or scarce at different times through Earth's history. The ability to identify these secular variations through time provides a critical first-pass exploration tool (Goldfarb et al., 2010a). Rocks that formed during particular time periods may be more permissive for given mineral deposit types and identification of rocks from less favourable time periods helps to eliminate large regions during mineral exploration programs.

6.1 Sedimentary basins deposited during Nuna supercontinent amalgamation

Sediments deposited in the 1910 Ma ─ 1840 Ma basins within northern Australia were deposited during the Nuna supercontinent amalgamation. These fine-grained mudstones, deposited before the Great Oxidation Event, formed the Dead Bullock Formation in the Tanami region and the Koolpin Formation in the Pine Creek Orogen and consisted of fine-grained iron-rich/mafic mudstones and siltstones.

These iron-rich/mafic sediments can be geochemically identified by high FeO values, high Cr/Th and low Th/Sc values. The gold-bearing stratigraphy of the iron-rich Callie Member (of the Dead Bullock Formation) was deposited as part of a deep-water

condensed section below storm wave base. The Callie Member is conformably overlain by the relatively iron-poor Killi Killi Formation. Geochemistry of these two units indicate that the Callie Member has a more mafic provenance, whereas the Killi Killi Formation had a felsic-dominated provenance. The depositional model of the Tanami Group is discussed in Chapter 2. Potentially thick sequences of Dead Bullock Formation are identified at the Old Pirate Prospect through isopach maps, suggesting this is a region for potentially deep exploration holes to intersect the gold-bearing Dead Bullock Formation.

The combined Tanami and Ware groups are interpreted to thicken to the northwest based on facies analysis and seismic data described in Chapter 2. The general thickening corresponds to generally coarser grains, less mud to sand ratio, within the Killi Killi Formation. Based upon these data, the provenance of the Killi Killi Formation sediments is inferred to have been from the northwest, possibly from the Kimberley Craton.

Two different tectonic models have been proposed that could help explain the source of the Killi Killi Formation sediments. The initial basin model of Etheridge et al. (1987) is based on continental crust consisting of basin convergence and little horizontal movement. The source of the sediments is interpreted to be from an eroding continent directly to the northwest of the Tanami region. This model is contrasted by the plate tectonic model of Griffin et al. (2000), based on work by Sheppard et al. (1999) and Tyler et al. (1999), with interpreted convergence between the Kimberley and proto-North Australian cratons. Collision of the plates is interpreted to occur at ca. 1850 Ma. In this model, the Tanami region was a foreland basin as subsequently proposed by Tyler et al. (2005) and Huston (2006). However, more detailed geochronology in the Tanami region is required to test these hypotheses.

The development of a Tanami geochemical regional stratigraphy and the identification of possible Dead Bullock Formation stratigraphy at depth at the Titania/Oberon Prospect outlined in Chapter 3 led to a follow-up drilling program. Using the results of this study, Newmont Tanami Operations designed a drilling program to test the potential of intersecting Dead Bullock Formation at depth at the Titania/Oberon prospect. Newmont drilled a 900 m exploration diamond hole which intersected a wide zone of gold mineralisation within sediment that consisted of high Cr/Th and low Th/Sc values which is interpreted as Dead Bullock Formation.

In Proterozoic Australia, 1910 Ma ─ 1840 Ma, iron-rich sedimentary basins host significant orogenic gold mineralisation. Orogenic gold mineralisation in Australia could be related to a global spike in orogenic gold (Goldfarb et al., 2001). The Tanami region and Pine Creek Orogen can be linked to global processes that host major gold deposits in Homestake, U.S.A, Ghana, West Africa, and Guiana Shield, South America. Similar whole-rock and trace element geochemical techniques as applied in northern Australia could be applied as potential exploration techniques in the Homestake terrain of USA, Ghana, West Africa and in the Guiana Shield South America as discussed in Chapter 4. Identifying the deepest parts of sedimentary basins and discriminating the prospective stratigraphy using the suggested geochemical proxies discussed in this thesis could increase exploration effectiveness.

The rise in oxygen content in oceans after 1840 Ma in northern Australia and globally (Cloud 1972; Holland 1984; Huston and Logan 2004) led to increasing sulfate content

and the end of deposition of banded iron formations and iron-rich sediments (Canfield 1998; Poulton et al., 2004; Goldfarb et al., 2010b). While complex, this transition led to a change from iron-rich sediments to iron-poor sediments and corresponds broadly to a change in mineralisation style in northern Australia. This change is reflected in Australia from predominantly orogenic gold to lead-zinc deposits, with a major period of lead-zinc mineralization in Australia occurring between 1710 – 1575 Ma.

6.2 Sedimentary basins deposited during Nuna supercontinent break-up

The timing of zinc-lead-silver deposition between 1710 and 1575 Ma in Australia also broadly corresponds with the timing of the Nuna supercontinent break-up (Huston et al., 2010; Leach et al., 2010). Changes in tectonic stresses and plate movement directions at 1650 Ma (Idnurm 2000) are interpreted to have driven episodes of fluid circulation into non-iron-rich siltstones and mudstone sequences, where zinc, lead and silver were deposited.

The timing of Mt Isa-style zinc-lead deposits within northern Australia corresponds to an abrupt Sm-Nd isotopic change within sedimentary provenances recorded throughout eastern Proterozoic Australia (Chapter 5). This change in sedimentary provenance from an evolved to a more juvenile composition is associated with a change in magmatic source at ~1650 Ma. Sources for these juvenile compositions within Proterozoic Australia (e.g. Warumpi Province 1639 Ma – 1631 Ma, the St Peters Suite at 1620 Ma – 1610 Ma or the Sybella Suite at 1670 Ma) are unlikely as these events are either too young or the compositions are too evolved.

Intracratonic bimodal volcanism within Proterozoic Australia was active over a 50 Ma period documenting a time of continental extension between 1690 – 1640 Ma. A previously unrecognised intracratonic source of juvenile volcanism is the most probable source to explain the tuffs/peperites recorded in regional Australia. The voluminous juvenile sedimentary detritus in sediments between 1690 – 1640 Ma is potentially evidence of an eroded magmatic province that was active in Proterozoic Australia or adjacent (since rifted away) provinces.

Regional extension and influx of felsic volcanism which began at ca. 1780 Ma and potentially concluded by ca. 1650 Ma in Proterozoic Australia may have been part of the rifting and break-up of Nuna. The extension and rifting could have been associated with the divergence between Proterozoic Australia and the cratonic block to the east during Nuna time (either Laurentia or Baltica). Like-wise the extension and rifting could have also been part of back-arc extension associated with a convergent margin along eastern Proterozoic Australia.

The use of Sm-Nd isotopic compositions and U-Pb zircon geochronology is providing new regional constraints in deformed and metamorphosed terrains of Proterozoic Australia where absolute ages are difficult to determine leading to difficulties with regional stratigraphic correlations within and between regional provinces. This work shows that Sm-Nd isotopic data has the potential to provide a rapid way to ‘fingerprint’ this important reference boundary for Mt Isa-style Zn-Pb-Ag sediment hosted mineralisation in regional Palaeoproterozoic sequences. The Sm-Nd isotopic data presented in chapter 5, which shows a significant change in ε_{Nd} values at ~1650 Ma, offers a significantly cheaper and complementary technique for well constrained zircon-based stratigraphic age determination. Therefore Sm-Nd analyses could potentially be

used as a future exploration and correlation tool for an important reference boundary for Mt Isa–style Pb-Zn-Ag style deposits elsewhere in the Mt Isa Inlier, the Etheridge Province, and elsewhere in Proterozoic Australia.

6.3 References

Canfield, D.E., 1998. A new model for Proterozoic ocean chemistry. Nature, 396: 450–453.

Cloud, P., 1972. A working model of the primitive Earth. American Journal of Science, 272: 537–548.

Goldfarb, R.J., Bradley, D. and Leach, D.L., 2010a. A Special Issue Devoted to Secular Variation in Economic Geology. Economic Geology, 105(3): 459-712.

Goldfarb, R.J., Bradley, D. and Leach, D.L., 2010b. Secular Variation in Economic Geology. Economic Geology, 105(3): 459-465.

Goldfarb, R.J., Groves, D.I. and Gardoll, S., 2001. Orogenic gold and geologic time: a global synthesis. Ore Geology Reviews, 18(1-2): 1-75.

Holland, H.D., 1984. The Chemical Evolution of the Atmosphere and Ocean. . Princeton Series in Geochemistry,, Princeton University Press, New Jersey.

Huston, D.L. and Logan, G.A., 2004. Barite, BIFs and bugs: evidence for the evolution of the Earth's early hydrosphere. Earth and Planetary Science Letters, 220(1-2): 41-55.

Huston, D.L., Pehrsson, S., Eglington, B.M. and Zaw, K., 2010. The Geology and Metallogeny of Volcanic-Hosted Massive Sulfide Deposits: Variations through Geologic Time and with Tectonic Setting. Economic Geology, 105(3): 571-591.

Idnurm, M., 2000. Towards a high resolution Late Paleoproterozoic-earliest Mesoproterozoic apparent polar wander path for northern Australia. Australian Journal of Earth Sciences, 47: 405-429.

Leach, D.L., Bradley, D.C., Huston, D., Pisarevsky, S.A., Taylor, R.D. and Gardoll, S.J., 2010. Sediment-Hosted Lead-Zinc Deposits in Earth History. Economic Geology, 105(3): 593-625.

Poulton, S.W., Fralick, P.W. and Canfield, D.E., 2004. The transition to a sulphidic ocean ~ 1.84 billion years ago. Nature, 431(7005): 173-177.

Alexis Lambeck

PhD THESIS TITLE

“Basin analysis and the geochemical signature of Paleoproterozoic sedimentary successions in northern Australia: Constraints on basin development in respect to mineralisation and paleoreconstruction models”

APPENDIX

SHRIMP U-Pb detrital & volcanic zircon results, Georgetown Inlier, Mt Isa, Eastern Succession

Lambeck, A.[1,2]
Cross, A. [2]

[1] Centre for Tectonics Resources and Exploration, University of Adelaide, Adelaide, SA 5005.
[2] Geoscience Australia, GPO Box 378, Canberra, ACT 2601, Australia

Geoscience Australia Record – 2011, (to be submitted)

STATEMENT OF AUTHORSHIP

SHRIMP U-Pb detrital & volcanic zircon results, Georgetown Inlier, Mt Isa, Eastern Succession

Geoscience Australia Record – 2011, (to be submitted)

Alexis Lambeck (PhD. Candidate)

Collected all samples, interpreted data, wrote manuscript and acting as corresponding author

I hereby certify that the statement of contribution is accurate

Signed …… ……..Date 22 June 2011

Andrew Cross (co-author name)

Supervised development of work, provided assistance with data interpretation and manuscript evaluation

Appendix: Supplementary U-Pb zircon data collected during A. Lambeck's PhD program

To be published as: Lambeck, A., Cross, A., (to be submitted). SHRIMP U-Pb detrital & volcanic zircon results, Georgetown Inlier, Mt Isa, Eastern Succession. GA Record XX2011.

Introduction

A.1.1 Overview

This report presents SHRIMP U-Pb detrital zircon results for four sedimentary samples and SHRIMP U-Pb zircon results from a felsic volcanic sample collected and analysed as part of A. Lambeck's PhD program (2008-2011) through the University of Adelaide and supported by Geoscience Australia. Three sedimentary samples and the felsic volcanic sample are from the Georgetown Inlier and the final sedimentary sample is from the Mount Isa Eastern Succession.

Numerous intracratonic volcano-sedimentary basins form part of the evolution of the interior of the proto-Australian continent between 1800 and 1600 Ma (e.g. Southgate et al., 2000; Betts et al., 2006). Characterising potential isotopic changes within these volcano-sedimentary basins could provide important information about tectonic events and key stratigraphic marker horizons within major mineralising time periods.

The work was undertaken by Geoscience Australia (GA) as part of its Onshore Energy and Security Program in collaboration with the Mount Isa Mapping Project of the Geological Survey of Queensland. Further reference to SHRIMP U-Pb detrital and volcanic zircon studies in the region carried out by Lambeck between 2008-2011 are found in Lambeck (2011); Lambeck et al., (in review); Lambeck et al., (in prep).

A.1.2 Analytical procedures

SHRIMP U-Pb isotopic analysis were conducted on Geoscience Australia's SHRIMP IIe using the procedures outlined in Carson et al. (2008). The unknown zircons were mounted together with the $^{206}Pb/^{238}U$ standard zircon Temora 2 (416.8; Ma Black et al., 2004) and $^{207}Pb/^{206}Pb$ standard zircon OG1 (3465; Stern et al., 2009). Cathodoluminescence (CL) images were taken of the zircons to reveal their internal zoning using a JEOL JSM-6490LV scanning electron microscope located at Geoscience Australia, operating at 15kV with a working distance of 16mm. Data reduction was carried out using SQUID 1.13b and ISOPLOT 3 Microsoft Excel-based macros of (Ludwig 2001; 2003). The pooled ages were calculated from the ^{204}Pb corrected $^{207}Pb/^{206}Pb$ ages using ISOPLOT 3 (Ludwig, 2003), and the final age is given at the 95% confidence interval. Error ellipses on the concordia diagram are plotted at the 1σ level.

For all SHRIMP U-Pb isotopic ages reported here, zircons that are over 1000 Ma are reported as $^{207}Pb/^{206}Pb$ ages. For zircons younger than 1000 Ma, $^{206}Pb/^{238}U$ ratios have been used as the $^{207}Pb/^{206}Pb$ ratios become too imprecise to be of any use. Additionally, for zircons older than 1000 Ma, both the $^{207}Pb/^{206}Pb$ and $^{206}Pb/^{238}U$ ratios can be used to access the level of concordance of each analysis, and thereby determine the degree to

which a given zircon has remained a closed system. In this report Pb isotopic ratios are corrected for common Pb by reference to the measured ^{204}Pb and all errors are quoted as 1σ. For zircons older than 1000 Ma, an arbitrary cut-off of 10% discordance has been used to exclude disturbed analyses from age considerations. However, for zircons younger than 1000 Ma, concordance cannot be properly determined because the ^{207}Pb/^{206}Pb ratios are too imprecise. Therefore, the degree of concordance cannot be used to identify and remove disturbed analyses.

Acknowledgements

I'd like to acknowledge the meticulous care and professionalism taken with the crushing of samples, SHRIMP mount preparation, photography and SEM imaging of zircons undertaken by members of the Geoscience Australia Geochronology Laboratory: David DiBugnara, Emma Chisholm, Chris Foudoulis and Stephen Ridgeway. Patrick Burke ensured the SHRIMP was optimally tuned during all analytical sessions and Les Sullivan's readiness to assist with any computer related or data storage issues is much appreciated. Chris Carson, Chuck Magee and Andrew Cross are thanked for helping with the running of the SHRIMP, data presentation and many fun and thoughtful geochronology discussions.

Samples Analysed

A.1.3 GA sample ID **1977852**: Georgetown Inlier, Etheridge Group, Lane Creek Formation

GA sample No: 1977852
GA Sample ID: 2008165300
GSQ Sample ID: IWGT550
GA mount No: GA6083
1:100 000 sheet: FOREST HOME (7561)
1:250 000 sheet: GEORGETOWN (SE5412)
Geographic area: Georgetown Inlier
Region: Georgetown, Robertson River Subgroup
Grid Reference (MGA94 Zone 54) 758347 mE 7958097 mN
Formal name: Lane Creek Formation
Lithology: Grey feldspathic fine-grained sandstone

A.1.4 Sample information

This sample was collected from the Lane Creek Formation which sits stratigraphically at the top of the Robertson River Subgroup in the Etheridge Province of the Georgetown Inlier. SHRIMP U–Pb dating was undertaken to establish the maximum depositional age of the Lane Creek Formation. The Lane Creek Formation is constrained by the 1655.9 ± 2.2 Ma leucogabbro sill which intrudes this unit and is thought to approximate the depositional age of the Lane Creek Formation (Black et al., 1998). The sample was collected to test if the maximum timing of deposition of the Lane Creek Formation could potentially be correlated with the ca. 1658 Ma maximum depositional age of the Toole Creek Volcanics (sandstone unit) in the Mount Isa Eastern Succession (Carson et al., 2008). The sample collected for analysis is a poorly sorted fine-grained sandstone collected by Ian Withnall GSQ.

A.1.5 Zircon description

Zircons from this sample range from ~100 μm to ~270 μm in length, and are clear to brown in colour. Ninety-eight percent of grains are well rounded commonly with surficial pitting and frosting and lacking prismatic edges. The remaining grains are heavily cracked fragments of probably rounded grains. Cathodoluminescence images recording oscillatory zoning within ninety-five percent of grains with the remainder of grains showing no zoning (Fig. A.1).

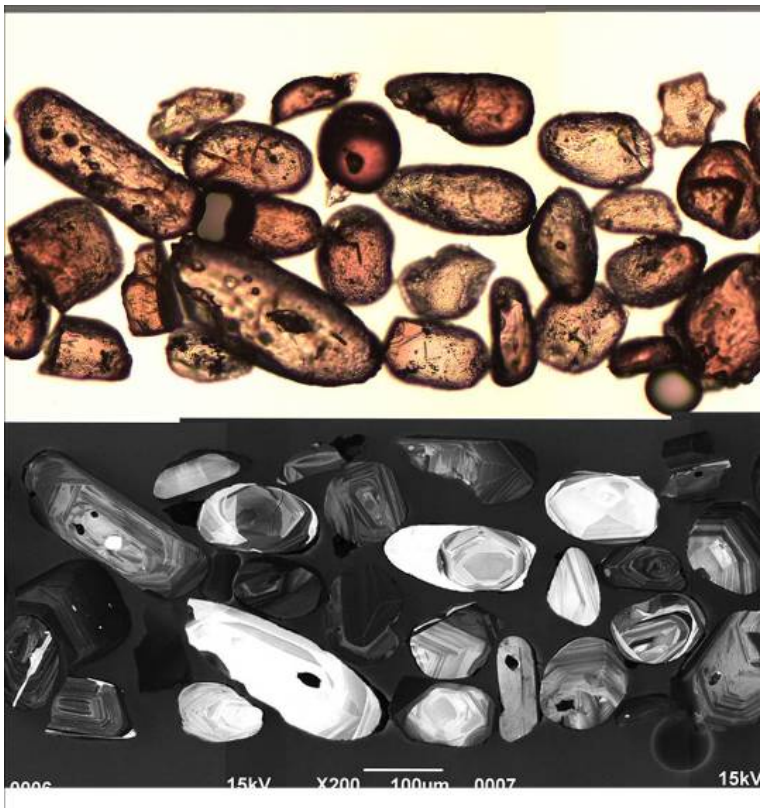

Figure A.1. Selected transmitted light (top) and cathodoluminescence (bottom) images of zircon grains from the Lane Creek Formation (Forest Hill, 1977852).

A.1.6 U–Pb isotopic results

Eighty-five analyses were undertaken on eighty-three zircons from this sample (Fig. A.2, Table A.1). Uranium contents range from 36-1175 ppm and Th/U from 0.08 – 1.55. Common Pb contents are all below 1% (f^{206}). One poor analysis with a large error range is plotted as an open ellipse (Fig. A.2). Figures A.2 & A.3 display a Tera-Wasserburg Concordia diagram and a cumulative probability diagram of isotopic data, respectively, from the Lane Creek sample. The MSWD value for the weighted mean age of this entire group indicates that it is not a single population. The youngest statistical grouping (readily apparent in Fig. A.2, Table A.1) forms a population which returns a weighted mean of **1789 ± 8** Ma (95% confidence; n = 13, MSWD = 1.7) which can be used as a maximum depositional age for this sample.

The maximum depositional age of the formation suggests that it cannot be directly compared to the maximum depositional age of the ~1658 Ma Toole Creek Volcanics in the Mount Isa Eastern Succession (Carson et al., 2008). The result shows that the Lane Creek Formation sediments have a volumetrically dominant Paleoproterozoic/Archean

source that is not as evident in the Toole Creek Volcanics sediments (Carson et al., 2008).

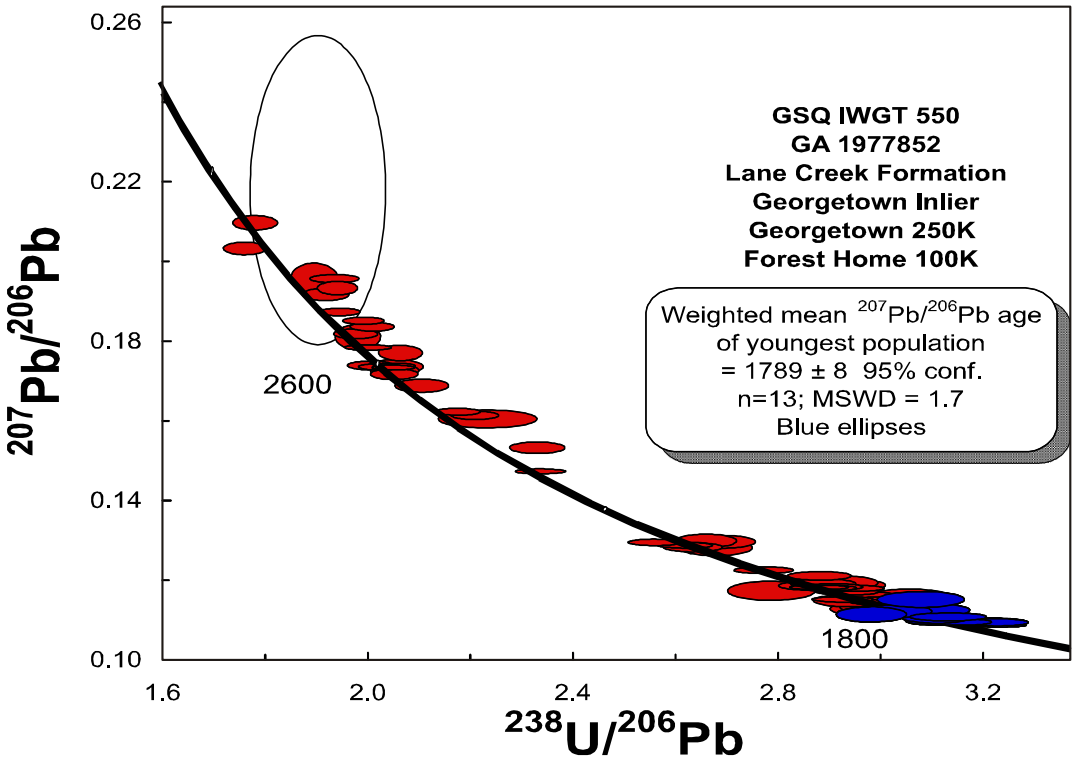

Figure A.2. Tera-Wasserburg Concordia diagram of isotopic data from the Lane Creek Formation (GA 200816300; GSQ IWGT-550), Forest Home, Georgetown Inlier. Blue ellipses indicate analyses included in weighted mean determination of 1789 ± 8 Ma. Open ellipse not included in age determination.

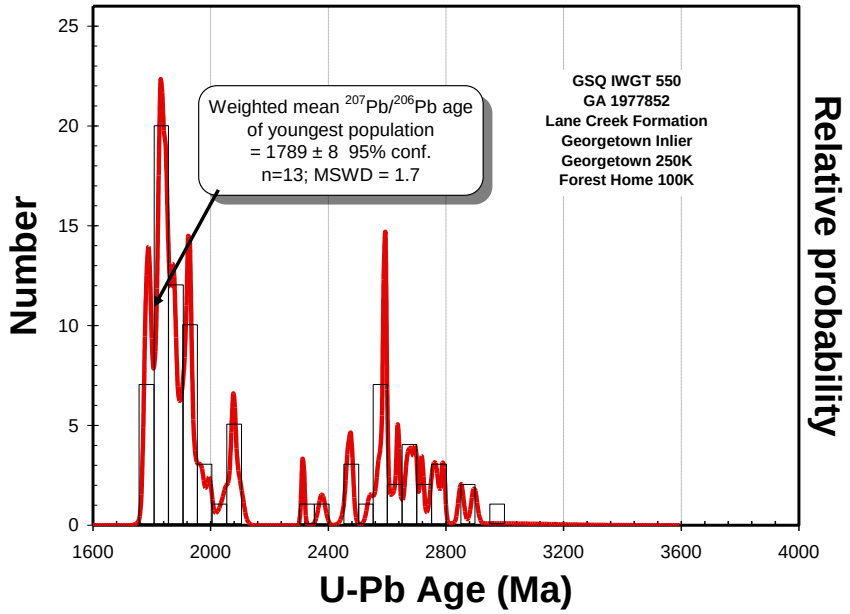

Figure A.3. Cumulative probability diagram of isotopic data from the Lane Creek Formation (GA 200816300; GSQ IWGT-550), Forest Home, Georgetown Inlier. The youngest population at 1789 ± 8 Ma (n = 13; MSWD = 1.7) is taken as the Maximum Deposition Age for this unit. Total number of accepted analyses = 85.

Table A.1: SHRIMP U–Pb zircon isotopic data from Lane Creek Formation grey feldspathic sandstone (1977852). Grey shading displays youngest statistical grouping.

Grain area	$^{206}Pb_c$ (%)	U (ppm)	Th (ppm)	$^{232}Th/^{238}U$	$^{238}U/^{206}Pb^*$	± (%)	$^{207}Pb^*/^{206}Pb^*$	± (%)	$^{206}Pb/^{238}U$ Age (Ma)	± (1s)	$^{207}Pb/^{206}Pb$ Age (Ma)	± (1s)	Discordance %
Detrital zircons													
852.61.1.1	0.02	906	298	0.34	3.2208	1.31	0.1087	0.3	1743	20.8	1775	5.5	3
852.22.1.1	0.02	439	237	0.56	3.1215	1.35	0.1093	0.4	1791	22.6	1785	7.9	2
852.20.1.1	0.04	239	102	0.44	3.2034	1.68	0.1095	0.6	1750	27.2	1785	11.1	2
852.25.1.1	-0.01	434	172	0.41	3.1904	1.35	0.1092	0.4	1757	21.8	1787	7.8	2
852.5.1.1	0.00	327	133	0.42	3.2237	1.38	0.1093	0.5	1743	22.2	1788	9.0	1
852.81.1.1	0.03	294	104	0.37	3.1155	1.40	0.1097	0.5	1794	23.0	1790	10.5	2
852.8.1.1	-0.01	478	395	0.86	3.1536	1.34	0.1094	0.5	1777	23.3	1792	8.5	0
852.57.1.1	0.05	147	61	0.43	3.1089	1.50	0.1109	1.1	1796	24.8	1806	20.7	0
852.84.1.1	0.22	82	44	0.55	3.0951	1.69	0.1124	1.0	1805	28.6	1807	22.7	1
852.49.1.1	0.14	81	63	0.80	3.0252	1.66	0.1121	0.9	1845	29.7	1815	21.9	2
852.53.1.1	0.04	138	75	0.56	2.9820	1.51	0.1114	1.1	1863	26.3	1817	21.2	0
852.55.1.1	-0.07	237	88	0.38	3.1333	1.57	0.1107	0.6	1785	25.8	1820	11.0	1
852.66.1.1	0.41	56	54	1.00	3.0784	1.83	0.1151	1.2	1807	33.4	1824	30.8	1
852.10.1.1	0.05	267	94	0.36	3.0805	1.39	0.1122	0.5	1812	23.0	1828	10.5	1
852.46.2.1	0.13	85	63	0.76	3.0532	1.72	0.1129	0.9	1835	30.3	1829	20.7	3
852.82.1.1	-0.01	458	129	0.29	3.0383	1.63	0.1117	0.4	1836	26.9	1829	7.4	1
852.47.1.1	0.01	645	349	0.56	3.0939	1.32	0.1119	0.3	1805	22.3	1829	6.4	2
852.54.1.1	0.05	227	92	0.42	3.0417	1.42	0.1122	0.6	1831	23.9	1829	10.8	3
852.71.1.1	0.14	83	60	0.75	3.0010	1.76	0.1131	0.9	1856	31.4	1830	22.3	3
852.59.1.1	0.03	577	50	0.09	3.0492	1.41	0.1123	0.4	1829	22.8	1833	6.7	1
852.41.1.1	-0.01	424	304	0.74	3.1077	1.35	0.1121	0.4	1797	23.3	1835	7.5	1
852.31.1.1	0.01	315	330	1.08	3.0753	1.38	0.1122	0.5	1817	25.2	1835	8.8	0
852.11.1.1	0.13	107	44	0.43	3.0492	1.57	0.1134	0.8	1827	26.3	1837	17.6	1
852.64.1.1	0.04	60	42	0.72	2.9861	1.88	0.1128	1.1	1857	33.5	1838	20.5	0
852.40.1.1	0.01	1175	92	0.08	3.0320	1.30	0.1129	0.2	1837	20.9	1845	4.5	1
852.56.1.1	-0.01	252	101	0.41	3.0444	1.41	0.1128	0.5	1831	23.6	1847	9.7	0
852.29.1.1	0.00	282	166	0.61	3.0578	1.39	0.1130	0.5	1824	23.9	1848	9.0	0
852.33.1.1	0.01	449	57	0.13	3.0426	1.34	0.1132	0.4	1831	21.7	1851	7.2	0
852.32.1.1	0.02	728	272	0.39	3.0338	1.32	0.1136	0.3	1837	22.2	1855	5.8	1
852.14.1.1	0.07	95	54	0.59	3.0407	1.60	0.1144	0.8	1821	27.7	1861	16.9	-1
852.73.1.1	0.02	433	108	0.26	3.0746	1.35	0.1141	0.4	1814	22.1	1864	7.9	1
852.18.1.1	-0.02	485	229	0.49	3.0010	1.34	0.1144	0.4	1852	22.9	1873	6.7	-1
852.43.1.1	0.04	449	120	0.28	2.9888	1.34	0.1150	0.4	1862	22.4	1874	7.7	-1
852.21.1.1	0.01	88	12	0.14	2.9412	1.62	0.1148	0.9	1886	27.0	1875	15.7	1
852.50.1.1	0.04	385	216	0.58	2.9252	1.36	0.1151	0.4	1894	24.0	1877	7.9	-3
852.42.1.1	-0.02	159	127	0.83	3.0599	1.48	0.1148	0.7	1822	26.2	1880	12.3	1
852.63.2.1	0.24	36	36	1.03	2.7862	2.05	0.1173	1.3	1972	40.3	1883	39.5	2
852.27.1.1	0.01	54	21	0.41	3.0535	1.81	0.1157	1.2	1823	30.4	1890	21.5	2
852.16.1.1	-0.01	156	30	0.20	2.9676	1.48	0.1159	0.7	1872	24.7	1896	11.9	-1
852.4.1.1	0.04	304	246	0.84	2.9350	1.39	0.1170	0.5	1886	25.4	1906	9.3	1
852.3.1.1	0.07	125	75	0.62	2.9383	1.54	0.1178	0.8	1890	27.4	1914	14.6	1
852.9.1.1	0.13	134	201	1.55	2.9421	1.51	0.1187	0.8	1881	31.0	1919	16.8	-1
852.28.1.1	0.04	351	179	0.53	2.9459	1.36	0.1180	0.4	1884	23.8	1921	8.0	3
852.13.1.1	0.02	336	184	0.57	2.9053	1.36	0.1182	0.4	1907	24.2	1927	8.1	2
852.17.1.1	0.00	426	197	0.48	2.8941	1.35	0.1180	0.4	1912	23.6	1927	7.0	1
852.44.1.1	0.05	152	83	0.57	2.8646	1.48	0.1186	0.7	1929	26.6	1928	12.9	1
852.19.1.1	0.01	713	265	0.38	2.8792	1.32	0.1182	0.3	1921	22.9	1928	5.5	1
852.30.1.1	0.09	166	222	1.38	2.8877	1.47	0.1190	0.7	1916	29.5	1930	13.4	3
852.48.1.1	-0.07	75	49	0.68	2.9053	1.69	0.1187	0.9	1906	30.4	1947	17.6	0
852.52.1.1	-0.05	133	67	0.52	2.9280	1.51	0.1193	0.9	1894	26.6	1953	17.3	0
852.62.1.1	0.01	197	189	0.99	2.8797	1.44	0.1210	0.6	1918	27.3	1970	10.2	-5
852.67.1.1	-0.02	285	196	0.71	2.7704	1.39	0.1225	0.5	1985	25.9	1995	8.3	0
852.12.1.1	0.28	63	55	0.89	2.6767	1.74	0.1280	1.0	2045	34.4	2036	23.0	3
852.85.1.1	0.14	173	93	0.55	2.6314	1.48	0.1282	0.6	2076	28.1	2056	12.6	0
852.80.1.1	0.11	433	143	0.34	2.5578	1.36	0.1294	0.4	2125	25.7	2077	7.6	2
852.65.1.1	0.02	439	193	0.45	2.6165	1.35	0.1288	0.4	2087	25.3	2078	6.5	-1
852.38.1.1	0.03	150	59	0.41	2.6572	1.48	0.1298	0.8	2058	27.4	2092	14.7	0
852.26.1.1	-0.03	88	46	0.54	2.6888	1.62	0.1296	0.8	2038	30.3	2096	14.2	-2
852.60.1.1	0.01	618	328	0.55	2.3327	1.41	0.1473	0.3	2300	29.0	2314	4.8	1
852.6.1.1	0.04	129	119	0.95	2.3262	1.53	0.1533	0.6	2301	33.3	2378	11.3	3
852.70.1.1	0.03	246	109	0.46	2.2041	1.41	0.1613	0.4	2413	29.8	2467	7.4	2
852.34.1.1	-0.08	49	22	0.47	2.2283	2.88	0.1604	0.9	2387	60.6	2467	15.6	3
852.39.1.1	0.01	287	127	0.46	2.1698	1.38	0.1623	0.4	2443	29.6	2479	6.2	1
852.23.1.1	0.03	83	36	0.44	2.0995	1.63	0.1689	0.7	2514	35.7	2543	11.4	1
852.15.1.1	0.05	122	85	0.72	2.0446	1.52	0.1717	0.5	2563	35.0	2570	9.3	0
852.51.1.1	0.02	291	104	0.37	2.0463	1.54	0.1725	0.6	2564	33.9	2581	10.2	1
852.76.1.1	-0.01	522	411	0.81	2.0433	1.34	0.1734	0.3	2567	31.0	2591	4.4	1

Table A.1: (Continued)

Grain area	$^{206}Pb_c$ (%)	U (ppm)	Th (ppm)	$^{232}Th/^{238}U$	$^{238}U/^{206}Pb^*$	± (%)	$^{207}Pb^*/^{206}Pb^*$	± (%)	$^{206}Pb/^{238}U$ Age (Ma)	± (1s)	$^{207}Pb/^{206}Pb$ Age (Ma)	± (1s)	Discordance %
Detrital zircons													
852.77.1.1	0.00	382	112	0.30	2.0165	1.36	0.1735	0.3	2596	30.0	2592	5.2	0
852.72.1.1	0.01	76	36	0.50	2.0499	1.70	0.1737	0.7	2557	37.9	2593	11.7	1
852.7.1.1	0.01	416	62	0.15	2.0449	1.37	0.1738	0.3	2566	29.5	2594	4.9	1
852.75.1.1	0.01	202	93	0.47	1.9985	1.49	0.1738	0.4	2616	33.6	2594	7.2	-1
852.45.1.1	0.02	353	289	0.84	2.0573	1.37	0.1770	0.7	2549	31.7	2624	12.4	3
852.1.1.1	0.02	521	85	0.17	1.9939	1.50	0.1785	0.3	2620	32.8	2637	4.4	1
852.36.1.1	0.05	172	58	0.35	1.9738	1.49	0.1810	1.2	2645	33.5	2658	19.5	1
852.35.1.1	0.00	160	96	0.62	1.9693	1.47	0.1819	0.4	2647	34.1	2670	7.4	1
852.83.1.1	0.03	222	76	0.35	2.0015	1.43	0.1836	0.4	2616	31.8	2684	6.7	3
852.69.1.1	0.02	391	218	0.57	1.9852	1.35	0.1851	0.3	2624	31.0	2697	5.4	3
852.37.1.1	0.01	250	177	0.73	1.9368	1.39	0.1873	0.3	2687	33.1	2718	5.8	1
852.68.1.1	0.88	85	67	0.81	1.8887	1.64	0.1957	1.3	2741	40.4	2723	42.1	0
852.78.1.1	0.03	109	78	0.74	1.9110	1.57	0.1918	0.5	2714	37.7	2755	9.2	2
852.74.1.1	0.02	430	51	0.12	1.9328	1.35	0.1933	0.6	2689	30.1	2769	9.3	3
852.2.1.1	0.00	278	321	1.19	1.9279	1.69	0.1957	0.3	2693	42.5	2791	5.7	4
852.79.1.1	0.03	110	33	0.31	1.7525	1.58	0.2033	0.5	2909	38.2	2851	8.7	-2
852.24.1.1	0.12	82	75	0.94	1.7719	1.63	0.2098	0.6	2879	42.0	2896	9.9	1
Discordant													
No discordant analyses													
high comm Pb													
No samples with high comm Pb													
Poor analysis													
852.58.1.1	-0.05	107	113	1.10	1.8954	4.65	0.2180	11.8	2712	121.1	2969	189.1	9

A.1.7 GA sample ID: **1999372**, Georgetown Inlier, Etheridge Group, Candlow Formation volcanic rock

GA sample No: 1999372
GA mount No: GA6108
GA Sample ID: 2009165047
1:100 000 sheet: NORTH HEAD (7560)
1:250 000 sheet: GEORGETOWN (SE54-12)
Geographic area: Georgetown Inlier
Region: Georgetown, Robertson River Subgroup
Grid Reference (MGA94 Zone 54) 54 716921 mE 7933866 mN
Formal name: Candlow Formation
Lithology: Felsic volcanic
Drill core intervals: 153.39-158.13m and 160.20-161.64m

A.1.8 Sample information

The sample was collected from a volcanic rock within the Candlow Formation, Etheridge Province of the Georgetown Inlier. The Candlow Formation lies stratigraphically above the Lane Creek Formation and is therefore potentially younger than the ca. 1655 Ma leucogabbro sill in that unit (Withnall et al., 1988; Black et al., 1998; Baker et al., 2010). Black and McCulloch (1984) completed Sm-Nd analysis on the volcanic rock within the Candlow Formation which suggests a juvenile magmatic input. This juvenile magmatic input was dismissed by Black and McCulloch (1984) as alteration effects. However more detailed isotopic work by Lambeck (2011), Lambeck et al., (in review), and Lambeck et al., (in prep) suggests the juvenile input is part of a larger juvenile volcanic suite that is represented through out Proterozoic Australia. The drill core was re-examined by A. Lambeck as part of his PhD program in collaboration

with I.Withnall (Geological Survey of Queensland). The volcanic unit was interpreted by A. Lambeck and I.Withnall to have basal peperitic textures. Dating the volcanic rock was thought to be able to provide direct timing of felsic magmatism and deposition of sedimentation in the Georgetown Inlier. The sample was collected by I. Withnall from drill core, GSQ Georgetown 4, at two intervals and combined during crushing to maximise potential zircon yield.

A.1.9 Zircon description

Zircons from this sample range from ~20 μm to ~220 μm in length, and are clear to brown in colour. The zircons are sub angular to rounded and lack clearly defined prismatic edges (Fig. A.4). This suggests that there are a high percentage of inherited components within this sample.

Figure A.4. Selected transmitted light (top) and cathodoluminescence (bottom) images of zircon grains from the volcanic rock within the Candlow Formation (North Head, 1999372).

A.1.10 U–Pb isotopic results

Thirty-eight analyses were undertaken on twenty-seven zircons from this sample (Fig. A.5, Table A.2). Uranium contents range from 13-854 ppm and Th/U from 0.02 – 1.30. Common Pb contents are all below 1% (f_{206}). Three analyses are discordant and have been removed form further consideration. Figures A.5 & A.6 respectively display Tera-Wasserburg Concordia diagrams of Proterozoic data and Phanerozoic data. Figure A.7 displays a cumulative probability diagram of all isotopic data from the Candlow Formation volcanic rock. Inspection of these diagrams indicated multiple zircon populations. The youngest population is defined by three analysis on one zircon (372.Z.1.1.1, 372.Z.1.2.1 & 372.1.3.1), with a $^{206}Pb/^{238}U$ Phanerozoic age of 301 ± 8 Ma, MSWD = 0.33, Table A.2; Figs. A.6 & A.8). Two analysis (372.Z.10.1.1 & 372.Z.10.2.1) on the same zircon grain with low $^{232}Th/^{238}U$ values (0.05 and 0.02 respectively: Table A.2, Figs. A.9 & A.10) are interpreted to be zircon recrystallisation as described in detail by Hoskin and Black (2000) and indicate an age of 1549 ± 26 Ma.

The remaining analyses do not form a coherent group (MSWD 162, n = 29). The youngest statistical grouping (Figs. A.5 & A.7, Table A.2) form a population which returns a weighted mean of **1675 ± 8 Ma** (95% confidence; n = 23, MSWD = 1.5).

Determining the depositional age of the Candlow Formation is complex. The sample includes a Phanerozoic zircon grain, zircon recrystallisation at ~1550 Ma, and a large range in zircons from ca. 1573 ± 39 Ma to 2656 ± 15 Ma. The youngest Phanerozoic grain is problematic. This age is not consistent with geological relationships in the region, and is interpreted as either a contaminant or the consequence of Phanerozoic isotopic disturbance.

With respect to the major zircon distribution, interpreting the youngest statistical grouping of **1675 ± 8 Ma** as a depositional or volcanic age is not geologically consistent with the current understanding of the Georgetown stratigraphy (Withnall et al., 1988; Black et al., 1998; Baker et al., 2010). Rather, this age is interpreted as a maximum depositional age, an interpretation consistent with the morphology of the zircons. Hence, the age of the Candlow Formation is interpreted to lie between the age of the ca. 1655 Ma leucocratic gabbro sill that intrudes the underlying Lane Creek Formation and ca. 1550 Ma, the age of the zircon recrystallisation identified in this sample.

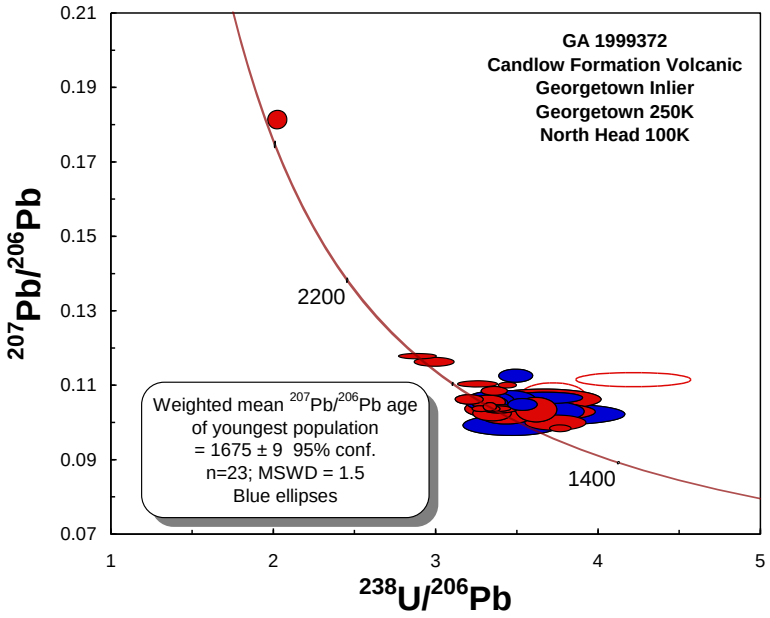

Figure A.5. Tera-Wasserburg Concordia diagram of isotopic data from the Candlow Formation Volcanic rock (GA 2009165047;1999372), Forest Home, Georgetown Inlier. Red open ellipses = omitted analyses with >10% discordance and/or high common ^{206}Pb (>1%). Blue ellipses indicate analyses included in weighted mean determination of 1675 ± 9 Ma.

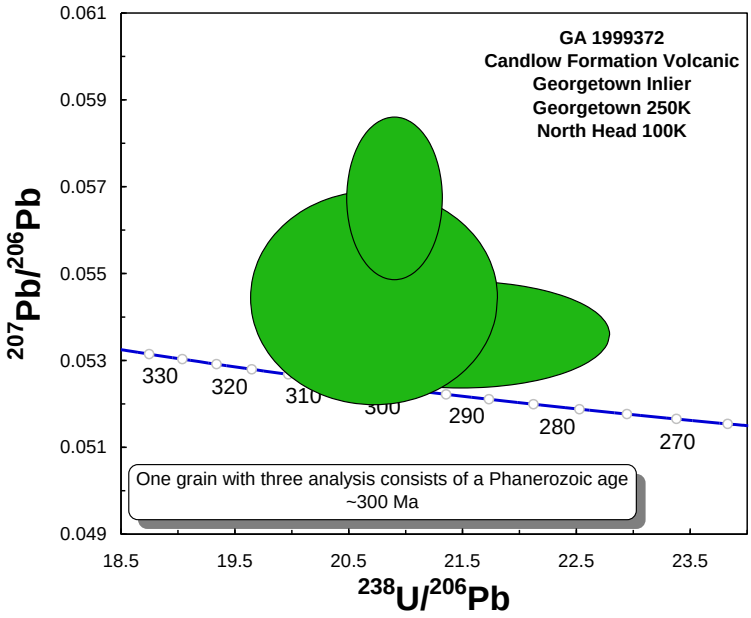

Figure A.6. Tera-Wasserburg Concordia diagram of isotopic data from three analysis on one zircon in the Candlow Formation Volcanic rock (GA 1999372), North Head, Georgetown Inlier. Green ellipses included in weighted mean determination of 300 ± 8 Ma (MSWD = 0.33, Table A.2)

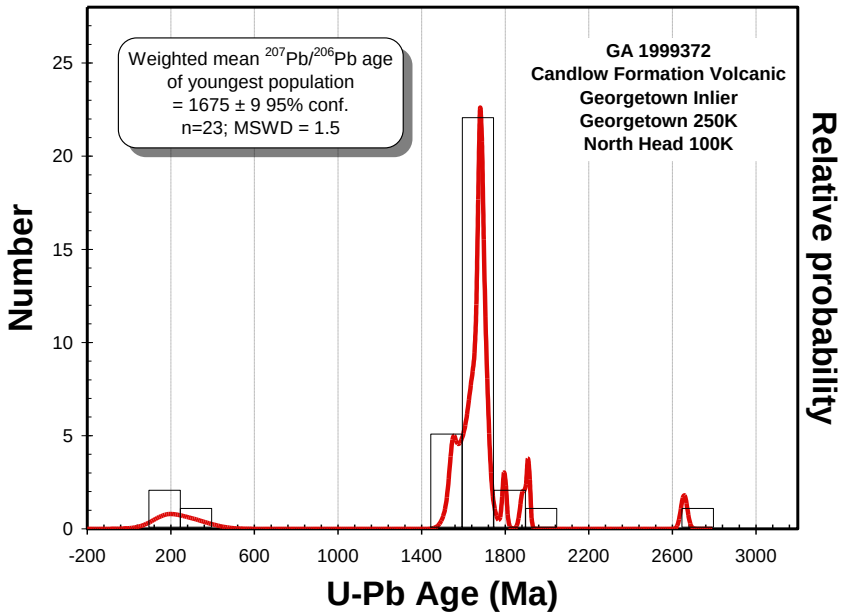

Figure A.7. Cumulative probability diagram of isotopic data from the Candlow Formation volcanic rock (GA 1999372), North Head, Georgetown Inlier. Three analyses on one zircon provide a Phanerozoic age (Fig. A.6). The youngest statistical population at 1675 ± 9 Ma (n = 23; MSWD = 1.5) is interpreted as a 'maximum depositional age' and is not regarded as a representative volcanic age. Total number of accepted analyses = 34.

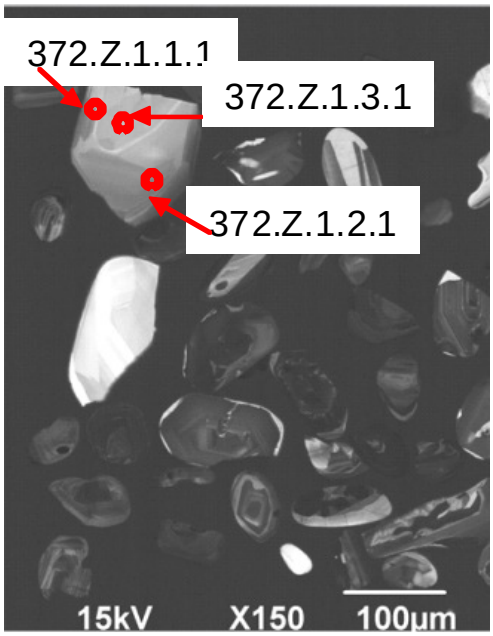

Fig. A.8. Cathodoluminescence images of zircon grains from the volcanic rock within the Candlow Formation (North Head, 1999372). Analysis with sample numbers 372.Z.1.1.1, 372.Z.1.2.1 & 372.Z.1.3.1 yielded a Phanerozoic age (Table A.2, Fig. A.6).

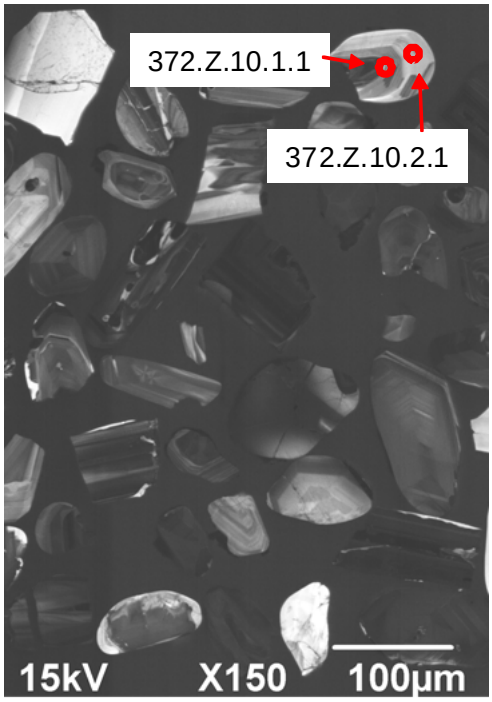

Fig. A.9. Cathodoluminescence images of zircon grains from the volcanic rock within the Candlow Formation (North Head, 1999372). Analysis with sample numbers; 372.Z.10.1.1 & 372.Z.10.2.1 consisting of low 232Th/238 U values (Fig. A.10) are interpreted as zircon recrystallisation (Table A.2, see Hoskin and Black (2000) for more details).

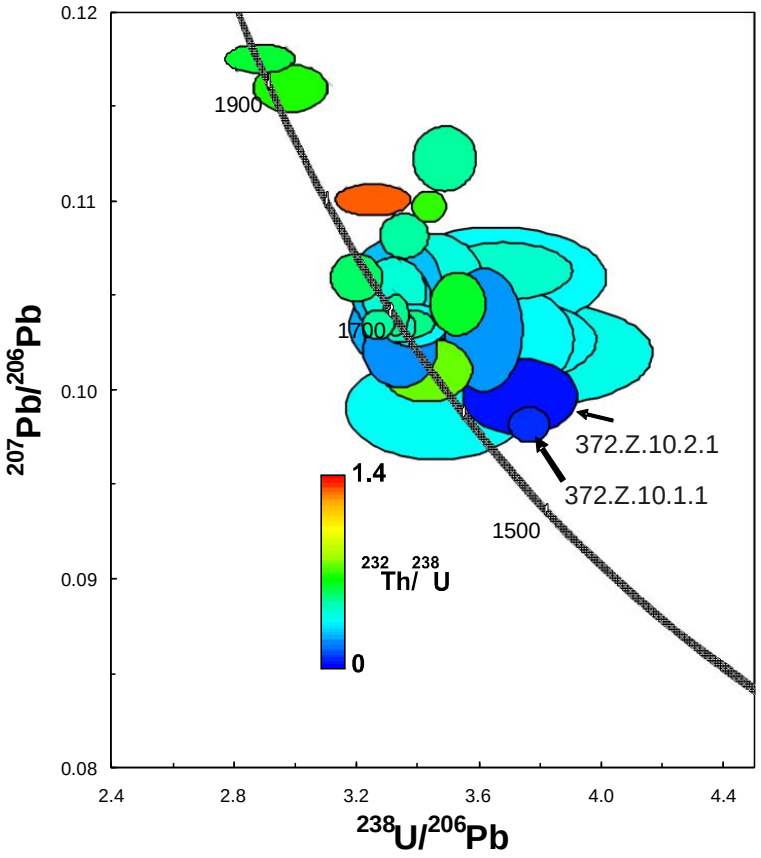

Figure A.10. Tera-Wasserburg Concordia diagram of isotopic data from the Candlow Formation volcanic rock (GA 200816500), North Head, Georgetown Inlier. Ellipses are coloured by $^{232}Th/^{238}U$ values with analyses 372.Z.10.1.1 and 372.Z.10.2.1 consisting of low $^{232}Th/^{238}U$ values, 0.05 and 0.02 respectively. These two analyses are interpreted as zircon recrystallisation (see Fig. A.9).

.

Table A.2: SHRIMP U–Pb zircon isotopic data from felsic volcanic intrusive in the Candlow Formation (1999372). Grey shading displays youngest statistical grouping

Grain area	$^{206}Pb_c$ (%)	U (ppm)	Th (ppm)	$^{232}Th/^{238}U$	$^{238}U/^{206}Pb^*$	± (%)	$^{207}Pb^*/^{206}Pb^*$	± (%)	$^{206}Pb/^{238}U$ Age (Ma)	± (1σ)	$^{207}Pb/^{206}Pb$ Age (Ma)	± (1σ)	Discordance %	
Volcanic zircons														
372.Z.1.2.1	0.51	234	136	0.60	21.4883	4.02	0.0536	1.52	291	12.8	173	62.7	-71	Phanerozoic
372.Z.1.3.1	0.42	92	52	0.58	20.7353	3.44	0.0544	2.98	304	11.3	242	114.9	-25	Phanerozoic
372.Z.1.1.1	0.57	125	86	0.71	20.9144	1.32	0.0567	2.18	302	4.6	292	89.3	-2	Phanerozoic
372.Z.10.1.1	0.24	165	9	0.05	3.7666	1.17	0.0981	0.63	1517	16.0	1548	14.3	2	zircon recrystallisation
372.Z.10.2.1	0.39	62	1	0.02	3.7371	3.30	0.0996	1.33	1528	45.0	1553	33.9	2	zircon recrystallisation
372.Z.16.2.1	0.19	16	5	0.35	3.4642	5.58	0.0989	1.81	1640	84.1	1573	39.3	-4	
372.Z.13.2.1	0.45	18	6	0.37	3.7648	7.04	0.1019	1.81	1522	99.8	1587	43.8	5	
372.Z.15.2.1	0.52	22	8	0.35	3.6250	6.52	0.1025	1.54	1562	95.2	1588	38.5	2	
372.Z.2.1.1	0.75	21	5	0.24	3.3356	2.97	0.1054	1.61	1693	45.5	1603	46.2	-5	
372.Z.25.1.1	0.46	31	6	0.21	3.3943	4.12	0.1033	1.64	1662	62.1	1611	42.8	-3	
372.Z.4.1.1	0.31	34	6	0.19	3.6195	2.27	0.1031	2.09	1570	32.6	1632	43.2	4	
372.Z.23.1.1	0.02	212	154	0.75	3.4356	2.82	0.1010	1.11	1643	45.4	1639	20.7	0	
372.Z.8.2.1	0.19	42	14	0.34	3.6575	4.59	0.1026	1.91	1561	66.3	1641	37.7	6	
372.Z.13.1.1	0.49	18	7	0.38	3.4567	3.12	0.1054	1.76	1638	47.6	1646	44.0	1	
372.Z.3.1.1	0.34	77	45	0.60	3.5354	1.68	0.1045	1.04	1601	26.1	1653	23.9	4	
372.Z.8.1.1	0.00	32	6	0.18	3.3476	2.35	0.1021	1.31	1688	35.7	1663	24.3	-2	
372.Z.5.1.1	0.07	234	107	0.47	3.2766	1.04	0.1034	0.50	1719	16.6	1675	9.7	-3	
372.Z.14.1.1	0.23	44	13	0.31	3.3388	2.12	0.1049	1.14	1683	32.8	1677	24.7	-1	
372.Z.9.1.1	0.25	44	17	0.40	3.3259	2.09	0.1051	1.16	1688	33.0	1677	25.6	-1	
372.Z.12.1.1	0.03	217	90	0.43	3.3442	1.04	0.1033	0.50	1684	16.4	1680	9.5	0	
372.Z.6.1.1	0.02	241	116	0.50	3.3698	1.78	0.1034	0.49	1673	28.0	1683	9.1	1	
372.Z.22.1.1	0.00	157	50	0.33	3.3933	2.08	0.1034	0.73	1664	31.9	1685	13.4	1	
372.Z.7.1.1	0.05	522	245	0.49	3.3336	0.80	0.1039	0.70	1690	12.7	1688	13.2	0	
372.Z.18.1.1	0.26	277	142	0.53	3.2061	1.74	0.1059	0.79	1751	28.7	1691	17.4	-4	
372.Z.4.2.1	0.30	56	22	0.41	3.6822	4.00	0.1063	0.95	1546	58.2	1691	21.1	10	
372.Z.19.1.1	0.49	333	151	0.47	3.3615	1.56	0.1081	0.73	1671	24.6	1694	19.2	2	
372.Z.17.1.1	0.96	214	99	0.47	3.4923	1.96	0.1122	1.01	1612	30.0	1695	61.0	6	
372.Z.2.2.1	0.22	22	7	0.33	3.6586	6.47	0.1059	1.67	1557	93.5	1697	35.6	9	
372.Z.20.1.1	0.57	854	571	0.69	3.4417	1.06	0.1097	0.49	1638	17.0	1709	12.9	5	
372.Z.15.1.1	0.09	37	13	0.35	3.4155	3.81	0.1058	1.24	1657	58.2	1713	24.3	4	
372.Z.21.1.1	0.03	269	339	1.30	3.2595	2.47	0.1100	0.50	1722	45.0	1796	9.3	5	
372.Z.27.1.1	0.06	136	88	0.67	2.9915	2.67	0.1159	0.70	1860	46.9	1886	13.3	2	
372.Z.24.1.1	0.05	355	202	0.59	2.8904	2.63	0.1175	0.42	1913	46.9	1911	7.9	0	
372.Z.26.1.1	0.07	108	70	0.67	2.0275	1.84	0.1810	0.90	2579	42.4	2656	15.1	3	
Discordant														
372.Z.14.2.1	0.23	13	3	0.25	3.7219	3.49	0.1074	2.01	1529	49.6	1721	42.7	12	
372.Z.7.2.1	0.83	825	649	0.81	4.2183	5.56	0.1115	1.13	1366	76.9	1702	34.8	22	
372.Z.11.1.1	5.09	2056	38	0.02	7.4162	3.23	0.1476	0.97	775	25.0	1687	30.2	57	
high comm Pb														
No analyses														

A.1.11 GA sample ID: **1977975,** Georgetown Inlier, Unnamed unit

GA sample No: 1977975
GA Sample ID: 2008837024
GA mount No: GA6083
1:100 000 sheet: WALLABADAH (7362)
1:250 000 sheet: NORMANTON (SE54-7)
Geographic area: Wallabadah
Region: Georgetown Inlier
Grid Reference (MGA94 Zone 54) 54 647940 mE 8025110 mN, A2 Prospect
Formal name: Unnamed
Lithology: Silty mudstone
Drill core interval: A2-006, depth 397.7 to 398.5 m

A.1.12 Sample details

This sample was collected to provide a maximum depositional age of an unnamed silty mudstone unit within the Georgetown Inlier. Dating these rocks was thought to provide a maximum depositional age of the upper stratigraphy within the Georgetown Inlier. The sample was collected from drill core from the A2 Prospect, near Croydon, by D. Huston, Geoscience Australia.

A.1.13 Zircon description

Zircons from sample 1977975 range from ~30 μm to ~125 μm in length with three large grains up to 300 μm in length. The poorly-sorted zircons are rounded to sub-angular and lack prismatic edges. Cathodoluminescence images records oscillatory zoning within most grains. Two large grains (ca. 300 μm in length) record oscillatory zoning and a third large grain (ca. 250 μm in length) exhibits a bright (low-U) CL response (Fig. A.11).

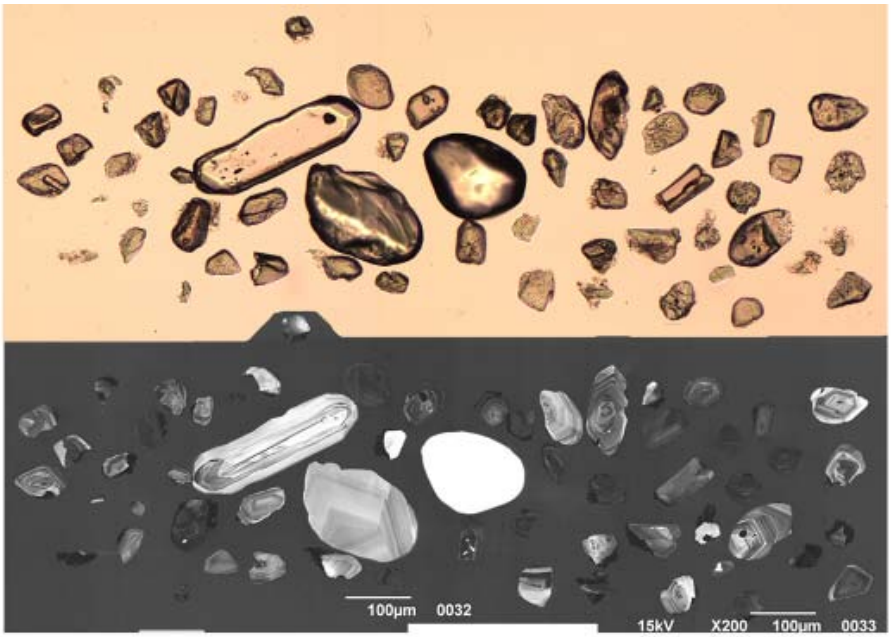

Figure A.11. Selected transmitted light (top) and cathodoluminescence (bottom) images of zircon grains from an unnamed silty mudstone (Croydon A2 Prospect, 1977975). Large zircons in this sample are Phanerozoic in age.

A.1.14 U–Pb isotopic results

Thirty eight analyses were undertaken on thirty-four zircons from sample 1977975 (Table A.3). Uranium contents range from 132-1310 ppm and Th/U from 0.1 – 1.71, common Pb contents are all below 1% (f^{206}). Figures A.12 & A.13 display Tera-Wasserburg Concordia diagrams of the Proterozoic and Phanerozoic data. The MSWD value for the weighted mean age of this entire group and presence of Phanerozoic zircons indicates that this sample does not contain a single zircon population.

The largest grains yielded ^{206}Pb-^{238}U ages of between ca. 432 Ma and ca. 574 Ma, with the two youngest analyses (on two different grains) yielding ages of 432 ± 6 Ma and 446 ± 6 Ma (1σ) that form a discrete population. The MSWD value for the weighted mean age of the Phanerozoic group indicates that it is not a single population (MSWD = 83). Although the Phanerozoic zircons are the best constraint on the age of sedimentation at the A2 prospect, the zircon population is dominated by Proterozoic zircons, which are characterised by a youngest statistical grouping that returns a weighted mean of **1622 ± 9** Ma (95% confidence; n = 12, MSWD = 1.9).

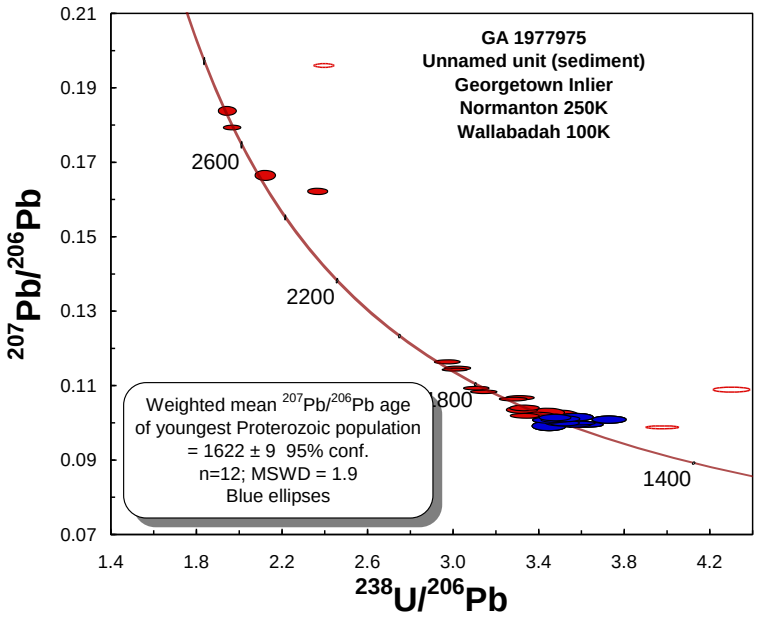

Figure A.12. Tera-Wasserburg Concordia diagram of older isotopic data from the silty mudstone from the A2 prospect (GA 1977975), Wallabadah, Georgetown Inlier. Red open ellipses = omitted analyses with >10% discordance and/or high common ^{206}Pb (>1%). Blue ellipses indicate analyses included in weighted mean determination of 1622 ± 9 Ma.

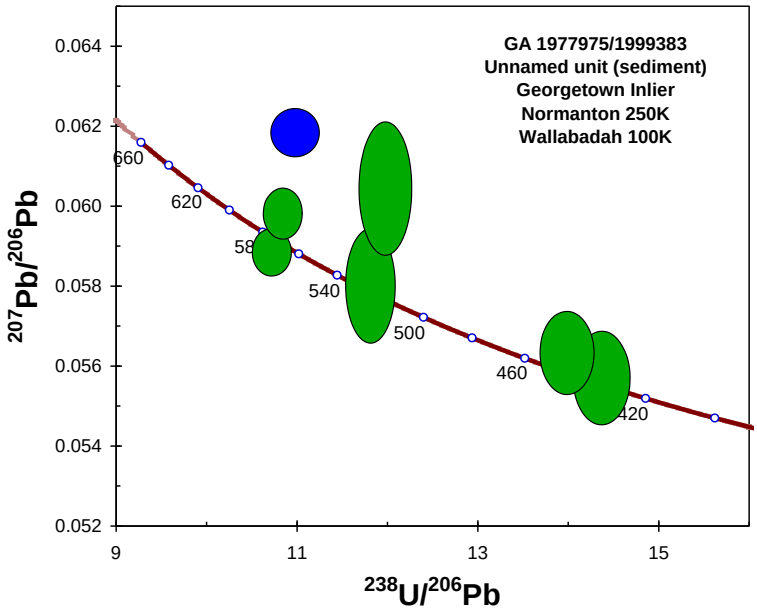

Figure A.13. Tera-Wasserburg Concordia diagram of younger isotopic data from the silty mudstone from the A2 prospect, Wallabadah, Georgetown Inlier. Green ellipses are of analyses from 1977975 and blue ellipsis is an analysis from 1999383.

A.1.15 GA sample ID: **1999383**, Georgetown Inlier, Unnamed unit.

GA sample No: 1999383
GA Sample ID: 2009165058
GA mount No: GA6108
1:100 000 sheet: WALLABADAH (7362)
1:250 000 sheet: NORMANTON (SE54-7)
Geographic area: Wallabadah
Region: Georgetown Inlier
Grid Reference (MGA94 Zone 54) 54 647940 mE 8025110 mN, A2 Prospect
Formal name: Unnamed
Lithology: Silty mudstone
Drill core interval: A2004 527 ─ 530.2 m

A.1.16 Sample details

This sample was collected by A. Lambeck from the Croydon A2 prospect, Georgetown Inlier, to assess if the Phanerozoic input in sample 1977975 was possible zircon contamination.

A.1.17 Zircon description

Zircons from sample 1999383 contained a similar poorly sorted zircon population to 1977975. All the small zircons display oscillatory zoning. Two large grains, ~300 µm in length, have variable cathodoluminescence responses. One grain displays prominent oscillatory zoning, whereas the other grain exhibits a bright (low-U) CL (Figure. A.14).

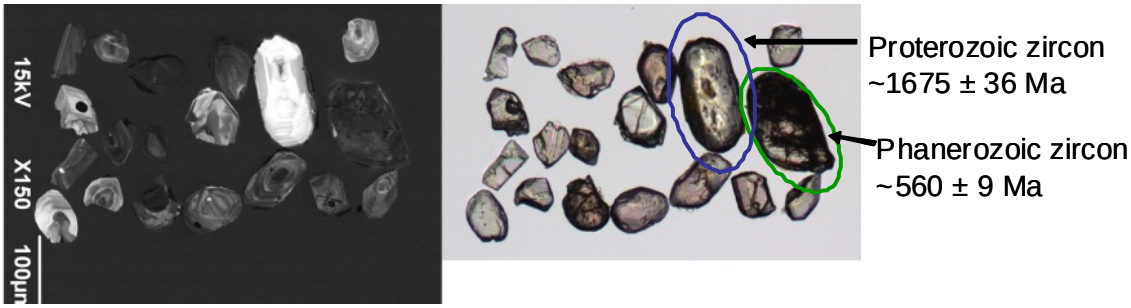

1999383

Figure A.14. Selected transmitted light (top) and cathodoluminescence (bottom) images of zircon grains from a silty mudstone (Croydon A2 Prospect, 1999383). One of the two large zircons in this sample returned a Phanerozoic age.

A.1.18 U–Pb isotopic results

Two further analyses were completed on the two large zircon grains from sample 1999383 (Table A.3). Uranium contents are 1007 ppm and 111 ppm and Th/U content is 0.66 and 0.83, respectively. Common Pb contents for both analyses are below 1% (f^{206}). Figure A.13 illustrates the younger analysis on a Tera-Wasserburg Concordia diagram in comparison with analyses from sample 1977975. This analysis yielded a ^{206}Pb-^{238}U age of 560 ± 8 Ma. The second analysis yielded a ^{207}Pb-^{206}Pb age of 1675 ± 36 Ma, which is not shown.

As younger and larger Phanerozoic zircons are present in both samples (1977975 & 1999383), these grains are unlikely to be contamination, and Phanerozoic successions may be present in these subsurface rocks currently interpreted as Mesoproterozoic units. Figure A.15 shows the cumulative probability distribution of acceptable analyses from samples 1977975 and 1999383. The youngest grains in this spectrum should be interpreted to constrain the maximum depositional age of the unnamed silty mudstone. This Phanerozoic interpretation is consistent with recent ^{40}Ar-^{39}Ar analyses on undeformed muscovite within sulphide veins from the A2 prospect. These analyses established a robust age of ca. 284 Ma for zinc-tin mineralisation at A2 (Huston et al., 2010). Although more work is required to further constrain the depositional age of the rocks that host the A2 prospect, data presented here constrain the age of these rocks to between ca. 432 Ma and ca. 284 Ma (i.e., Silurian, Devonian, Carboniferous or Permian). In any case, the data indicate a greater Phanerozoic sedimentary input into the Croydon region.

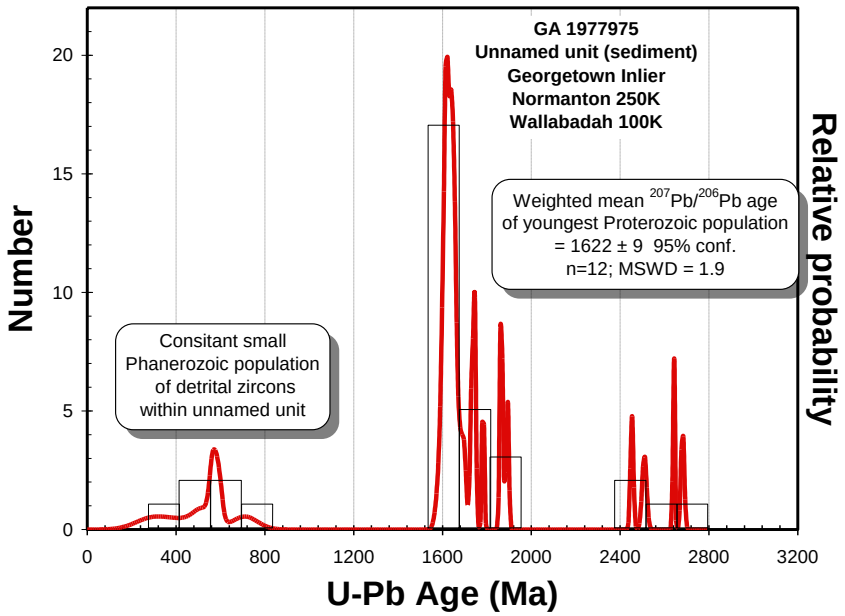

Figure A.15. Cumulative probability diagram of isotopic data from the unnamed sedimentary rocks at the Croydon A2 prospect (GA 1977975 and 1999383), Wallabadah, Georgetown Inlier. A Phanerozoic input is observed in both samples (Fig. A.14). The youngest statistical Proterozoic population is 1622 ± 9 Ma (n = 12; MSWD = 1.9; 2σ); the youngest Phanerozoic zircon yielded an age of 432 ± 6 Ma (1σ). Total number of accepted analyses = 36.

Table A.3: SHRIMP U–Pb zircon isotopic data from unnamed sedimentary rocks at the Croydon A2 prospect (1977975/1999383). Grey shading displays youngest Proterozoic statistical grouping.

Table 3

Grain area	$^{206}Pb_c$ (%)	U (ppm)	Th (ppm)	$^{232}Th/^{238}U$	$^{238}U/^{206}Pb^*$	± (%)	$^{207}Pb^*/^{206}Pb^*$	± (%)	$^{206}Pb/^{238}U$ Age (Ma)	± (1)	$^{207}Pb/^{206}Pb$ Age (Ma)	± (1)	Discordance %	
Detrital zircons														
975.16.1.1	0.46	289	58	0.21	14.3626	1.44	0.0557	1.39	432	6.05	285	73.3	-34	Phanerozoic
975.15.1.1	0.33	165	50	0.31	11.8296	1.53	0.0580	1.63	521	7.73	426	84.7	-18	Phanerozoic
975.16.2.1	-0.19	385	122	0.33	13.9829	1.41	0.0563	1.22	446	6.08	525	44.3	18	Phanerozoic
975.17.2.1	-0.01	1003	235	0.24	10.7464	1.32	0.0588	0.67	574	7.23	565	14.5	-2	Phanerozoic
975.17.1.1	0.02	797	119	0.15	10.8661	1.32	0.0598	0.70	567	7.18	591	15.8	4	Phanerozoic
975.15.2.1	-0.32	140	33	0.24	11.9923	1.59	0.0604	1.82	518	7.97	710	57.3	37	Phanerozoic
975.12.1.1	0.07	132	85	0.66	3.4485	1.53	0.0989	0.82	1640	22.12	1592	17.7	-3	
975.33.2.1	0.21	239	211	0.91	3.7275	1.42	0.1005	0.64	1529	19.38	1600	16.0	5	
975.13.1.1	0.02	442	535	1.25	3.6264	1.34	0.0992	0.45	1570	18.73	1605	9.3	2	
975.26.1.1	0.05	326	279	0.89	3.5041	1.39	0.0997	0.54	1618	19.88	1610	11.2	0	
975.33.1.1	0.02	281	255	0.94	3.5715	1.40	0.0995	0.59	1591	19.80	1611	11.4	1	
975.20.1.1	0.00	983	401	0.42	3.5928	1.30	0.0997	0.33	1583	18.29	1618	6.1	2	
975.31.1.1	-0.02	683	442	0.67	3.5171	1.33	0.0996	0.49	1613	18.94	1620	9.3	0	
975.27.1.1	0.04	303	327	1.11	3.4454	1.40	0.1004	0.57	1642	20.30	1625	11.7	-1	
975.14.1.1	0.00	379	381	1.04	3.4819	1.35	0.1005	0.46	1628	19.46	1633	8.6	0	
975.22.1.1	0.06	226	205	0.94	3.5756	1.47	0.1012	0.64	1589	20.73	1636	13.7	3	
975.4.1.1	0.00	523	752	1.49	3.5190	1.34	0.1008	0.52	1612	19.06	1638	9.6	2	
975.19.1.1	0.01	309	379	1.27	3.4767	1.39	0.1011	0.54	1630	19.97	1643	10.2	1	
975.30.1.1	0.04	370	135	0.38	3.4015	1.38	0.1017	0.52	1661	20.25	1648	11.4	-1	
975.10.1.1	0.09	150	248	1.71	3.4414	1.50	0.1024	0.76	1643	21.77	1653	16.1	1	
975.5.1.1	-0.01	489	379	0.80	3.3354	1.34	0.1015	0.42	1691	19.95	1654	7.8	-2	
975.6.1.1	-0.07	148	123	0.86	3.5108	1.50	0.1012	1.14	1617	21.46	1658	21.8	3	
975.28.1.1	0.06	233	115	0.51	3.3207	1.43	0.1031	0.62	1696	21.38	1672	12.4	-1	
975.1.1.1	-0.04	310	353	1.18	3.3338	1.38	0.1037	0.52	1692	20.53	1697	10.2	0	
975.7.1.1	0.02	814	450	0.57	3.2801	1.31	0.1061	0.32	1715	19.74	1729	6.1	1	
975.8.1.1	-0.03	749	115	0.16	3.3125	1.31	0.1064	0.33	1701	19.65	1742	6.5	2	
975.21.1.1	0.14	1310	905	0.71	3.1415	1.29	0.1080	0.28	1779	20.09	1745	5.7	-2	
975.25.1.1	0.00	1066	810	0.79	3.1085	1.30	0.1090	0.27	1798	20.42	1783	5.0	-1	
975.11.1.1	0.01	1039	97	0.10	3.0081	1.30	0.1139	0.26	1850	20.89	1862	4.7	1	
975.34.1.1	0.00	772	352	0.47	3.0217	1.31	0.1143	0.31	1843	21.07	1869	5.7	1	
975.3.1.1	0.02	703	237	0.35	2.9735	1.32	0.1160	0.31	1869	21.35	1893	5.8	1	
975.29.1.1	0.23	969	494	0.53	2.3670	1.31	0.1618	0.36	2266	24.95	2453	6.5	8	
975.9.1.1	0.11	132	58	0.46	2.1240	1.51	0.1661	0.53	2484	31.10	2509	9.9	1	
975.24.1.1	0.01	604	428	0.73	1.9685	1.32	0.1789	0.24	2648	28.72	2642	4.0	0	
975.18.1.1	0.03	177	112	0.66	1.9463	1.46	0.1834	0.43	2672	31.94	2682	7.3	0	
		1310	1310	1.71									35	
high comm Pb		132	132	0.10										
No analyses														
Discordant														
975.32.1.1	0.06	1764	1255	0.74	3.9780	1.29	0.0988	0.26	1445	16.69	1592	5.2	10	
975.2.1.1	0.40	1281	1359	1.10	2.3965	1.29	0.1960	0.16	2238	24.40	2763	3.3	23	
975.23.1.1	0.00	690	223	0.33	4.3015	1.33	0.1089	0.40	1347	16.12	1782	7.2	32	

Sample 199383 confirms pressence of CAMBRIAN zircons.

Grain.area	$^{206}Pb_c$ (%)	U (ppm)	Th (ppm)	$^{232}Th/^{238}U$	$^{238}U/^{206}Pb^*$	± (%)	$^{207}Pb^*/^{206}Pb^*$	± (%)	$^{206}Pb/^{238}U$ Age (Ma)	± (1)	$^{207}Pb/^{206}Pb$ Age (Ma)	± (1)	Discordance %	
Sample 1999383 confirmed pressence of Cambrian zircons.														
Detrital zircons														
383.Z.1.1.1	0.11	1007	639	0.66	11.0011	1.59	0.0618	0.65	560	8.54	2160	55.4	13	Phanerozoic
383.Z.2.1.1	-0.05	111	89	0.83	3.2940	1.92	0.1058	1.33	1710	28.87	1675	36.2	2	
Discordant														
No analyses														
high comm Pb														
No analyses														

A.1.19 GA sample ID: **1976838**: Mount Isa Inlier, Eastern Succession, Hampden Slate

GA sample No: 1976838
GA Sample ID: 2008165036
GA mount No: GA6083
1:100 000 sheet: KURIDALA
1:250 000 sheet: MT ISA 1:250
Geographic area: Mount Angelay and Malbon
Region: Mt Isa Eastern Succession
Grid Reference (MGA94 Zone 54) 54 447829 mE 7648096 mN
Formal name: Hampden Slate; formerly Kuridala Formation
Lithology: Grey feldspathic fine-sandstone

A.1.20 Sample information

This sample was collected from the Eastern Succession of the Mount Isa Inlier. SHRIMP U–Pb dating was undertaken to establish the maximum depositional age of the Hampden Slate in the Kuridala region. The Hampden Slate sample was sampled to directly compare with the maximum timing of deposition of the Toole Creek Volcanics (sandstone unit) in the Mount Isa Eastern Succession (Carson et al., 2008). The Hampden Slate was thought to be a direct stratigraphic equivalent to the Toole Creek Formation as indicated by mapping completed by Parsons et al. (2008) as part of the GSQ Mt Isa Mapping Project. The sample collected for analysis is a black sandy siltstone collected by A. Lambeck and A. Parsons.

A.1.21 Zircon description

Zircons from this sample range from ~30 μm to ~180 μm in length with one grain ~300 μm. The zircons range from clear to brown in colour and display well rounded equant to slightly elongate morphology. Recognisable crystal facets are rare and broken and fragmented grains are common. Cathodoluminescence images record oscillatory zoning within ninety-eight percent of grains (Fig. A.16).

Figure A.16. Selected transmitted light (top) and cathodoluminescence (bottom) images of zircon grains from the Kuridala siltstone (Mount Angelay and Malbon, 1976838).

A.1.22 U–Pb isotopic results

Ninety analyses were undertaken on eighty-eight zircons from this sample (Fig. A.17, Table A.4). Uranium contents range from 28-1096 ppm and Th/U from 0.1 – 1.56. Five analyses greater than an arbitrary threshold of ~10 % discordance have been removed as were eleven samples with high common f^{206} values (> 1 %). Figures A.17 & A.18 display Tera-Wasserburg Concordia and cumulative probability diagrams, respectively, of isotopic data from the Hampden Slate. The sample contains a significant Archean detrital population but is dominated by Paleoproterozoic zircons. The dominant group displayed in the cumulative probability diagram (Fig. A.18) does not represent a single population (MSWD = 6.5). The youngest statistical grouping (readily apparent in Fig. A.17 and Table A.4) forms a population which returns a weighted mean of **1686** ± **7** Ma (95% confidence; n = 28, MSWD = 1.3). A conservative estimate on the maximum age of deposition of the Hampden Slate at this location is best represented by the youngest statistical grouping at **1686 ± 7** Ma.

The maximum depositional age of the Hampden Slate at this site suggests it cannot be directly compared to the maximum depositional age of the ~1658 Ma Toole Creek Volcanics in the Mount Isa Eastern Succession. The result suggests that the Hampden Slate sediments have a volumetrically dominant Paleoproterozoic/Archean source that is not as evident in the Toole Creek Volcanics sediments (Carson et al., 2008).

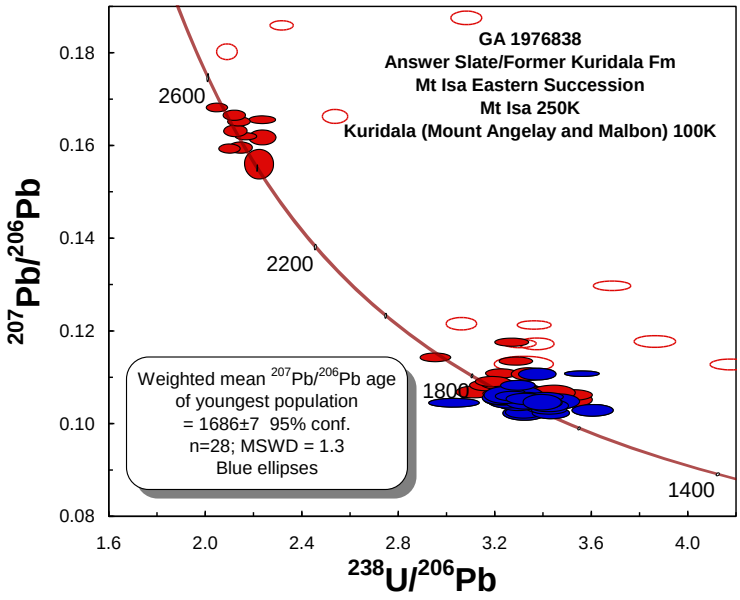

Figure A.17. Tera-Wasserburg Concordia diagram of isotopic data from the Hampden Slate (GA 1976838), Eastern Succession, Mount Isa region. Red open ellipses = omitted analyses with >10% discordance and/or high common ^{206}Pb (>1%). Blue ellipses indicate analyses included in weighted mean determination of 1686 ± 7 Ma.

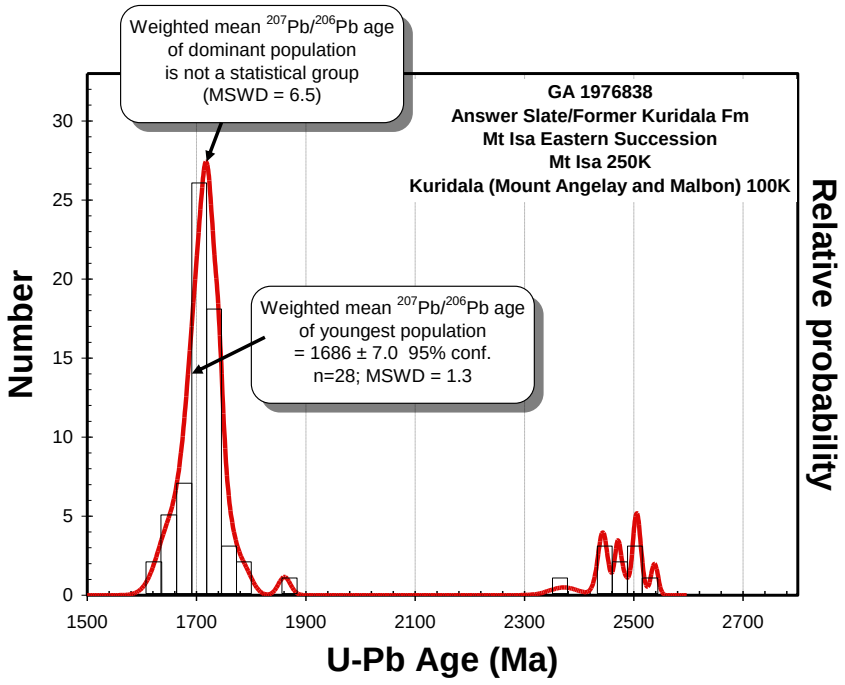

Figure A.18. Cumulative probability diagram of isotopic data from the Hampden Slate (GA 1976838), Kuridala region, Mount Isa Inlier. The youngest statistical population at 1686 ± 7 Ma (n = 28; MSWD = 1.3) is taken as the maximum deposition age for this unit. Total number of accepted analyses = 74.

Table A.4: SHRIMP U–Pb zircon isotopic data from Kuridala Formation grey feldspathic sandstone (1976838). Grey shading displays youngest statistical grouping.

Grain area	$^{206}Pb_c$ (%)	U (ppm)	Th (ppm)	$^{232}Th/^{238}U$	$^{238}U/^{206}Pb^*$	± (%)	$^{207}Pb^*/^{206}Pb^*$	± (%)	$^{206}Pb/^{238}U$ Age (Ma)	± (1σ)	$^{207}Pb/^{206}Pb$ Age (Ma)	± (1σ)	Discordance %
Detrital zircons													
838.63.1.1	0.17	90	51	0.58	3.3220	1.76	0.1020	1.0	1694	26.2	1634	21.3	-4
838.11.1.1	0.18	123	80	0.67	3.3211	1.53	0.1022	0.8	1694	22.8	1635	20.1	-3
838.77.1.1	0.16	160	135	0.87	3.6050	1.53	0.1026	0.8	1576	21.5	1647	18.2	5
838.10.1.1	0.05	143	113	0.81	3.4324	1.50	0.1020	0.8	1647	21.8	1653	16.2	0
838.27.1.1	0.30	76	109	1.49	3.4635	1.69	0.1045	1.0	1630	24.4	1660	28.7	2
838.69.1.1	0.13	138	94	0.70	3.4056	1.53	0.1032	0.8	1657	22.4	1662	19.0	0
838.79.1.1	0.16	127	101	0.83	3.4167	1.53	0.1035	0.8	1652	22.4	1663	23.6	1
838.31.1.1	0.01	247	156	0.65	3.4243	1.41	0.1027	0.6	1651	20.5	1672	10.9	1
838.21.1.1	0.24	28	37	1.39	3.2972	2.23	0.1053	1.7	1704	33.4	1683	39.3	-1
838.29.1.1	0.17	127	102	0.82	3.3346	1.54	0.1048	1.1	1688	22.8	1685	22.5	0
838.3.1.1	0.16	64	96	1.56	3.2558	1.74	0.1048	1.1	1724	26.4	1686	29.4	-2
838.42.1.1	0.23	181	189	1.07	3.2383	1.52	0.1055	0.7	1731	23.1	1687	16.1	-3
838.52.1.1	0.08	262	134	0.53	3.0311	2.25	0.1043	0.6	1837	35.9	1689	12.9	-8
838.28.1.1	0.78	675	416	0.64	3.5604	1.32	0.1105	0.4	1583	18.6	1692	11.3	7
838.51.1.1	0.14	141	88	0.65	3.2272	1.53	0.1050	0.8	1738	23.3	1693	18.2	-3
838.23.1.1	0.07	155	110	0.73	3.3798	1.49	0.1044	0.7	1670	21.9	1693	15.1	1
838.15.1.1	0.75	147	147	1.03	3.3758	1.49	0.1104	0.7	1660	21.9	1694	24.1	2
838.37.1.1	-0.03	130	97	0.77	3.4241	1.54	0.1036	0.8	1652	22.5	1694	15.7	3
838.4.1.1	0.15	98	47	0.49	3.2268	1.59	0.1053	0.9	1738	24.2	1697	21.9	-2
838.40.1.1	0.09	271	191	0.73	3.3594	1.41	0.1048	0.6	1678	20.8	1697	12.2	1
838.39.1.1	0.17	244	145	0.61	3.4109	1.42	0.1055	0.6	1655	20.8	1698	13.8	3
838.87.1.1	0.04	93	73	0.81	3.3259	1.64	0.1044	1.0	1694	24.4	1698	18.4	0
838.48.1.1	0.20	68	69	1.04	3.2438	1.77	0.1059	1.1	1729	26.9	1699	26.4	-2
838.54.1.1	0.43	222	200	0.93	3.2942	1.43	0.1080	0.6	1702	21.5	1701	17.3	0
838.65.1.1	0.01	114	81	0.74	3.3984	1.57	0.1043	0.9	1663	23.0	1701	16.2	2
838.45.1.1	0.13	220	162	0.76	3.2741	1.45	0.1057	0.6	1716	21.9	1706	13.9	-1
838.41.1.1	0.05	157	108	0.71	3.3236	1.50	0.1050	0.7	1695	22.4	1707	15.8	1
838.74.1.1	-0.03	139	110	0.82	3.3962	1.54	0.1043	1.1	1664	22.6	1707	19.8	3
838.6.1.1	0.07	293	284	1.00	3.2470	1.38	0.1055	0.5	1729	21.0	1713	10.5	-1
838.33.1.1	0.05	320	217	0.70	3.3462	1.38	0.1054	0.5	1685	20.5	1713	10.7	2
838.44.1.1	-0.03	177	211	1.23	3.2607	1.48	0.1046	0.7	1725	22.4	1713	13.2	-1
838.76.1.1	-0.04	147	121	0.85	3.3090	1.53	0.1046	0.8	1703	22.9	1714	15.5	1
838.20.1.1	0.09	294	194	0.68	3.3142	1.39	0.1057	0.5	1698	20.7	1714	10.8	1
838.73.1.1	-0.01	100	95	0.98	3.5153	1.66	0.1049	1.0	1614	23.7	1715	18.4	6
838.43.1.1	0.08	329	178	0.56	3.2794	1.38	0.1059	0.6	1714	20.8	1716	11.6	0
838.62.1.1	0.19	261	198	0.78	3.2605	1.41	0.1068	0.6	1721	21.4	1717	14.4	0
838.67.1.1	0.06	106	99	0.96	3.3303	1.63	0.1057	0.9	1692	24.3	1717	19.7	2
838.72.1.1	0.10	182	50	0.29	3.4373	1.48	0.1061	0.8	1644	21.5	1718	16.9	4
838.60.1.1	0.14	126	133	1.09	3.3233	1.57	0.1064	0.9	1693	23.4	1718	20.6	1
838.56.1.1	-0.01	573	417	0.75	3.2722	1.34	0.1052	0.4	1719	20.2	1720	7.3	0
838.61.1.1	0.05	434	383	0.91	3.2653	1.36	0.1057	0.4	1721	20.5	1720	8.7	0
838.34.1.1	0.20	140	75	0.55	3.3126	1.52	0.1071	0.8	1697	22.7	1720	18.2	1
838.30.1.1	0.00	164	129	0.81	3.2993	1.87	0.1055	0.7	1707	28.0	1724	12.9	1
838.25.1.1	0.58	400	273	0.71	3.2269	1.35	0.1106	0.6	1730	20.6	1724	14.8	0
838.70.1.1	0.04	189	106	0.58	3.5238	1.52	0.1059	0.7	1610	21.6	1724	14.4	7
838.18.1.1	0.03	159	127	0.82	3.2953	1.48	0.1060	0.7	1708	22.2	1726	13.2	1
838.64.1.1	0.07	149	59	0.41	3.1135	1.58	0.1066	0.8	1794	24.8	1730	16.3	-4
838.9.1.1	0.03	367	148	0.42	3.2949	1.36	0.1062	0.5	1708	20.4	1731	8.9	1
838.35.1.1	0.04	103	84	0.85	3.2908	1.61	0.1063	0.9	1710	24.2	1731	17.2	1
838.81.1.1	0.05	165	59	0.37	3.3842	1.51	0.1065	0.8	1668	22.2	1734	15.9	4
838.58.1.1	0.49	229	170	0.77	3.3403	1.44	0.1104	0.8	1680	21.3	1735	19.9	3
838.90.1.1	-0.04	151	178	1.21	3.2986	1.51	0.1060	0.8	1708	22.7	1736	14.7	2
838.78.1.1	0.01	90	90	1.03	3.4413	1.76	0.1064	1.0	1644	25.6	1737	18.8	6
838.13.1.1	-0.01	260	205	0.81	3.2182	1.40	0.1062	0.5	1744	21.4	1737	10.0	0
838.66.1.1	0.04	379	180	0.49	3.3113	1.37	0.1067	0.5	1701	20.5	1738	9.4	2
838.71.1.1	0.04	204	65	0.33	3.2739	1.47	0.1068	0.7	1718	22.1	1740	13.6	1
838.2.1.1	0.06	779	686	0.91	3.3020	1.31	0.1071	0.3	1704	19.6	1742	6.4	2

Table A.4: (continued)

Grain area	$^{206}Pb_c$ (%)	U (ppm)	Th (ppm)	$^{232}Th/^{238}U$	$^{238}U/^{206}Pb^*$	± (%)	$^{207}Pb^*/^{206}Pb^*$	± (%)	$^{206}Pb/^{238}U$ Age (Ma)	± (1°)	$^{207}Pb/^{206}$ Pb Age (Ma)	± (1°)	Discordance %
Detrital zircons													
838.5.1.1	0.74	238	182	0.79	3.2863	1.40	0.1132	0.5	1700	21.0	1745	17.1	3
838.32.1.1	0.02	160	133	0.86	3.2681	1.48	0.1073	0.7	1721	22.4	1751	13.3	2
838.16.1.1	0.07	163	93	0.59	3.1689	1.52	0.1080	0.7	1767	23.5	1755	14.6	-1
838.88.1.1	0.03	210	119	0.59	3.2137	1.44	0.1083	0.7	1746	22.1	1767	13.7	1
838.14.1.1	0.98	277	142	0.53	3.2690	1.42	0.1173	0.5	1703	21.3	1778	16.0	4
838.24.1.1	-0.08	156	71	0.47	3.1900	1.48	0.1088	0.7	1759	22.8	1791	14.1	2
838.19.1.1	0.03	210	75	0.37	2.9545	1.43	0.1140	0.6	1879	23.3	1861	11.0	-1
838.53.1.1	0.37	95	27	0.29	2.2254	1.76	0.1556	1.4	2383	35.2	2372	26.0	0
838.49.1.1	0.08	162	74	0.47	2.1480	1.49	0.1593	0.5	2462	30.4	2440	9.4	-1
838.86.1.1	0.02	1096	108	0.10	2.1026	1.41	0.1591	0.4	2507	29.3	2444	7.0	-3
838.68.1.1	0.25	102	62	0.63	2.2384	1.61	0.1615	0.7	2375	32.1	2448	13.4	3
838.47.1.1	0.03	440	226	0.53	2.1703	1.35	0.1617	0.3	2442	27.4	2471	5.4	1
838.38.1.1	0.07	146	101	0.71	2.1276	1.50	0.1629	0.5	2482	31.0	2479	9.6	0
838.57.1.1	0.08	505	215	0.44	2.2378	1.63	0.1653	0.3	2379	32.3	2503	6.0	5
838.7.1.1	0.01	223	132	0.61	2.1409	1.41	0.1649	0.4	2471	28.9	2506	6.9	1
838.59.1.1	0.12	218	115	0.54	2.1221	1.43	0.1662	0.4	2486	29.6	2509	7.8	1
838.22.1.1	-0.01	243	157	0.67	2.0503	1.39	0.1679	0.4	2561	29.5	2538	6.4	-1
high comm Pb													
838.75.1.1	1.01	326	214	0.68	1.5082	1.38	0.2864	0.3	3240	35.3	3349	5.6	3
838.80.1.1	1.03	91	61	0.70	3.3208	2.44	0.1128	1.0	1679	36.2	1695	36.8	1
838.1.1.1	1.29	261	168	0.66	3.3737	1.42	0.1172	0.7	1652	20.8	1731	23.4	5
838.46.1.1	1.40	423	283	0.69	2.0898	1.35	0.1802	0.6	2483	28.0	2534	15.4	2
838.85.1.1	1.61	315	226	0.74	3.3030	1.38	0.1173	0.5	1677	20.5	1683	20.8	0
838.8.1.1	1.77	325	189	0.60	3.0616	1.37	0.1215	0.7	1790	21.5	1734	22.8	-3
838.36.1.1	1.86	323	181	0.58	3.3634	1.38	0.1213	0.5	1646	20.1	1716	18.4	4
838.55.1.1	2.71	390	166	0.44	2.1252	1.36	0.1925	0.3	2413	27.6	2539	11.0	5
838.26.1.1	2.98	294	111	0.39	2.3166	1.38	0.1859	0.4	2239	26.2	2447	13.7	9
838.50.1.1	4.25	966	54	0.06	2.2913	1.30	0.1974	0.3	2228	24.7	2448	11.3	10
838.82.1.1	9.32	332	232	0.72	3.0822	1.37	0.1875	0.5	1640	20.4	1737	44.5	6
Discordant >10 %													
838.12.1.1	3.11	267	195	0.76	3.6864	1.40	0.1297	0.5	1498	18.9	1674	29.8	12
838.84.1.1	0.96	430	197	0.47	2.5381	1.37	0.1663	0.6	2119	24.7	2431	12.2	15
838.17.1.1	1.64	158	153	1.00	3.8638	1.47	0.1177	0.7	1459	19.4	1687	30.0	16
838.83.1.1	13.53	258	157	0.63	2.9473	1.40	0.2349	0.4	1618	23.1	1897	93.9	17
838.89.1.1	1.37	452	280	0.64	4.1777	1.35	0.1128	0.7	1364	16.7	1641	20.7	20

References

Betts, P.G., Giles, D. and Schaefer, B.F., 2008. Comparing 1800-1600 Ma accretionary and basin processes in Australia and Laurentia: Possible geographic connections in Columbia. Precambrian Research, 166(1-4): 81-92.

Baker, M.J., Crawford, A.J. and Withnall, I.W., 2010. Geochemical, Sm-Nd isotopic characteristics and petrogenesis of Paleoproterozoic mafic rocks from the Georgetown Inlier, north Queensland: Implications for relationship with the Broken Hill and Mount Isa Eastern Succession. Precambrian Research, 177(1-2): 39-54.

Betts, P., Giles, D., Mark, G., Lister, G., Goleby, A.B. and Ailleres, L., 2006. Synthesis of the Proterozoic evolution of the Mt Isa Inlier. Australian Journal of Earth Sciences, 53: 187-211.

Black, L. and McCulloch, M.T., 1984. Sm-Nd ages of the Arunta, Tennant Creek and Georgetown Inliers of northern Australia. Australian Journal of Earth Sciences, 31: 49-60.

Black, L.P., Gregory, P., Withnall, I.W. and Bain, J.H.C., 1998. U-Pb zircon age for the Etheridge Group, Georgetown region, north Queensland: Implications for relationship with the Broken Hill and Mt Isa sequences. Australian Journal of Earth Sciences: An International Geoscience Journal of the Geological Society of Australia, 45(6): 925 - 935.

Black, L.P., Kamo, S.L., Allen, C.M., Davis, D.W., Aleinkoff, J.N., valley, J.W., Mundil, R., Campbell, I.H., Korsch, R.J., Williams, I.S. and Foudoulis, C., 2004. Improved 206Pb/238U microprobe geochronology by the monitoring of a trace-element-related matrix effect; SHRIMP, ID–TIMS, ELA–ICP–MS and oxygen isotope documentation for a series of zircon standards. Chemical Geology, 205: 115–140.

Carson, C., Hutton, L.J., Withnall, I.W. and Perkins, W., 2008: Joint GSQ-GA NGA geochronology project Mount Isa region, 2007-2008. Queensland Geological Record 2008/05

Hoskin, P.W.O. and Black, L.P., 2000. Metamorphic zircon formation by solid-state recrystallization of protolith igneous zircon. Journal of Metamorphic Geology, 18: 423-439.

Huston, D.L., Champion, D.C. and Kositcin, N., 2010. Metallogenesis of eastern Australia: links to the tectonic evolution of the Tasman Orogen. Australian Institute of Geoscientists Bulletin, 52: 45-57.

Lambeck, A., 2011. Basin analysis and the geochemical signature of Paleoproterozoic sedimentary successions in northern Australia: Constraints on basin development in respect to mineralisation and paleoreconstruction models. Unpublished PhD thesis, The University of Adelaide.

Lambeck, A., Barovich, K., Gibson, G.M. and Huston, D., in review. An abrupt change in Nd isotopic composition in Australian basins at 1650 Ma: implications for the tectonic evolution of Australia and its place in Nuna. Precambrian Research.

Lambeck, A., Parsons, A., Withnall, I., Huston, D. and Gibson, G.M., in prep. Juvenile sediments at 1650 Ma in the Mt Isa & Georgetown Inliers: Constraints on basin development. Australian Journal of Earth Sciences.

Ludwig, K.R., 2001. Squid 1.03: a user's manual. Berkeley Geochronology Center, Special Publication 2.

Ludwig, K.R., 2003. Isoplot 3.00: a user's manual. Berkeley Geochronology Center, Special Publication 4.

Parsons, A., Withnall, I.W., Neumann, N.L., Carson, C.J. and Lambeck, A., 2008. The Tectono-Stratigraphic framework of the Cloncurry-Selwyn Zone: working towards a resolution. Digging Deeper 6 Proceedings, Geological Survey of Queensland.

Southgate, P., Bradshaw, B., Dimagala, J., Jackson, M.J., Idnurm, M., Krassay, A.A., Page, R.W., Sami, T., Scott, D., Lindsay, J., McConachie, B. and Tarlowski, C., 2000. Chronostratigraphic basin framework for Palaeoproterozoic rocks (1730-1575 Ma) in northern Australia and implications for base-metal mineralisation. Australian Journal of earth Sciences, 47(3): 461-483.

Stern, R.A., Bodorkos, S., Kamo, S.L., Hickman, A.H. and Corfu, F., 2009. Measurements of SIMS instrumental mass fraction of Pb-isotopes during zircon dating. Geostandards and Geoanalytical Research, 33(2): 145-168.

Withnall, I.W., Bain, J.H.C., Draper, J.J., MacKenzie, D.E. and Oversby, B.S., 1988. Proterozoic stratigraphy and tectonic history of the Georgetown Inlier, northeastern Queensland. Precambrian Research, 40-41: 429-446.